46

21

NASA TECHNICAL MEMORANDUM

NASA TM X-52876
Volume II

NASA TM X-52876
Volume II

SPACE TRANSPORTATION SYSTEM TECHNOLOGY SYMPOSIUM

II - Dynamics and Aeroelasticity

NASA Lewis Research Center
Cleveland, Ohio
July 15-17, 1970

1. Report No.	2. Government Accession No.	3. Recipient's Catalog No.
TM X-52876 - Volume II		

4. Title and Subtitle	5. Report Date
SPACE TRANSPORTATION SYSTEM TECHNOLOGY SYMPOSIUM II - Dynamics and Aeroelasticity	July 1970 6. Performing Organization Code
7. Author(s)	8. Performing Organization Report No. E-5866
9. Performing Organization Name and Address	10. Work Unit No. 11. Contract or Grant No.
12. Sponsoring Agency Name and Address National Aeronautics and Space Administration Washington, D. C. 20546	13. Type of Report and Period Covered Technical Memorandum 14. Sponsoring Agency Code

15 Supplementary Notes

Held at the NASA-Lewis Research Center, July 15-17, 1970

16. Abstract

The Symposium encompassed seven technical areas, each published in a separate volume of NASA Technical Memorandum X-52876:

Volume I - Aerothermodynamics and Configurations
(includes aerodynamics; atmospheric operations; and aerodynamic heating)

II - Dynamics and Aeroelasticity
(includes dynamic loads and response; aeroelasticity; and flight dynamics and environment)

III - Structures and Materials
(includes structural design technology; thermal protection systems; and materials technology)

IV - Propulsion
(includes main propulsion; auxiliary propulsion; and airbreathing propulsion)

V - Operations, Maintenance, and Safety (Including Cryogenic Systems)
(includes general and cryogenics)

VI - Integrated Electronics (Including Electric Power)
(includes system integration; data management, systems monitoring, and checkout; navigation, guidance, and control; communication, instrumentation, and display; and power subsystems)

VII - Biotechnology

17. Key Words (Suggested by Author(s))	18. Distribution Statement
	Unclassified - unlimited

19. Security Classif. (of this report)	20. Security Classif. (of this page)	21. No. of Pages	22. Price*
Unclassified	Unclassified	367	$3.00

*For sale by the Clearinghouse for Federal Scientific and Technical Information
Springfield, Virginia 22151; also as microfiche
at $.65 per copy

FOREWORD

The prospect of undertaking a reusable launch vehicle development led the NASA Office of Manned Space Flight (OMSF) to request the Office of Advanced Research and Technology (OART) to organize and direct a program to develop the technology that would aid in selecting the best system alternatives and that would support the ultimate development of an earth-to-orbit shuttle. Such a Space Transportation System Technology Program has been initiated. OART, OMSF, and NASA Flight and Research Centers with the considerable inputs of Department of Defense personnel have generated the program through the efforts of several Technology Working Groups and a Technology Steering Group. Funding and management of the recommended efforts is being accomplished through the normal OART and OMSF line management channels. The work is being done in government laboratories and under contract with industry and universities. Foreign nations have been invited to participate in this work as well. Substantial funding, from both OART and OMSF, was applied during the second half of fiscal year 1970.

The Space Transportation System Technology Symposium held at the NASA Lewis Research Center, Cleveland, Ohio, July 15-17, 1970, was the first public report on that program. The Symposium goals were to consider the technology problems, their status, and the prospective program outlook for the benefit of the industry, government, university, and foreign participants considered to be contributors to the program. In addition, it offered an opportunity to identify the responsible individuals already engaged in the program. The Symposium sessions were intended to confront each presenter with his technical peers as listeners, and this, I believe, was substantially accomplished.

Because of the high interest in the material presented, and also because the people who could edit the output are already deeply involved in other important tasks, we have elected to publish the material essentially as it was presented, utilizing mainly the illustrations used by the presenters along with brief words of explanation. Those who heard the presentations, and those who are technically astute in specialty areas, can probably put this story together again. We hope that more will be gained by compiling the information in this form now than by spending the time and effort to publish a more finished compendium later.

A. O. Tischler
Chairman,
Space Transportation System
Technology Steering Group

CONTENTS

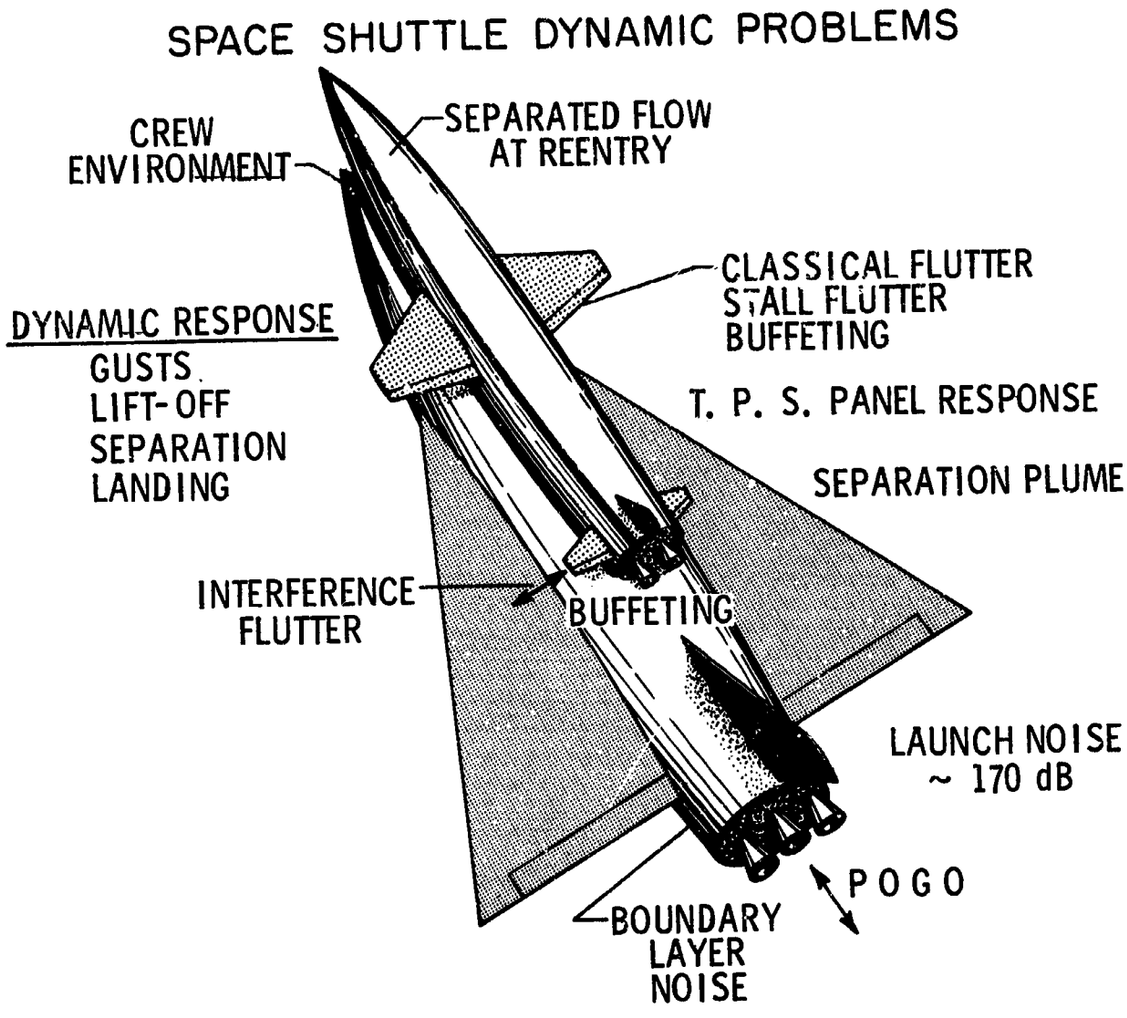
SPACE SHUTTLE DYNAMIC PROBLEMS
CREW ENVIRONMENT
SEPARATED FLOW AT REENTRY
CLASSICAL FLUTTER
STALL FLUTTER
BUFFETING
DYNAMIC RESPONSE
GUSTS
LIFT-OFF
SEPARATION
LANDING
T. P. S. PANEL RESPONSE
SEPARATION PLUME
INTERFERENCE FLUTTER
BUFFETING
LAUNCH NOISE ~ 170 dB
POGO
BOUNDARY LAYER NOISE

Dynamics and Aeroelasticity

Introductory Statement

by Harry L. Runyan

The Space Shuttle, being an hybrid - an airplane and a launch vehicle - represents the greatest challenge that the dynamicist and the aeroelastician have faced. Some specific problem areas related to the Space Shuttle are listed on figure 1.

Dynamics and aeroelasticity envelop many disciplines, including aerodynamics, vibration, random processes, structures, fluid flow, mechanics, etc., but, of more importance, they involve the interaction and coupling of many of these various disciplines. Fundamentally, we are concerned with structural integrity and safe flight, i.e., trying to ensure that the vehicle will remain structurally intact as well as function properly in the presence of the many faceted dynamic environment.

A new area which may have an impact on our task is the effect of the high temperature environment. In the past, we have been able to successfully decouple the temperature effects from our problem formulation. For the Space Shuttle, this problem must be closely reexamined.

As has been pointed out in the opening remarks of the Conference, the Dynamics and Aeroelasticity Technology Group comprises one of several technology groups which are attempting to provide the necessary research to support a successful and safe vehicle. The group has members from most of the

NASA Centers as well as from the Air Force groups. We meet periodically to review ongoing work, search for new problem areas; and we are constantly updating and revising our program. The group is organized into three panels as shown on figure 2: a panel on Dynamic Loads and Response, one on Aeroelasticity, and one on Flight Dynamics and Environment. The Conference papers accordingly have been grouped in these same three areas, with each Panel Chairman acting as moderator for his particular session.

TECHNOLOGY AREA
DYNAMICS AND AEROELASTICITY

H. L. Runyan, LRC

DYNAMIC LOADS AND RESPONSE

H. G. Morgan, LRC

Vibration Characteristics
- Parallel Staging
- Thermal Effects
- Dynamic Models

Dynamic Loads
- Lift-off Transients
- Staging Transients
- Docking Impacts
- Landing Impacts

Liquid Dynamics
- Propellant Slosh
- Baffles

Separation Dynamics

AEROELASTICITY

W. H. Reed, LRC

Flutter
- Primary and Control Surface
- Buzz
- Panel
- Stall

Buffet
- Launch Configuration
- Reentry Configuration

Ground Wind Loads

FLIGHT DYNAMICS AND ENVIRONMENT

R. W. Schock, MSFC

Coupled dynamics and interactions of structural components, propulsion systems, and control systems in full-scale structures

Pogo

Wind, Gust, and Control Loads

Acoustic Environment and Sonic Fatigue

ASSESSMENT OF CURRENT METHODS FOR DYNAMIC ANALYSIS OF COMPLEX STRUCTURES

K. J. Forsberg

Lockheed Missiles & Space Company

INTRODUCTION

An accurate, detailed dynamic analysis of the space shuttle must be made if it is to survive the combined environments of launch vehicle, satellite, reentry vehicle, and aircraft. Moreover, these dynamic analyses must be initiated as early as possible in the preliminary design phase, so that dynamic guidance can be given to the program.

Basically, there are two ways to compute dynamic response of a vehicle: direct integration of the equations of motion, and modal synthesis. Direct integration is used primarily for nonlinear problems or for impact or impulsive loads when one is interested only in early-time behavior. Modal superposition is the primary method for predicting the linear dynamic behavior of aerospace vehicles. For most problems, the dynamic response of a structure can be adequately predicted by less than 100 modes (although this is a function of the loading). Once the modal parameters (eigenvalues, mode shapes, generalized masses) are known, prediction of peak dynamic loads is a straightforward, though nontrivial, task. Perhaps the most difficult step in the process is the determination of the eigenvalues of large complex structures, since, as will be shown, accurate dynamic analysis requires models often involving more than 10,000 degrees of freedom.

There are many problems in the area of dynamics which require further research to insure proper design of the space shuttle, and the other speakers will discuss a number of these in detail. However, there is one problem which underlies all of the work to be discussed today: i.e., the analytical prediction of the modal characteristics of a vehicle. It is appropriate, then, to limit this paper to an assessment of the state-of-the-art for determining eigenvalues of large systems.

BASIC METHODS OF DYNAMIC ANALYSIS

TIME INTEGRATION

- IMPACT
- EARLY TIME RESPONSE
- NONLINEAR BEHAVIOR

MODAL SUPERPOSITION

- PRIMARY TOOL FOR ANALYSIS OF SPACE SHUTTLE VEHICLES
- MAJOR EFFORT-DETERMINATION OF EIGENVALUES FOR LARGE SYSTEM

STRUCTURAL MODELING

Many aircraft flying today have been adequately analyzed, using simple dynamic models having 100 to 200 degrees of freedom. Such analyses are usually based on simple "stick" models such as that shown for the Cheyenne helicopter. In cases where the structure does not act like an assemblage of compact beams, however, a "stick" model cannot accurately predict all of the modes of interest to the engineer, and a more sophisticated model must be used, as shown in the figure on the opposite page.

In practice, it has proven to be necessary to construct detailed finite element or finite difference models for aerospace vehicles. Such models produce large systems of simultaneous equations, involving 1000 to 10,000 or more degrees of freedom. The problems encountered in accurately modeling a complex structure (such as the treatment of liquid-filled shells) are recognized, but will not be discussed here.

MODELS OF CHEYENNE (AH-56A) HELICOPTER

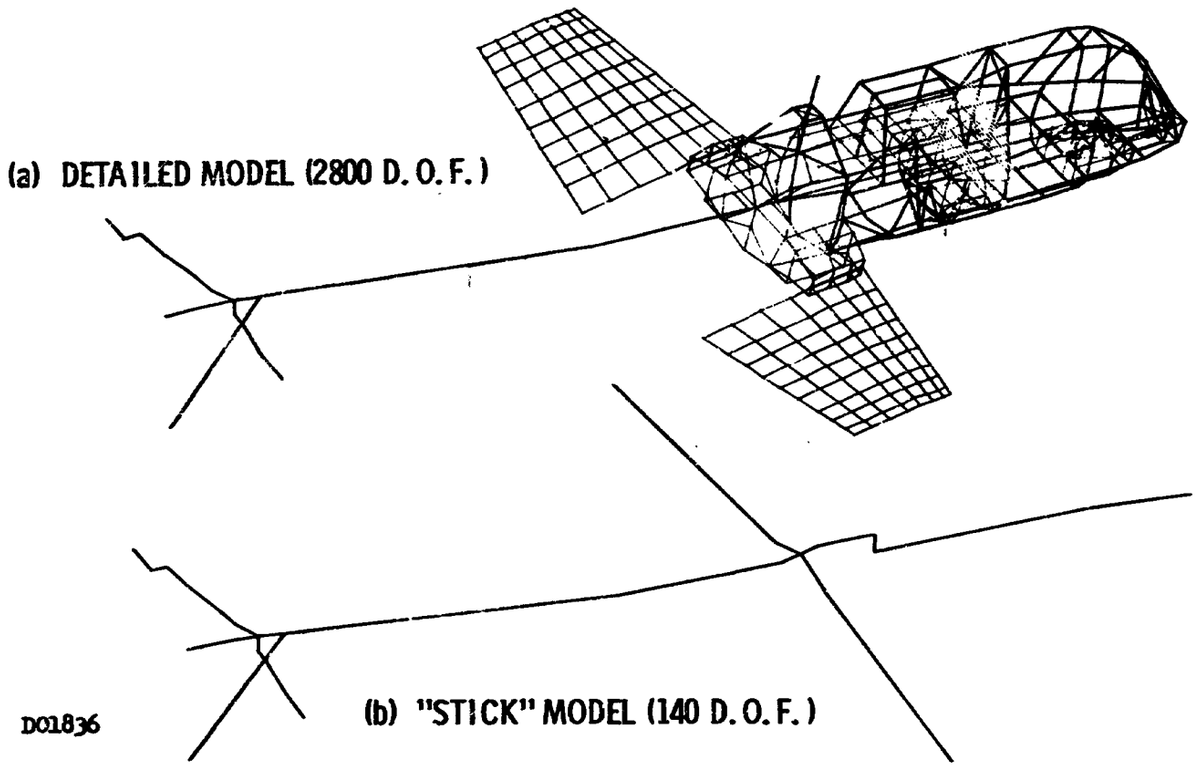

(a) DETAILED MODEL (2800 D.O.F.)

(b) "STICK" MODEL (140 D.O.F.)

D01836

AH-56A HELICOPTER (Movie)

The deficiency of a simple stick model is clearly illustrated in the analysis of the Cheyenne helicopter. It was necessary to determine the effect of the flexibility of large fuselage access doors on the dynamic behavior of the vehicle. The stick model showed no change in mode shape and only a small decrease in frequency for the lowest modes. The detailed model predicted the same small reduction in frequency; however, it also predicted a dramatic change in mode shape (basically a change from pure bending to coupled bending and torsion). This change in mode shape, which is of vital engineering importance, is clearly illustrated in the movie. (The movie also illustrates the value of animated graphic displays. The movie is simply an animation of the SC4020 computer plot shown on the opposite page, with the dashed lines and numbers omitted. The modes shown in the movie can be immediately visualized, whereas the static plot shown here requires considerable study to interpret.)

Note that the significant change in the dynamic behavior of the Cheyenne occurred because of the introduction of a large, "nonstructural" reinforced cutout in the fuselage. Current shuttle orbiter designs call for a nonload-carrying payload door, which will cause similar bending and torsional coupling. This can only be predicted by a detailed three-dimensional dynamic model of the orbiter.

AH-56A HELICOPTER (FIRST MODE)

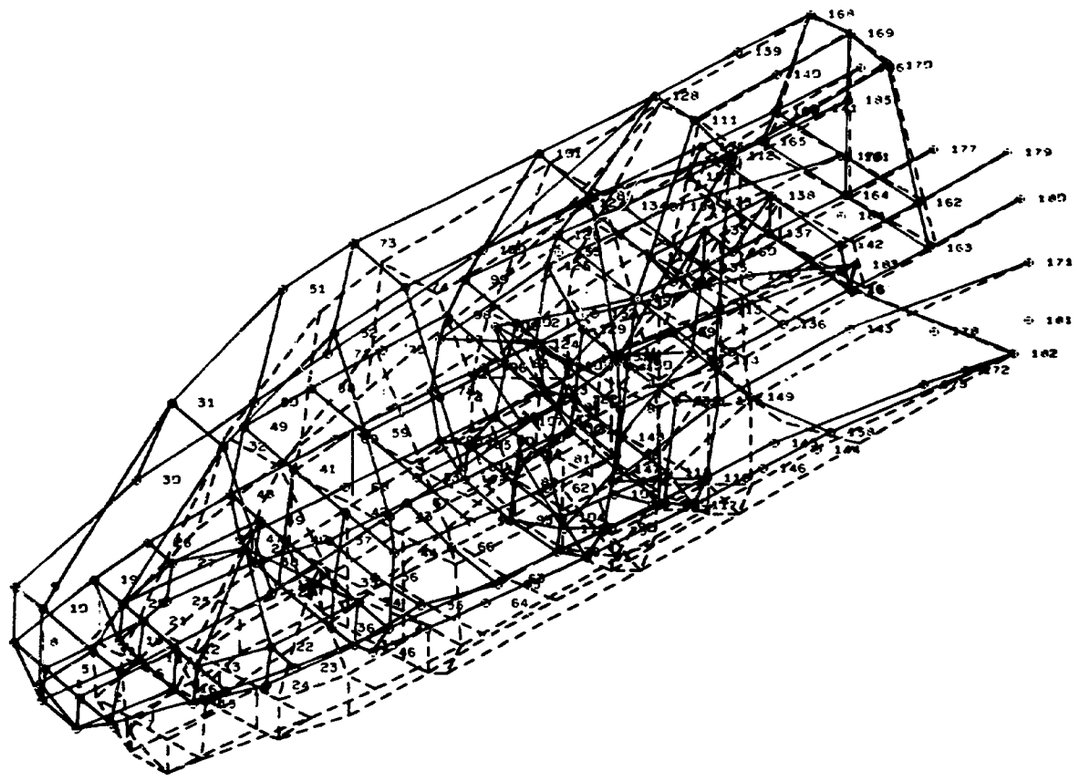

D01837

TECHNIQUES FOR FINDING EIGENVALUES

The usual formulation of a finite element or finite difference model yields a standard eigenvalue problem of the form

$$(A - \lambda B)\ x = 0$$

The matrices A and B are usually strongly banded, symmetric, and positive definite. The mass matrix is usually diagonal (although this is not necessary).

Basically, there are six methods for finding eigenvalues of such a system of equations, and these are noted on the opposite page.

TECHNIQUES FOR FINDING EIGENVALUES

- DIRECT SOLUTION
- INVERSE POWER ITERATION
- ASSUMED FUNCTIONS (RAYLEIGH-RITZ)
- MATRIX REDUCTION
- COMPONENT MODES (SUBSTRUCTURES)
- DETERMINANT SEARCH

DIRECT SOLUTION

During the past decade, the Choleski-Householder-Givens method has become the standard procedure for finding eigenvalues for engineering use. This highly reliable, very efficient routine finds all of the eigenvalues in ascending order; computer time can be saved, however, by limiting the number of eigenvectors to be computed. Both the mass and stiffness matrices are treated as if they were full, and hence the direct solution approach is usually limited to problems which can be contained "in-core" (200 degrees of freedom or less). Extensions have been made to accommodate larger problems (up to 400 degrees of freedom) but the cost increases rapidly with problem size, as shown in the accompanying graph. The run times shown are based on a double precision program running in FORTRAN V on the UNIVAC 1108 with an EXEC 2 compiler.

The Jacobi method is another commonly used "direct solution" technique for finding eigenvalues of full matrices. This method was the standard approach for many years and is still widely used. Experience at Lockheed has shown that the Choleski-Householder-Givens method is more accurate and more reliable than the Jacobi approach; however, the Jacobi is satisfactory for well-behaved problems and may be faster than the Householder-et al approach.

The primary deficiency of these approaches is that, for economic reasons, they are limited to small systems (less than 400 degrees of freedom).

The direct solution procedure is a vital part of other eigenvalue routines (Assumed Functions, Matrix Reduction, and Component Modes). It is a standard subroutine in most large-scale structural analysis programs (NASTRAN, STARDYNE, ASTRA, REXBAT, SNAP, FORMAT, etc.).

RUN TIME VS MATRIX SIZE

DIRECT SOLUTION OF EIGENVALUE PROBLEM

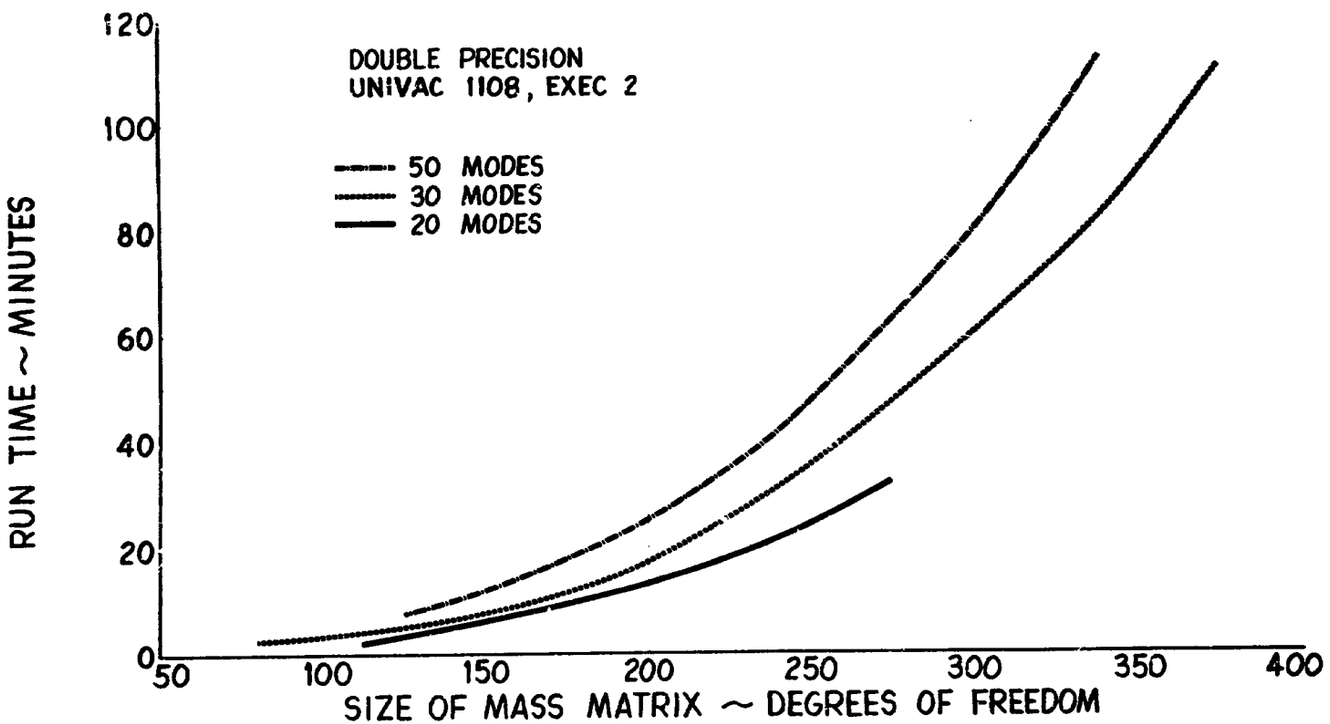

D01839 7-1-70

INVERSE POWER ITERATION

Proper structural dynamic characterization of a vehicle often results in problems in excess of 400 degrees of freedom. For instance, the preliminary model of the fixed-wing orbiter (shown on the opposite page) had 900 degrees of freedom, and required approximately 2 minutes of UNIVAC 1108 computer time to compute each eigenvalue. The most widely used method to handle such problems is inverse power iteration.

The accuracy of the inverse power iteration solution (without spectral shifts) depends on the:

- Bandwidth and constrained degrees of freedom
- Numerical conditioning of the stiffness matrix
- Spacing of the eigenvalues
- Number of previously computed modes
- Decomposition routine (usually a variation of Gaussian Elimination)

As an example of the accuracy which can be obtained, results from an analytical model of a cylinder with a cutout were compared with results obtained by experiment; the frequencies agreed within 0.1 percent. The analytical model had 4200 unknowns, with a semibandwidth of 150, and required 10 minutes on the UNIVAC 1108 to compute each eigenvalue (in single precision). For well-conditioned problems one can obtain accurate results in single precision (8 digits) for systems of 5000 to 6000 unknowns. Dr. C. Fellipa at Boeing has found that the accuracy of a 14-digit (single precision CDC-6600) solution deteriorates for practical problems in excess of 30,000 unknowns.

The rate of convergence of the solution to a given eigenvalue λ_0 depends upon the ratio of λ_0 to its nearest neighbor λ_1. By shifting the origin of the system to a point very near λ_0, the rate of convergence can be greatly improved. The iterations then converge to a new eigenvalue $\lambda^* = \lambda_0 - \Omega$, where Ω is the value of the spectral shift. This technique not only improves convergence, but it also allows one to determine higher modes without first finding all of the lower eigenvalues. Moreover, to find higher modes using the inverse power iteration without shifting one must orthogonalize the eigenvector with all previously computed eigenvectors; in practice this limits the usefulness of the method to the first five or six modes. However, with a spectral shift all such restrictions are removed. Each spectral shift requires a refactoring of the matrix, and hence is relatively expensive; each iteration is relatively cheap. For instance, for a 1140 degree of freedom problem, with a maximum semibandwidth of 630, and an average bandwidth of 90, each spectral shift required 48 seconds, while it took less than 1 second per iteration. Generally, one would like to make a bold shift to minimize the number of matrix factorizations; such a philosophy was adopted in the LMSC REXBAT code, which requires 1 to 2 shifts per eigenvalue. On the other hand, a bold shift can (and does) skip many eigenvalues of interest; hence a more conservative philosophy was adopted in NASTRAN, which may require 3 or 4 shifts per eigenvalue.

The primary deficiency of this technique lies in its inefficient and often inaccurate treatment of clustered roots. Also pathological cases can be constructed for which the inverse iteration procedure will coverge completely – to an invalid result. While one can determine whether all of the eigenvalues below a specified value (a spectral shift) have been computed, it is not possible to tell whether the modes have been accurately determined.

The inverse power iteration method with spectral shifts is a standard part of most large engineering codes.

FIXED-WING ORBITER (FIRST MODE)

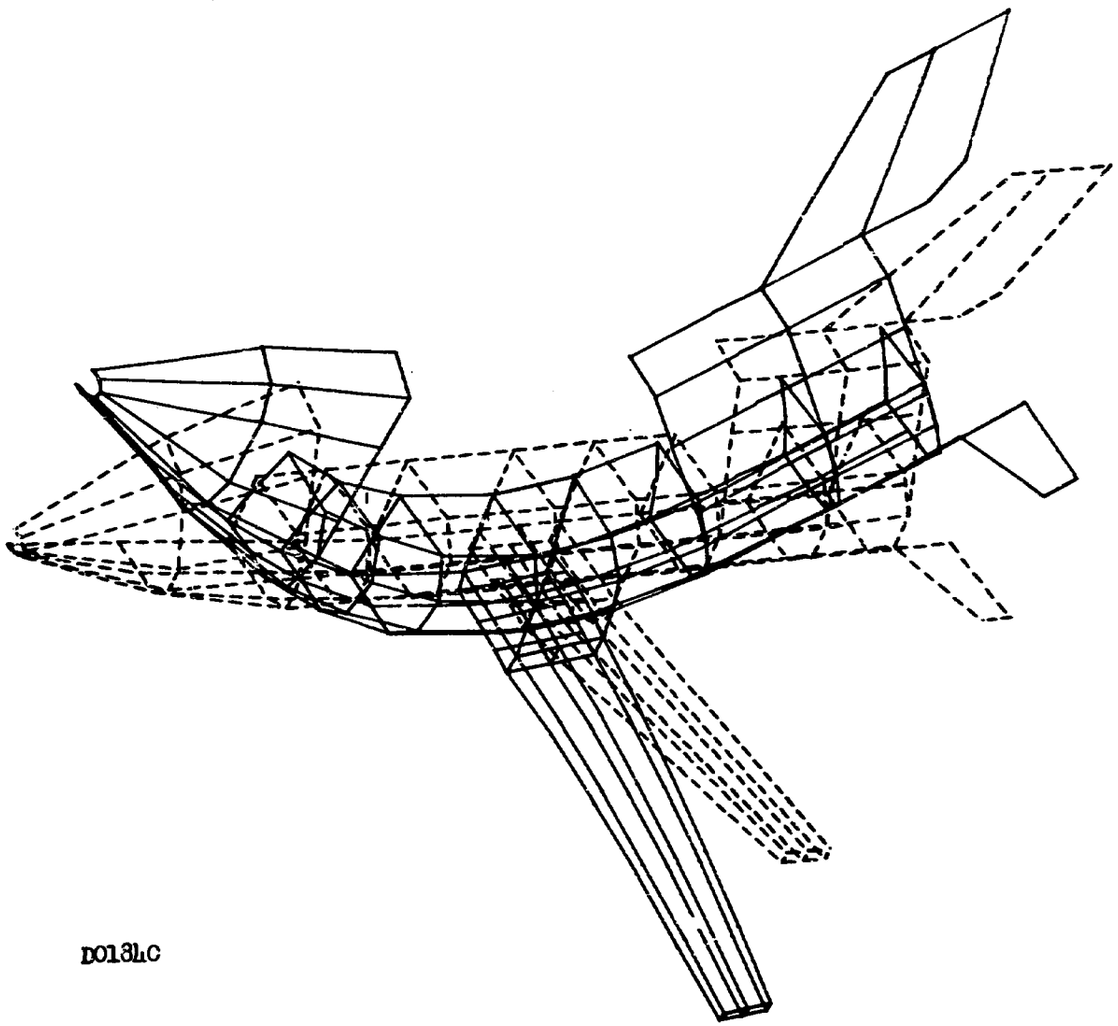

D013LC

ASSUMED FUNCTION

In order to avoid solving large eigenvalue problems, people have turned to alternate techniques. The traditional Rayleigh-Ritz procedure is an excellent tool for this purpose. The difficulty lies in the selection of suitable displacement functions for a complex vehicle. One widely used approach is to use "judiciously chosen" static deformation solutions obtained from a detailed finite element or finite difference model for the structure. Of course, one must take care not to choose functions which are orthogonal to modes of interest; for a complex structure, this may not be a trivial task.

For some purposes, the modes and frequencies obtained from the Rayleigh-Ritz analysis may be regarded as sufficiently accurate for engineering use. However, if these eigenvectors are used as initial estimates to the mode shape for an inverse power iteration, and if the Rayleigh-Ritz eigenvalues are used as spectral shifts, one can obtain excellent results with very few iterations per mode. The advantage of following the Rayleigh-Ritz solution by an inverse power iteration using the original model is that one obtains much more accurate results for the higher modes.

The Stodola approach is quite similar to the procedure just described; the static displacement functions are substituted directly into the iteration process without the benefit of an intermediate Rayleigh-Ritz eigenvalue determination, however. This technique works quite well, and is in engineering use in several firms.

The primary disadvantage of these methods, as with the power iteration method itself, is that one can still miss modes of engineering importance. To minimize this risk one usually takes at least 2n functions when one wants n eigenvalues.

ASSUMED FUNCTION

- RAYLEIGH-RITZ
- FORM SMALL EIGENVALUE PROBLEM
- USE RESULTS AS INITIAL INPUT TO INVERSE ITERATION
- STODOLA APPROACH

MATRIX REDUCTION

A second means to avoid large eigenvalue problems is to reduce the original problem size to one of manageable proportions. The most common procedure is to mathematically reduce the stiffness matrix while maintaining a diagonal (lumped) mass matrix. Conceptually this technique is equivalent to lumping all of the vehicle mass and applied forces at a few grid points in the structural model. All "mass-less" grid points can then be mathematically condensed out of the eigenvalue problem. The resulting eigenvalue problem is then solved using a direct solution (e.g., Choleski-Householder-Givens).

It is also possible to start from a model of the structure in which the mass is distributed at all the grid points, and then reduce both the mass and stiffness matrices simultaneously. This procedure avoids spurious modes which often arise from lumping the system masses at a few points. Although this approach produces a full mass and stiffness matrix, this poses no problem for finding the eigenvalues. However the reduction scheme is iterative and is much more complex and time consuming than when the stiffness matrix is considered alone. Where it has been implemented (e.g., Boeing's ASTRA code), it is apparently seldom used; users prefer the approach in which only the stiffness matrix is mathematically condensed. Evidently the high cost of reducing both mass and stiffness matrices simultaneously is not compensated for by the increased accuracy.

An example of the use of the matrix reduction technique for engineering purposes at Lockheed is provided by the recent analysis, design, fabrication, and test of a large vehicle equivalent in structural complexity to the space shuttle orbiter. The analytical model consisted of 20 substructures, each having 500 to 1000 degrees of freedom. The total 12,000 degree of freedom static model was condensed to a 380 degree of freedom eigenvalue problem, and 30 modes were computed. The complete runtime (including substructure setup, matrix reduction, and eigenvalue determination) was approximately 5 hours on the UNIVAC 1108.

A comparison between analytical and experimental results is shown in the table on the opposite page. The excellent comparison illustrates the power of this technique.

COMPLEX STRUCTURE MODAL ANALYSIS

MODE	FREQUENCY ~ CPS ANALYSIS	TEST	DESCRIPTION
1	2.6	2.6	1ST YAW BENDING
2	2.6	2.6	1ST PITCH BENDING
3	7.4	7.9	FRAME YAW
4	8.7	9.4	2ND YAW BENDING
5	10.8	10.7	2ND PITCH BENDING
6	11.3	11.3	1ST TORSION
7	13.95	13.7	PKG θ_x + − − +
8	14.55	14.7	θ_x + − + −
9	16.7	15.9	θ_x + + − −
10	17.5	17.1	1ST LONG
11	19.31		PKG θ_x + − − −
12	20.4	18.9	PKG X + + − −
13	23.3	↑	PKG X
14	23.6	EXPERIMENTAL DATA AVAILABLE ONLY FOR COMBINED MODES	↓
15	23.6		
16	23.8		
17	24.8	↓	
⋮	⋮	⋮	

NOTE: •12,000 D.O.F. STATIC MODEL CONDENSED TO 380 D.O.F. EIGENVALUE PROBLEM
•COMPLEXITY COMPARABLE TO SPACE SHUTTLE VEHICLES

MATRIX REDUCTION (Cont.)

The chart on the opposite page demonstrates that the matrix reduction procedure can be used to accurately predict mode shapes as well as natural frequencies.

The major advantage of the matrix reduction approach is that one can use a standard, reliable eigenvalue routine to guarantee that all the specified modes have been found.

The disadvantages, however, are numerous:

- Long run times are required to reduce equations (3 hours for reduction alone in the above example).
- Extraneous modes can be generated (modes which are a result of the lumping of the masses at a few points).
- Reconstruction of dynamic forces in the original model is time-consuming and costly.
- Evaluation and interpretation of modes of the reduced system is often difficult.
- Modes of engineering interest can be inadvertently omitted in the reduction process.

This procedure has been implemented in many of the large-scale computer programs (e.g., NASTRAN, STARDYNE, REXBAT, SNAP, ASTRA, etc.).

COMPARISON OF RESULTS FOR COMPLEX STRUCTURE

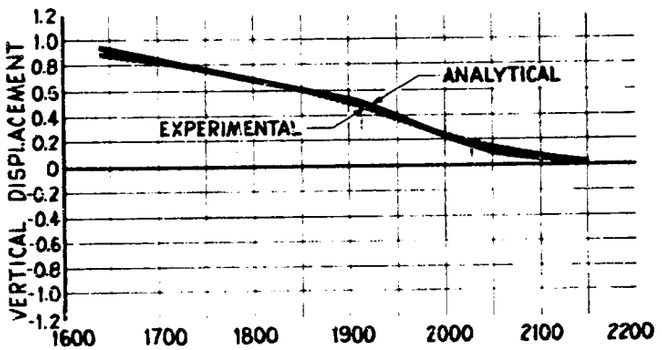

FIRST MODE
$f = 2.6$ cps

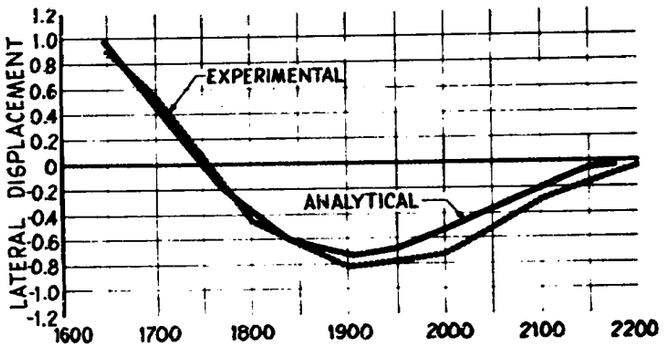

FIFTH MODE
$f = 10.85$ cps

COMPONENT MODES

The component modal method (also known as Hurty's method and the method of substructures) is a very powerful technique for computing the modal behavior of a complex vehicle. One first divides the overall structure into a number of substructures, and computes a set of normal-modes for each substructure. These normal modes are then used as generalized functions to describe the overall structural behavior. Any set of substructure modes (constrained or free) can be used; in fact, a generalization of this technique will allow any complete set of functions to be used for each substructure. Use of quasi-static functions (static deformation of the substructure to unit loads) will greatly improve convergence (especially for stresses), as will a judicious choice of modes to be used.

A major advantage of this approach is that one can utilize results from detailed analyses of subsystems which may have been initiated for other reasons. For instance, modal data from the orbiter and booster can be used to predict the modal behavior of the combined vehicle, as illustrated in the figure. (Note the excellent agreement between the results from the 23 degree of freedom component modal analysis and the 1149 degree of freedom direct analysis.) To illustrate more clearly the detail of the mode shapes predicted by component modal analysis for the shuttle vehicles, a short movie generated by Mr. D. Whetstone (Lockheed – Huntsville) will be shown.

In the examples shown here, the orbiter and booster are connected at only three points. One of the major deficiencies of the component modal method at present is the cumbersome means for handling multipoint elastic boundaries. If the two vehicles were elastically joined at 30 points instead of 3, 180 boundary functions would be needed to describe the interconnection, while only 20 functions are required to describe both vehicles completely.

The component modal method is widely used and many of the large codes have this capability.

COMPONENT MODAL ANALYSIS OF SS VEHICLES

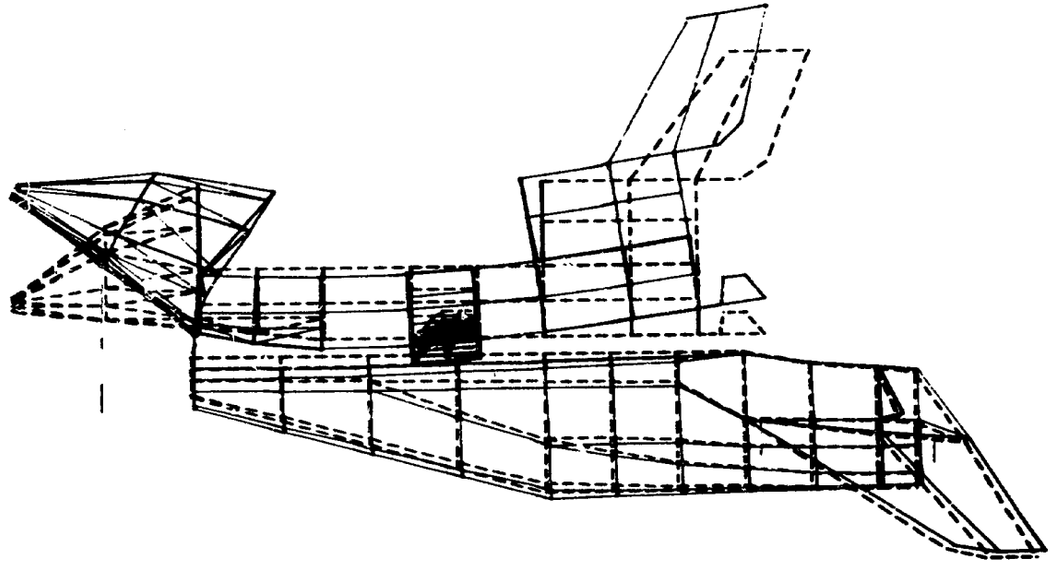

DIRECT FINITE ELEMENT ANALYSIS 1149 VARIABLES	COMPONENT MODES ANALYSIS 10 MODES/COMPONENT 23 VARIABLES
3.137 CPS	3.141 CPS
3.630	3.632
4.355	4.365
4.908	4.916
5.366	5.367

D01844

DETERMINANT SEARCH

For certain types of eigenvalue problems, the only feasible means for finding the eigenvalues is to use the determinant search method, which involves finding zeros of the determinant. As noted in the chart, this method would be used for transcendental problems, to find damped modes, or for control systems problems.

This technique is entirely unsuited for engineering use, except as a last resort. It is very easy to miss roots (in pairs), and one must have considerable insight into the problem being studied in order to select initial estimates and step width for the incrementing process.

Avoid this approach if the problem can be put into a standard form $(A - \lambda I)\, x = 0$.

DETERMINANT SEARCH

- USE FOR TRANCENDENTAL EQUATIONS
- USE FOR COMPLEX EIGENVALUE PROBLEMS
  $(A+\lambda B-\lambda^2 C)\,X=0$
- USE WITH NUMERICAL INTEGRATION OF SPATIAL COORDINATES
- USE ONLY AS A LAST RESORT !

RESEARCH OBJECTIVES

A number of specific research objectives are indicated on the chart on the opposite page. The general objective is to reduce the cost and improve the reliability of methods for finding the eigenvalues of large equation systems. Until the costs of computing eigenvalues are reduced by a factor of 10 or more, it will continue to be prohibitively expensive to make the dynamic parametric studies which should be a vital part of the space shuttle design process.

It would be remiss not to mention several key areas of structural modeling which need immediate attention. The items on the chart are self-explanatory and only two will be expanded upon here. First, the use of a common static and dynamic model of a structure is more of an engineering goal than a research objective. A major part of the expense of any engineering analysis lies in translating blueprint information via engineering judgment into an appropriate mathematical model. It is essential to reduce engineering costs by minimizing these modeling costs. By having compatible models, dynamic stress data can then be directly superimposed on static stress data, further reducing engineering costs and saving calendar time. Second, experimental and analytical analyses of a vehicle must go hand-in-hand. Neither one can do the job alone (e.g., it is very hard to obtain meaningful dynamic loads data from experimentally determined modes; it is very hard to analytically predict the stiffness and damping of manufactured joints). Much work is still required to improve experimental techniques for separating modes in regions of densely spaced eigenvalues.

We have made great strides during the past decade, but much remains to be done if we are to insure a safe and reliable space shuttle design.

RESEARCH OBJECTIVES

EIGENVALUE COMPUTATION

- REDUCE COMPUTATION TIME
- GUARANTEE CALCULATION OF ALL MODES WITHIN SPECIFIED BOUNDS FOR LARGE SYSTEMS
- GENERALIZE COMPONENT MODE BOUNDARY FUNCTIONS FOR MULTIPOINT ELASTIC CONNECTION
- DEVELOP MATRIX PERTURBATION TECHNIQUE

STRUCTURAL MODEL

- USE COMMON STATIC AND DYNAMIC MODEL
- IMPROVE PREDICTION OF PEAK TRANSIENT LOADS
- DEVELOP MODEL OF LIQUID-FILLED SHELL WITH PLANAR SYMMETRY
- DEVELOP SCALING TECHNIQUE FOR THERMAL AND DAMPING EFFECTS
- IMPROVE EXPERIMENTAL TECHNIQUE FOR MODAL TESTING

APPLICATION OF DYNAMIC MODELS

by

H. Wayne Leonard and Homer G. Morgan

NASA-Langley Research Center

SUMMARY

Structural dynamic models have been widely used to obtain vibration data required in launch vehicle development. A generalized model is now being used to obtain lateral response data on space shuttle configurations to account for new factors such as parallel staging, lifting surfaces, and interface stiffness. A second generation generalized model that would have representative longitudinal responses is also believed to be necessary. Finally, a detailed nearly-replica dynamic model of the final space shuttle configuration is proposed as the most cost-effective technique for obtaining timely vibration data to establish confidence in the design. Such a model would be an integral part of the development program, and would be closely coordinated with analysis and limited full-scale vibration tests.

INTRODUCTION

Many kinds of dynamic models have been used to solve special problems in the development of airplanes and spacecraft. This paper is concerned with one particular type of dynamic model - the subscale model for predicting vibration properties and structural dynamic response of a complete vehicle. Slide 1 shows models of this type that have been used in recent launch vehicle development programs. These models of Saturn I, Titan III, and Saturn V have demonstrated their versatility, usefulness, and cost effectiveness for obtaining the modal vibration data that are required to verify analytical methods used in response and stability studies. Each of these models employed different degrees of sophistication in their design and construction, and each was related to the development program in a different way, as discussed in references 1 through 6.

This background of structural dynamic models technology can be utilized in the space shuttle program to develop both new technology and the vehicle itself. However, such models can only be utilized effectively when closely coordinated with analysis. In this paper, a series of structural dynamic models is described which will complement the development of analytical methods for the space shuttle program. The series of models would culminate in a near-replica model that would provide most of the experimental data that have usually been obtained on full-scale test vehicles.

LAUNCH VEHICLE DYNAMIC MODELS

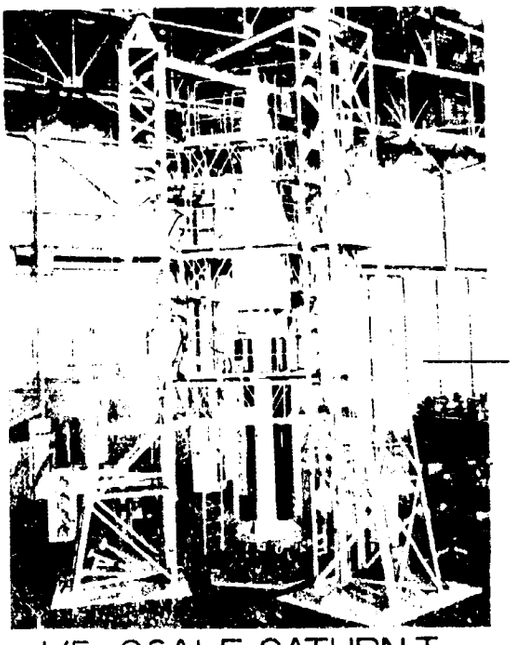

1/5-SCALE SATURN I

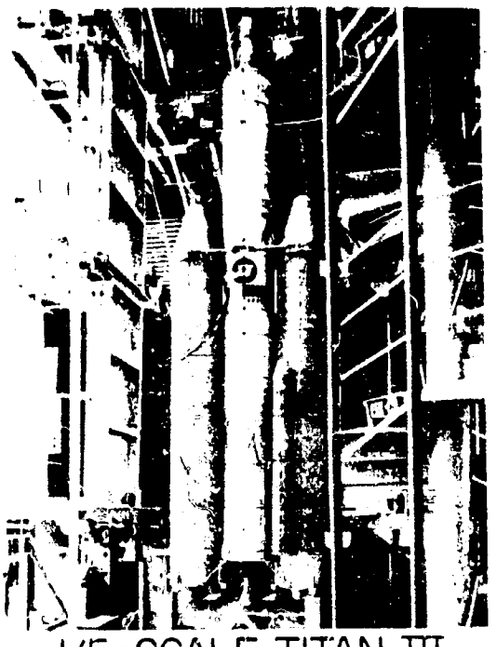

1/5-SCALE TITAN III

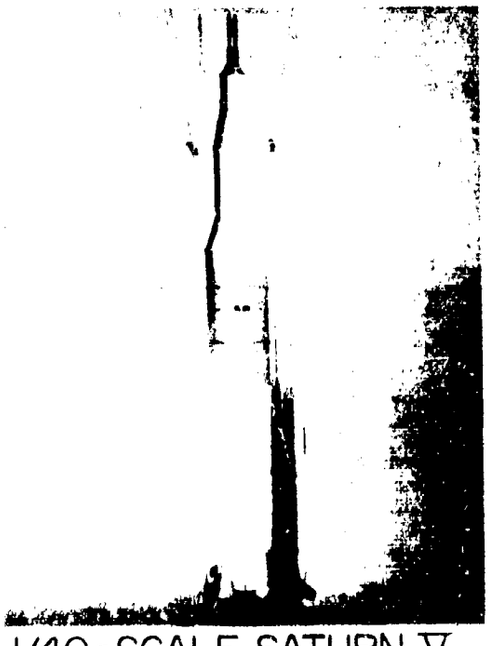

1/40-SCALE SATURN V

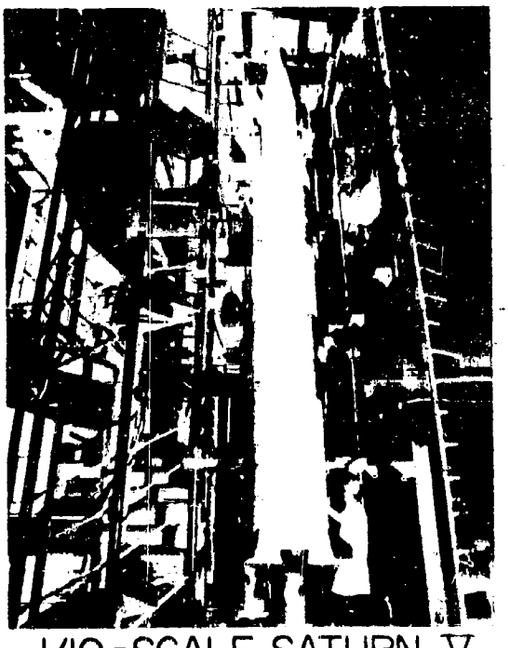

1/10-SCALE SATURN V

FIRST GENERATION MODEL

The complexity of dynamic models in use at a given time must reflect the definition of the space shuttle system at that time. The accompanying analysis will generally be no more complex than the model to which it is applied. At the present time, very few definitive details are known about the final space shuttle configuration. Thus, any model at this time must be a generalized structure for studying classes of problems rather than for generating quantitative data for specific application.

A first generation generalized model has been built, and is shown in Slide 2. Now being prepared for testing at Langley Research Center, it will be used in conjunction with analysis to study the coupled dynamic response of winged parallel-staged bodies. The interface connection spring rate will be varied parametrically over a wide range. The model is approximately 1/15-scale, based on 6-month old mass and stiffness data from a Manned Spacecraft Center 12,500-pound payload vehicle. However, it is generalized in that the orbiter can be mounted forward or aft on the booster, as illustrated here, and both orbiter and booster can have either straight wings (as shown) or delta wings. The model contains no liquids, but propellant mass and inertia are simulated by ballast masses to obtain liftoff, maximum dynamic pressure, and booster burnout weight conditions. Since the parallel bodies are scaled as beams, this model will exhibit representative coupled lateral vibrations of importance in flight loads and control system analyses. However, its longitudinal response will not be representative of an actual vehicle.

/15 SCALE DYNAMIC MODEL

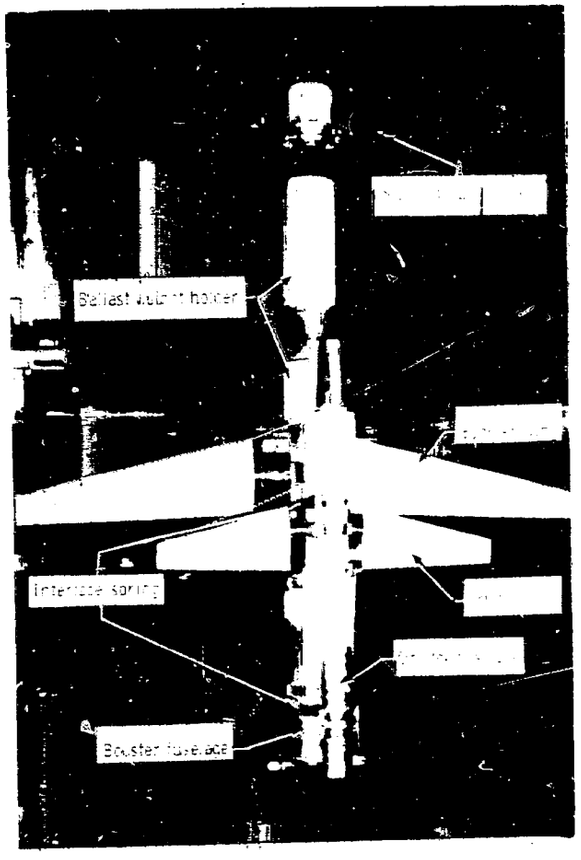

(a) Orbiter aft

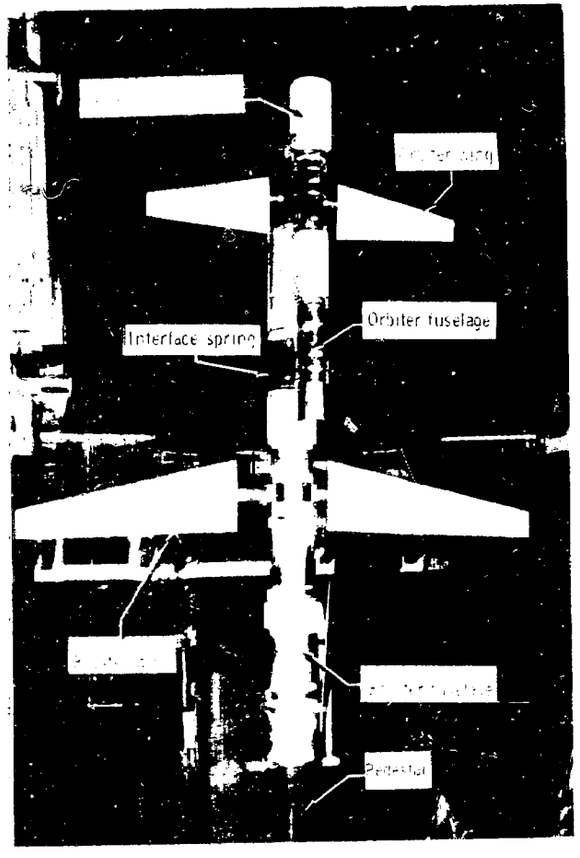

(b) Orbiter forward

SECOND GENERATION MODEL

As the space shuttle configuration becomes better defined, an advanced second generation structural dynamics model, such as shown schematically in Slide 3, will be used to study coupled behavior of a more representative vehicle. Such a model will be of 1/10- to 1/5-scale in size, and can be built very early in Phase C of space shuttle development. Stiffness and mass distributions will be refined, and liquid-carrying tankage will be included to obtain the first meaningful experimental data on coupled longitudinal responses. Thus, early data on the structural part of the Pogo problem for the space shuttle configuration could be obtained. To be useful for this purpose, the model should have representative liquid-shell interactions, propellant feedline characteristics, and thrust structure details. Other configuration features such as the interface connection, lifting surface geometry, and relative position of the orbiter and booster would be incorporated in this model.

ADVANCED DYNAMICS MODEL FOR SPACE SHUTTLE

MASS-STIFFNESS DISTRIBUTION

LONGITUDINAL DYNAMICS

POGO

- LIQUID-SHELL INTERACTIONS
- PROPELLANT-FEEDLINE DYNAMICS
- THRUST STRUCTURE DETAILS

INTERFACE CONNECTION

LIFTING SURFACE GEOMETRY

BOOSTER-ORBITER POSITIONING

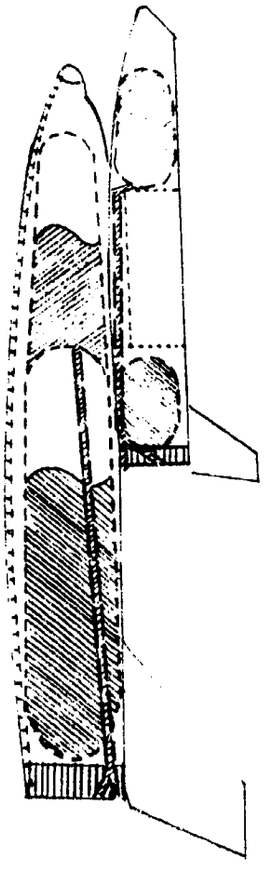

THIRD GENERATION MODEL

First and second generation models will be used essentially to develop structural dynamics technology for space shuttle configurations. However, the primary purpose of the final or third generation model would be to directly support development and testing of the selected vehicle. Design and fabrication of this model should parallel final design, should lead fabrication of the prototype, and could be most efficiently performed by the prototype contractor. It would be a subscale replica of the prototype structure within practical limits. Final scale selection would depend on tradeoffs involving available facilities, ease of construction, testing convenience, and cost, but would probably be in the range of 1/3- to 1/5-scale. Some advancements in modeling technology may be required to properly account for the thermal protective system.

The role of such a model in the development of the space shuttle is illustrated in Slide 4. Model tests, full-scale tests, and flight operations are shown to be unified by a constantly refined analytical model of the vehicle. The time sequence of tests is roughly indicated from left to right. Early test and analysis of the model, sitting airplane-fashion on its wheels, followed by test and analysis of the mated vehicle would lead to a verified analytical model prior to the availability of full-scale hardware. Some full-scale airplane-type ground vibration tests on flight hardware would then be conducted as checks and to develop more confidence in the analysis.

The complexity and importance in dynamic response of the structural interface between the orbiter and the booster will require some limited testing on full-scale hardware to check both the model and analysis.

MODEL APPROACH

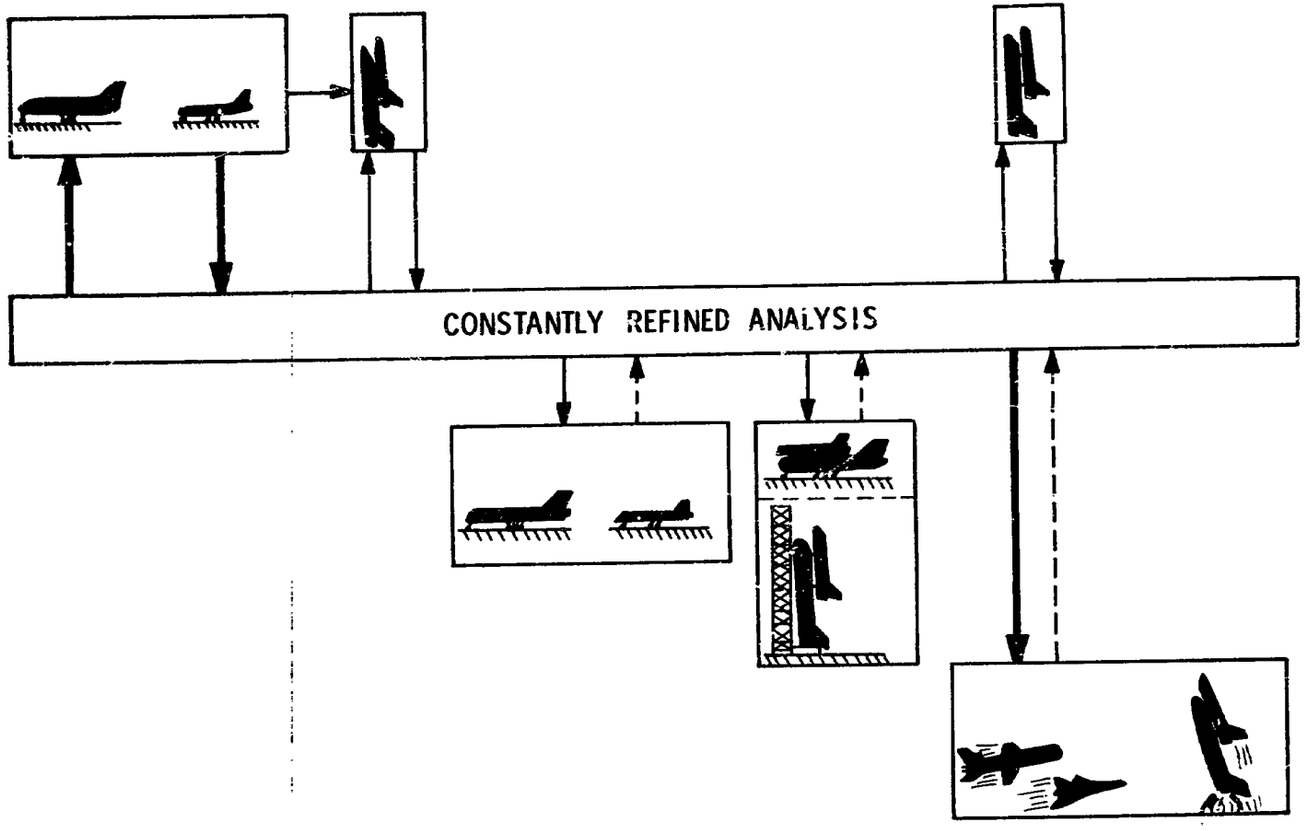

These tests could be static deflection measurements or vibration tests on the mated vehicles. Such tests could be done in the empty weight condition with the vehicle horizontal, if the configuration permits, or cantilevered from the launch tower.

The primary data source for supporting flight operations would be analysis. However, the model, being more inexpensive to maintain on standby than a full-scale dynamic test vehicle, would become the primary tool for evaluation of structural modifications and payload changes, and for investigation of operational problems.

RECOMMENDED DYNAMIC MODEL PROGRAM

Slide 5 presents recommendations for the utilization of a detailed structural dynamic model to achieve the most cost-effective and reliable space shuttle. First, the model must be an integral part of the development program. Then, it must be closely coordinated with analysis and full-scale tests. If these factors are achieved, then only limited full-scale testing is required. Analysis, thoroughly verified by model tests and further checked by some full-scale testing, would provide the final data for all flight decisions. However, since configurations change and maintaining a model on standby is relatively inexpensive, the model should be kept current so that it can be used throughout the program for evaluating configuration or payload changes, and for operational problem solving.

RECOMMENDATIONS

REPLICA MODEL TO BE INTEGRAL PART OF DEVELOPMENT PROGRAM

COORDINATED MODEL--ANALYSIS--FULL-SCALE PROGRAM

LIMITED FULL-SCALE TESTS REQUIRED

VERIFIED ANALYSIS PROVIDES FINAL DATA FOR FLIGHT DECISIONS

MODEL CONFIGURATION KEPT CURRENT AND USED FOR EVALUATION OF CONFIGURATION OR PAYLOAD CHANGES AND FOR OPERATIONAL PROBLEM SOLVING

ALTERNATIVE TO DYNAMIC MODELS

The alternative to an integrated dynamic model program in space shuttle development leads to the situation described in Slide 6. A more extensive full-scale test program would be required. This would probably require a special dynamic test vehicle and a new test facility. An order-of-magnitude increase in manpower is required. Test operations and logistics also become more complex so that the overall cost-effectiveness of this approach is questionable.

A significant factor in this approach is that data generated would be available late in the development cycle. Any changes to design resulting from the tests could only be implemented with considerable delay to the total program.

The scope and complexity of an extensive full-scale test program necessitates detailed long-range planning with a resultant loss of flexibility. The rate of data generation is also slower than in a model program due to the time required to effect configuration or test condition changes.

ALTERNATIVE TO MODEL APPROACH

EXTENSIVE FULL-SCALE TEST PROGRAM REQUIRED

- SPECIAL TEST VEHICLE
- LARGE TEST FACILITY
- INCREASED MANPOWER
- COMPLEX TEST OPERATIONS
- INCREASED COST

LOSS OF TIMELINESS

- DATA AVAILABLE LATE IN PROGRAM
- LESS IMPACT ON DESIGN

LESS FLEXIBILITY IN TEST PROGRAM

- COMPLEXITY OF OPERATION
- NUMBER OF PEOPLE INVOLVED
- DIFFICULTY OF MODIFICATIONS
- LONG LEAD TIME PLANNING

CONCLUDING REMARKS

Structural dynamic models have been successfully applied in previous launch vehicle development programs to obtain vibration data. Models can also be used early in space shuttle development to quickly and inexpensively obtain the data required for verifying analytical methods for treating new configurations.

A detailed structural dynamic model of the final space shuttle vehicle can also be used effectively and inexpensively to provide most of the experimental data for verifying analytical design methods. Only limited testing of full-scale flight hardware would be needed to supplement model data. The alternative to a dynamic model approach, without sacrifice of confidence in the design, is extensive, expensive, and less timely full-scale testing.

REFERENCES

1. Mixson, John S.; and Catherines, John J.: Comparison of Experimental Vibration Characteristics Obtained From a 1/5-Scale Model and From a Full-Scale Saturn SA-1. NASA TN D-2215, 1964

2. Jaszlics, Ivan J.; and Morosow, George: Dynamic Testing of a 20 Percent Scale Model of the Titan III. AIAA Symposium on Structural Dynamics and Aeroelasticity, August-September 1965, pp. 477-485

3. Catherines, John J.; and Stephens, David G.: Effectiveness of External Dampers for Attenuating Launch Vehicle Oscillations. Journal of Spacecraft and Rockets, Vol. 3, No. 12, December 1966, pp. 1798-1799

4. Leadbetter, Sumner A., Coordinator: Application of Analysis and Models to Structural Dynamic Problems Related to the Apollo-Saturn V Launch Vehicle. NASA TN D-5831, 1970

5. Grimes, P. J.; McTigue, L. D.; Riley, G. F.; and Tilden, D. I.: Advancements in Structural Dynamic Technology Resulting From Saturn V Programs. Volume I, NASA CR-1539, 1970

6. Grimes, P. J.; McTigue, L. D.; Riley, G. F.; and Tilden, D. I.: Advancements in Structural Dynamic Technology Resulting From Saturn V Programs. Volume II, NASA CR-1540, 1970

PANEL VIBRATION AND RANDOM LOADS

by William C. Walton, Jr.

and

Eugene C. Naumann

NASA-Langley Research Center
Hampton, Virginia

RESEARCH OBJECTIVES FOR TPS PANELS

We are working to establish procedures to predict basic vibration characteristics and random response of TPS panels. The purpose of this talk is to tell you what we are doing and why. Please consider my remarks as an invitation to constructive criticism on our efforts.

I emphasize that the work on vibration characteristics is general and not restricted to providing inputs to our own random response studies. For example, we are committed to provide structural inputs to support the panel flutter work which will later be discussed by Dr. Dixon of the Structures Research Division.

RESEARCH OBJECTIVES FOR TPS PANELS

CAPABILITY TO PREDICT BASIC VIBRATION CHARACTERISTICS

CAPABILITY TO PREDICT RESPONSE TO FLUCTUATING PRESSURE LOADS

SINGLE PANEL SYSTEM

This slide shows two things. It shows our delineation of the panel vibration problem which is necessarily somewhat arbitrary although, we think, logical. It shows also what we presently see as the possibly significant effects to be considered in characterizing the TPS skin for vibrations. We have decided to concentrate for the time being on what we call a single panel system – defined as a portion of elastic skin bounded by thermal expansion joints and resting on elastic standoff fixtures which in turn rest on a rigid underlying structure. What are our reasons for defining the problem within these particular limits? First, like anyone else, we are motivated by the desire to work with as simple and reasonably sized piece of structure as we can, consistent with retaining essential engineering information. Second, since the purpose of thermal expansion joints is to statically isolate a portion of skin from surrounding skin, it is plausible that such joints will decouple vibrations as well. Thirdly, the TPS skin and standoff fixtures carry only local pressure loads and, therefore, should be relatively light structures. The primary structure which carries integrated loads should generally be relatively stiff making the assumption of a rigid base reasonable. Finally, even if it should turn out that vibrations of the single panel system do couple significantly to surrounding skin or underlying structure, an understanding of the single panel system will still be necessary before the behavior of the coupled system can be intelligently assessed.

Now I will go over all the effects which we believe should be considered. We know we will be dealing with very thin skins – down around .01 inch. This means that random local shape imperfections may be larger than the skin thickness, substantially affecting local stiffness and stresses. This has already caused us problems in attempts to measure vibration modes of very thin flat plates as a subsequent slide will show. Next, we are going to have to deal with skin configurations and support fixtures which have complicated geometries. Typical candidate configurations feature corrugated skins. We have seen proposed standoff fixtures ranging from simple posts to truss arrangements and webs with cutouts. The different types of standoff fixtures attach at variously located points on the skin, sometimes on the edge and sometimes in the interior. Proposed methods for securing skin to standoff fixtures have included fixed attachments, such as spot welds, and sliding attachments, which allow more free thermal expansion. Some designs involve thin walled stiffeners running perpendicular to the corrugations. Major effects, which it will strain our capacities to understand and represent, stem from the fact that these panels will get hot, some perhaps well in excess of 2000°F. We shall have to deal, therefore, with the material changes, such as lowered modulus of elasticity which occur at elevated temperatures and perhaps with permanent material changes caused by thermal cycling. Also, there will be some thermal prestress which would affect vibrations. It is true that every effort will be made to design

SINGLE PANEL SYSTEM

VERY THIN SKIN

COMPLEX GEOMETRY

PRESSURE

HOT

STANDOFF FIXTURE

PRIMARY STRUCTURE ASSUMED RIGID

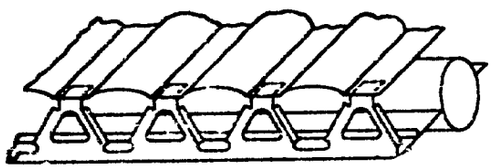

THERMAL EXPANSION JOINTS

SLIDE 2

panels which can expand so as to relieve thermal stress but we cannot assume that such designs will be completely effective. We know these panels will also be affected by the presence of a static pressure differential. It has been proposed to reduce pressure differentials during atmospheric flight by introducing a gas flow in the space between the TPS skin and the primary structure – and in fact some such pressure equalizing system may be necessary in order to allow a TPS skin of sufficiently light weight which can still endure the steady aerodynamic loads in the atmospheric portions of the Shuttle trajectory. However, complete equalization will certainly not be realized and the prestress from the remaining pressure differential could profoundly affect vibration response.

APPROACH FOR BASIC VIBRATION CHARACTERISTICS

This slide states the two main ideas in our approach as presently conceived. As is frequently done, we propose to determine natural vibration modes of the system and pass these modes along as the basic structural description of the panel for any subsequent response analysis. We will measure success in terms of the confidence which can be attached to these modes which we determine. I emphasize that I mean the modes of vibration while the system is in a general prestressed state. Thus, to accomplish our objectives, we require supporting capability to predict static stress due to general thermal and pressure loadings. We have placed a requirement on our output modes which I want to be particularly clear about since this requirement is probably the determining factor as to the level of effort required. We will require for any mode that the modal stress distribution be predicted with good accuracy at all points within a panel. We want to feel that if several modes are responding, the response analyst can add up the individual stress histories and find all points of significant stress. Among other things we hope to provide in this way a more rational basis for fatigue life prediction.

We propose to predict modes by analysis, supporting the analytical results by the best tests feasible. There is really no alternative to ultimately relying on analysis for, in the upper temperature ranges, we will be very limited as to what we can measure. Even for cold panels, analysis is necessary to get the modal stress definition we require.

With regard to structural damping, we recognize that in addition to reliable definition of vibration modes there may be a need for characterization of the energy dissipation processes in a panel. We have a desire and a responsibility to respond in this area, and in our test program, we are providing capability to measure vibration decays as a possible basis for specifying modal damping coefficients. However, we are dissatisfied about damping on a number of counts. The main reason is that for panel flutter and response to random pressure loads – two major concerns – we are not really clear on the role which structural damping plays.

APPROACH FOR BASIC VIBRATION CHARACTERISTICS

STRUCTURAL DESCRIPTION BY VIBRATION MODES

DAMPING DESCRIPTION BY MODAL DAMPING

SLIDE 3

PROJECTS FOR VIBRATION TEST CAPABILITY

This slide lists the projects currently under way to develop needed test capability. As you know, the big problem in testing is instrumentation for the higher temperatures. Our understanding of the capabilities of currently available instrumentation is as follows: (1) There are proximity probes for measuring displacements which should work at temperatures up to 1200°F. (2) There are strain gauges which should work up to 1000°. (3) There are accelerometers which should work throughout temperature ranges of interest for the Shuttle.

LRC has underway an in-house program to develop a traveling probe which will simultaneously sense local vibration amplitude and local temperature. Displacement is measured by a state-of-the-art non-contacting capacitance proximity probe. Temperature is sensed by a state-of-the-art non-contacting thermistor. It is recognized that it is questionable whether very accurate absolute temperature values can be determined with a non-contacting and moving thermistor. However, experience has indicated the shape of the temperature profile can be obtained with reasonable accuracy by this method and such profiles, when supplemented by spot temperature measurements from fixed thermocouples, give a very detailed description of the temperature state.

With regard to strain gauges, there is a substantial effort underway at LRC to perfect strain gauge technology for the temperature range from 1000° to 1500°F. However, we, the authors of this paper, are not at this time in a position to assess the status of this research.

LRC has a contract with TRW to demonstrate feasibility of a holographic system to measure the vibration mode shapes of hot panels. The suitability of continuous laser, strobed-continuous laser, and pulsed-laser systems are being investigated. This work, which will take place over the next thirteen months, is being viewed with great interest because holography appears to offer the best chance for vibration measurements above 1200°.

We have a high priority in-house project nearing operational status to develop and assemble the equipment necessary to excite and measure vibrations of panels at high temperatures and with various boundary supports. This test setup utilizes the dual sensor probe and the state-of-the-art strain gauges, accelerometers, and thermocouples mentioned previously. It is illustrated schematically in the next slide.

PROJECTS FOR VIBRATION TEST CAPABILITY

DISPLACEMENT AND TEMPERATURE PROBE

HIGH TEMPERATURE STRAIN GAUGES

HOLOGRAPH

SHAKE TEST EQUIPMENT FOR HOT PANELS

SLIDE 4

SCHEMATIC REPRESENTATION OF TEST SETUP

Let me emphasize that this representation is schematic and for the purposes of illustration. Some items of equipment, particularly heat shields are not shown. This is a half section view with the cut along the shaded portions. Shown at the top is a quartz tube radiant heater capable of sustaining temperatures at the panel specimen here of up to 1200°F. This frame here represents a hydraulically actuated clamping system which will accommodate panels up to two feet square. The unheated panel is placed in this support system with the clamps not actuated. Heat is applied and the panel brought to steady temperature. Clamps may then be applied along any combination of edges. It is felt that with this system we can simulate conditions for TPS non-ablative panels which will get hot but which according to present thinking will be free to expand. This is a 1-1/2 lb force electrodynamic shaker mounted through soft springs upon a pneumatic lift for positioning. There is a vacuum cup attachment connecting the force rod to the panel and there is a force gauge in the force rod. The vacuum attachment and pneumatic lift allow quick disengagement of the shaker for damping decay measurements. The shaking point can be located anywhere in the middle 75 percent of the panel. This is the dual sensor probe which is servo-controlled to maintain a constant distance of the tip from the mean position of the vibrating panel. This box contains a remotely controlled motor which moves the probe along this track. The track upon which the probe rests in turn moves in the perpendicular direction along this track beneath. The second track rests on a turntable allowing the entire system to be rotated. These movements allow scanning of over 90 percent of the panel surface. Actually there is a second dual sensor probe on a second track not shown. The two moving probes are operated simultaneously for fast scanning. It is believed that it will be possible to make a complete scan in about five minutes. In anticipation of eventual higher temperature requirements the support system, probe tracking systems and shaker system are designed for modal temperatures of 2000°F.

SCHEMATIC REPRESENTATION OF
SETUP

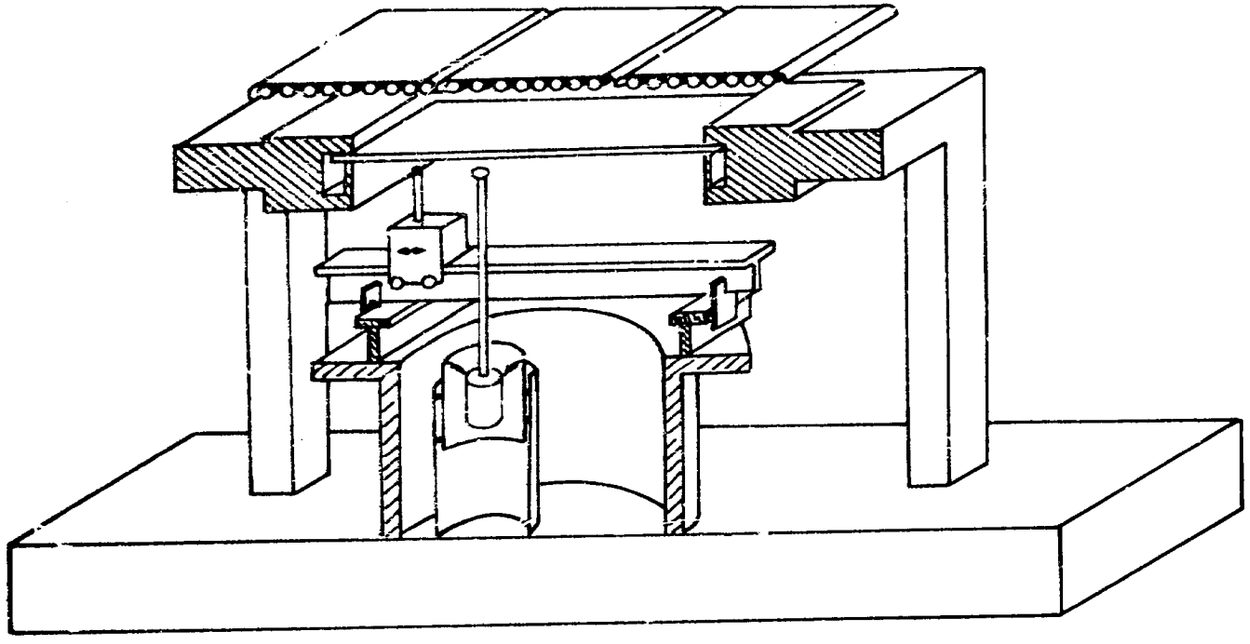

SLIDE 5

NASTRAN ANALYSIS

For the analytical side of the job, we expect to use the NASTRAN computer program – supporting it with other programs if necessary. This slide illustrates an application of NASTRAN which we are attempting in order to ascertain the capabilities of the program to predict vibration modes and give accurate and detailed descriptions of the modal stress distributions. The panel is corrugated and has two channel stiffeners..... Our initial goal is to compute the free-body modes, assuming no prestress. We take advantage of the four quadrants of symmetry so that we only have to deal with a quarter of the panel. We make a very fine subdivision of the panel into elements, from the element library of the NASTRAN program. Note that even the floor of the channel stiffener is subdivided.

With a six-degree-of-freedom mass at each node, the quarter panel system has about 3600 degrees of freedom. Utilizing the capabilities of the NASTRAN program to provide advance estimates of computing time, we have determined that a direct attack on the 3600 × 3600 eigenvalue problem would require from about 10 to 20 hours on our CDC 6600 computer to get the first mode. The time would very probably be closer to 10 hours than to 20. This amount of required time we consider to be prohibitive, but for two reasons we do not consider it discouraging. First, the time reflects the fact that the present version of NASTRAN uses double precision arithmetic. Double precision is probably not necessary on the CDC. Single precision on this machine is almost the equivalent of double precision on most machines. Steps are being taken to provide a single precision version of NASTRAN and this alone should reduce the time by a factor of four or more. Secondly, we feel there is a good chance we can reduce the time substantially by Guyan reduction techniques and we are positive we can reduce it drastically by substructuring. We have a high priority in-house program underway exploring both these avenues.

NASTRAN ANALYSIS

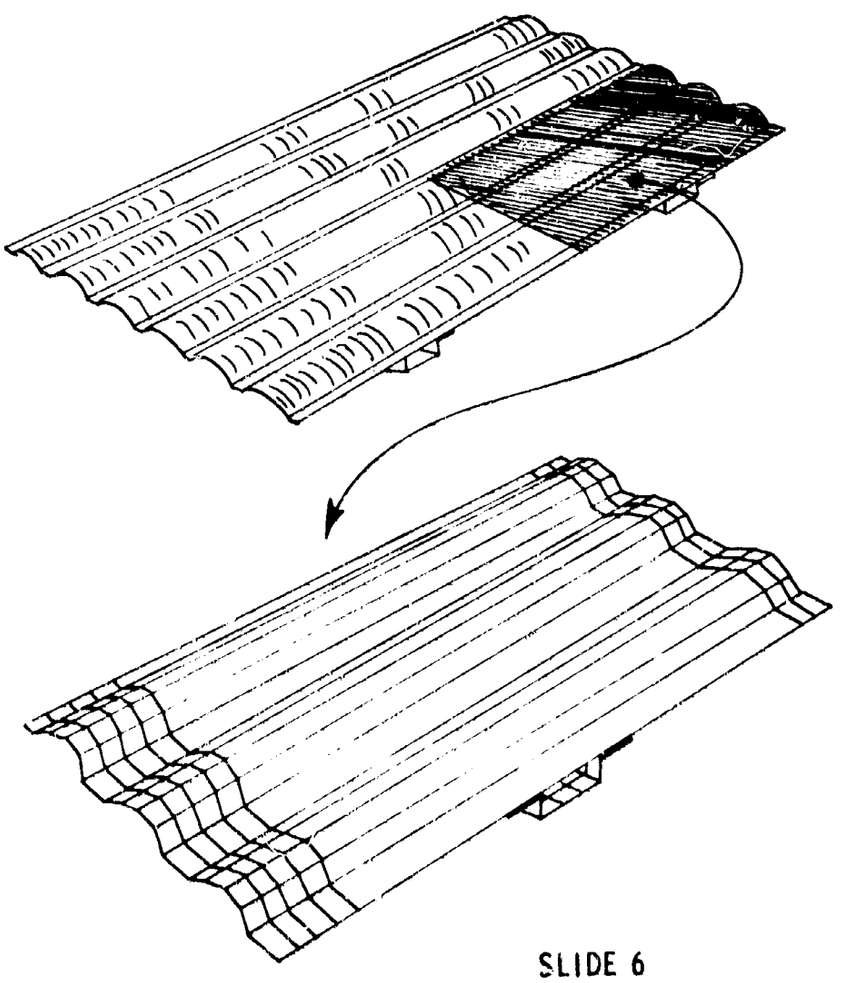

SLIDE 6

RESPONSE TO FLUCTUATING PRESSURE LOADS

I'm going to switch now from basic vibrations to response to fluctuating pressure loads; Charles Coe of Ames is going to speak on the aerodynamic aspects of fluctuating pressure loads. My purpose is to state our needs, as we presently see them, with regard to load description for predicting vibration stress response. I think it is fair to say that engineering techniques for predicting panel response to flight fluctuating pressure loads have been profoundly influenced by the assumption that there is always extremely limited information about the actual load environment and nearly always limited information about the structure. We favor an attempt to break out of this pattern. As I have indicated, at LRC we are laying the groundwork for a structural description of the TPS surface which which should allow prediction of the details of vibration response. It would be most gratifying to see a wind tunnel test program aimed at predicting with comparable detail the fluctuating pressure fields which will occur throughout the flight trajectory. Assuming adequate scaling laws, we think we could make effective use of wind tunnel pressure measurements in which a dense array of pressure gauges is packed within a scaled panel dimension giving details of the distribution of pressure in space as well as time. Utilizing such measured pressures and the computed panel modes, we would compute directly the generalized forces and from them the panel time history of response. From such response time histories corresponding to a number of points in the trajectory, we should be able to count stress cycles and from them make rational estimates of fatigue life.

RESPONSE TO FLUCTUATING PRESSURE LOADS

LIMITED UNDERSTANDING OF TURBULENT FLOWS

MORE SEVERE TURBULENCE

THINNER SKINS

REPEATED FLIGHTS

SLIDE 7

VIBRATION OF A SQUARE CLAMPED PLATE

As indicated in the discussion of a previous slide, we have some data which illustrate the effe[illegible] of shape imperfections on vibrations of square panels. Plotted here are ratios of experimentally and analytically determined natural frequencies for 24-inch by 24-inch flat aluminum alloy plates with several values of plate thickness. The plates were clamped on all four edges. The horizontal axis gives the plate thickness as a multiple of the thickness of the thinnest plate. Here beneath is noted the corresponding approximate ratios of thickness to edge length. The analytical results were obtained using the NASTRAN computer program. Comparisons were made for the first six modes of each plate. The moderate errors for the thickest panel are attributed to observed boundary motions due to the fact that the plate was quite heavy. Neglecting the thickest plate, the agreement passes from very good to unacceptable as the plates are made thinner and thinner. This same trend was observed for free-body vibration tests of the same panels. For each plate measurements were made of the deviations from flatness. The maximum deviations increased from 20 percent of the thickness for the 2nd thickest plate to approximately 2.5 times the thickness for the thinnest plate. It is noted that for the two thinnest plates, which had the largest percentage deviations from flatness, the first mode exhibits the greatest error. This is consistent with the observed long-wave-length character of the imperfections.

VIBRATION OF A SQUARE CLAMPED PLATE

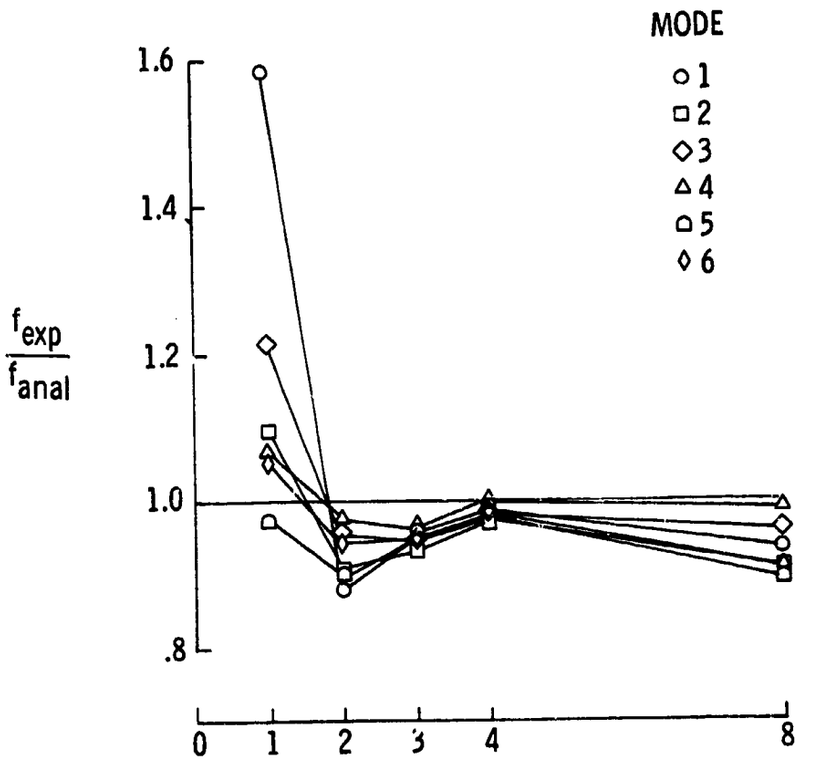

$$\frac{X}{L} = \frac{1}{750} \quad \frac{1}{375} \quad \frac{1}{250} \quad \frac{1}{187} \qquad \frac{1}{90}$$

SLIDE 8

PROPELLANT DYNAMICS PROBLEMS IN SPACE SHUTTLE VEHICLES

H. Norman Abramson, Franklin T. Dodge, and Daniel D. Kana
Southwest Research Institute
San Antonio, Texas

ABSTRACT

The dynamic behavior of liquid propellants in launch vehicles and spacecraft has been of great design importance for past and current generations of vehicles, and will be of equal or even greater importance for future space shuttle vehicles. Large masses of propellants, possibly contained in nonaxisymmetric tanks and subjected to many varying forms and levels of acceleration, may lead to slosh forces of such magnitude as to require extensive baffling or may lead directly to other important dynamic loads by interaction or coupling with the elastic structure. This paper will outline some of these problems and indicate the directions in which preliminary efforts are being made to delineate the problems in more detail or to effect their solution.

INTRODUCTION

Seventy to eighty percent of the lift-off mass of proposed space shuttle vehicles consists of cryogenic liquids; the "orbiter" vehicle itself will carry a larger amount of liquid into orbit than has any previous vehicle. It is therefore evident that the dynamic loads exerted by the contained liquids, which were of much importance in the design of present-generation vehicles, will be even more important in the design of the space shuttle. In fact, the nonsymmetric configuration of most proposed shuttle vehicle structures, the requirement of airplane-like maneuverability, and the stringent requirements imposed on structures and materials by a planned 100 re-use cycle all emphasize the need to understand and design for the influence of liquid

propellant dynamics on shuttle performance. Southwest Research Institute, under contract to NASA-Langley Research Center*, is presently attempting to delineate and evaluate some of these liquid dynamics loads and liquid-structure interactions that may be important in the design of the shuttle vehicle. These problems are discussed briefly in this paper.

We will first review some of the liquid dynamics problems that appear to be of consequence with respect to loads, mention some of the means of controlling those loads, and then discuss some preliminary plans for studying liquid-structure interaction problems peculiar to shuttle vehicles. We will specifically omit discussing pogo phenomena and problems comprising what has come to be known as "propellant management in orbit." Pogo problems applicable to space shuttles have been outlined by Runyan [1] who pointed out that pogo oscillations cannot be tolerated because of the magnitude of the dynamic loads exerted on the vehicles as a result of the large offset masses. Certain pump and feed line phenomena, such as water hammer and bubble collection in the impellers and inducers, are known to couple with pogo instabilities. Propellant management in orbit encompasses such problems as (1) "recapturing" the liquid propellant after an extended period of zero-g coasting and repositioning at least some minimum amount of propellant over the feed line intakes prior to engine restarting, and (2) ensuring that only vapor is released during venting operations meant to relieve excessive buildup of pressure in the tanks

*Contract NAS1-9890.

through boil-off. Needless to say, all these problems must be recognized and accounted for in the design and operation of the shuttle; in some cases, substantial developments in technology will be required.

LOADS ASSOCIATED WITH LIQUID PROPELLANT MOTIONS

In the present part of this paper, we will describe a number of general problems associated with liquid motions, assuming that the structures and tankage containing the liquid are rigid. The arrangement of the discussion follows the general sequence of events during a mission.

Propellant Slosh During Ascent

Although liquid propellant sloshing has been studied extensively in the past [2-5], the nonsymmetric geometry of the space shuttle introduces several new facets to the problem.

First of all, a side-by-side arrangement of the booster and orbiter causes the roll mode of the vehicle and the propellant slosh to be coupled; that is, the slosh can induce roll motions of the vehicle, and vice versa. Thus, large, resonant slosh torques should be expected at several excitation frequencies that depend upon the propellant tank diameters and the thrust acceleration. Large, rigid-body-like torques, because of the offset of the liquid masses from the roll axis, also should be expected. This effect was only of minor importance with respect to the outboard tanks of the Saturn I vehicle and was handled quite readily; however, in the space shuttle, such torques will be very large and difficult to control.

In some designs, the tanks themselves are not symmetric, and an orbiter-tanker probably will have compartmented payload tanks, thus creating further asymmetry. Nonaxisymmetric tanks will have slosh coupling to roll excitation about their own axes in addition to that caused by offsetting the tank from the vehicle roll axis. Consequently, shuttle vehicle propellant sloshing will be susceptable to roll, yaw, and pitch excitations, which is a further complication in booster design over past experience [6]. Equivalent mechanical models (mathematical) of the slosh characteristics, as commonly employed in guidance and control analyses, will be complicated by the fact that several slosh modes (having different resonant frequencies) can be excited, depending upon the orientation of the excitation to the tank. Figure 1 shows a typical slosh model for a tank chosen to fit the structural envelope of the shuttle; this mechanical model contains two "slosh masses" (i.e., two slosh modes are important), a rigidly attached mass m_o which simulates the rigid body inertia of the liquid to lateral excitations, and two mass moment-of-inertias I_o and J_o which simulate the rigid body reactions to pitch, roll, and yaw.

Another problem caused by asymmetrical conditions, and one which can occur even with an axisymmetrical tank and an in-line booster and orbiter, arises during maneuvering whenever the thrust axis is not aligned with the tank axis. For this condition, the steady-state free surface of the liquid is not perpendicular to the tank axis; this, in effect, creates asymmetry and therefore will bring additional slosh modes into being.

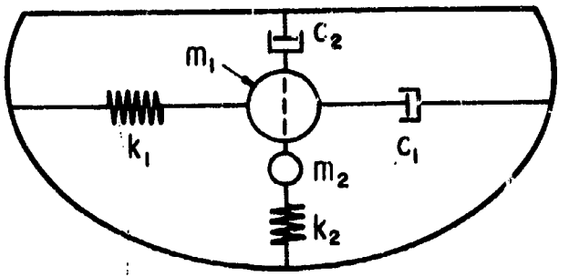

PLAN VIEW

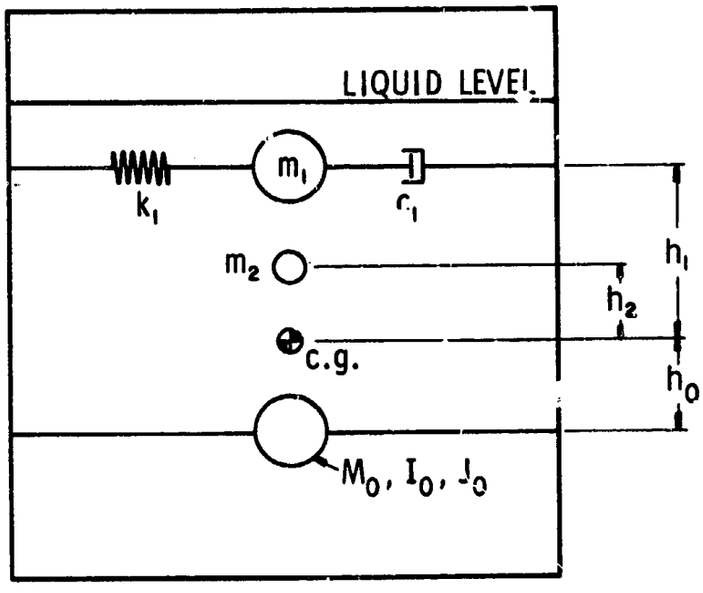

m_1 , m_2 = SLOSH MASSES

$\sqrt{k_1/m_1}$, $\sqrt{k_2/m_2}$ = SLOSH FREQUENCIES

c_1 , c_2 = SLOSH DAMPING

M_0 = RIGID MASS I_0 = PITCH & YAW INERTIA J_0 = ROLL INERTIA

FIGURE 1. EQUIVALENT MECHANICAL MODEL FOR SLOSHING IN SHUTTLE-TYPE TANK

Many of these problems are being investigated at SwRI under sponsorship of NASA-Langley Research Center and NASA-Marshall Space Flight Center*. In addition to analytical studies, slosh force-frequency response characteristics will be measured in the laboratory for several typical non-axisymmetric tank geometries in order to provide information comparable to what has been made available previously for symmetric tank slosh.

Liquid Motions Induced at Separation

Rather large, transverse, impulsive forces will be required to separate the booster and the orbiter in the side-by-side configuration. Assuming that the thrust level for the orbiter is small during and just after separation, transverse impulses will cause gross liquid motions and large disturbing forces and torques at a critical period in the control of the orbiter. It is probable that some of the propellants will impact on tank bulkheads. In any event, significant residual liquid motions will remain when thrusting begins and it important that these not be amplified.

Liquid Behavior in Orbit and During Docking

Besides those propellant management problems mentioned in the Introduction, other fluid motions during orbital operations can cause large loads on the vehicle structure and exert disturbing effects on the guidance and control system. There may be a large mass of liquid onboard at this time, especially when the orbiter is used as a tanker so that it contains liquids other than its own propellants.

*Contract NAS8-25920.

It is likely that the orbiter will "stop" several times, each time docking with some other vehicle. When the payload or propellant tanks are partially empty, the docking deceleration has the potential to move the liquid bodily from one end of a tank to the other, and the impact loads that result might cause "de-latching" (i.e., an aborted docking) or perhaps even damage the tank bulkheads. On the other hand, the impact loads might be used to advantage to eliminate the rocket thrust requirement for completion of a "hard" docking. But the fluid mechanics of docking have so far been almost entirely neglected, especially as regards analysis, and consequently our knowledge of liquid motions during docking is meager.* It is believed that the motions that can occur are similar to those shown in Figure 2. The nonsymmetrical type of motion shown in Figure 2c is the most probable, for free-surface stability reasons, unless extreme care is taken to insure that the docking is aligned perfectly with the tank axes; these nonsymmetric fluid motions obviously impose the largest delatching torques. It is known, also, that a certain minimum deceleration is required to disrupt the steady free surface before the liquid can move bodily. Thus, if the docking deceleration could be maintained below this value then only small disturbances would occur; unfortunately, the destabilizing acceleration is very small. For example, the acceleration that will destabilize a zero-g interface with a zero degree contact angle in a cylindrical tank is

*A study of this problem is being sponsored by NASA-MSFC (Contract NAS8-25712).

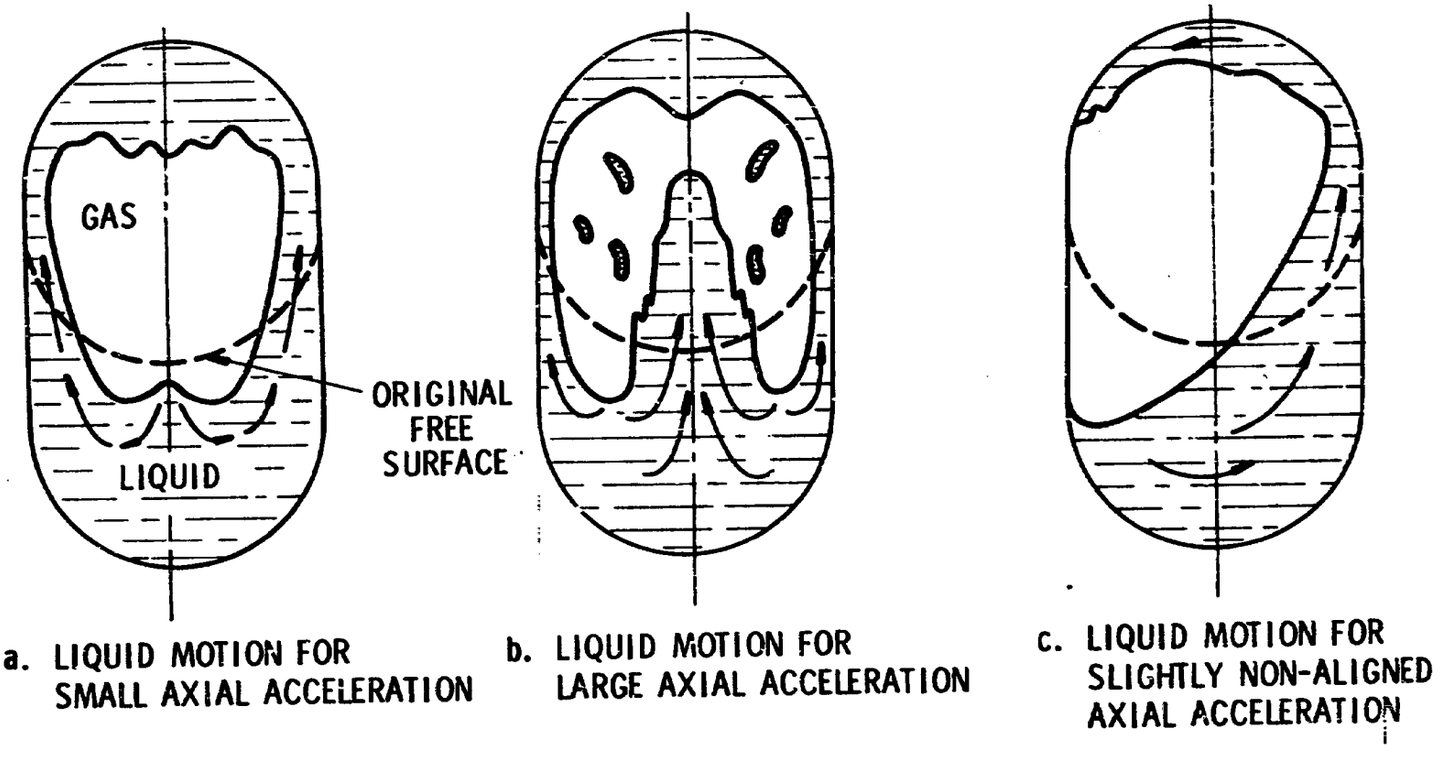

FIGURE 2. TYPICAL LIQUID MOTIONS DURING DOCKING

$0.84\sigma/\rho r_o^2$ (σ = surface tension, ρ = density, r_o = tank radius) which, for a lox tank of say 250 cm diameter, is less than 10^{-3} cm/sec^2.

During the periods when an orbiter-tanker is thrusting and in the process of changing orbits and speeds, both the propellants and the payload can slosh, similarly as experienced during the vehicle boost phase, and thereby impose significant disturbing forces and torques on the orbiter.

Flyback of Orbiter or Booster

During the normal "flyback" of an orbiter or booster, residual propellants in the amount of five to ten percent of capacity may remain in the tanks even after venting. Although this a relatively small mass, it can cause large disturbances because of the way in which the liquids are oriented during both the high angle-of-attack return and maneuvering just prior to landing. In both cases, the effective gravity is directed more or less perpendicularly to the sides of the tanks rather than along the tank axis, and hence the liquids, during flyback, are contained in what are effectively long, shallow tanks, as shown in Figure 3. Tests have shown that liquids in partially filled, long shallow tanks are very susceptible to small excitations and response in violent, large amplitude nonlinear motions [7]. The response can take the form of normal sloshing but, more commonly, traveling waves occur which reflect back and forth along the tank, impacting on the bulkheads each time; these possible reponses are shown in Figure 4. Such liquid responses can impose severe disturbances on vehicle guidance and control.

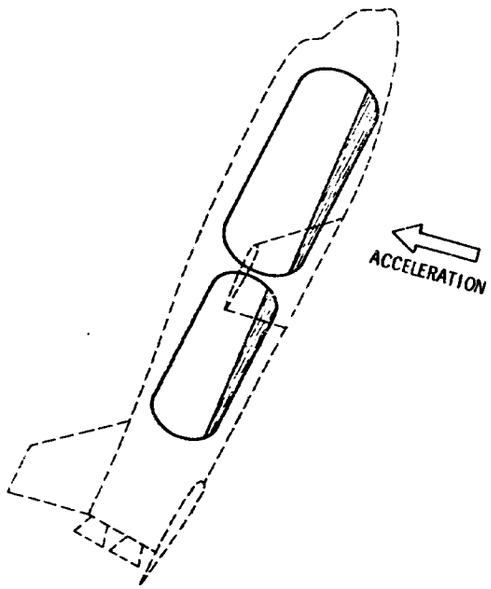

FIGURE 3. RESIDUAL PROPELLANT LOCATION DURING HIGH ANGLE-OF-ATTACK FLYBACK

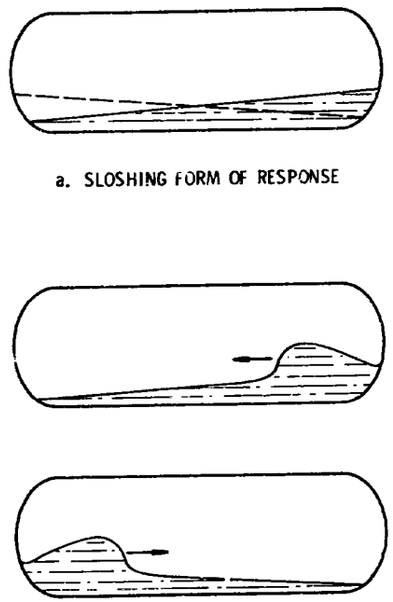

a. SLOSHING FORM OF RESPONSE

b. TRAVELING WAVE RESPONSE

FIGURE 4. POSSIBLE LIQUID MOTIONS IN LONG, SHALLOW TANKS

In some designs, water impact landing is contemplated. Large loadings on the tank structure due to the gross motions of the rapidly decelerated propellants will occur during such landings, and may be of equal importance in the event of any "hard" landing.

Aborted Flybacks

If a mission is aborted, it is likely that at least a brief period of maneuvering and airplane-like flying will be necessary before the propellant tanks can be dumped or vented. Because of the large mass of liquid still onboard during this period, various propellant motions could be extremely deleterious to vehicle stability.

If the main engines are shut down while the vehicle is flying through the sensible atmosphere, the liquids may impact on the upper bulkheads of the tanks because of the sudden deceleration resulting from air drag. This "dome impact" can rupture the bulkheads, and a fireball may result if hypergolic propellants are employed [8, 9].

During the flying phase of abort, the large shifts in liquid cg and the fluctuating forces and torques caused by propellant motions such as shown in Figures 3 and 4 would be difficult to compensate for by the pilots. Obviously, then, the possible propellant motions occurring during an aborted flyback need to be carefully investigated, and preventive measures provided for in the design of the space shuttle.

CONTROL OF LIQUID PROPELLANT MOTIONS

Because of the 100 re-use cycle requirement, the flyback capability, and the need to maximize the payload, the space shuttle is a weight-critical

vehicle. Therefore, the devices used to control or dampen the propellant motions must be kept as light as possible. Flexible baffles, which effectively control sloshing and other forms of motion, are attractive in this respect.

Although they have been shown to be feasible in tests with model tanks and conventional liquids [10-12], flexible baffles need to be investigated with regard to (1) fatigue life, (2) compatibility with cryogenic liquids, (3) fastening techniques, (4) manufacturing techniques, and (5) in-place cleaning. SwRI, under contract to NASA-Langley Research Center*, is conducting such an engineering design analysis for space shuttle applications, which will attempt to answer these questions. This study is oriented toward eventually conducting a large-scale, proof-of-concept test program.

Other specific measures to control liquid motions will undoubtedly rely upon adaptations of baffle and deflector configurations successfully employed in present vehicles [5]. Tank compartmentation may be particularly effective in shifting liquid frequencies and in reducing the magnitudes of sloshing masses.

INTERACTION OF LIQUID PROPELLANTS WITH ELASTIC STRUCTURE

Experience to date has indicated that the overall dynamic response of essentially axisymmetric launch vehicle structures can be separated into basically (1) longitudinal accordion-like motions (pogo) and (2) lateral bending motions. Both kinds of response are highly influenced by the presence

*Contract NAS1-10074.

of liquid propellants in the system; however, because of symmetry, these responses have, in the past, been essentially decoupled from one another (except for possible localized motions). On the other hand, the radically different and nonaxisymmetric designs for shuttle vehicles will no longer permit this simplification. Therefore, studies have already been initiated with the objective of making a relatively simplified parametric analysis of coupling between lateral and longitudinal structural motions for a typical shuttle design and, further, to determine the influence of the liquid propellant dynamics on the coupled response.

One study is being performed in-house at NASA-Langley Research Center and is described in detail elsewhere. Its objective, however, is to investigate the effects of joint stiffness between the booster and orbiter vehicles on the coupled vehicle vibration response, emphasizing rigid body and lateral bending modes and considering only solid mass representations of the contained propellants.

Complementary efforts are in progress at SwRI* to determine the influence of the liquid propellants on the coupled system of elastic shells. For this latter study, a sketch of the design of a simplified shuttle vehicle model is shown in Figure 5 and the model booster is shown in Figure 6. The two-tank booster is joined to a smaller two-tank orbiter by means of a common spar, and intermediate skirts and various rigid masses are utilized to simulate various components. This arrangement is an extension of some

*Contract NAS1-9890.

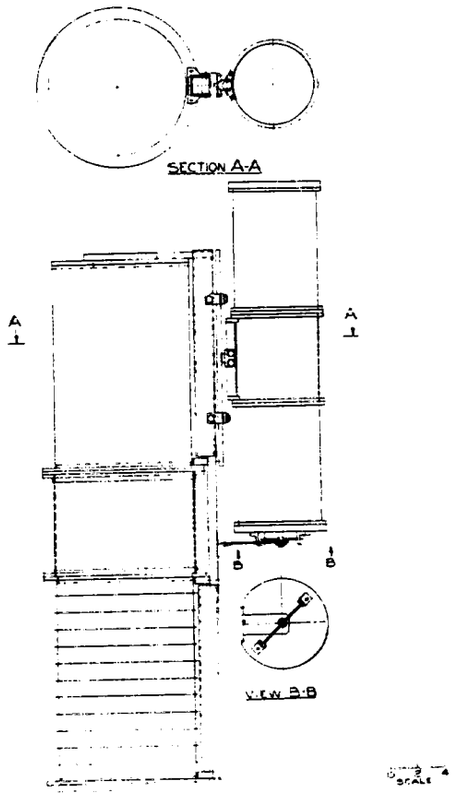

FIGURE 5. SIMULATED SHUTTLE VEHICLE MODEL

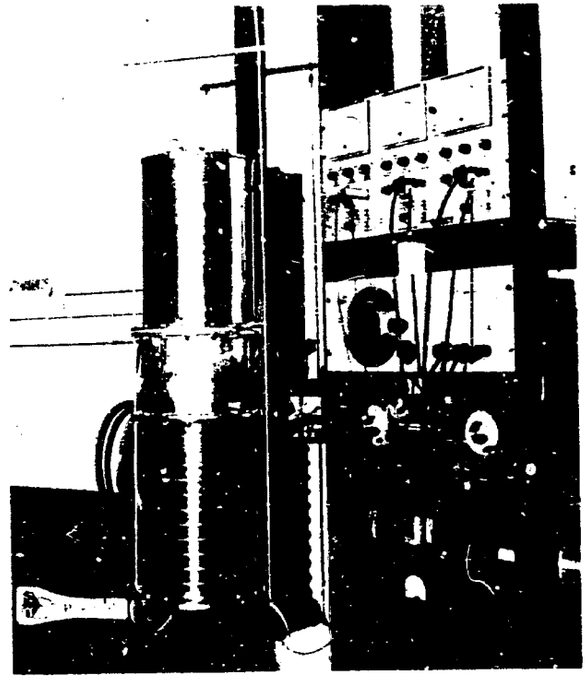

FIGURE 6. SIMULATED SHUTTLE VEHICLE BOOSTER

recent research on purely axisymmetric longitudinal dynamics of a simplified launch vehicle dynamic model sponsored by NASA-Marshall Space Flight Center [13]. Since the principal objective of this study is to determine the influence of liquid propellants on coupled longitudinal-lateral bending modes, natural frequencies will be measured on the model suspended in a simulated free-free condition (Fig. 6) for a variety of parameters such as propellant depths, ullage pressures, and orbiter attachment spring rates and position. Initial tests will be conducted with the tanks containing a simulated frozen liquid (using materials such as a mixture of sand and flour, or plastic beads); subsequent tests will be performed with liquids having the same density. Forced responses will also be determined by excitation at various simulated gimbal angles, required by the antisymmetric design. The gimbal angle changes with the varying lateral position of the center of gravity as a result of propellant depletion during the boost phase. Also, both longitudinal and lateral components are required. It is anticipated that two preferential axes of motion will exist; one in the plane of, and the other normal to the plane of the drawing in Figure 5. A comparison of results using both simulated frozen and free liquids will permit an overall determination of the significance of the liquid coupling as well as provide some perspective regarding the increased complexity which will be required for pogo analyses of shuttle vehicle designs. To aid in these analyses, a complementary analytical model is also being developed consisting of a series of linear and torsional springs, flexible beams, and rigid masses. Each mass is to be capable of two degrees of translational and one degree of rotational motion,

except for those representing the lateral sloshing and longitudinal liquid contributions. Mechanical models for lateral sloshing are those previously given in [2], while those for longitudinal liquid motion were recently given in [14]. Initial plans are to study motion in the plane of the model only.

CONCLUDING REMARK

We have pointed out in the foregoing discussion some of the areas in which developmental efforts are required in order to insure that problems of propellant dynamics in shuttle vehicles can be satisfactorily analyzed and solved. Many of these are already being studied, either to delineate them in more detail or to effect their solution. Some of the more significant problems include: (1) propellant slosh characteristics in nonsymmetric tank configurations; (2) propellant impact on tank bulkheads, either at high-g as a consequence of abort, hard landing, etc., or at low-g as a consequence of docking, maneuvering, etc.; (3) flexible baffle technology; and (4) influence of propellant dynamics on elastic shell and vehicle vibrations. The coupling of the latter with other elements of the system, thereby leading to overall vehicle instability (pogo), is of primary importance in shuttle vehicle design.

REFERENCES

1. Runyan, H. L., and Morgan, H. G., "Structural Dynamic Problems of the Space Shuttle," Paper presented at the AIAA/ASME 11th Structures, Structural Dynamics, and Materials Conference, Denver, April 23, 1970.

2. Abramson, H. N., Ed., The Dynamic Behavior of Liquids in Moving Containers, NASA SP-106 (1966).

3. Abramson, H. N., "Some Current Aspects of the Dynamic Behavior of Liquids in Rocket Propellant Tanks," Applied Mechanics Surveys, Spartan Books, Washington, D. C., pp 941-949 (1966).

4. Anon., "Propellant Slosh Loads," NASA Space Vehicle Design Criteria (Structures), NASA SP-8009, August 1968.

5. Anon., "Slosh Suppression," NASA Space Vehicle Design Criteria (Structures), NASA SP-8031, May 1969.

6. Stephens, D. G., and Leonard, H. W., "The Coupled Dynamic Response of a Tank Partially Filled with a Liquid and Undergoing Free and Forced Planar Oscillations," NASA TN D-1945 (1963).

7. Chu, W. H., Dalzell, J. F., and Modisette, J. E., "Theoretical and Experimental Study of Ship-Roll Stabilization Tanks," J. Ship Research, 12, pp 165-180, September 1968.

8. Epperson, T. B., Brown, R. B., and Abramson, H. N., "Dynamic Loads Resulting from Fuel Motion in Missile Tanks," Proc. 4th Symposium on Ballistic Missile and Space Technology, Vol II, Pergamon Press, New York, pp 313-327 (1961).

9. Stephens, D. G., "Experimental Investigations of Liquid Impact in a Model Propellant Tank," NASA TN D-2913 (1965).

10. Schwind, R., Scotti, R., and Skogh, J., "Analysis of Flexible Baffles for Damping Tank Sloshing," J. Spacecraft and Rockets, 4, pp 47-53, January 1967.

11. Garza, L. R., and Dodge, F. T., "A Comparison of Flexible and Rigid Baffles for Slosh Suppression," J. Spacecraft and Rockets, 4, pp 805-806, June 1967.

12. Stephens, D. G., and Scholl, H. F., "Effectiveness of Flexible and Rigid Ring Baffles for Damping Liquid Oscillations in Large-Scale Cylindrical Tanks," NASA TN D-3878 (1967).

13. Kana, D. D., and Nagy, A., "An Experimental Determination of the Longitudinal Modes of a Simulated Launch Vehicle Dynamic Model," Interim Report, Contract NAS8-30167, Southwest Research Institute, March 1970.

14. Glaser, R. F., "Longitudinal Mass-Spring Modeling of Launch Vehicles," NASA TN D-5371, August 1969.

TRANSIENT LOADING CONSIDERATIONS FOR SHUTTLE DESIGN

E. F. Baird

Grumman Aircraft

Introduction

This paper will review some of the transient-response problems of the space shuttle vehicle, and also introduce a combined test and analytic technique that could be a valuable supplement to the standard methods for calculating transient response. The technique relies on using experimentally determined impulse transfer functions to predict structural responses to longer-duration inputs. Before going into this technique, the transient loadings the shuttle will encounter from liftoff to landing will be summarized.

Fig. 1 lists the more important transient loadings due to launch, separation, docking, and landing. Since other papers will discuss some of these conditions in detail, such as launch and separation, comments on these items will be limited. Pyrotechnics have been omitted since these will probably not be important to overall structural response.

SHUTTLE TRANSIENT LOADINGS

- LAUNCH
  - ENGINE IGNITION & SHUTDOWN
  - RELEASE CHARACTERISTICS
  - WIND LOADS
- NORMAL & ABORT SEPARATION
- DOCKING & UNDOCKING, PAYLOAD HANDLING
- LANDING

Fig. 2 lists recommendations for limiting transient response during ignition and release at liftoff. Reference 1 will cover this subject in some detail, so only some of the more important considerations will be mentioned. These include flexibility of the launch pad structure, including the operation of the release mechanism, control system interactions, and lateral excitation due to wind effects and thrust build-up differences among the various engines.

Since these are principally ground conditions, it has been suggested that research in this area be directed primarily toward the design of ground-load alleviation devices. These studies, including dynamic-model and wind-tunnel tests, should focus on such items as shielding systems to protect against wind loads, and holddown and release systems which would limit the response of the vehicle elastic modes during engine start and at liftoff.

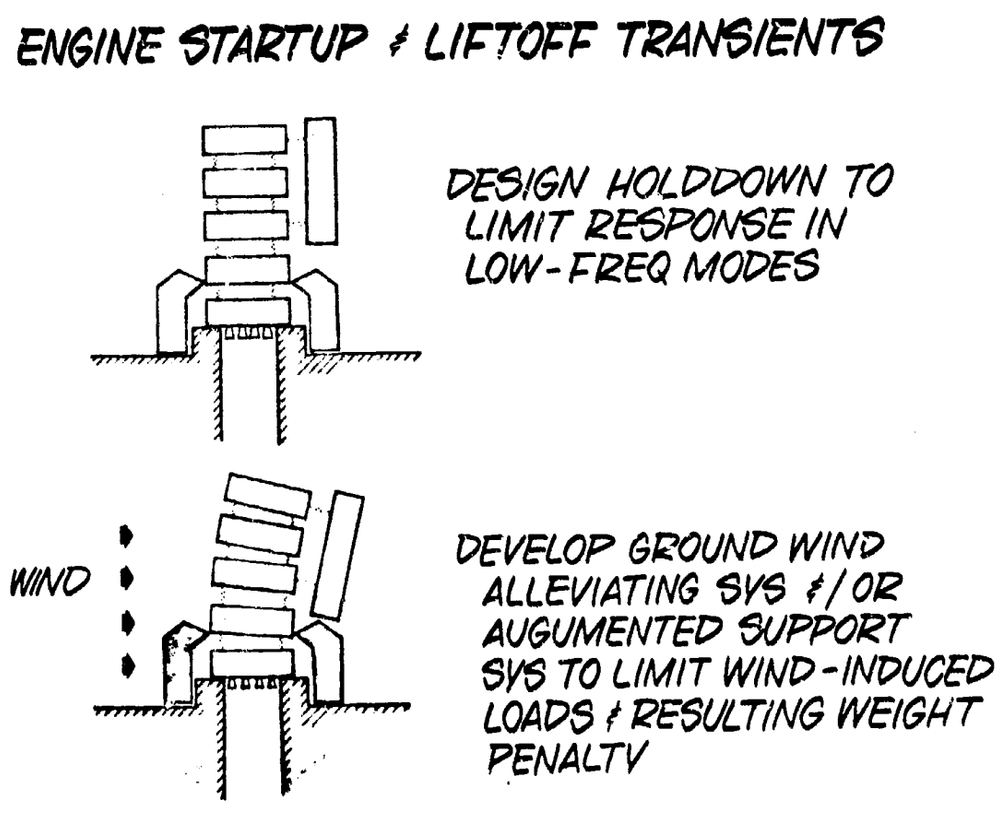

Booster engine shutdown transients should be mentioned briefly. On the Apollo Saturn V, the largest lateral accelerations on the LM during the launch phase occur after engine shutdown as a result of the longitudinal-lateral coupling (X-Z) between booster and spacecraft.

In the shuttle, the relatively large eg offset between booster and orbiter is expected to result in fundamental modes which exhibit considerable coupling. A relatively refined elastic analysis and model program is, therefore, recommended to evaluate this transient condition. The large sizes of the matrices required can make this analysis expensive, so improved matrix reduction techniques will become highly desirable. In addition, analytical and experimental studies should be performed to determine an optimum interstage arrangement and stiffness to minimize the adverse transient loads due to X-Z coupling.

LM-3 (APOLLO 9) ASCENT STAGE RESPONSE DURING 1ST STAGE OUTBOARD ENGINE CUTOFF

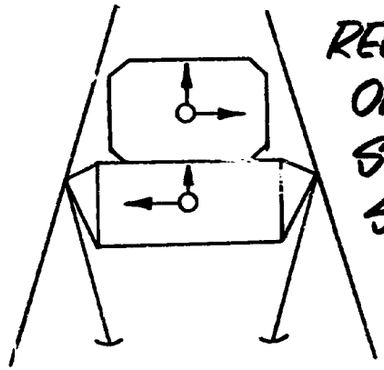

REL RESPONSE ON ASC & DESC STAGES AT 5.5 HZ

The next problem to be reviewed, separating the orbiter and booster, is one of the most critical in the shuttle mission.

One concept for accomplishing separation is shown in Fig. 4. The prime objectives of the scheme are to provide reliable operation for both normal and abort situations; to avoid, where possible, the harmful plume impingement of the rocket exhaust of one vehicle on the other; and to give positive assurance of no recontact of the vehicles under widely varying aerodynamic conditions.

The dynamics of separation involve a number of complex problems: transients due to mechanism operation, engine shutdown and startup, and aerodynamic interactions of the two vehicles in proximity to each other. A combination of wind-tunnel testing and analytic backup is recommended to gain a fundamental understanding of the aerodynamic problems. Reference 2 will cover this topic in more detail.

SEPARATION DYNAMICS

NORMAL - PARALLEL MOTION

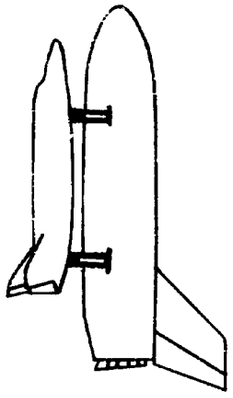

MATED

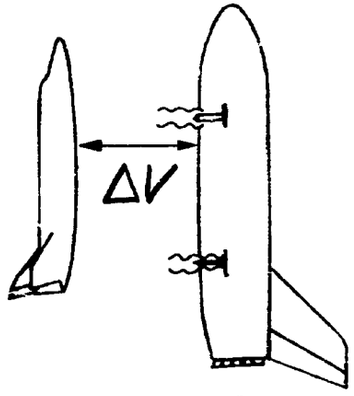

RELEASED

ABORT - ROTATE BEFORE RELEASE, OBTAIN AERO ASSIST

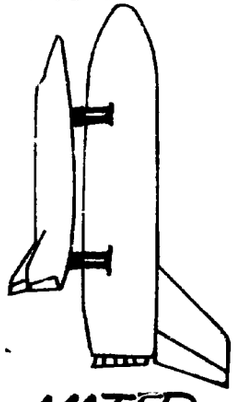

MATED

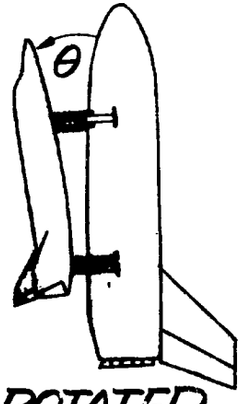

ROTATED

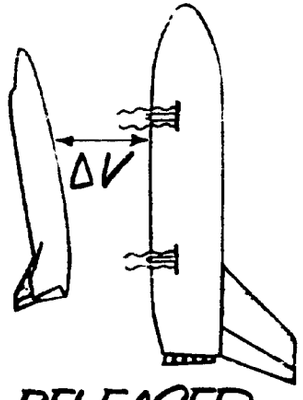

RELEASED

Another problem in the shuttle mission is docking, as shown in Fig. 5. While docking-impact loads will probably not design major portions of the orbiter structure, they will be important in developing docking mechanism hardware and designing local structure, and will influence payload handling and orbiter control system design. Propellant behavior, as affected by docking loads, is another important consideration that will require study.

Two basic schemes for docking the orbiter to a space station are shown, together with some of the advantages of each.

There are many other schemes for docking and payload deployment that range from using the payload structure as the docking interface to designing for free-flying payload modules. Tradeoff studies involving the interaction of control-system dynamics, docking impact, and post-latching loads must be performed to establish a practical system. Manned simulations of the approach phase of docking should be considered, as well as model testing again backed by an analytic program.

DOCKING DYNAMICS

NOSE DOCK

- GOOD VISIBILITY
- MIN CG OFFSET

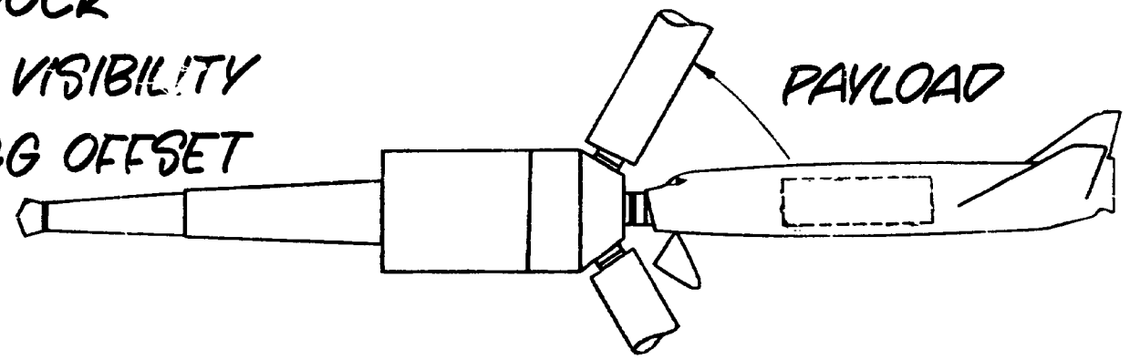

TOP DOCK

- PAYLOAD CLOSE TO STATION
- NO FOLDING NOSE

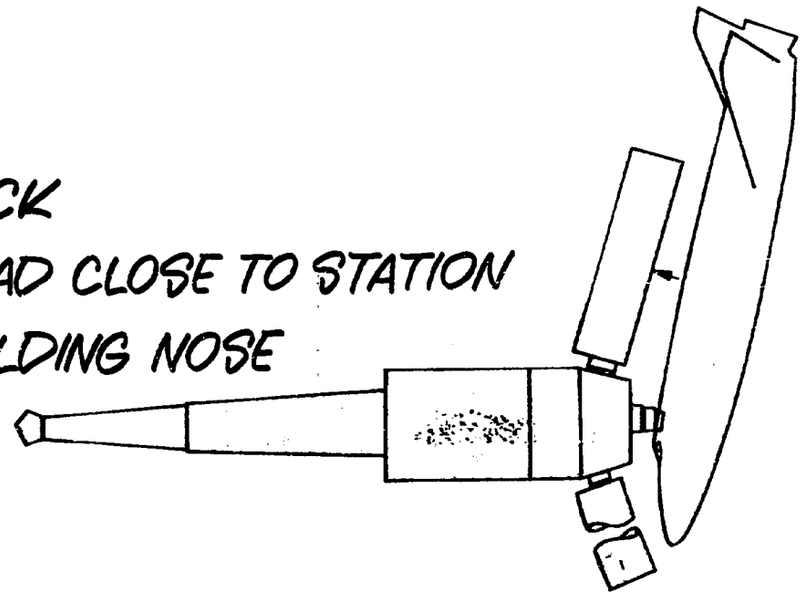

87

87

The final step in the shuttle mission is landing. In the early stages, shuttle gear design will probably follow transport-aircraft practices. Studies of the weight penalties associated with landing gear design criteria, as illustrated in Fig. 6, should be performed to learn where significant savings can be made. The sensitivity of strut weight to sink speed is shown here. Since the landing gear itself is of sizable weight and since landing imposes design-level loads on local structure and is of importance to overall vehicle response, advanced landing systems should be investigated. These should range from replacing wheels with brushes or skids to studies of air-cushion-type landing schemes.

ORBITER LANDING GEAR CONSIDERATIONS

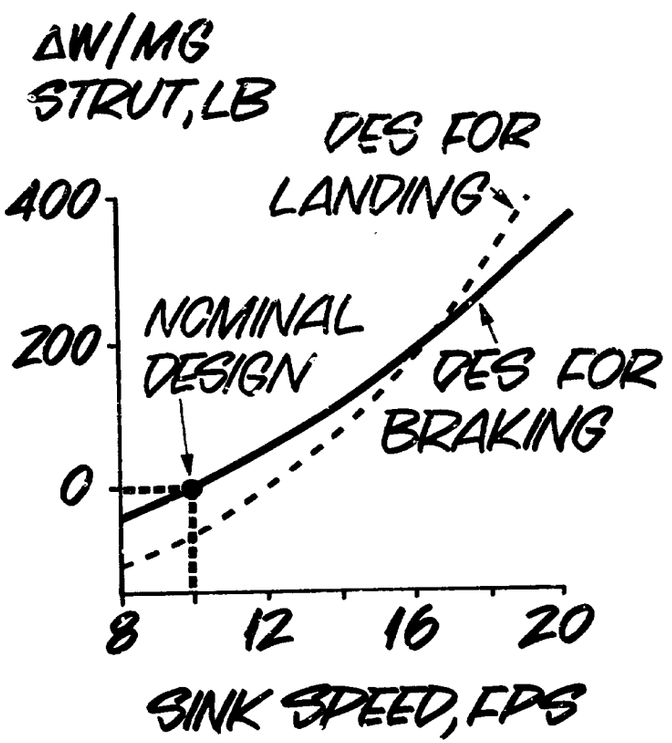

BASIC DESIGN DATA

- LDG LOAD FACTOR = 1.4
- SPINUP MAG FACTOR = 1.3
- SPINUP μ = 0.55
- BRAKING DGW = 1.2 LDGW
- BRAKING μ = 0.8

In addition to analyses, conventional aerospace practice makes extensive use of testing. This would include mode surveys, vibration testing, and dynamic simulations. Modal information obtained from test is still difficult to use to predict internal load distributions, stress levels, or component accelerations. Dynamic simulations may verify the integrity of the structure, but may not yield basic information which can be applied to conditions that were not tested or which arise after the testing is completed. To overcome these limitations, Grumman has been developing, under MSC sponsorship, a combined analytical and testing technique that is called "impulse testing." This is expected to become a valuable supplement to the standard tests and analyses planned for the shuttle.

The technique is based on experimentally determining the responses, such as strains, forces, or accelerations, to short-duration pulses that approximate an impulse. These responses or transfer functions may then be used to predict the responses to long-duration loadings. Fig. 7 and 8 give a quick review of the principles involved in the method.

Suppose we are concerned with determining an internal response at R due to a transient loading at I. The loading of interest could arise from landing or separation dynamics or docking impact. The structure, which may be a portion of the SSV hardware or a detailed model of the entire vehicle, is mounted so as to simulate the desired support condition, and a short-duration pulse, in the desired direction, is applied at I. As in modal analysis, the structure is assumed linear, and thus the response at R is directly proportional to the area under the impulse. When the response is normalized to a unit impulse, an "impulse transfer function" is obtained.

IMPULSE TRANSFER FUNCTIONS

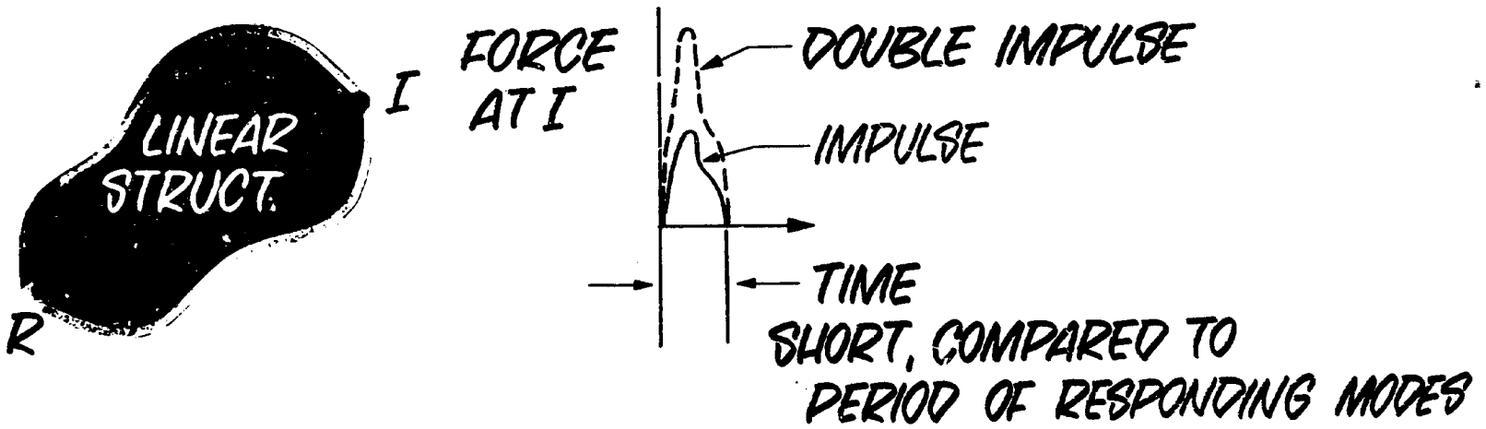

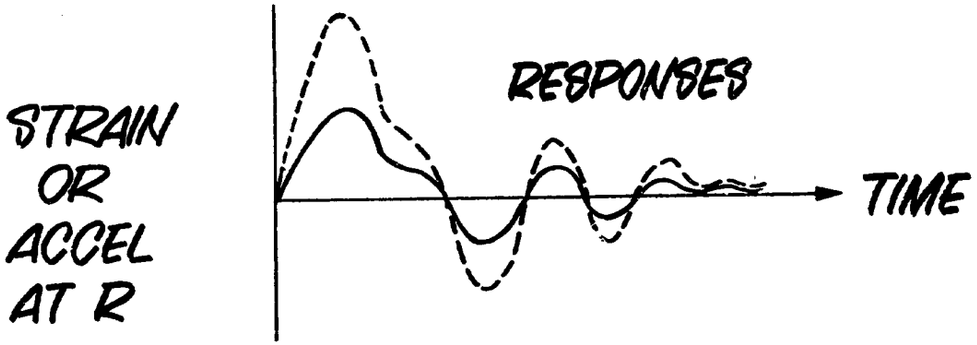

The next step in the procedure, shown in Fig. 8, consists of approximating a given time history of load application by a series of impulses. The response to this long-duration forcing function is then determined by performing a Duhamel integration.

While the approach is straightforward, the problems of experimentally generating an approximation to an impulse, accurately measuring the area under it, and measuring the resulting low-level responses required a demonstration test to prove the feasibility of the method.

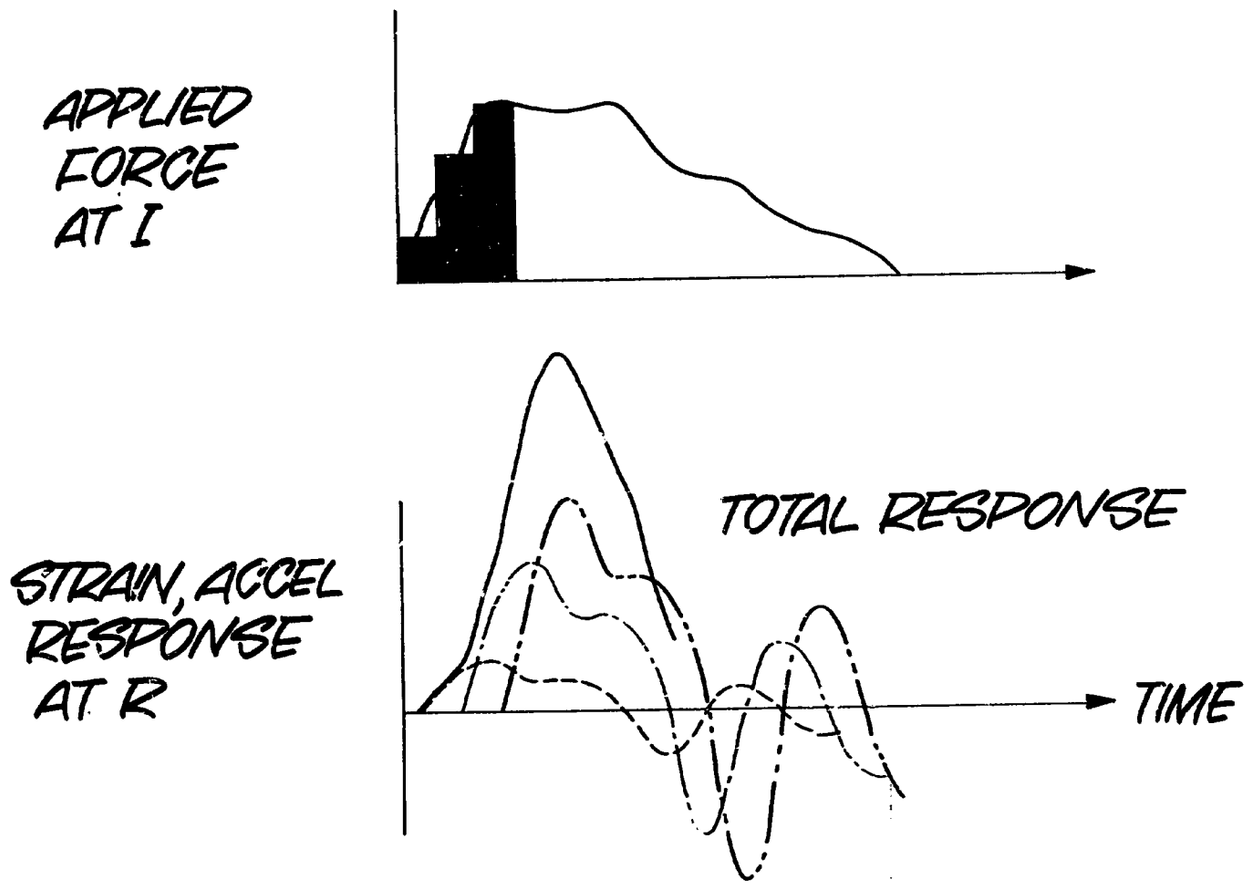
APPLIED FORCE AT I
TOTAL RESPONSE
STRAIN, ACCEL RESPONSE AT R
TIME

A typical test setup with a LM structural test article is shown in Fig. 9. The LM is supported from the apex of its outrigger trusses through a set of air springs to simulate a "free-free" condition. An electrodynamic shaker, programmed using an exact-waveform synthesizer, was used to apply impulses as large as 10,000 lb with a time base of about 1 millisecond to one landing gear attachment point. A force transducer mounted to the shaker head was used to measure the impulse time history. Instrumentation to measure both strain and acceleration response was located at various points on the vehicle. A few gages were located on the outrigger truss members themselves, very close to the impact point, while others were placed about 15 ft away, on the ascent stage aft equipment bay.

IMPULSE TEST SETUP

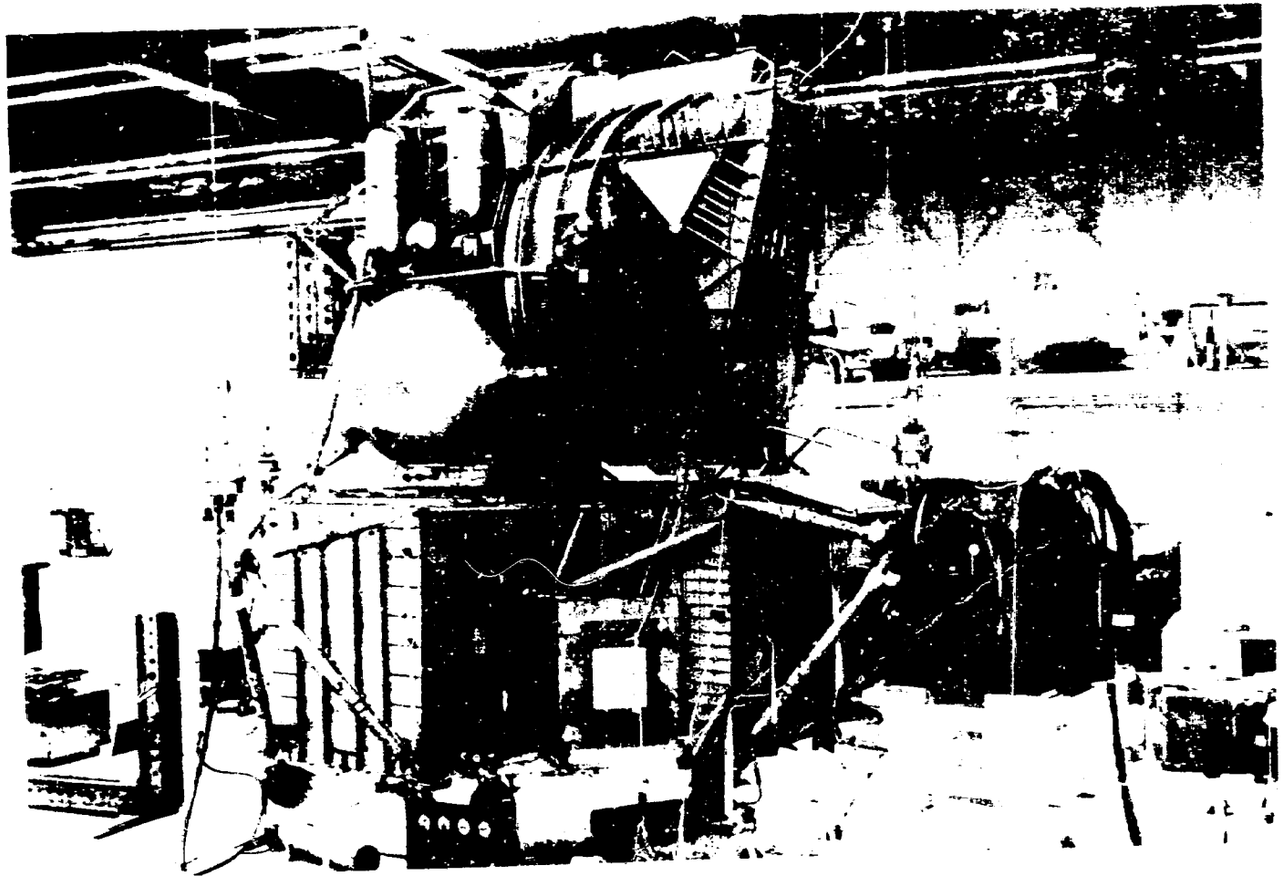

A typical impulse and several normalized response time histories are shown in Fig. 10. The actual responses, as well as the pulse itself, were recorded on magnetic tape, digitized, and then normalized to obtain the impulse transfer functions. The degree of variability in the technique, and in the test article, was assessed by comparing impulse transfer functions derived from various short-duration pulses. In spite of suspected nonlinearities in the vehicle, repeatability was good for both strain and accelerometer measurements over a wide range of input forces and for many transducer locations.

LH FWD INTERSTAGE FITTING IMPULSE TRANSFER

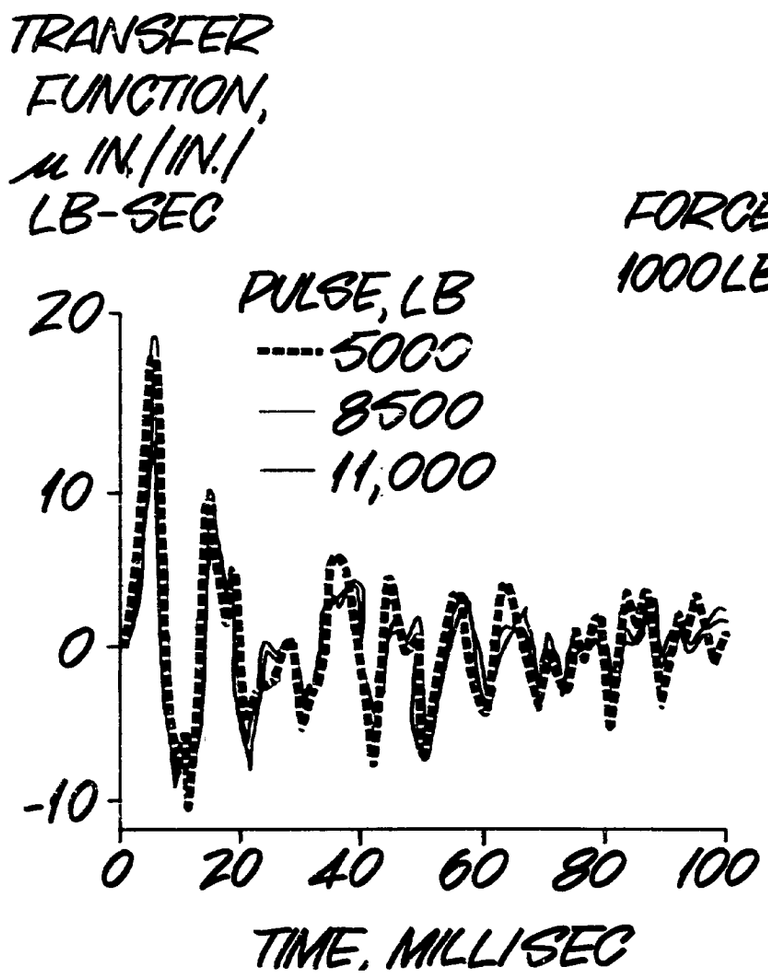

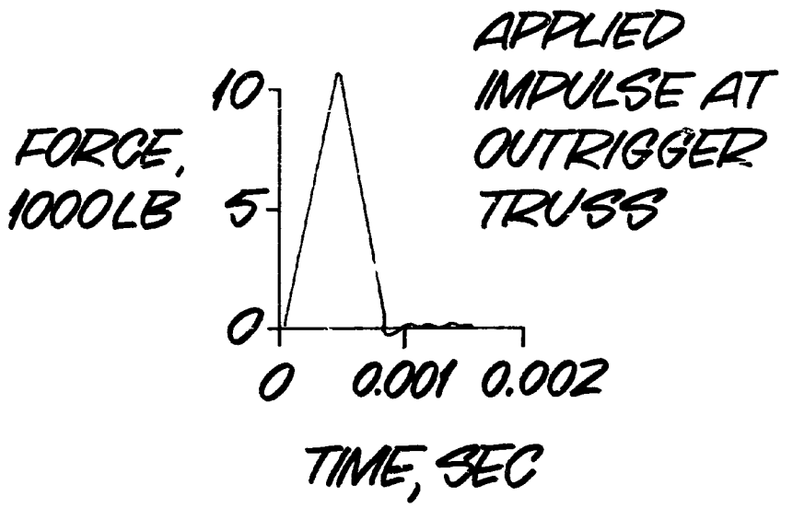

Application of the impulse transfer functions to obtain LM responses to a long-duration transient loading is illustrated in Fig. 11. It is seen that excellent correlation is obtained between the response calculated using the impulse transfer function and the actual measured response to the long-duration loading. The results shown are for a response location that is far from the input force location, and involve a complex load path from impact point to response point. Similar agreement between experimental and predicted responses has been shown at other locations, for both strain-gage and accelerometer measurements. What has been demonstrated then is a technique which consists of measuring and cataloging structural dynamic characteristics in the form of impulse transfer functions, storing these intermediate results in a memory bank, and then recalling them to predict responses to arbitrary transient loads. Applying this technique to the shuttle or detailed replica models will permit the prediction of loads due to a variety of transients.

RH AFT EQUIP. BAY LOWER OUTBD STRUT RESPONSE

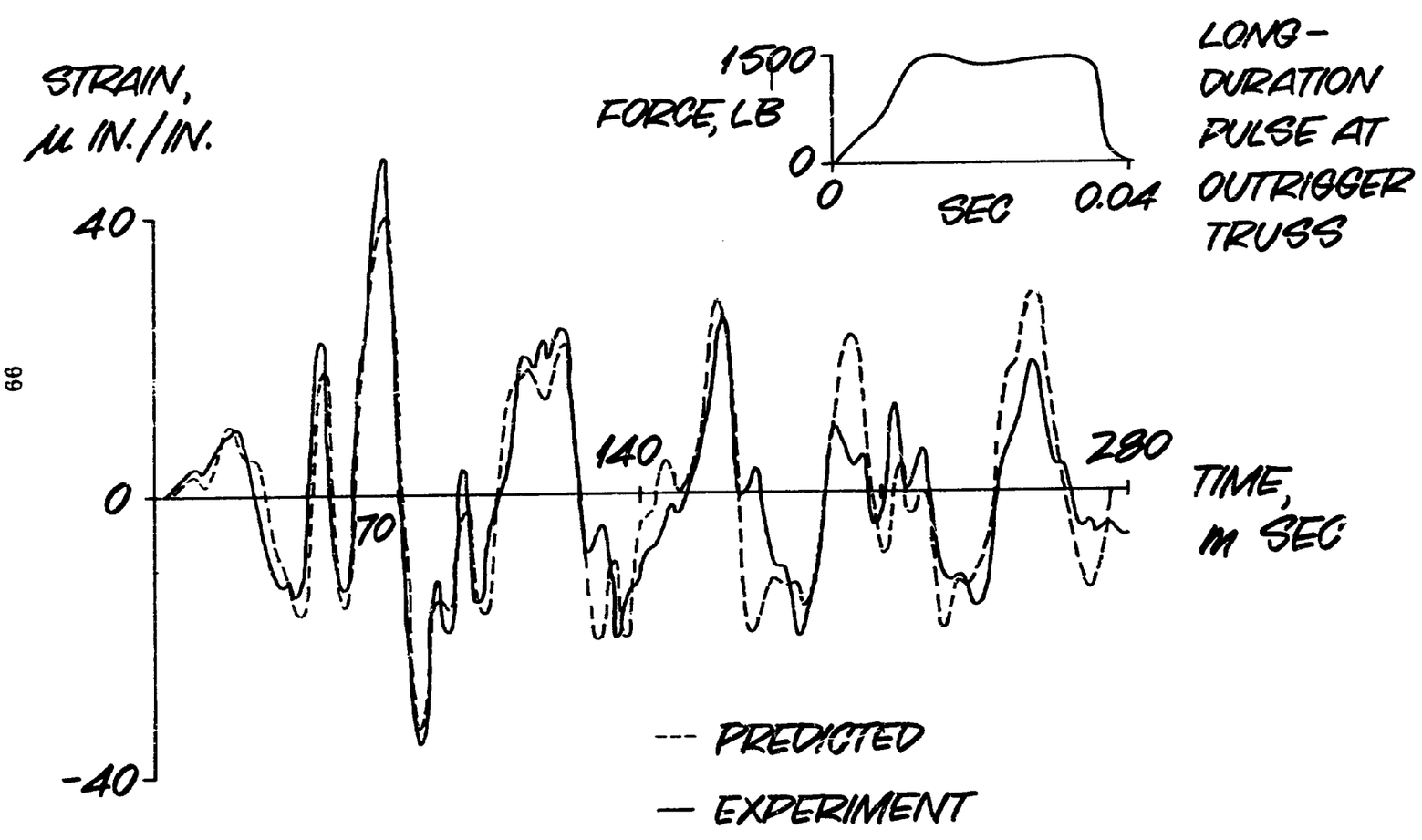

Summary

Prompt advances in several areas of technology will be required to handle the transient loading problems that will be encountered by the shuttle.

The large amount of complex structure which has to be analytically represented to obtain reliable results will require extensions of current computing capability. Therefore, methods such as modal synthesis, which will relieve the size of the required programs associated with comprehensive idealizations, will have to be utilized more extensively.

Studies of launch holddown devices and aerodynamic model studies of ground-wind alleviation systems should be pursued to reduce shuttle weight penalties for ground-loading conditions.

Analytical and experimental studies to determine an optimum interstage arrangement and stiffness should be performed to minimize the adverse transient loads due to X-Z coupling, and the effects of aerodynamic interactions during separation.

Since the size and complexity of the vehicle will limit the type of testing which can be performed to verify structural integrity, an impulse-transfer function technique should be considered for determining the loads and accelerations associated with many of the transient conditions which can not be tested directly.

Sound judgment will be required to decide the depth of analysis, the extent of model testing, and the necessity for full-scale testing.

The challenge, even when one considers only the transient-loading problems, is indeed formidable.

References

1. Wade, D. C., "Space Shuttle Liftoff Dynamics," Space Shuttle Technology Conference, Cleveland, Ohio, July 15-17, 1970.

2. Schuett, R. H., Clark, M.O., and Hurley, M. J., "Space Shuttle Staging Dynamics," Space Shuttle Technology Conference, Cleveland, Ohio, July 15-17, 1970.

SPACE SHUTTLE LIFTOFF DYNAMICS

Donald C. Wade

NASA Manned Spacecraft Center
Houston, Texas

SUMMARY

Because of the potential impact on structural weights and on crew and payload environments, space shuttle liftoff dynamics constitute an important design consideration. The analytical simulation of space shuttle liftoff dynamics poses both an interesting and complex problem. This presentation discusses many factors associated with liftoff dynamics and the potential areas affected by them. The merits of discrete versus statistical analyses of the condition are discussed and recommendations are made to assist in finding an optimum blend of criteria, analysis, and operations which will result in an efficient and adequate design.

INTRODUCTION

Probably no other space vehicle operation is characterized by a busier schedule of electrical, propulsion, and mechanical systems operations that excite the dynamics of the structure than liftoff. For example, the Saturn V ignition sequence begins 9 seconds prior to release. During this 9-second period, ignition signals are sent to engines in exacting order, valves open and close, engine thrusts build up, chamber pressures and scores of other parameters are sensed for an internal go-no go decision, and holddown and access arms are retracted to free the vehicle for liftoff. Variations in these parameters, coupled with a loading environment complicated by wind, gusts, vortex shedding, and engine gimbaling, result in a very complex structural design loading condition. A realistic structural simulation of shuttle liftoff is important because the resulting loads can affect the design of portions of the structure, as well as sensitive systems and payloads. An accurate simulation of liftoff is also important in establishing operational wind restrictions and for studying the effects on the crew and passengers. The unique configuration of a piggyback, winged shuttle orbiter configuration with a winged twelve-engine booster adds more complexity to the problem.

NASA-S-70-3404-V

SPACE SHUTTLE LIFTOFF DYNAMICS

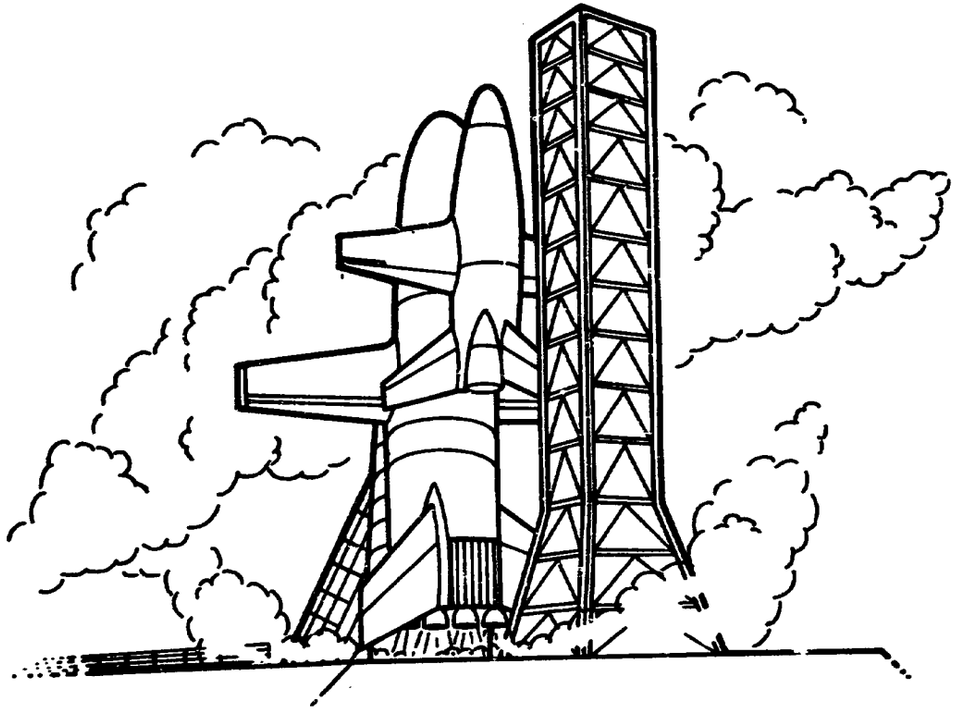

The importance of an efficient structural design can be seen by examining the percentage of total vehicle burnout weight that is structure. The distributions of weight indicate that for a straight wing or delta wing orbiter and a straight wing booster, the structure accounts for approximately forty percent of the total burnout weight.

STRUCTURAL & SUBSYSTEM WEIGHT DISTRIBUTION

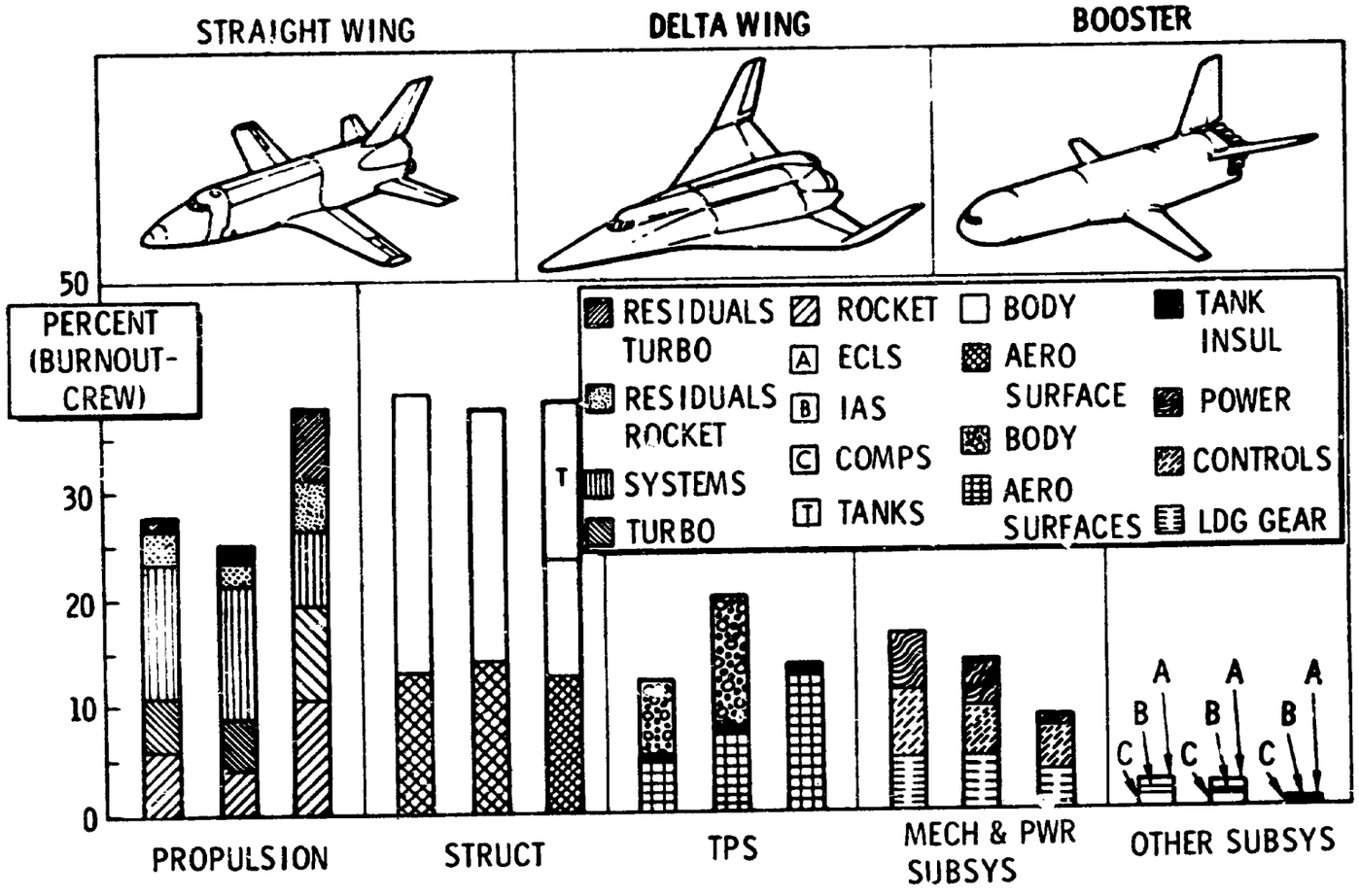

60SV3066

The requirement for efficiency is further magnified by examining payload sensitivity to weight changes. For both low and high cross-range vehicles, a ten-percent variation in booster structural weight can cause an approximate variation of 3,000 pounds, and a ten-percent variation in orbiter structural weight can result in an approximate variation of 7,000 pounds in payload capability.

PAYLOAD/SENSITIVITY TO WEIGHT & I_{SP}

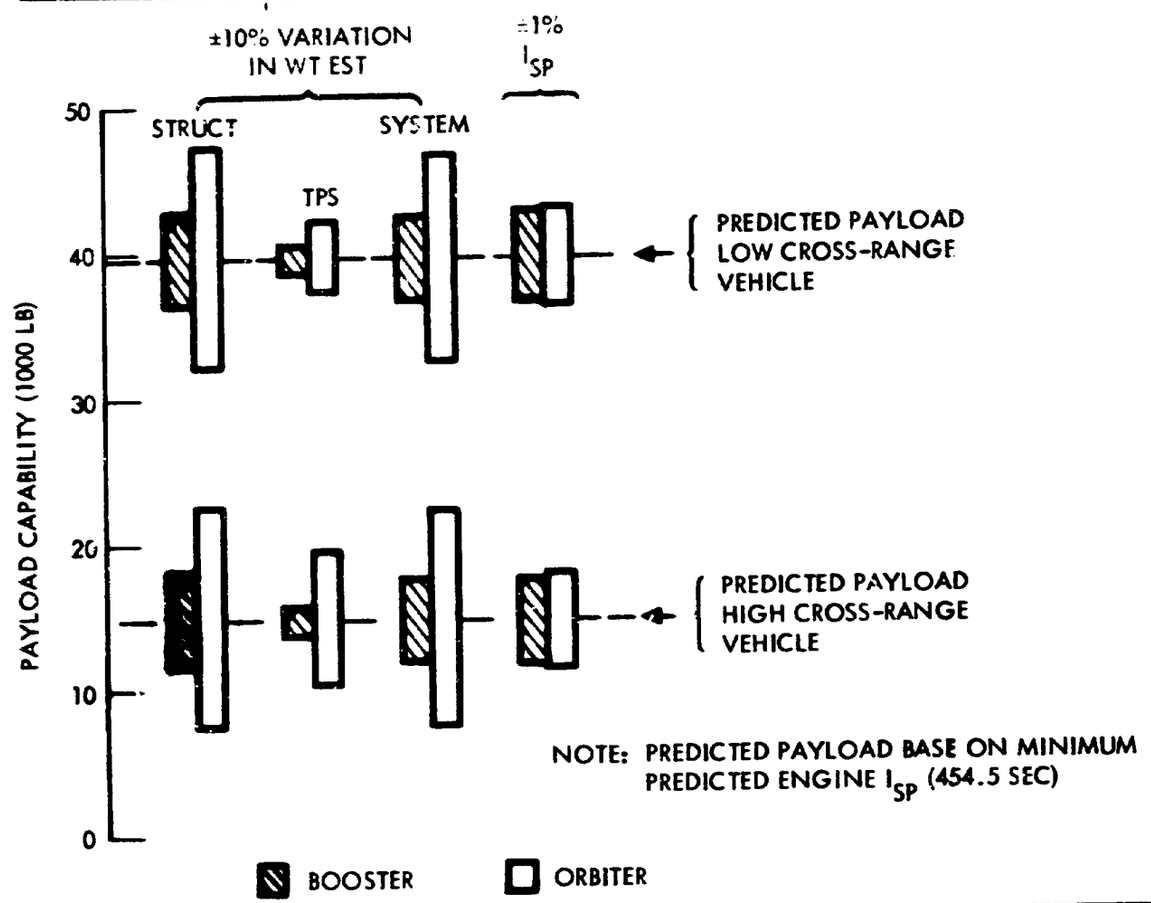

60SV2972

The importance of liftoff dynamics to shuttle design is shown by the variety of areas potentially affected. The constraining loads immediately prior to liftoff can affect the design of the vehicle thrust and holddown structure. Tension-critical elements may be designed by the low acceleration field plus high dynamic environment of liftoff. The hydroelastic interactions of the propellant and the tank structure can result in significant bulkhead loads. Onboard instruments and payloads sensitive to vibrations must be evaluated for the expected liftoff dynamic environment. This environment could potentially affect crew and passenger comfort and impair vision at a time when scanning the instrument panel is most important. These impacts on shuttle design dictate the need for a good simulation of liftoff dynamics. A good simulation is necessary not only to define the design environment but also to establish wind restrictions. The liftoff dynamics are directly influenced by the magnitude of the constraining loads at the time of release. Since this loading can be determined from load-measuring devices or wind measurements, operational restrictions can be established which will provide for a safe liftoff environment. A realistic liftoff simulation is therefore necessary to establish these operational limits without the need to resort to numerous conservative assumptions. Note that the impact on vehicle design of liftoff dynamics can be greatly reduced by loads alleviation. Pursuit of loads alleviation methods should therefore be a goal of space shuttle designers. A similar pursuit on Apollo led to a damper system which reduced the design prelaunch vortex shedding loads.

NASA-S-70-3400-V

STRUCTURAL AREAS POTENTIALLY AFFECTED BY LIFTOFF LOADS

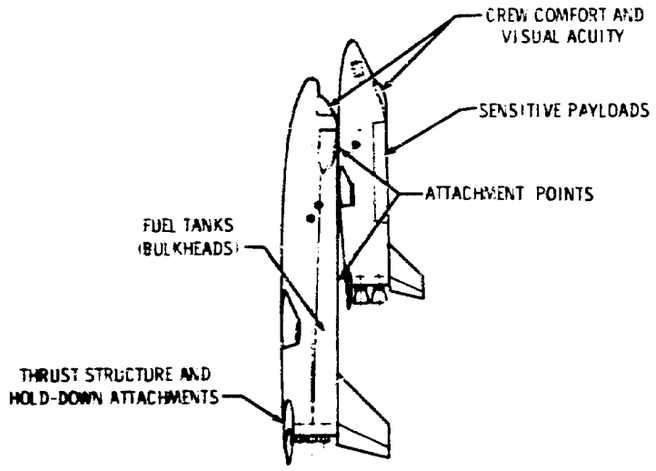

STRUCTURAL LOADING AT LIFTOFF

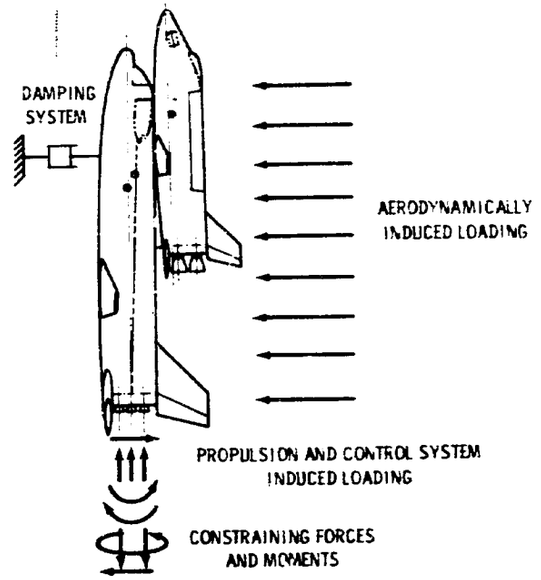

The vehicle liftoff dynamics primarily result from the release of constraining forces and moments at the instant of liftoff. The magnitude of these constraining loads, however, is determined by external loading and vehicle dynamics occurring prior to release. Perhaps the largest effects, those which are wind induced, underscore the need for a good wind tunnel program. The vehicle is loaded with thousands of pounds of drag due to both steady winds and gusts. The gusts and turbulence cause the vehicle to sway in the drag direction. Von Karman vortices (vortex shedding) occur at critical windspeeds, causing the vehicle to sway in a direction essentially normal to the wind. One proposed cross-sectional shape of the shuttle booster is approximately semi-circular. A swaying vehicle with this shape, in conjunction with a particular relative wind direction, can result in a flutter-like interaction of elastic and aerodynamic forces. This phenomenon is known as "galloping transmission line" instability. The vehicle can be further excited by unsymmetric thrust buildup of the multi-engined vehicle. This unsymmetric buildup is caused by variations in buildup rates, engine misalignments, engine-to-engine thrust variations, and dispersions from nominal ignition times. On the shuttle this effect will be magnified by the vectoring of thrust through a center of gravity which is significantly removed from the booster centerline for piggyback configurations. The liftoff dynamics are also affected by the mechanical characteristics of the release mechanisms and the manner and time at which the vehicle is released. Still another factor is engine motion prior to and during liftoff. The vehicle control system actively attempts to stabilize the vehicle and perform maneuvers, such as those to clear the tower under high winds. An additional engine motion is induced when the servo-driven engines responding to these commands experience an oscillation often described as "engine dither."

FACTORS AFFECTING LIFTOFF LOADING

- STEADY STATE WIND EFFECTS
- GUSTS
- TURBULENCE
- VORTEX SHEDDING
- 'GALLOPING TRANSMISSION LINE' INSTABILITY
- PROPULSION
  - BUILDUP RATES
  - ENGINE ALIGNMENTS
  - THRUST VECTOR/C. G. OFFSET
  - ENGINE TO ENGINE THRUST VARIATIONS
- SEQUENCING AND MECHANICAL SYSTEMS
  - IGNITION TIME DISPERSIONS
  - RELEASE TIME DISPERSIONS
  - RELEASE MECHANISM CHARACTERISTICS
- CONTROL SYSTEM
  - ENGINE GIMBALING
  - MANEUVERS
  - ENGINE 'DITHER'

A good example of the vehicle dynamics due to unsymmetric thrust buildup is shown in spacecraft accelerometer data for AS-202, an uprated Apollo Saturn I mission. The significant lateral dynamics before liftoff were due primarily to unsymmetric thrust buildup, as winds were light and there was no evidence of vortex shedding. The source of unsymmetric thrust buildup is seen in the thrust curves where diametrically opposed engine pairs did not ignite and buildup simultaneously. The data indicate significant lateral and longitudinal structural dynamics after liftoff due to the release of constraining forces and moments at the base of the vehicle. It should be noted that a high wind environment, coupled with the indicated unsymmetric buildup, could have resulted in far more severe liftoff dynamics.

NASA-S-70-3403-V

TYPICAL APOLLO LIFTOFF FLIGHT DATA

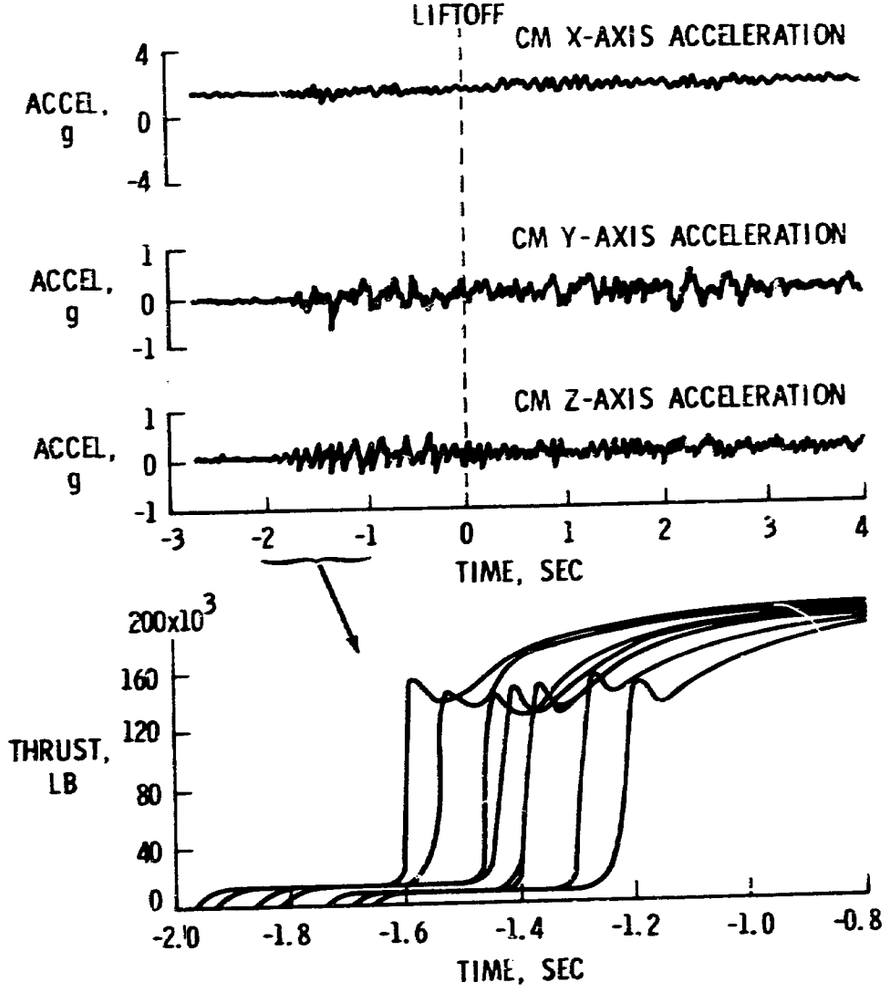

There are two primary methods of analytically evaluating the dynamic loads resulting from space shuttle liftoff the discrete method and the statistical method.

The first was the route chosen to calculate Apollo spacecraft dynamic loads for liftoff. The method entails selecting "worst-case" wind-induced and propulsion-induced forcing functions, running independent cases using a detailed structural model and root-sum-squaring the results. Considerable judgment is required in selecting worst-case input forces and determining whether results should be combined by root-sum-squaring time histories or maximum values. The discrete approach generally leads to a conservative design case; however, because only a small number of cases evolve from a selection of worst-worst inputs, a critical condition could be missed. In short, the selection of design loads is not based on a physically realistic condition with a determinable probability of occurrence but rather depends primarily on judgment.

A statistical Monte Carlo approach offers an alternative which removes several of the drawbacks in the discrete method. It, too, has several disadvantages. For example, two analytical structural models are generally required--a simplified model to use in running many cases and a detailed model to refine the results of the selected design cases. Input forces are constructed from data randomly selected from probability distributions. Each case represents as realistically as possible a simulation of a physically possible liftoff. Although distributions of some data are not available or must be assumed during the early design phases, with proper planning, all required parameters for a liftoff dynamic analysis can be described by distribution functions in time to support the final design effort. The desired maximum outputs from all cases are ordered and a distribution function established. A design value can then be selected from the distribution based on a desired probability of occurrence. It is this selection of a rational design case with a statistical meaning that makes a Monte Carlo analysis a desirable goal during the course of shuttle design. A statistical approach, however, requires planning at the criteria development stage so that the design criteria, analytical techniques, and necessary data are consistent and can be encompassed into a meaningful design effort. (It is important to note that even the selection of worst-case inputs for a discrete analysis often depends on statistical data, such as wind and wind direction. In conjunction with this, it will be necessary to fill a possible void in wind data should launch sites other than KSC be selected for the shuttle.)

DISCRETE VERSUS STATISTICAL ANALYSIS

DISCRETE	STATISTICAL
● DETAILED STRUCTURAL MODEL	● DETAILED STRUCTURAL MODEL PLUS SIMPLIFIED MODEL
● DISCRETE INPUT DATA	● INPUT DATA DESCRIBED BY PROBABILITY DISTRIBUTIONS
● SELECTION OF DESIGN CASE BASED ON JUDGEMENT	● SELECTION OF DESIGN CASE BASED ON DESIRED PROBABILITY OF OCCURRENCE
● DESIGN CASE IS GENERALLY CONSERVATIVE BUT A CRITICAL CASE MAY BE MISSED	● RATIONAL DESIGN CASE WITH A STATISTICAL MEANING

A Monte Carlo Apollo liftoff dynamic loads analysis carried out at MSC (NASA TMX-58046) helps to illustrate the comparison of loads calculated by discrete and statistical methods. The load chosen was the maximum bending moment at the command module/service module interface. A moment for that interface was obtained by the Apollo design method of root-sum-squaring the maximum moments from three cases, each of which was constructed from the selection of "worst-case" wind, unsymmetric thrust, and thrust misalignment forcing functions. Probability distributions of the same input data were then prepared from which 200 independent sets of forcing functions were selected for the Monte Carlo analysis. A compilation of the maximum CM/SM interface moment from all cases established a log-normal distribution. The log of the CM/SM moment obtained by the root-sum-square method (the "design moment") was then compared to the Monte Carlo distribution. The "design moment" was not once exceeded in the 200 Monte Carlo cases and would not be expected to be exceeded at least 99.99 percent of the time. This example indicates the potential conservative nature of a liftoff design load obtained by the root-sum-square of several discrete worst cases.

NASA-S-70-3402-V

STATISTICAL EVALUATION OF APOLLO DESIGN LIFTOFF LATERAL LOAD

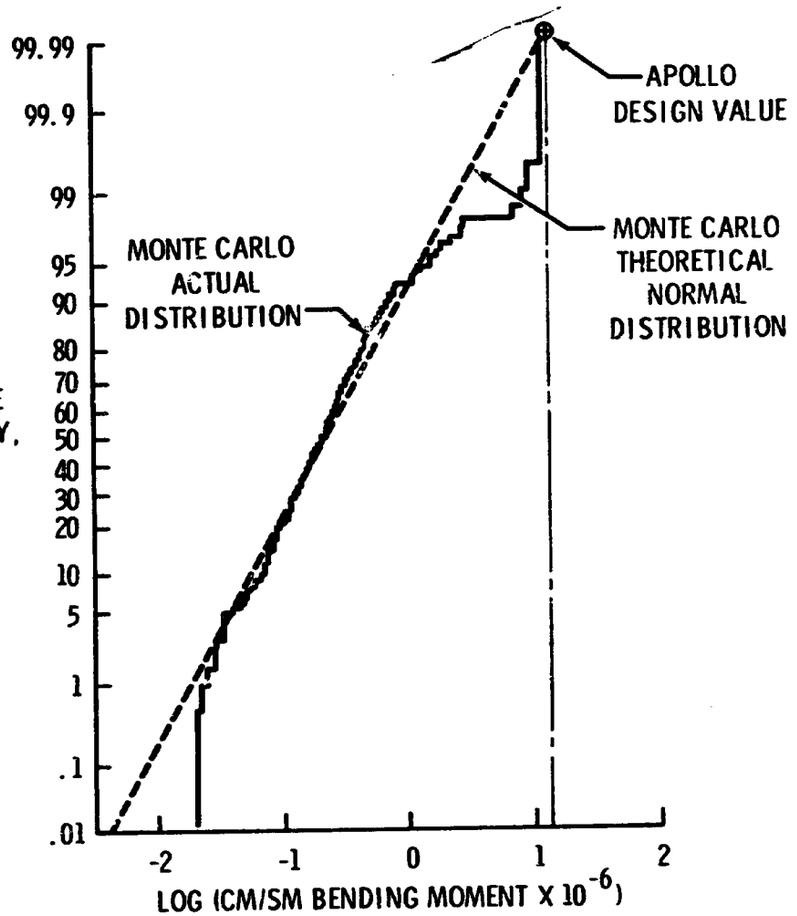

Because of the planned rapid turn-around, high launch frequency and small launch windows, an effective wind monitoring system is necessary to obtain maximum operational capability. The early Apollo system utilized only wind measurements in the system. There was no means of detecting the wind distribution or the vehicle dynamic effects, which resulted in an undesirably high wind restriction for launch. Later, Saturn IB load measurements at the SIB/SIVB interface and Saturn V load measurements at the SIC intertank region were calibrated to read out bending moment while the vehicle was still on the pad. While load measurements at the holddown structure would better indicate the entire loading on the vehicle, these measurements were able to detect the presence of lack of vehicle dynamics due to gusts and vortex shedding. As a result, load measurement became the primary mode in the wind monitoring system, and wind measurement served only as a backup. The new procedure provided for greater and more realistic operational capability. The Apollo experiences have shown that an effective space shuttle wind monitoring system should rely primarily on load measurements in the launch support structure. It should be possible to calibrate these measurements to assess the total external and dynamic loading on the vehicle. The load measurement device should be incorporated into the design of the launch complex. Appropriate planning in the development of a wind monitoring system can ensure low operational restrictions and simple operational procedures.

WIND MONITORING SYSTEMS

	TYPE OF SYSTEM	CHARACTERISTICS
EARLY APOLLO	WIND MEASUREMENT	CONSERVATIVE VORTEX SHEDDING AND GUST DYNAMICS ASSUMED NO VEHICLE LOAD MEASUREMENTS HIGH OPERATIONAL RESTRICTIONS
LATE APOLLO	PRIMARY - LOAD MEASUREMENT ON LAUNCH VEHICLE BACKUP - WIND MEASUREMENT	UNSTEADY WIND EFFECTS MEASURED LOW OPERATIONAL RESTRICTIONS
SHUTTLE (PROPOSED)	PRIMARY LOAD MEASUREMENT ON LAUNCH SUPPORT STRUCTURE INCORPORATED IN LAUNCH COMPLEX DESIGN BACKUP - WIND MEASUREMENT	UNSTEADY WIND EFFECTS MEASURED AT VEHICLE BASE LOW OPERATIONAL RESTRICTIONS SIMPLE OPERATIONAL PROCEDURES

Because of the shuttle payload capability sensitivity to structural weight changes and the potential effects of the vehicle dynamics on primary structure, crew, and payloads, liftoff dynamics constitute an important shuttle design area. Not only is liftoff an important design area, but the many factors affecting liftoff dynamics present the designer with a complex analytical problem. The unique aerodynamic shape of the space shuttle requires a good wind tunnel program to detect the presence of vortex shedding and "galloping transmission line" instabilities, in addition to the static aerodynamic effects. A thorough and efficient liftoff design effort should include a statistical analysis. To complete such an analysis the designer must plan now to acquire the necessary statistical data. Should launch sites other than KSC be selected, efforts must be undertaken to gather statistical wind data for either a discrete or a Monto Carlo analysis. Although most of the input parameters for a Monte Carlo liftoff analysis can be expressed by probability distributions, this form of input requires advanced planning and should be a desired goal of test programs. The statistical basis for selection of design loads should be expressed in improved criteria and analysis methods. Unlike other design conditions, physical access to the vehicle is attainable via a launch support structure until liftoff which the designer could use advantageously in seeking loads alleviation methods to reduce the impact of liftoff dynamics on design loads. Finally, project Apollo taught that an effective wind monitoring system can greatly enhance operational capability and that it should be planned into the design of the launch complex.

CONCLUSIONS

- LIFTOFF DYNAMICS ARE IMPORTANT TO SHUTTLE STRUCTURAL DESIGN
  - STRUCTURE IS A MAJOR PORTION OF VEHICLE WEIGHT
  - PAYLOAD IS SENSITIVE TO STRUCTURAL WEIGHT
  - STRUCTURAL WEIGHT IS SENSITIVE TO DESIGN LOADS
- STATISTICAL DATA AND ANALYSES ARE NEEDED TO DEFINE REALISTIC LIFTOFF DESIGN LOADS
- STATISTICAL WIND DATA ARE REQUIRED FOR LAUNCH SITES OTHER THAN KSC
- IMPROVED CRITERIA AND ANALYSIS METHODS ARE NEEDED
- LOADS ALLEVIATION SYSTEM IS NEEDED FOR DESIGN LOADS REDUCTION
- AN EFFECTIVE WIND MONITORING SYSTEM IS REQUIRED TO OBTAIN MAXIMUM OPERATIONAL CAPABILITY
- A COMPREHENSIVE GROUND WINDS WIND TUNNEL PROGRAM SHOULD BE PLANNED

RECOMMENDATIONS

- BASE FINAL LIFTOFF DESIGN LOADS ON STATISTICAL ANALYSIS
- OBTAIN STATISTICAL WIND DATA FOR LAUNCH SITES OTHER THAN KSC
- DEVELOP IMPROVED CRITERIA AND ANALYSIS METHODS
- PLAN COMPREHENSIVE GROUND WINDS WIND TUNNEL PROGRAM
- INVESTIGATE LOADS ALLEVIATION SYSTEMS TO MINIMIZE EFFECT ON DESIGN
- PLAN A WIND MONITORING SYSTEM IN THE DESIGN OF THE LAUNCH SUPPORT STRUCTURE

SPACE SHUTTLE STAGING DYNAMICS

R. H. Schuett, M. C. Clark, and M. J. Hurley

General Dynamics Convair Division

Stage separation is recognized as a major Space Shuttle problem area. The piggyback arrangement precludes utilization of separation techniques developed for tandem vehicle stages. Also, since most shuttle configurations are not symmetrical, thereby complicating interactions, experience gained from Titan III C solid motor separation and Atlas-Centaur fairing jettison is not directly applicable. Unlike present day launch vehicle stage separation, the depleted space shuttle booster is as massive as the orbiter element so that large intervehicular interaction is probable. Abort separation is likely to yield the most severe separation condition since aerodynamic loading is significantly higher during the abort regime. Aerodynamics, including interference effects, will dominate the separation dynamics for all but the lowest dynamic pressures.

The separating booster must clear or withstand the orbiter exhaust plume, as well as clear its hard structure under all probabalistic conditions. Following separation, the booster element must initiate a capture mode and reorient to a trimmed attitude for subsequent reentry. The orbiter continues on its mission, or, for abort, prepares for reentry.

This paper summarizes separation analyses conducted during the NASA Phase A Space Shuttle Study, the Air Force (SAMSO) Space Transportation System Study, and company sponsored research which evaluated separating multiple bodies placed symmetrically about a center core. An aft hinge system with separation force supplied by inertial and aerodynamic reactions was recommended. With the piggyback arrangement, other schemes could be required. Concepts using rails, links, thrusters and pistons are discussed with advantages and shortcomings of each system identified. Factors to be evaluated for system comparison include system weight, performance losses, separation clearance time history, abort capability, and costs.

Supporting research and technology necessary for selection and definition of a space shuttle separation system are identified. Covered in brief discussions are the three topics, interference aerodynamics, plume impingement heating and pressures, and propellant motions during abort.

PROBLEMS

UNSYMMETRIC, PIGGYBACK ARRANGEMENT

CONTROL & RECOVERY REQUIREMENT

SEPARATION OF BODIES OF EQUAL MASS

SEPARATION IN HIGH DYNAMIC PRESSURE

SEPARATION DYNAMICS

Separation is a combination of many transient events over a relatively short time period and the implication of one event on succeeding events must be considered in any analysis. The sequence is begun based on a pre-established staging velocity or time or could be triggered by a sensor which indicates some measure of propellant depletion. The first transient is then booster engine thrust decay. Associated with thrust decay is a relaxation of the structure responding to the changing acceleration vector. The combination of structural response and propulsion system characteristics have, on existing systems, resulted in thrust oscillations during engine decay. Gimbaling of the booster engines during this time period may be required for control in event of unsymmetric engine shutdown or to trim the vehicle under additional forces such as orbiter thrust or separation system forces if those are activated prior to booster engine shutdown. Control forces after engine shutdown are provided by the ACPS.

The second series of events is associated with activation of the separation mechanism. Releasing the structural tie between stages by means of retraction pins, explosive bolts, or whatever, introduces two transients; the first is the shock associated with the mechanism and the second is the redistribution of loads due to breaking the tie point. These conditions are followed by activating the separation forces such as thrusters, pistons, inertial and aerodynamics forces, and the kinematics of linkages, guide rails, or hinges as may be necessary to control initial movements.

The next major series of events are associated with orbiter engine ignition. Orbiter engine ignition could be commanded at a pre-selected time after separation initiation. The rigid body and transient motions associated with engine thrust and activation of the orbiter control system are significant in separation system evaluation. Orbiter exhaust plume impingement causes a hostile environment to be imposed on the booster and could be a prime factor in establishing separation required at time of orbiter ignition, or establish design requirements for portions of the booster structure.

Present during the separation sequence will be the aerodynamic forces. The interference effects must be determined and included in simulations of separation dynamics. Aerodynamics will be of major importance for abort separation and of minor importance during normal separation.

The separation dynamics through the preceeding events must consider the separation of energy and momentum of one body into two bodies and the shift in points of body rotations after separation. For abort conditions, the phenomena of propellant motions in the booster tanks will add to the complexity of the analyses.

Separation dynamics can be divided into two categories - rigid body motions and elastic response. The discussions in this paper will concentrate on the rigid body motions and required timing sequences and forces necessary to provide an acceptable, safe separation. Elastic response should not be neglected in overall evaluation and selection of a separation concept.

SEPARATION DYNAMICS

SEPARATION SYSTEM

- RELEASE MECHANISM
- SEPARATION FORCE
- SEPARATION GUIDES

AERODYNAMICS

- LIFT
- DRAG
- MOMENT
- INTERFERENCE VS. DISTANCE

ORBITER

- THRUST BUILDUP
- TIME HISTORY
- GIMBAL REQUIREMENT
- PLUME IMPINGEMENT

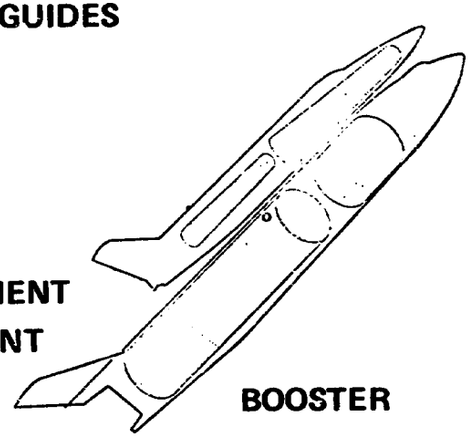

INERTIAS

- BOOSTER
- ORBITER
- PROPELLANT MOTION

BOOSTER

- THRUST DECAY TIME HISTORY
- STRUCTURAL RELAXATION
- THRUST OSCILLATIONS
- CONTROL REQUIREMENT

PHASE A & STS STUDY RESULTS

During the Phase A and STS studies Convair evaluated several separation systems for separating multiple bodies located symmetrically about the central or core vehicle. An aft hinge separation of the outer bodies from the core element while the core is under thrust was selected as being the most promising scheme for symmetric vehicles. Other concepts evaluated included a translational-rotational linkage system, an inclined ramp, and a system of lateral thrusters. The bases for selection of the aft hinge were; experience on Titan III C solid motors and Atlas Centaur fairings; the system is passive; readily extendable to abort; and maximum energy was imparted to the payload. Aft hinge system separation was initiated by releasing forward attach points. The boosters then are free to rotate about the aft hinge and will do so under the combined aerodynamic and inertial reaction loads. To determine aerodynamic interference effects, captive trajectory wind tunnel testing was conducted.

The captive trajectory system permits the trajectory of a body separating from another (stationary) body to be determined experimentally in a wind tunnel. An analog computer uses force and moment data from a balance within the separating body to compute the resultant trajectory. Trajectory motion is simulated by the six-degree-of-freedom support shown.

The simulation includes the aerodynamic characteristics of the separating body during and just after separation, as influenced by the flow field generated by the stationary body, together with the mass properties and propulsion characteristics of the body itself. In this way, the effects of body release position and attitude can be studied.

The model support, an electromechanical positioning system with all axes of motion contained within a single mechanism, is independent of the stationary body. This mechanism has an envelope of motion lying within a cube about 30 inches on a side. Drive motors, located in a case below the tunnel floor, are printed-armature electric motors with extremely fast response characteristics.

After the free-stream flow has been established, the analog computer computes the trajectory using model strain-gage balance data in conjunction with body mass, moment of inertia, rocket thrust, altitude, and other data. This trajectory, transformed into velocity components, is then supplied to the support control drive motors, thus positioning the separating model in a smooth, accurate simulation of the separation trajectory. The analog program is time-scaled; thus, what is seen is an apparent slow-motion movement of the separating body through its separation trajectory. The balance outputs are converted to aerodynamic coefficients, and the actual position and angle outputs are processed into full-scale parameters.

CAPTIVE TRAJECTORY MODELS IN SUPERSONIC TEST SECTION

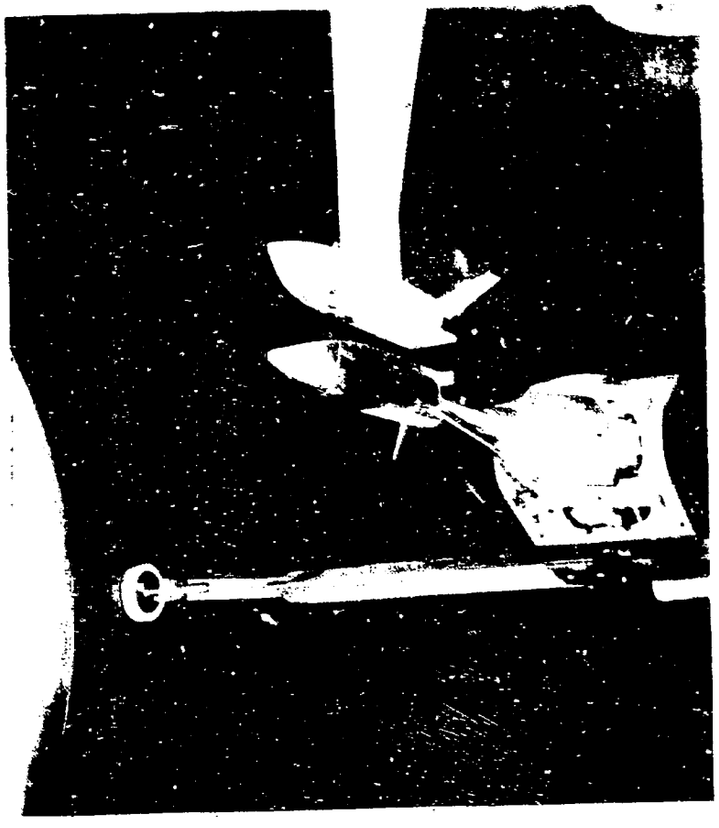

PHASE A & STS STUDY RESULTS (CONT'D)

In conjunction with the analysis of space-shuttle separation, a digital computer simulation was developed to analyze the separation dynamics of hinged or linked lifting-entry vehicle clusters. The program computes the kinematics of separation of as many as five auxiliary (booster) elements attached around the periphery of a central core (orbiter) element in six rigid-body degrees of freedom for the core plus three for each auxiliary element. After separation, all elements are computed in six-degrees-of-freedom.

Aerodynamic forces provided by the captive trajectory testing were used in the computer simulation. A typical abort separation display is shown on the opposite page. The correlation with the captive trajectory results was acceptable.

Most present space shuttle configurations are not suitable for aft hinge separation because the aft hinge system does require that the aft ends of all stages be reasonably flush. Also, the hinge reaction on the core, which, for symmetrical vehicles was canceled by the body on the opposite side, could cause vehicle control problems. Therefore, this staging system evaluation must re-examine all concepts in view of the present shuttle configurations.

TYPICAL OUTPUT DISPLAY FOR ABORT SEPARATION
(Near Maximum Q)

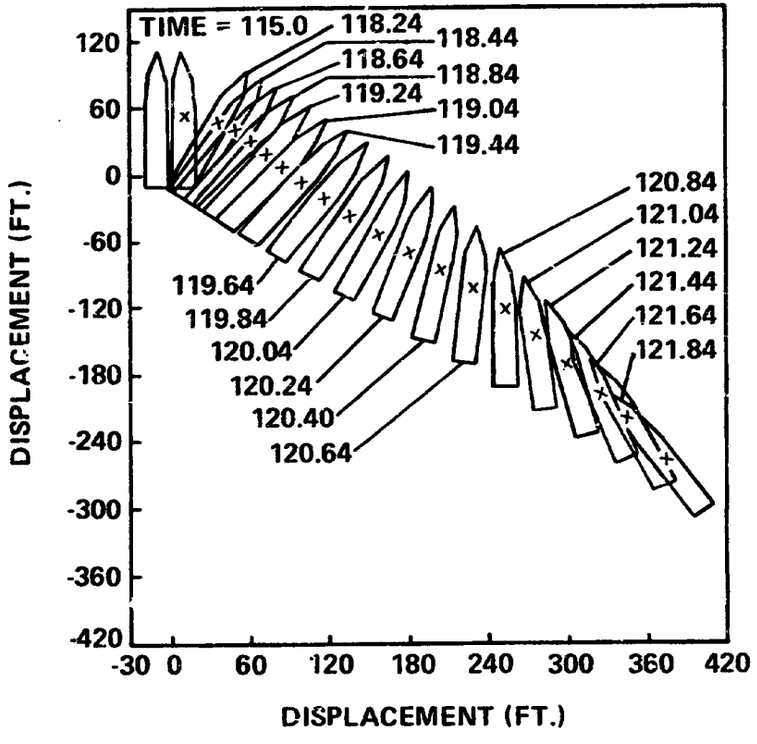

CONCEPTS

LINKS-BOOSTER THRUST - Staging is initiated by a sensor which detects near propellant depletion, required velocity, or time. A signal is sent to release the links. With the links free to rotate, the booster, still under thrust, will move forward relative to the orbiter and the link rotation will also provide a relative lateral velocity. By the time the booster plume comes in contact with the orbiter, the booster thrust is near zero. The orbiter engines are then ignited. By the time orbiter engines are at full thrust, the relative lateral velocity will have provided enough lateral separation to minimize plume impingement effects. The depletion sensor could be near the top of the LO_2 line, thus provide about one second of burn time before booster engine shutdown.

LINKS-ORBITER THRUST - Staging is again initiated by a sensor which detects near propellant depletion. A signal is sent to start the orbiter engines. As the orbiter engine comes up to full thrust, the booster engines are gimbaled to reduce vehicle rotation. When booster thrust has decayed to about 10% of full thrust, the orbiter T/W is greater than the booster T/W, the links are released and the orbiter moves forward of the booster, with the links also providing relative lateral velocity. Plume pressures will impart lateral velocity to the booster.

RAMP/RAILS - This sequence is very similar to the preceeding system with initial separation travel being guided by ramps or rails in place of linkages.

PISTON - Staging is initiated by an accelerometer which indicates zero or very small acceleration. The interstage structural ties are released and the piston provides a relative lateral velocity of about 10 feet per second for a 100,000 pound force acting for 1 second. The orbiter engine is ignited, and by the time it is up to full thrust, the vehicles are separated sufficiently to reduce impingement effects. To account for differential vehicle motions during piston action, it will be desirable to hinge both ends of the system.

ROCKET - Very similar to the previous concept, with incremental lateral velocity imparted to the booster by engines located in the wing root. Thrust could be provided by solid rocket motors or by liquid propellant engines fed from the booster tanks. In this concept, as well as the piston concept, the thrust could be oriented to provide a differential velocity in directions other than lateral if it is found beneficial to do so.

SEPARATION CONCEPTS

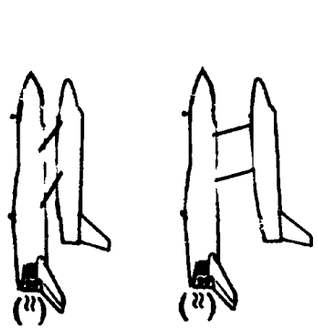

LINKS – BOOSTER THRUST

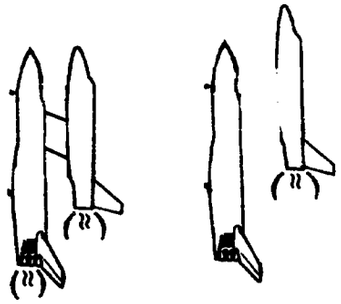

LINKS – ORBITER THRUST

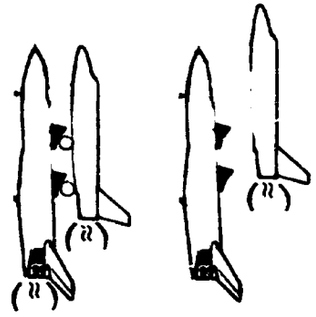

RAMP/RAILS

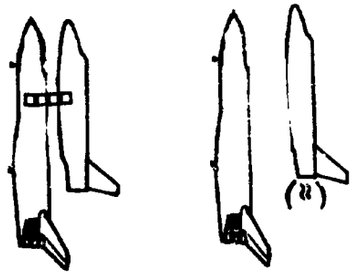

PISTON

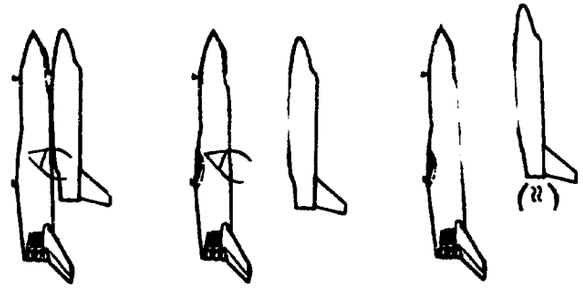

LATERAL THRUSTERS

S70CV1245

PRELIMINARY CONCEPT EVALUATION

LINKS-BOOSTER THRUST - This system has some potential for normal separation, however for abort conditions the aerodynamic forces during the coast time could generate large compressive forces between the vehicles thus preventing link motion. The structure supporting the orbiter during normal booster phase would be primarily in compression, leading to high system weights. The coast time for normal staging is moderate, on the order of 3 or 4 seconds, and compares favorably with other concepts in payload capability.

LINKS-ORBITER THRUST - Primary advantages of this system are no coast time and some probability of satisfying abort conditions. Performance is maximized with the elimination of coast time. The improved probability of satisfying abort conditions is due to having the orbiter under thrust immediately, reducing the time the orbiter is in the vicinity of the booster which in turn reduces the impact of aerodynamic forces. The support links are in tension during normal ascent flight tending to reduce weights. Plume impingement will be significant, but preliminary calculations have indicated pressures and temperatures are not intolerable. Primary disadvantage of the system is the timing and controllability required between the various engine shutdown and startup characteristics. Also, vehicle control during engine ignition and shutdown may be delicate. The separation dynamics and booster/orbiter controllability are quite sensitive to booster thrust decay and orbiter thrust rise time histories. The time phasing between booster engine decay and orbiter engine ignition will also affect controllability and separation dynamics.

RAMP/RAILS - No particular advantage can be cited for this concept over the previous system. Ramps/rails have more simplicity than linkages but also have more weight. Lateral separation would be less, and therefore the plume impingement effects would be more important.

PRELIMINARY CONCEPT EVALUATION

LINKS – BOOSTER THRUST

- CLEAN SEPARATION FOR ABORT QUESTIONABLE
- SUPPORT STRUCTURE RELATIVELY HEAVY – MOSTLY COMPRESSION MEMBERS
- MODERATE COAST TIME: 3 OR 4 SECONDS

LINKS – ORBITER THRUST

- NO COAST TIME. MAXIMIZES PERFORMANCE
- GOOD SEPARATION DISTANCE. HAS ABORT POTENTIAL
- SUPPORT STRUCTURE RELATIVELY LIGHT – MOSTLY TENSION MEMBERS
- PLUME IMPINGEMENT ON BOOSTER TO BE EVALUATED
- ENGINE IGNITION, DECAY, CONTROL, & GIMBALING REQUIRE DELICATE TIMING

RAMPS/RAILS

- SAME AS ABOVE
- RAMPS/RAILS HAVE MORE SIMPLICITY THAN LINKS, BUT ARE HEAVIER
- LATERAL SEPARATION NOT AS GOOD. INCREASES ABORT & PLUME IMPINGEMENT SENSITIVITY

S70CV1246

PISTON - This concept appears to be the most straight forward, simple approach. Sensors and timing requirements are very practical. Angular rates imparted to the orbiter can be minimized by placing the piston at the orbiter c.g. Assuming booster piston location between the LO_2 and LH_2 tanks, the angular rates imparted to the booster are not excessive. Negative aspects are: the relatively long coast time of 5 to 8 seconds reduces performance, large force will be required to separate the vehicles under abort conditions with additional complications due to booster/orbiter differential drag forces at abort which could require guides of some type to react moments and axial forces; redundancy for fail safe, or fail operational, fail safe requirements will increase the system complexity and weight.

ROCKET - Most of the comments of the piston concept apply to this system; however, the system does have more complexity and has the added problem of rocket plume impinging on the orbiter. The concept could use solid rockets or engines fed from the LO_2 and LH_2 tanks. Replacement or refurbishment would be necessary with solid rockets. An additional LO_2 tank and considerable LO_2 plumbing would be required with the second option. A preliminary reliability assessment utilizing solid rockets indicated a triple redundant system would be necessary. The abort condition would require much larger thrust than normal separation.

PRELIMINARY CONCEPT EVALUATION (CON'T)

PISTON

SIMPLE, STRAIGHTFORWARD APPROACH. SENSORS & TIMING NOT CRITICAL

LONG COAST TIME (5-8 SEC.). REDUCES PAYLOAD (100-200 LB./SEC.)

LARGE PISTON FORCE & LATERAL VELOCITY REQUIRED FOR ABORT

REDUNDANCY REQUIRED TO MEET FAIL SAFE REQUIREMENT

ROCKETS

SAME COMMENTS AS FOR PISTON

ADDED PROBLEM OF ROCKET PLUME IMPINGEMENT

REFURBISHMENT OF SOLID ROCKETS

ADDITIONAL TANKAGE & FEEDLINES FOR LIQUID SYSTEM

TYPICAL SEPARATION TIME-HISTORY

Lateral and axial separation time histories are shown for the Link-Orbiter Thrust and Piston concepts. Time zero is taken to be the time at which restraining members are disconnected. For the link concept, this means that the orbiter is up to full thrust at time zero, when the booster engines have decayed to about 10% of full thrust and the system is released. The lateral separation velocity is due to the rotating links and the impingement pressures on the booster. Axial separation is, of course due to T/W of the orbiter.

For the piston concept, to match the lateral separation of the link system will require a 200,000 pound force applied for 1 second. A 100,000 pound force applied for 1 second will provide half the lateral separation distance, A piston stroke of approximately 10 feet would be required with the 200,000 pound force and 5 feet for the 100,000 pound force. The orbiter was assumed to be up to full thrust at 4.0 seconds after separation is initiated, or 3.0 seconds after the piston has reached the end of its stroke.

The significant separation distance difference between the two concepts is the axial displacement. At 5 seconds the relative axial movement has been 600 feet for the link system and about 100 feet for the piston system. The greater separation distance reduces hazardous conditions during abort in event of an explosion.

The piston system, with its lateral separation at orbiter ignition reduces plume impingement effects. The timing of the sequence is easily established.

The link system maximizes performance, has abort potential, but suffers from the hostile impingement environment and could be sensitive to engine shutdown and startup characteristics.

TYPICAL SEPARATION TIME HISTORY

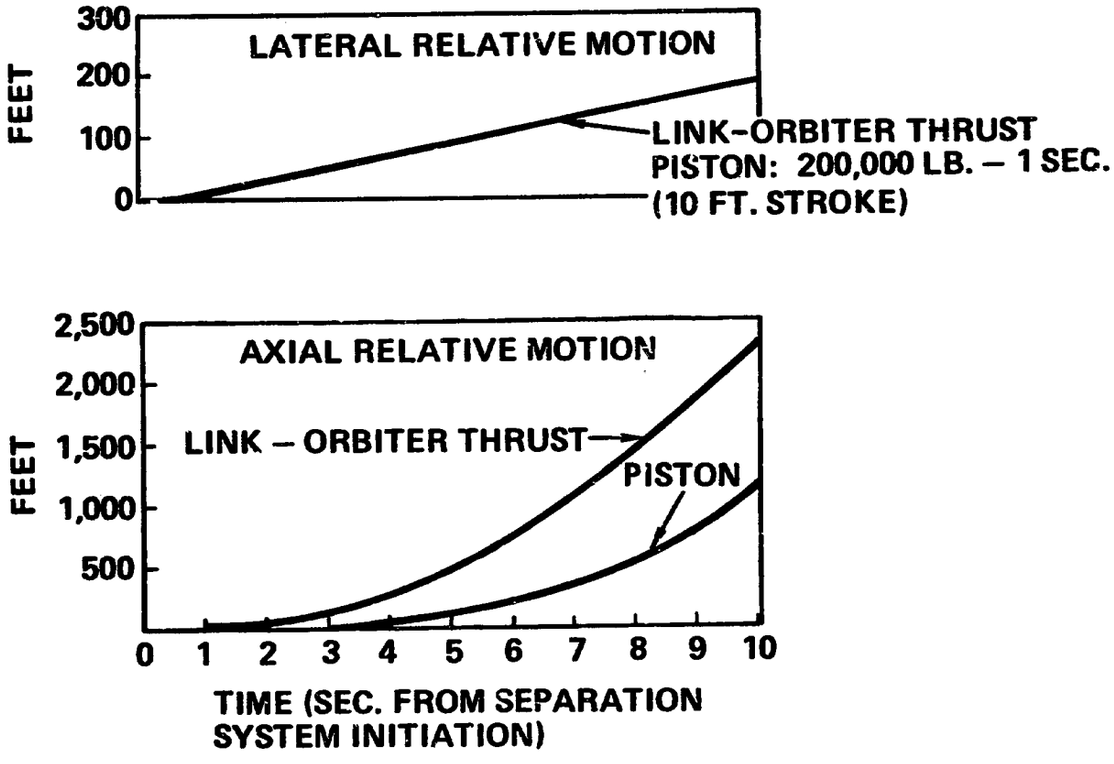

IMPINGEMENT PRESSURES

Typical orbiter exhaust exit conditions were expanded using a vacuum jet ecpansion program to obtain gas flow conditions throughout the exhaust plume. The boundary of the flow was determined by combining the flow conditions of the free stream air and the conditions in the nozzle flow. The plume boundary intersects the booster approximately 220 inches downstream of the nozzle exit plane. This is a result of the engine nozzles high expansion ratio producing pressures which do not cause a highly expanded plume. From the flow angle and the Mach number, the static pressure was determined downstream of the oblique shock which exists at the intersection of the flow stream and the element.

From the geometry of the system, the pressures on either side of the booster are the same and only one side is shown. The plane of intersection of the flows from the two engines will result in locally higher pressures on the top surface of the booster where it intersects the X-Z plane. It is estimated that the local pressure at the intersection will be greater than the sum of two engines, but probably less than 2 psia. This pressure would act over a strip possibly 2 feet wide.

The total force from one engine is 14,032 pounds, acting 492 inches from the orbiter nozzle exit. For two engines the force would be 28,064 pounds plus an allowance of approximately 10,000 pounds for the interference effects for a total of 38,000 pounds.

Pressures on the booster V-tail were calculated for one orbiter engine. The tail was described by a series of flat plate elements. Each section subtends an arc of approximately 7 degrees. The orbiter nozzle exit was assumed to be 780 inches forward of the aft end of the booster. The tail surface leading edge was assumed to be located approximately 420 inches forward of the booster base. The results show pressures less than 0.15 psia. From the initial orbiter location, forward movement of the orbiter will result in lower pressures on the surface. If the initial position of the nozzle exit is further aft, the pressures on the tail surface would be higher, but probably not exceed 0.3 psia.

Preliminary impingement heating analysis indicate that temperatures will exceed allowables at several local areas which can be protected with minor weight increase. Plume impingement analysis, particularly the interference effects of multiple plumes, is a key technology improvement item requiring further analysis and verification by testing.

TYPICAL IMPINGEMENT PRESSURES
One Engine

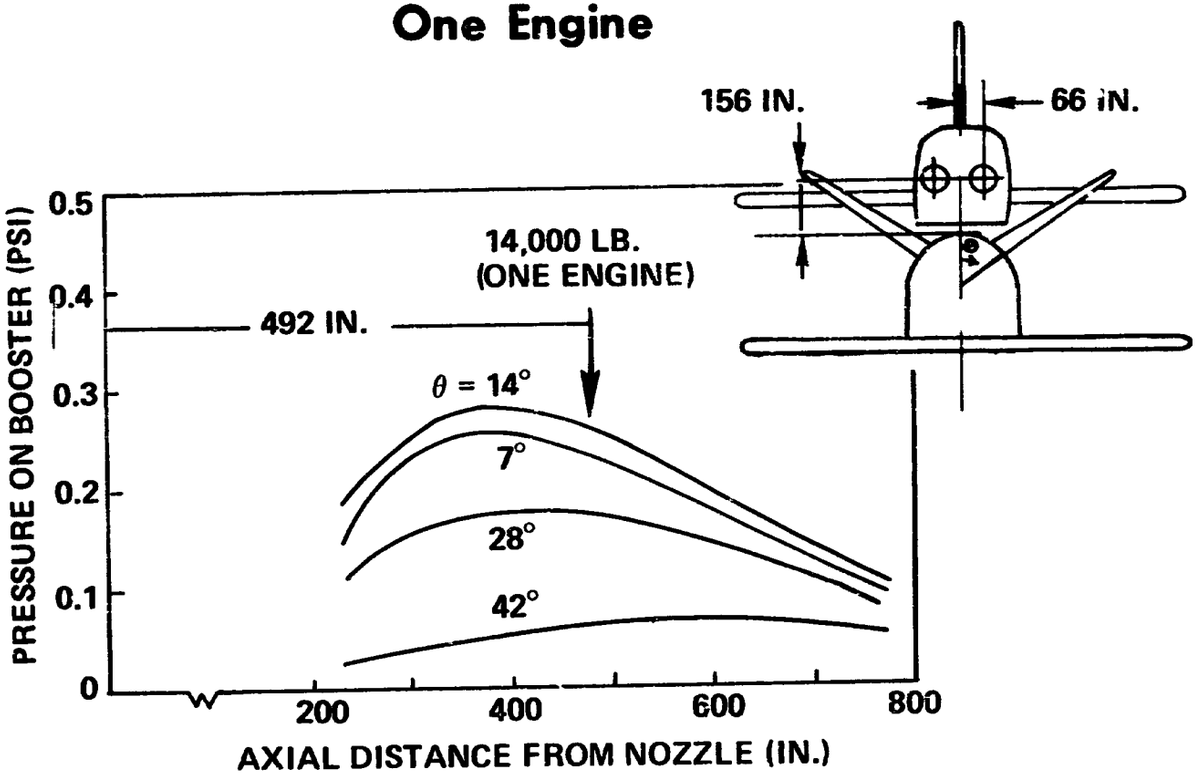

SUPPORTING RESEARCH & TECHNOLOGY

Several key areas have been identified as requiring definition before selection of a separation system is possible, or before requirements for the separation system can be fully described. These items, in order of importance, are described.

1. Interference Aerodynamics - Assuming the system must operate during portions of the trajectory when there is significant dynamic pressure, then the aerodynamic forces will undoubtedly define the separation force necessary for successful operation. Wind tunnel testing is required to provide the necessary aerodynamic force information. Force data must be provided for interference effects between the vehicles, for all possible relative positions of the booster and orbiter element, during the separation trajectory. The test program must account for abort at sufficient points on the trajectory as well as normal separation. If exhaust plumes are in the vicinity of the vehicle, these must also be simulated in the tests. Multi-degree of freedom captive trajectory capability, at least 8 or 9 degrees of freedom must be developed for final system verification. Buffet response testing will be necessary if separation is to occur in high dynamic pressure.

2. Plume Impingement - Several separation concepts will incur considerable plume impingement. Tests should be undertaken to define the heating and pressures incurred from exhaust plume for the relative orbiter/booster positions in separation trajectories for normal and abort separation. Particular attention should be devoted towards defining the interference effects of exhaust plumes from two engines. Analyses techniques, verified by the above tests, should be developed to predict impingement heat input, pressures, total forces, and total moments. The effects of aerodynamic/plume interference at abort conditions must be evaluated by testing.

3. Propellant Motions - Propellant in the booster tanks during abort will respond to changing vehicular linear and angular accelerations resulting in propellant motion in the tanks which in turn, will cause the booster to undergo erratic behavior. These motions, although probably too slow to affect separation clearance, could place excessive demands on the vehicle control system. Analyses techniques should be developed which describe the propellant motions under abort conditions.

SUPPORTING RESEARCH & TECHNOLOGY REQUIRED

INTERFERENCE AERODYNAMICS

- CAPTIVE TRAJECTORY WIND TUNNEL TESTS
- ORBITER-BOOSTER RELATIVE ORIENTATION
- ABORT & NORMAL SEPARATION PARAMETERS
- BUFFETING FOR HIGH-Q ABORT

PLUME IMPINGEMENT EFFECTS

- ANALYSIS TECHNIQUES VERIFIED BY TESTS
- PLUME/AERODYNAMIC INTERFERENCE EFFECTS
- TESTS FOR IMPINGEMENT HEATING & PRESSURES

BOOSTER ABORT PROPELLANT MOTIONS

- DESCRIPTION OF MOTION DURING ACCELERATION VARIATION
- TESTS FOR VERIFYING ANALYSIS

SUMMARY

Investigations should continue on the alternative staging methods such as separation rockets, pistons, rails, linkages or aerodynamic separation. Each technique has advantages and disadvantages. For example, pistons reduce plume heating effects. Rockets will require additional attach points and doors. Aerodynamic separation will require a higher staging dynamic pressure (i.e., performance reduction) but perhaps simplifying separation system hardware. These techniques must be reevaluated considering both nominal separation and abort separation. Abort, in addition to large aerodynamic forces, will introduce unknowns in engine controllability (for propulsion system failures) and many other additional factors to be considered in separation system requirements and design.

Evaluation criteria must consider separation distance time history from a clearance as well as potential explosion hazard for the abort conditions. Weight penalties associated with each concept must be identified, including systems and structures required in the concept and such factors as added thermal protection to account for plume effects. ΔV losses incurred during the coast period or by application of separation forces are to be considered. Disturbances to the orbiter and booster should not require excessive additional vehicle control capability. The ability of the system to perform under abort conditions for the total ascent phase or portions thereof must be established consistent with the abort philosophy.

Research must be conducted to establish interference effects on aerodynamics during separation. Exhaust plume impingement analyses must be developed and verified by tests for adequate representation of separation. For abort conditions, analysis techniques describing motions of the unused propellant in the booster must be developed and verified by tests.

BIBLIOGRAPHY

1. Hurley, M. J., "Digital Program P5255: A six-Degree, Multiple-Body Separation Simulation for Hinged and/or Linked Lifting-Entry Vehicles," Volumes I and II, Convair division of General Dynamics Report GDC-ERR-1377, December 1969.

2. Lanfranco, M.J., "Wind-Tunnel Investigation of the Separation Maneuver of Equal-Sized Bodies," AIAA Paper No. 70-260, presented at AIAA Advanced Space Transportation Meeting, Cocoa Beach, Fla., February 1970.

3. Black, R.L., "High-Speed Store Separation - Correlation Between Wind-Tunnel and Flight-Test Data," J. Aircraft, Vol. 6, No. 1, Jan.-Feb. 1969, pp 42-45.

4. SAMSO-TR-69-348, "Space Transportation Systems Study," Volume III, "FR-4 Studies, Study Trades and Conclusions," (Confidential), Section 19.12, "Separation System Analysis" (unclassified); November 1969.

GROUND-WIND-LOAD CONSIDERATIONS FOR SPACE SHUTTLE VEHICLES

by Wilmer H. Reed III

NASA-Langley Research Center
Hampton, Virginia

INTRODUCTION

Four years ago a technical meeting on ground-wind load problems in relation to launch vehicles was held at Langley Research Center (ref. 1). In the concluding session of that meeting, a panel addressed the question: "Where do we go from here? - the designer's viewpoint." We probably shouldn't be too critical of that panel for failing to include in their crystal-ball-look into the future, consideration of vehicle launch operations such as the following: Take an orbiter vehicle that resembles a Douglas DC-8 jet transport; strap it piggyback to a booster vehicle that resembles a Boeing 747 superjet transport; mount the combination vertically on a launch pad; design the system to withstand a 70-knot wind, and then be launched vertically in a 35-knot wind. Today, we call the concept Space Shuttle.

In the area of ground-wind loads, as in other technical areas, the space shuttle concept presents a full measure of challenging problems For example, in addition to the usual ground-wind load problems dealt with on previous launch vehicles, such as steady drag loads, gust loads and vortex shedding, we also foresee new problems, some with interesting names such as "stop-sign flutter" and "galloping" stability. In this paper, we will attempt to identify and focus attention on those areas which space vehicle designers have heretofore been able to ignore, but which are likely to be of key importance on Space Shuttle configurations.

SPACE SHUTTLE GROUND-WIND-LOAD CONSIDERATIONS

This figure presents a brief list of factors to be considered in designing a vehicle to withstand the effects of ground wind. First, one must specify an appropriate ground-wind environment for various phases of operation. The design wind environment for space shuttle vehicles is specified in reference 2 in terms of steady wind profiles and turbulence spectra. A requirement stated in reference 2 is that the space shuttle shall be capable of withstanding peak ground winds up to 72 knots at the 60-foot level during stay-periods on the launch pad. The ground-wind environment creates loads on the vehicle which are both steady and dynamic. The dynamic load components can be associated with fluctuations in the wind itself, vortices shed from the structure, or some form of aerodynamic instability such as "stop-sign flutter" or "galloping" stability.

These loads and responses create such problems as the following: stresses in the vehicle and the associated tie-down structures; clearance requirements to allow for relative deflections between vehicle and ground service structure; fatigue due to the accumulation of long wind-exposure times on reusable vehicles*; ground handling of winged vehicles during towing and erection operations; and finally, guidance alignment difficulties encountered on a swaying structure.

*Note: If the average time on the launch pad were one week per launch, a shuttle vehicle would accumulate approximately two years of wind exposure time during its design life span of 100 missions.

SPACE SHUTTLE GROUND WIND LOAD CONSIDERATIONS

- GROUND WIND ENVIRONMENT
  - STEADY WIND PROFILES
  - TURBULENCE SPECTRA
- VEHICLE LOADS AND RESPONSE
  - STATIC LOADS
  - DYNAMIC LOADS
    - VORTEX SHEDDING
    - TURBULENCE
    - GALLOPING
    - STOP SIGN FLUTTER
- PROBLEM AREAS
  - STRENGTH
  - DEFLECTION
  - FATIGUE
  - GROUND HANDLING
  - GUIDANCE ALIGNMENT

SPACE SHUTTLE GROUND-WIND-LOAD MODEL STUDIES

This figure depicts various ground-wind-load model studies which are planned for Langley wind-tunnel facilities in support of the space shuttle program. The approach is step-by-step, progressing from simple models in low-speed wind tunnels to the complete aeroelastic modeling at high Reynolds numbers of the vehicle-launch pad complex.

First, simple rigid models with interchangeable lifting surfaces will be utilized to isolate and study some specific aerodynamic instabilities. Galloping instabilities - the tendency of noncircular blunt bodies to oscillate in the cross-stream direction - are being explored in the Langley 12-Foot Low-Speed Wind Tunnel. More will be said about these studies later in this paper.

In a second phase, with the same model used in galloping studies, stop-sign flutter - a stall-flutter type phenomenon which involves single-degree-of-freedom oscillations of a lifting surface - will be investigated in the 7- by 10-Foot High-Speed Tunnel. These studies will employ a special oscillating-sting mount developed for measuring airplane roll damping derivatives.

The third phase of ground-wind-load model studies will be conducted in the Transonic Dynamics Tunnel in freon. In these studies, light-weight rigid models of coupled booster-orbiter configurations will be attached to a flexible mount system. The mount has variable stiffness and damping features in order to simulate the fundamental cantilever bending and torsion modes of the vehicle. During this phase of the study, in which Marshall Space Flight Center and Langley Research Center will be joint participants, it is expected that considerable effort will be devoted to the evaluation of methods for alleviating excessive wind-induced oscillations of the shuttle vehicle.

It will be recalled (ref. 3) that in similar ground-wind-load studies on Saturn V, a requirement for additional structural damping was established and was subsequently implemented at the launch site in the form of viscous dampers between the vehicle and launch tower. After the space shuttle vehicle design has been defined, studies of complete aeroelastic models of the vehicles and launch structures will be conducted in the Transonic Dynamics Tunnel. Included as an important aspect of these final studies will be evaluations of wind-load effects during vehicle erection.

SPACE SHUTTLE GROUND WIND LOAD MODEL STUDIES

GALLOPING

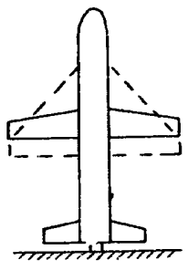

Static loads

STOP SIGN FLUTTER

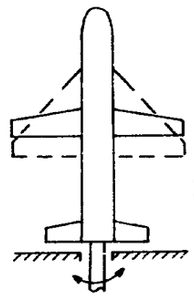

Forced oscillations

VORTEX SHEDDING AND INSTABILITIES

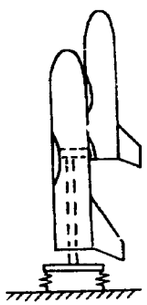

Variable mount
(Stiffness/damping)

FINAL DESIGN VERIFICATION

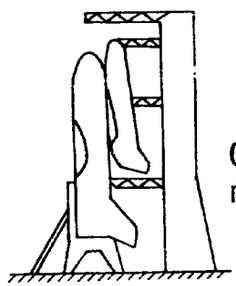

Complete aeroelastic
model

AERODYNAMIC FORCES AFFECTING GALLOPING STABILITY OF BLUFF BODIES

Galloping instability is so-named because it is descriptive of the low-frequency, high-amplitude oscillations that are sometimes observed on ice-loaded transmission conductor lines exposed to wind. For such instabilities, an essential feature is that the body cross-section shape is such that a steady-state lift force is developed, and that the rate of change of this force with wind incidence angle (angle of attack) is negative. With reference to figure 3, it can be seen that when this condition exists, the change in lift force associated with the change in relative wind direction due to body motion, $\dot{y}/v$, acts in the same direction as the motion, and therefore tends to reinforce, rather than dampen, the motion. As a necessary condition for galloping, Den Hartog gave the following criterion in reference 4: A section is dynamically unstable if the negative slope of the F_A^{lift} force is greater than the drag force,

i.e., $$\frac{\Delta L}{\Delta \alpha} + D < 0$$

Although the galloping phenomenon is well-known and has been studied extensively in relation to transmission lines, towers, and bridges (see, for example, references 4 through 8), it has received little attention by launch vehicle designers. This is not surprising since most existing launch vehicles have basically circular cross-sections which cannot produce the necessary steady-state lift forces required for galloping excitation. On of the other hand, looking at the typical D-shaped body cross-section of some space shuttle configurations, one might conclude that the prototype design had been Den Hartog's galloping demonstration model (ref. 4, page 301). Thus, it is expected at the galloping phenomenon will play a prominent role in space shuttle ground-wind-load studies.

Footnote: In the oral presentation, motion pictures were shown which demonstrated galloping and stop-sign flutter on small wind-tunnel models. Copies of the film are available for loan from NASA-Langley Research Center.

AERODYNAMIC FORCES AFFECTING GALLOPING STABILITY OF BLUFF BODIES

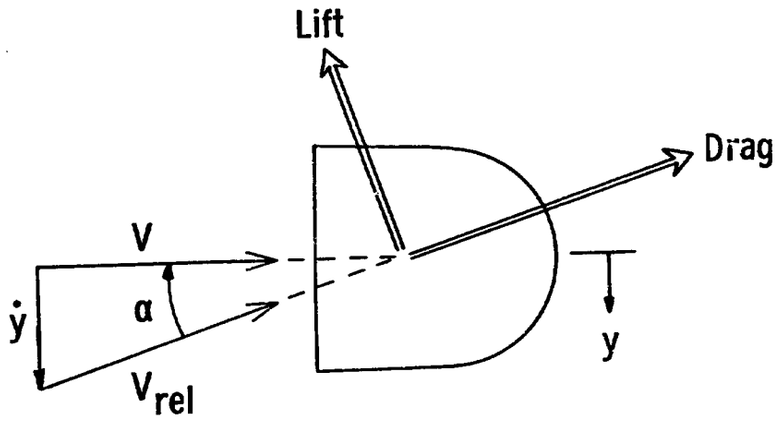

Galloping is possible when $C_{L_\alpha} + C_D < 0$

SPACE SHUTTLE GROUND-WIND-LOAD MODELS

To explore the galloping characteristics of representative space shuttle configurations, static aerodynamic forces and moments were measured on the models shown in figure 4. These studies, referred to earlier in figure 3, were conducted in the Langley 12-Foot Low-Speed Wind Tunnel. The model consisted of a basic body onto which various lifting surfaces could be attached. Fiberglas-foam sandwich construction resulted in a light-weight, rigid model structure. The model was mounted on a 5-component turntable balance located beneath a ground board, and could be rotated about its longitudinal axis so as to cover an 180-degree range of wind azimuth angles. In addition, two accelerometers were mounted near mid-body to sense horizontal accelerations of the model.

Some pertinent model properties are as follows: The body cross-section had an 8-1/2 inch wide flat bottom; flat sides slope inward at 7-1/2 degrees coming tangent to a 3-inch radius circle which forms the upper side; the bottom corners have 3/8-inch radii. Overall dimensions of the body are 62-inch length, 8-1/2 inch width, and 12-inch depth. The wing of the straight-wing configurations had a 7.36 aspect ratio, 0.42 taper ratio, 7 degree dihedral angle, and an NACA 0012-64 airfoil section. The wing of the delta-wing configuration had a 50 degree swept leading edge, 2.66 aspect ratio, 0.14 taper ratio, zero dihedral angle, and a 3-percent-thick symmetrical airfoil section.

SPACE SHUTTLE GROUND WIND [illegible]

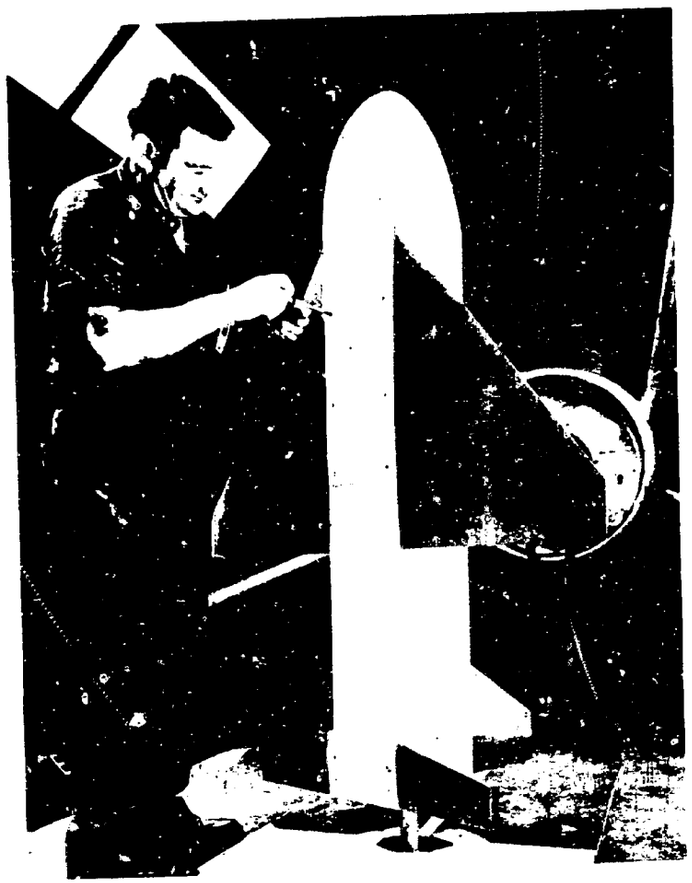

DELTA WING

STRAIGHT W[illegible]

STATIC AERODYNAMIC COEFFICIENTS FOR A SPACE SHUTTLE CONFIGURATION ON LAUNCH PAD

This figure shows the variation of static lift and drag coefficients with wind azimuth angle for the straight wing configuration pictured in the previous figure. (The reference area is taken to be the total projected area of the wings, body, and horizontal tail.) Regions of possible instability, as given by the Den Hartog criterion, are indicated by shaded sections on the C_L curve. (Note that negative C_L has been plotted.) From the slope of the lift-curve, it can be seen that galloping instability should be most pronounced when the flat bottom side of the body faces upstream ($\alpha = 0$); conversely, the system should be most stable when the flat side faces downstream ($\alpha = 180^0$). (These stability trends were clearly displayed in the motion picture demonstrating galloping stability.)

STATIC AERODYNAMIC COEFFICIENTS FOR A SPACE SHUTTLE CONFIGURATION
ON LAUNCH PAD

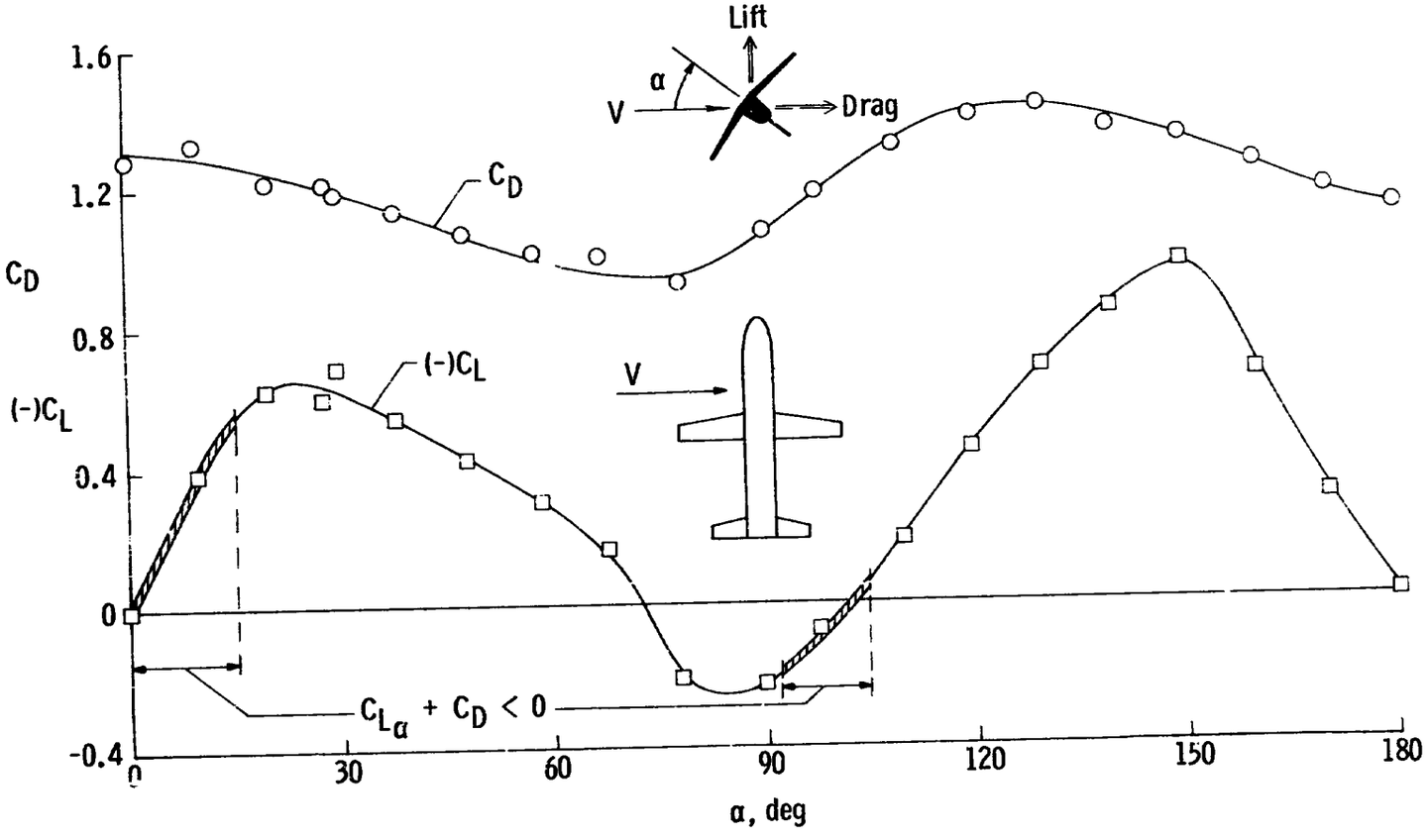

GALLOPING STABILITY AERODYNAMIC COEFFICIENTS FOR SOME SPACE SHUTTLE CONFIGURATIONS ON LAUNCH PAD

This figure shows lift and drag coefficients plotted against wind azimuth angle, as in the previous figure, for three configurations: fuselage alone, straight wing, and delta wing. The reference area in each case is the total projected area of the planform in question.

GALLOPING STABILITY AERODYNAMIC COEFFICIENTS FOR SOME SPACE SHUTTLE CONFIGURATIONS ON LAUNCH PAD

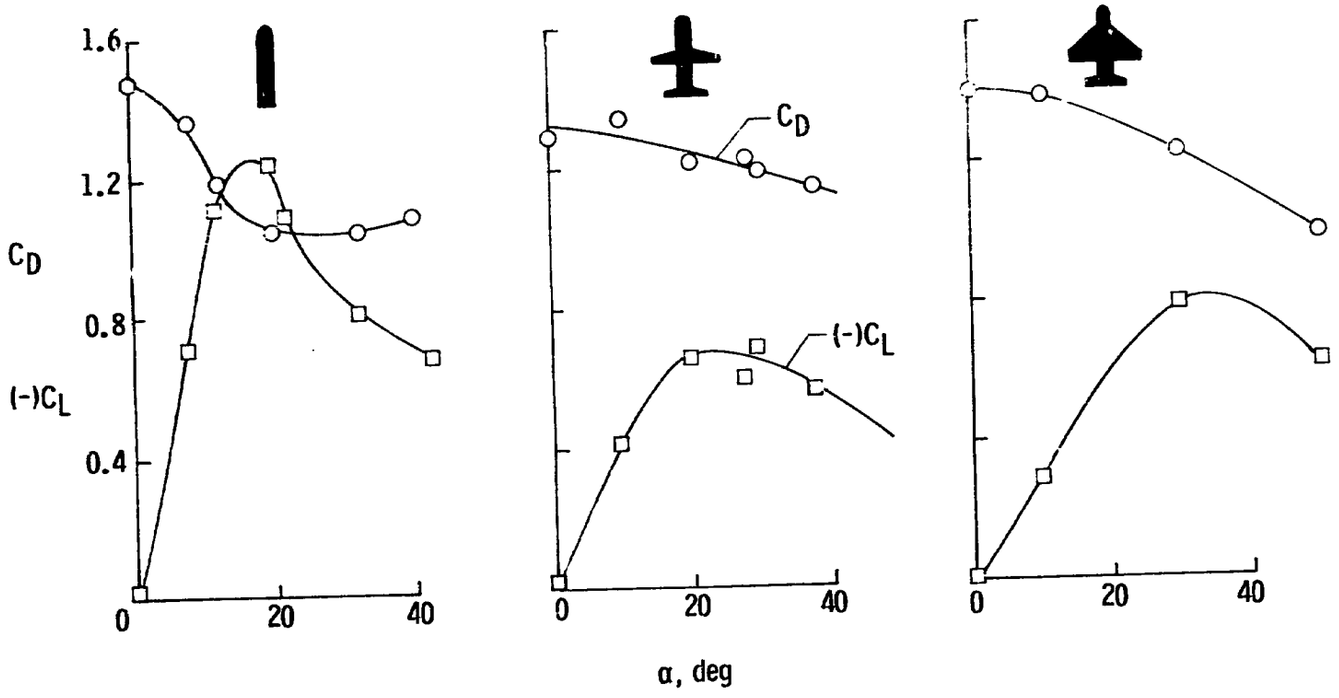

PREDICTED GALLOPING STABILITY BOUNDARIES

In this figure the aerodynamic coeffcients presented in figure 6 have been utilized to predict galloping stability boundaries for each of the three configurations. The ordinate in the figure is a nondimensional velocity ratio V/fD in which V is the wind velocity, D is the body width, and f is the natural frequency (in Hz) of the vehicle for an assumed single-degree-of-freedom translation mode in the cross-stream direction. The abscissa is a nondimensional inertia damping parameter

$$\frac{2\,\delta_s m}{\rho D^2}$$

in which δ_s is the log decrement damping of the structure, m, average vehicle mass per unit length, and ρ, air density. These stability boundaries can be derived by equating the work per cycle done on the body by aerodynamic forces to the work per cycle dissipated by structural damping. The shaded area in the figure gives an approximate indication of the region covered by representative cantilevered-mounted space shuttle boosters exposed to the design peak wind speed. (Structural damping was assumed to be one percent of critical damping.) The right side of the shaded area represents the full-fuel condition, and the left side the empty-fuel condition. Some key points to be made about this figure are: lifting surfaces attached to the body have a strong stabilizing influence on galloping; at the design peak ground-wind-speed for the space shuttle (72 knots at 60-foot height), the figure indicates that a straight wing shuttle booster configuration will experience galloping for the empty fuel condition; and, for the body without wings, galloping would occur for all weight conditions.

PREDICTED GALLOPING STABILITY BOUNDARIES

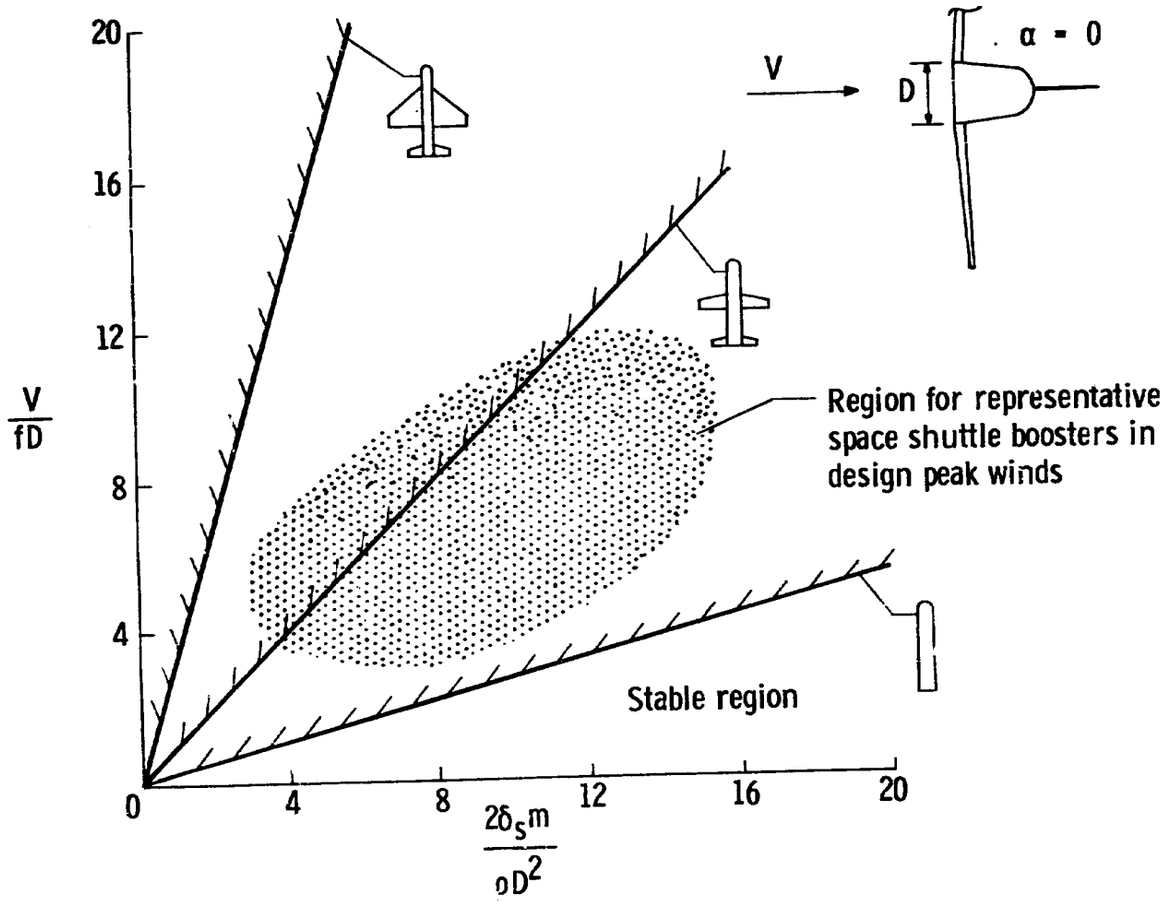

ACCELEROMETER TIME HISTORIES MEASURED ON SPACE SHUTTLE GROUND-WIND-LOAD MODELS

This figure shows sample acceleration time histories measured on the three models under identical wind tunnel conditions ($V = 50$ ft/sec, $\alpha = 0$). The fundamental frequency of the model in each case was approximately 7.0 Hz, and the corresponding mode shape was essentially that of a rigid model pivoted near its base. It is gratifying to note that these results support the predictions shown in figure 7 regarding the effects of the wing on galloping stability.

ACCELERATION TIME HISTORIES

MEASURED ON SPACE SHUTTLE GROUND WIND LOAD MODELS

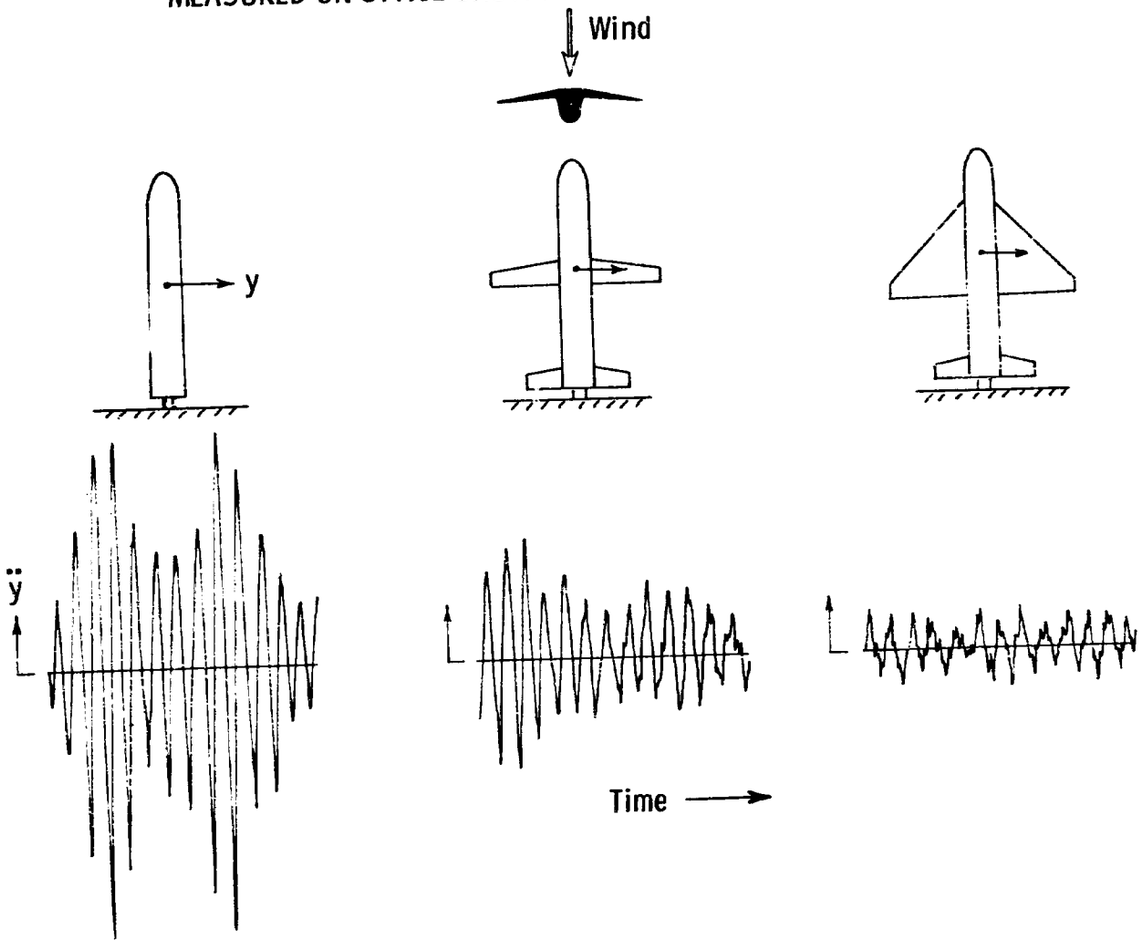

SUMMARY AND CONCLUDING REMARKS

The requirement for reusable space shuttle vehicles to withstand the effects of ground winds poses some formidable problems. This paper attempts to identify and focus attention on some new problem areas which designers of past launch vehicle systems have been able to ignore, but which are very likely to be significant on space shuttle vehicles. Among such problems are: structural fatigue due to the high accumulated wind exposure time on a reusable vehicle; ground handling during erection of large winged vehicles exposed to wind forces; vortex shedding, stop-sign flutter, galloping stability, and possibly other wind-induced aerodynamic instabilities associated with the geometric shape of space shuttle configurations.

Wind-tunnel results obtained from a preliminary investigation of galloping stability for models of typical space shuttle configurations are presented. Indications from this study are: wind-induced galloping oscillations could occur on shuttle vehicles within the design ground wind speed range; the light-weight vehicle condition is least stable; and lifting surfaces attached to the body tend to have a strong stabilizing influence on galloping stability.

REFERENCES

1. Meeting on Ground-Wind-Load Problems in Relation to Launch Vehicles. NASA TM X-57779, NASA-Langley Research Center, June 7-8, 1966, (N-66-32226)

2. Natural Environment Criteria for the NASA Space Shuttle Program. W. W. Vaughan, Coordinator, NASA TM C-53973, February 9, 1970

3. Jones, George W., Jr.; and Farmer, Moses G.: Wind-Tunnel Studies of Ground-Wind Loads on Saturn Launch Vehicles. Proceedings of AIAA/ASME Seventh Structures and Materials Conference, April 1966, pp. 377-381

4. Den Hartog: Mechanical Vibrations. McGraw-Hill Book Co., Inc., New York, N. Y., 4th Edition, 1956

5. Scruton, C.: On the Wind-Excited Oscillations of Stacks, Towers and Masts. Symposium on Wind Effects on Buildings and Structures, Teddington, England, 1963

6. Richardson, A. S.; Martucelli, J. R; and Prise, W. S.: Research Study on Galloping of Electric Power Transmission Lines. Symposium on Wind Effects on Buildings and Structures, National Physical Laboratory, Teddington, England, 1963, pp. 612-686

7. Parkinson, G. V.; Santosham, T. V.: Cylinders of Rectangular Section as Aeroelastic Nonlinear Oscillators. ASME Vibrations Conference, Boston, Mass., March 19-31, 1967

8. Novak, Milos: Aeroelastic Galloping of Prismatic Bodies. Journal of the Engineering Mechanics Div., Proceedings of the Am. Soc. of Civil Engineers, Vol. 95, February 1969

WIND TUNNEL SIMULATION OF GROUND WIND SHEAR AND TURBULENCE SPECTRA WITH POSSIBLE APPLICATION TO SPACE SHUTTLE LAUNCH PROBLEMS

R. J. Templin, National Research Council, Canada

INTRODUCTION

It seems to be generally agreed that wind tunnel testing of aeroelastic models is an essential part of the investigation of the dynamic effects of ground-level winds on launch vehicle configurations. However, a deficiency in practically all such tests so far carried out has been the failure to simulate, in the wind tunnel, the correct wind mean velocity shear, turbulence intensity and power spectrum. This deficiency becomes more serious when vehicle configurations depart from simple cylindrical shapes, as is the case with the space shuttle launch configuration, because of the increased difficulties in the analytical prediction of ground wind loads.

Three techniques are briefly described, which have been developed or put to use in Canada, for the wind tunnel simulation of low-altitude, neutrally stable winds, mostly for non-aerospace structural applications. Each has its advantages and disadvantages, but any of them may be applicable in future launch vehicle wind tunnel tests.

JUPITER MODEL IN SIMULATED TERRAIN ROUGHNESS

Probably the most reliable method of simulating the neutrally-stable gound wind layer in wind tunnels is that pioneered by Jensen in Denmark, and further developed in specially-designed wind tunnels at Colorado State University (Reference 1) and at the University of Western Ontario (Reference 2). In this technique, natural terrain roughness is simulated along the floor of the tunnel test section, which may be up to 90 feet in length. This permits the growth of a boundary layer between two and four feet thick near the downstream end. Measurements of mean velocity profile, turbulence intensity variation with height, and the power spectrum of turbulence within this layer are in good agreement with full-scale measurements over various types of terrain.

As far as is known, only one launch vehicle configuration has been tested using this wind tunnel technique. Figure 1 is a photograph of a 1:30 scale aeroelastic model of the Jupiter vehicle in the University of Western Ontario tunnel during 1966. This investigation was carried out under a NASA grant, as a part of a research program to compare dynamic model measurements with full-scale measurements of vehicle response.

Although this method appears to be the most highly developed technique for ground wind simulation in wind tunnels, it is not adaptable to conventional aeronautical tunnels, since it requires a test section length about 10 times the section width or height.

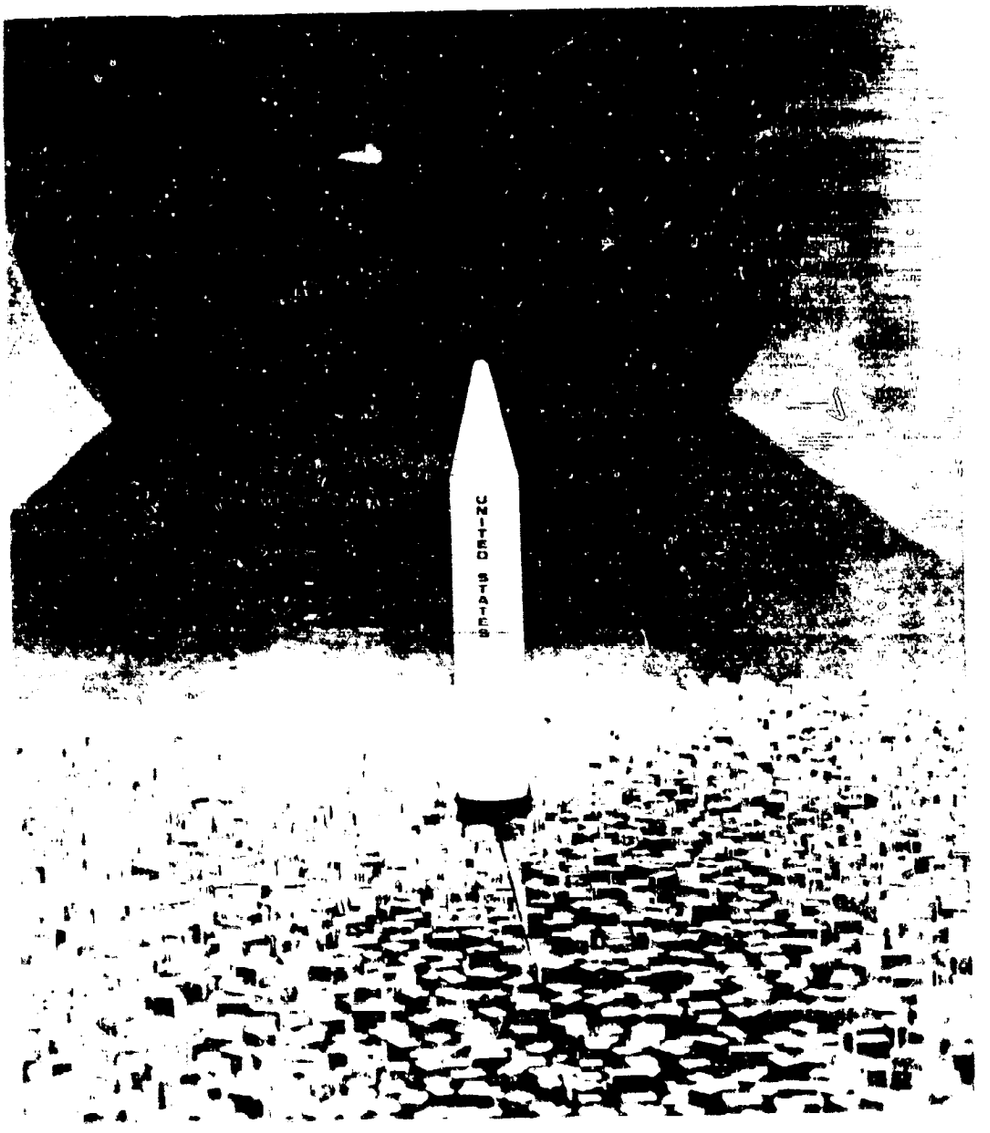

FIG. 1. JUPITER MODEL IN UNIVERSITY OF WESTERN ONTARIO TUNNEL

RESPONSE OF AEROELASTIC JUPITER MODEL IN TURBULENT BOUNDARY LAYER

Figure 2 shows the unsteady response, in non-dimensional form of the 1:30 scale aeroelastic Jupiter model in the University of Western Ontario boundary layer wind tunnel. The curve labelled σ_X shows the R.M.S. deflection at the top of the model in the wind direction and the curve labelled σ_Y is the transverse response. H is the total height of the model and the mean wind speed U_H is that at height H. The reduced wind velocity has been made non-dimensional by dividing by the product of model natural bending frequency f and the diameter D.

The figure illustrates one of the effects of simulating, as nearly as possible, the complete wind turbulence spectrum. In tests of similar models in smooth wind tunnel flow, the phenomenon of vortex shedding from tall cylindrical structures often results in a large-amplitude response over a narrow resonant speed range, with little response outside this range. In turbulent flow, especially with substancial low-frequency content, the vortex-shedding resonant response may be entirely absent or greatly reduced. The small peaks in the curves of Figure 2 occur at a value of the reduced velocity (which is a form of inverse Strouhal number) where vortex-shedding resonance would be expected. In this case, however, the amplitude is almost lost in the overall response which now extends over the whole velocity range.

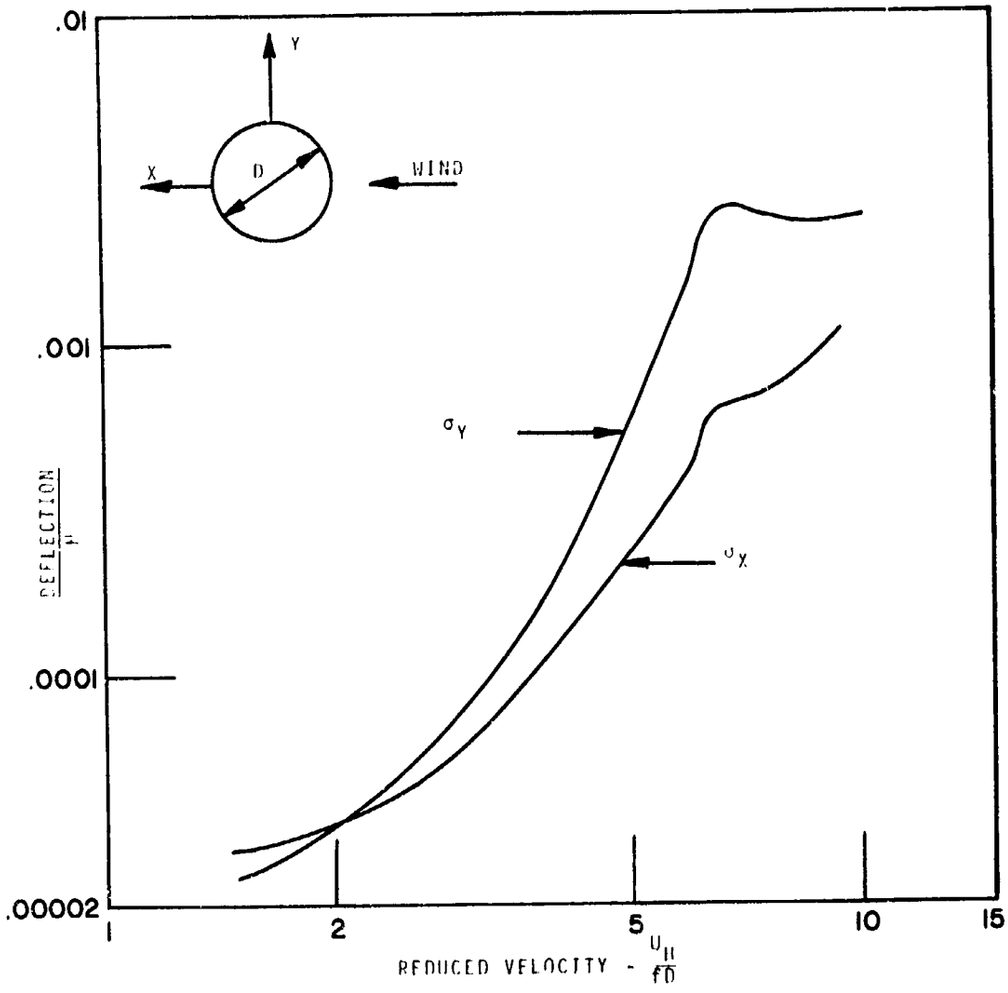

FIG. 2 RESPONSE OF AEROELASTIC JUPITER MODEL IN TURBULENT BOUNDARY LAYER

CITY OF MONTREAL MODEL IN N.R.C. 6 x 9 FOOT TUNNEL

Figure 3 is a photograph of a 1:400 scale model representing about one mile of downtown Montreal in the National Research/National Aeronautical Establishment 6 x 9 ft. wind tunnel in Ottawa. The purpose of this test was to obtain spectra of unsteady pressures on the face of the tall building near the centre of the picture, for comparison with full-scale measurements that had been made previously.

The photograph also shows an array of 4-foot plywood "spires" at the upstream end of the test section. This technique has been developed as a means of producing thick, turbulent shear layers in the relatively short test sections that are typical of aeronautical wind tunnels (Reference 3). At a downstream distance of about 3 or more spire heights, the boundary layer characteristics appear to settle down so that the mean velocity profile, turbulence intensity and spectrum are reasonably similar to corresponding full-scale data. The spires are tapered in order to control the mean velocity profile, and their coarse geometry is required in order to generate turbulence of sufficiently large scale. There is some similarity between this technique and one developed in the U. K. by Counihan at the Central Electricity Research Laboratories (Reference 4).

Techniques of this type appear to have reached a stage of development such that they can be used with some confidence for aeroelastic response measurements on tall structures. A possible disadvantage is that the drag of the spire array is large, and in some wind tunnels may cause fan stall.

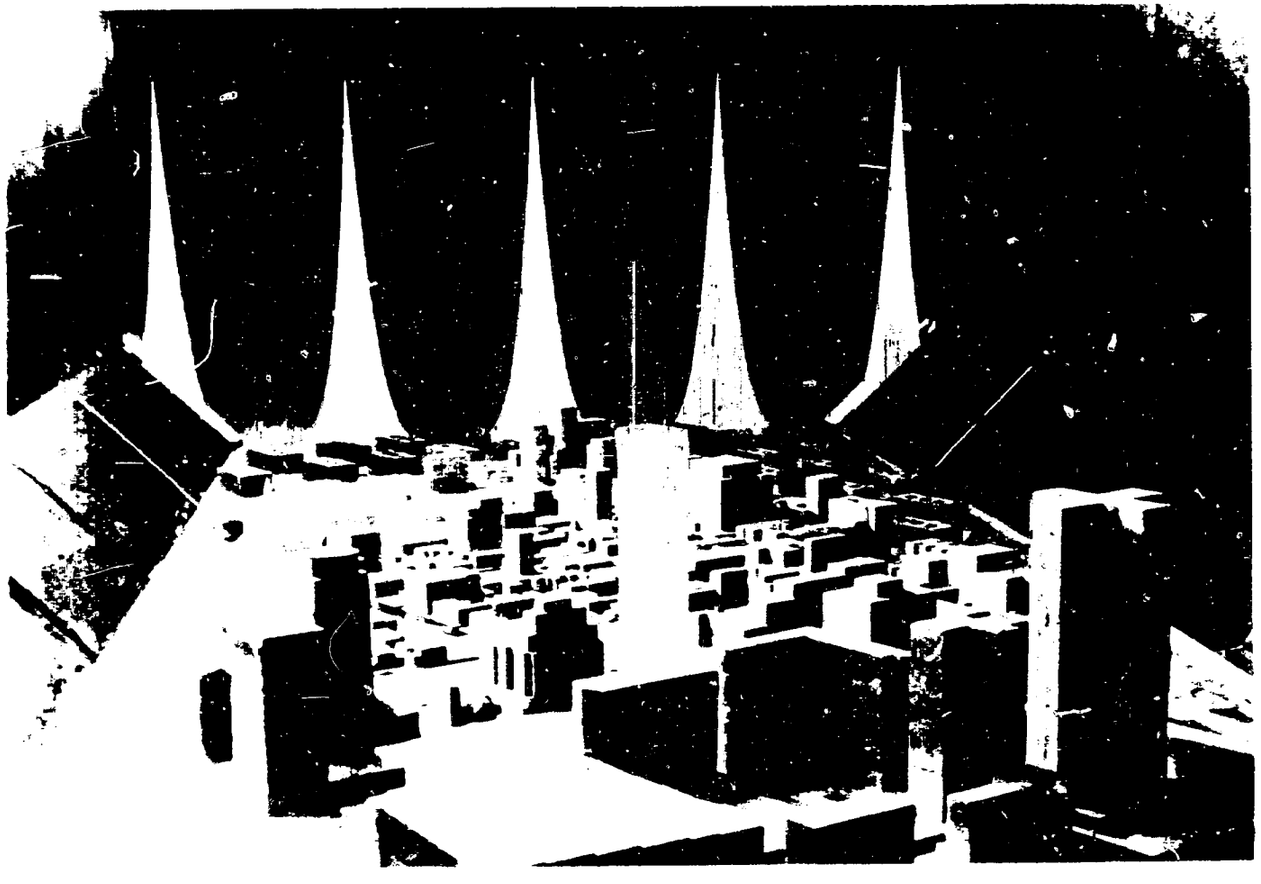

FIG. 3. CITY OF MONTREAL MODEL IN N.P.C. 6 x 9 FT. TUNNEL

TALL BUILDING PRESSURE SPECTRA

Using the spire technique, unsteady pressure spectra have been determined at several locations on the tall building model shown in the previous Figure. A representative result is shown for comparision with full-scale measurements in Figure 4.

In this graph the spectra are normalized with respect to the mean squared pressure fluctuation, and the reduced frequency has been made non-dimensional by multiplying by the height at the top of the roof tower (800 ft. full scale) and dividing by the mean wind speed measured at that height.

The shaded area representing full-scale measurements is an envelope drawn around a large number of separate spectra, which have considerable scatter among themselves. The agreement between model and full-scale measurements is reasonably good, although there are indications that the model spectrum is shifted toward higher frequencies. The comparision of the spectra of longitudinal turbulence measured at the height H (now shcwn here) displays the same trend, suggesting that the spire technique has not fully reproduced the largest scale motions in the lower atmosphere.

The advantage of this technique is its adaptability to any low speed wind tunnel, with a potential for producing shear layers of thickness approaching the tunnel height. A disadvantage in some cases is the large drag of the spire array.

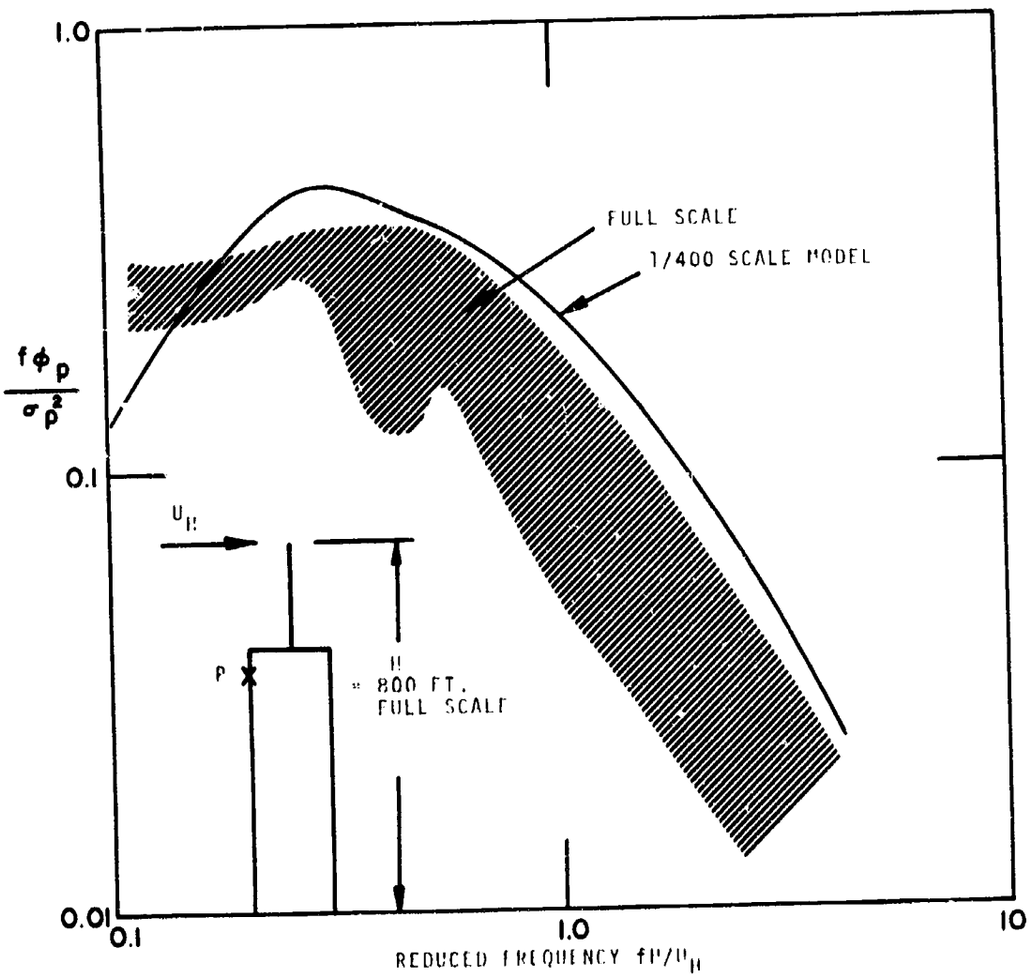

FIG. 4 TALL BUILDING PRESSURE SPECTRA AT POINT P

UNIVERSITY OF TORONTO TURBULENT JET LATTICE

A method for generating shear flow with associated large-scale turbulence in wind tunnels has been under development at the University of Toronto for about two years (Reference 5). In this method a lattice of jet outlets oriented parallel to the tunnel axis produces the turbulent flow, and by separate regulation of the jet pressures can be made to control the mean velocity gradient. A photograph of the small-scale experimental jet array is shown in Figure 5. In experiments carried out so far, the jet array also constitutes the sole method of propulsion of the wind tunnel, which is of the open circuit type.

Although this technique has not yet been applied in large-scale wind tunnels, it offers several possible advantages. It does not introduce large drag into the tunnel circuit, and in fact can be used for propulsive purposes. It would appear to be more flexible with respect to the control of mean velocity gradient. A possible disadvantage may be its cost and complexity when adapted to large scale, but if coupled to a short, large-scale open-circuit tunnel this complexity may be offset by the fact that the jet system can also act as the tunnel drive system.

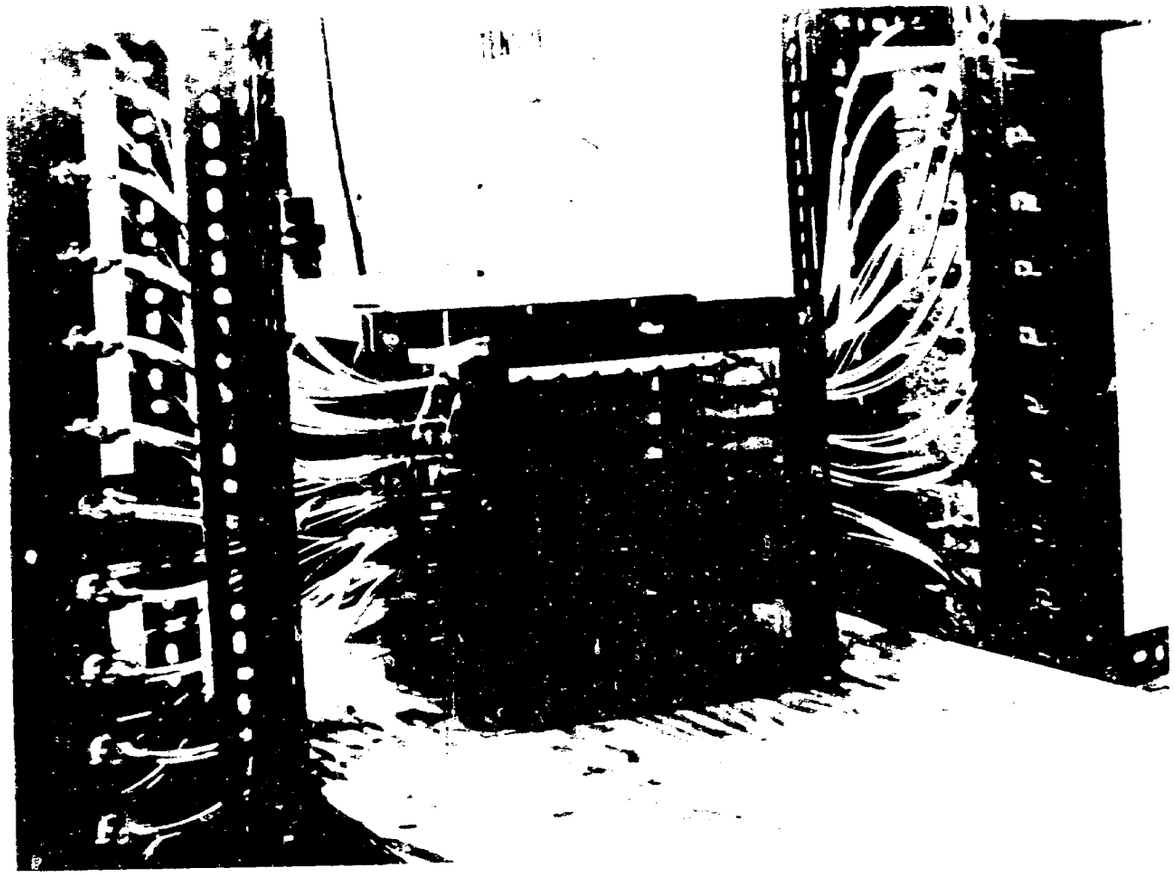

FIG. 5. UNIVERSITY OF TORONTO TURBULENT JET LATTICE

LONGITUDINAL VELOCITY SPECTRUM WITH JET-INDUCED SHEAR FLOW

When the array of jets shown in the previous Figure are blown with uniform momentum so as to produce a uniform mean velocity distribution further downstream, the turbulence characteristics are somewhat similar to those downstream of a square lattice of drag elements, except that, for a given lattice mesh size, the longitudinal integral scale of turbulence is about twice as large for the jets as for a drag lattice. The R. M. S. turbulence intensity decreases with increasing downstream distance, and is about 10 percent of the mean velocity at about 15 mesh widths.

The character of the turbulent flow changes in certain respects when the jets are controlled so as to produce an approximately uniform mean shear across the tunnel. The R. M. S. turbulence, as a percentage of mean velocity, now varies through the shear layer in a manner somewhat similar to that in a boundary layer, and on the tunnel centre-line it remains roughly constant with dowstream distance. Furthermore, the integral scale becomes comparable with the width of the shear layer itself, and is much larger than that produced in uniform flows. Figure 6 shows one measurement of the longitudinal power spectrum of turbulence in shear flow. Its overall shape is in at least qualitative agreement with that in the natural wind layer.

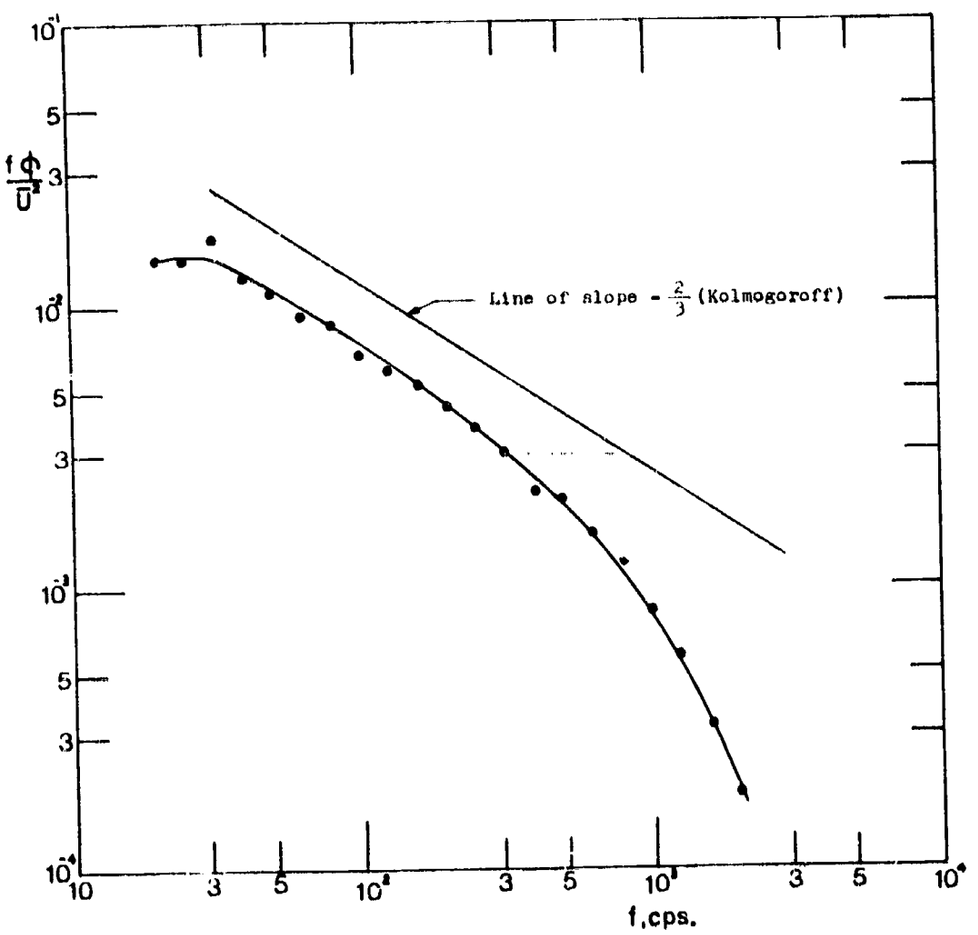

FIG. 6 LONGITUDINAL VELOCITY POWER SPECTHAL DENSITY - SHEAR FLOW

CONCLUSIONS

This paper has briefly described three techniques for the wind tunnel simulation of the natural wind layer at low altitudes, with possible application to space shuttle launch vehicle problems. All happen to have been recently developed or adopted in Canada, but this choice is due only to the author's familiarity with them, and related developments have taken place in other countries as well. They appear to offer means of rectifying a deficiency that has characterized almost all previous wind tunnel tests of aeroelastic launch vehicle models. In particular:

1. Thick turbulent boundary layers that simulate the neutrally stable ground wind layer can be generated over a long fetch of surface roughness in specially-designed wind tunnels with long test sections. Tunnels of this type have been in operation for some years at Colorado State University and at the University of Western Ontario. The latter has been used for exploratory aeroelastic model tests of a Jupiter launch vehicle.

2. At NRC/NAE in Ottawa, an array of shear layer "spires" has been developed, which generates thick shear layers in conventional tunnels, with velocity profiles, turbulence intensity, scale, and spectral shape similar to the neutral wind layer. A similar technique has been developed in England.

3. The University of Toronto Institute for Aerospace Studies has under development a technique for generating turbulent shear layers by means of an upstream array of controllable air jets. In an open circuit tunnel, the jet array appears to be capable of providing the tunnel propulsion system, and of generating shear layers with a depth comparable to the tunnel height, and with appropriate turbulence characteristics.

REFERENCES

1. Cermak, J. E. Laboratory Simulation of Atmospheric Motions in the Lowest One Hundred Meters. Paper presented at Meeting on Ground Wind Load Problems in Relation to Launch Vehicles, Langley Research Center, 7 - 8 January, 1966.

2. Davenport. A. G. and Isyumov, N. The Application of the Boundary Layer Wind Tunnel to the Prediction of Wind Loading. Proceedings of the International Research Seminar on Wind Effects on Buildings and Structures. Paper No. 7, Ottawa, Sept. 1967. University of Toronto Press.

3. Campbell, G. S., and Standen, N. M. Progress Report II on Simulation of Earth's Surface Winds by Artificially Thickened Wind Tunnel Boundary Layers. National Aeronautical Establishment Laboratory Technical Report LTR-LA-37. July 1969.

4. Counihan, J. A Method of Simulating a Neutral Atmospheric Boundary Layer in a Wind Tunnel. Paper No. 14, Proceedings of the AGARD Conference on Aerodynamics of Atmospheric Shear Flows, Sept. 1969. AGARD CP No. 48.

5. Teunissen, H. W. An Ejector-Driven Wind Tunnel for the Generation of Turbulent Fows with Arbitrary Mean Velocity Profile. University of Toronto Institute for Aerospace Studies Technical Note No. 133.

LIFTING AND CONTROL SURFACE FLUTTER

by Robert C. Goetz

National Aeronautics and Space Administration
Langley Research Center
Hampton, Virginia

SUMMARY

Employing the space shuttle vehicle as a center of discussion, several potential problem areas of lifting and control surface flutter are surveyed. Topics very briefly discussed include flutter of planar lifting surfaces, stall flutter, interference flutter, control surface instabilities, and lifting surface - body flutter. Proposed or needed research in those areas where the state of the art is not presently sufficient to insure a safe and reliable space shuttle mission are delineated.

INTRODUCTION

The degree of interaction between aerodynamic, elastic, and inertial forces - which are the basic ingredients causing lifting and control surface flutter - is very much a function of a vehicle's design and the severity of its operating mission. In the concepts for a recoverable and reusable space shuttle system, one sees emerging a new generation of vehicles: the offspring of a marriage between the design technologies of airplanes and launch vehicles. The vehicle mission includes vertical launch, separation, orbit, winged reentry, and conventional landing. This broad mission, together with the criticality of the vehicle's payload to weight ratio, highlights many areas of flutter technology that need refinement, and as with any new class of vehicle, new potential problem areas. The space shuttle program will thus push the state of the art of a great many disciplines, including the field of aeroelasticity as pointed out by Garrick (ref. 1) in a recent international talk.

In the present talk, several potential problem areas of lifting and control surface flutter will be discussed and indications given as to their relative importance to the space shuttle program. Proposed or needed research in those areas where the state of the art is not presently sufficient to insure a safe and reliable space shuttle mission are delineated.

IV

POTENTIAL FLUTTER PROBLEM AREAS

Some of the potential flutter problem areas and their relationship to the space shuttle operating mission are indicated in figure 1. Major events such as launch, maximum dynamic pressure (max q), booster descent, and orbiter reentry and transition are shown along the mission profile. The circled numbers immediately below each of these events are keys to the five flutter areas listed at the bottom of the figure.

The first area is flutter associated with planar lifting surfaces. It encompasses much of the past classical flutter research that has been conducted over the subsonic, transonic, and super-hypersonic speed regimes. A survey of some of the important milestones leading to the current state of the art in this area are given in reference 2. For the space shuttle mission, this area will have to be refined to include blunt, thick, lifting surfaces operating at high angles of attack over the complete speed spectrum as indicated by the flight events of ascent through the transonic flow region and max q, reentry, and booster and orbiter descent.

The second area listed is stall flutter. This is a special case of lifting surface flutter. In general, it has been found that as the angle of maximum lift is approached, the flutter velocity is reduced appreciably from the value obtained at zero lift. In addition, the mode of flutter at the higher angles of attack is usually predominantly a single-degree-of-freedom flutter occurring in the torsional mode. This type of flutter is associated with nonpotential separated flow and, hence, extremely difficult to analytically define. A large background of technology exists concerning the problems of stall flutter for normal aircraft flight regimes (refs. 3-7). However, the unusual operating requirements for proposed space shuttle vehicles, i.e., booster descent, and orbiter transition suggest the need for additional studies (ref. 8) of thick wings at very high angles of attack and high subsonic and transonic Mach numbers.

The third area is interference flutter - the interference effects of one lifting surface on the flutter characteristics of another lifting surface. Existing technology pertinent to this area is limited to the interference effects of wings on other surfaces such as horizontal tails (refs. 9-12) But in the launch configuration (for some designs of the space shuttle vehicle) these lifting surfaces take on a "biplane" appearance - a transonic, super-hypersonic biplane appearance at that. Very little is known about the flutter of two closely spaced lifting surfaces, particularly in the transonic and supersonic regimes.

POTENTIAL FLUTTER PROBLEM AREAS

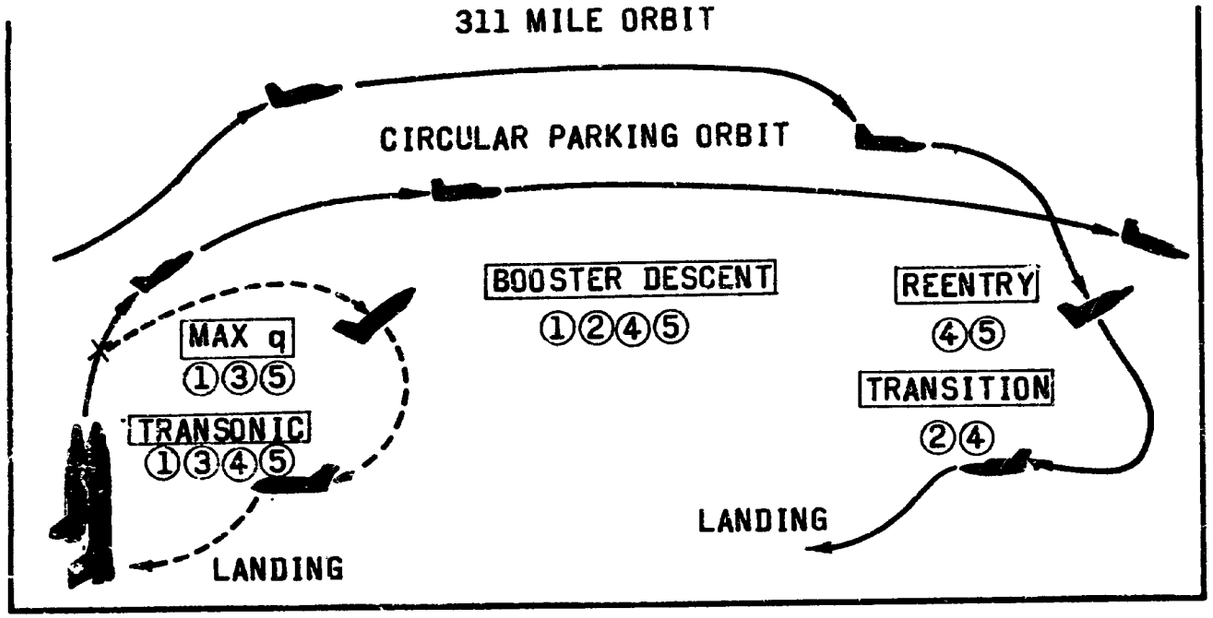

1 PLANAR LIFTING SURFACES

2 STALL FLUTTER

3 INTERFERENCE FLUTTER

4 CONTROL SURFACES

5 LIFTING SURFACE - BODY

The fourth area entitled control surfaces includes such known phenomena as transonic buzz (ref. 13) and phenomena referred to more recently in the literature (refs. 14 and 15) as hypersonic buzz. This latter case is an area where the technology learned in more recent hypersonic lifting-body vehicle programs is still being assessed. Also included in this area is the field of aeroservoelasticity. This field concerns the interaction of aerodynamic, elastic, inertial, and automatic control forces, which can considerably influence the control surface limit loads, fatigue load spectra, flutter speed, and the ride/handling/control qualities of the vehicle.

The fifth and final area is entitled lifting surface - body flutter. While the individual stages taken separately do not appear to be outside the realm of the current state of the art, the combined configuration is a more formidable problem. Obvious difficulties will be encountered in wind-tunnel aeroelastic testing programs, which in the past have always been conducted for any new vehicle design to prove flutter clearance and aeroelastic integrity. From an analytical viewpoint the problem is even more difficult. It is sufficient to mention here that the analytical technology at the present time is not adequate. A more detailed discussion of the status of unsteady aerodynamics associated with this area will be given by Mykytow in a subsequent talk.

For the remainder of my talk, I wish to briefly present some recent results obtained at Langley Research Center that are applicable to the space shuttle vehicle in three of these areas: (1) stall flutter, (2) interference flutter, and (3) control surfaces.

STALL FLUTTER STUDY OF SPACE SHUTTLE WING CONCEPTS

The first results are from an exploratory experimental study of the stall flutter characteristics of two space shuttle wing concepts (ref. 8). The two wall mounted semispan wing models are shown in figure 2. The wing configuration of the left of the figure was a 50° clipped delta. It had a symmetric airfoil with a constant 3-percent maximum thickness-to-chord ratio. The configuration shown on the right was a straight, aspect ratio 7 wing which had a 12-percent thick, 64 series airfoil shape. The investigation was conducted in the Langley transonic dynamics tunnel at Mach numbers from about 0.2 to 1.2 and Reynolds number per foot from about 0.15 to 2.5×10^6. The general testing procedure was, with the model at zero angle of attack, flow was established at a given Mach number and dynamic pressure. The model was then rotated at a nominal rate of 0.6 degree per second up to an angle of attack of 90 degrees. This angle of attack sweep rate is approximately 10 times slower than full-scale rotational rate during transition. Strain gages at the model root indicating the relative magnitude of the strains in the bending and torsion degrees of freedom were continuously recorded, thus allowing correlation between the model response, model altitude, and wind-tunnel conditions.

STALL FLUTTER STUDY OF SOME SPACE SHUTTLE WING CONCEPTS

Clipped-delta wing

Straight wing

STALL FLUTTER BOUNDARY FOR AR = 7 STRAIGHT WING

A summary of some of the stall flutter results obtained from this investigation is presented in figure 3. The stall flutter boundary shown is for the aspect ratio 7 straight wing. (Stall flutter was not encountered on the clipped delta wing over the range of the parameters of the investigation; this result being consistent with previous studies.) The stall flutter boundary is presented as a function of Mach number and angle of attack. A flutter velocity coefficient scale is also shown on the right of the figure. This coefficient is a function of the flutter velocity, V, wing semichord at the 3/4-semi-span, b, and the circular frequency associated with the wing torsion mode, w_α .

The boundary in figure 3 indicates that the stall flutter region for this wing model was confined to angles of attack less than about 20° and to Mach numbers less than 0.85. For the lower Mach numbers, the boundary limit for the stall flutter region is seen to occur near a value of the flutter velocity coefficient equal to 1. Thus, no new stall flutter regions were found beyond those which have been studied and discussed extensively in the literature. However, it should be noted that this stall flutter boundary is not general but rather the boundary found for this particular wing model of the present investigation. It has been found in previous studies (ref. 5) that stall flutter boundaries may be altered by configuration aerodynamics as well as by structural parameter changes. For example, stall boundaries are functions of Reynolds number as well as Mach number and flutter velocity coefficient.

Shifting gears now, I would like to turn your attention to another flutter area: Interference Flutter.

STALL FLUTTER BOUNDARY FOR AR = 7 STRAIGHT WING

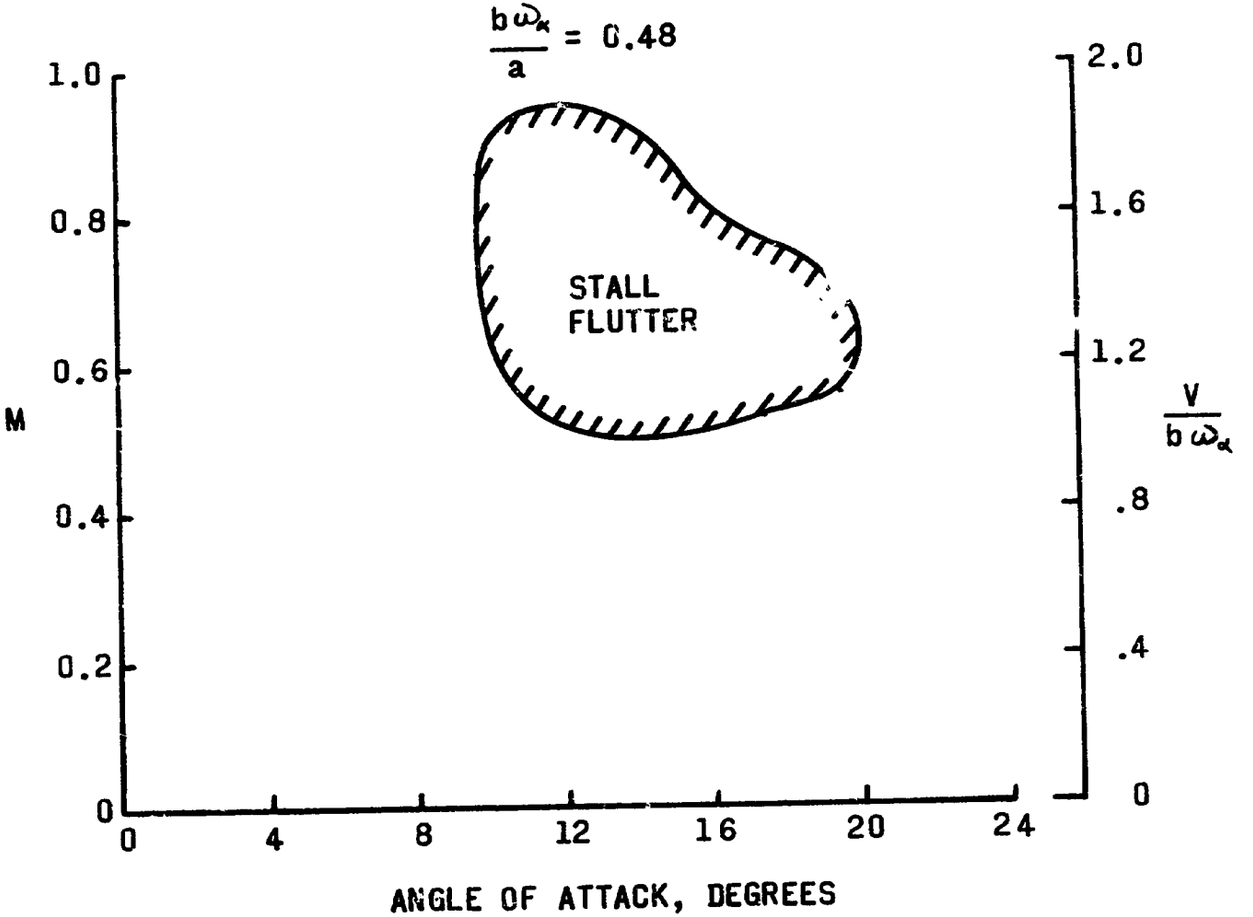

BIPLANE FLUTTER PROGRAM

An exploratory program was conducted in the Langley 26-inch transonic blowdown tunnel to determine the flutter characteristics of an aspect ratio 8, unswept wing model in proximity to a geometrically similar model as shown in figure 4. Both models had 12-percent thick, 64 series airfoil shapes. Flutter data have been obtained with the models' leading edges inline and the distance between them varied from about 1/4 to 2-1/4 mean aerodynamic chord lengths over the Mach number range from 0.4 to 1.3. Additionally, the coplanar separation distance between the models was also varied fore and aft one mean aerodynamic chord.

"TRANSONIC-BIPLANE" FLUTTER MODEL

FLUTTER CHARACTERISTICS OF WINGS IN CLOSE PROXIMITY

Some results of this flutter program of wings in close proximity are shown in the next figure (5). The effect of biplanar separation distance between two lifting surfaces is presented as a function of equivalent airspeed over the Mach number range from about 0.4 to 1.30. There are two predominant effects to be noted as the separation distance between the two wings is reduced. First, the Mach number at which the minimum flutter velocity is encountered shifts to progressively lower values. For example, along the boundary for the single wing, which is depicted by the solid curve, the Mach number corresponding to the minimum flutter speed (or bottom of the flutter bucket) occurs at a value of about 0.75, and for two wings with a separation distance $h/\bar{c} = 0.27$ the minimum flutter velocity occurs at a Mach number of about 0.45. The second effect resulting from reducing the separation distance between the wings is the reduction in equivalent airspeed or dynamic pressure at which flutter occurs over most of the Mach number range. For example, for the lower range of Mach numbers a reduction of about 50 percent is seen to result. Perhaps, more importantly, are the supersonic results since estimates for the space shuttle mission have the vehicle encountering maximum dynamic pressures of about 500-600 psf at a Mach number between 1.2 and 1.3. Again, the more flexible lifting surface is seen to flutter at lower values of equivalent airspeed or dynamic pressure as the wings are spaced closer together. The exact amount of the reduction is not known since no flutter data was obtained for the single wing in this Mach number range.

TRANSONIC FLUTTER CHARACTERISTICS OF WINGS IN CLOSE PROXIMITY

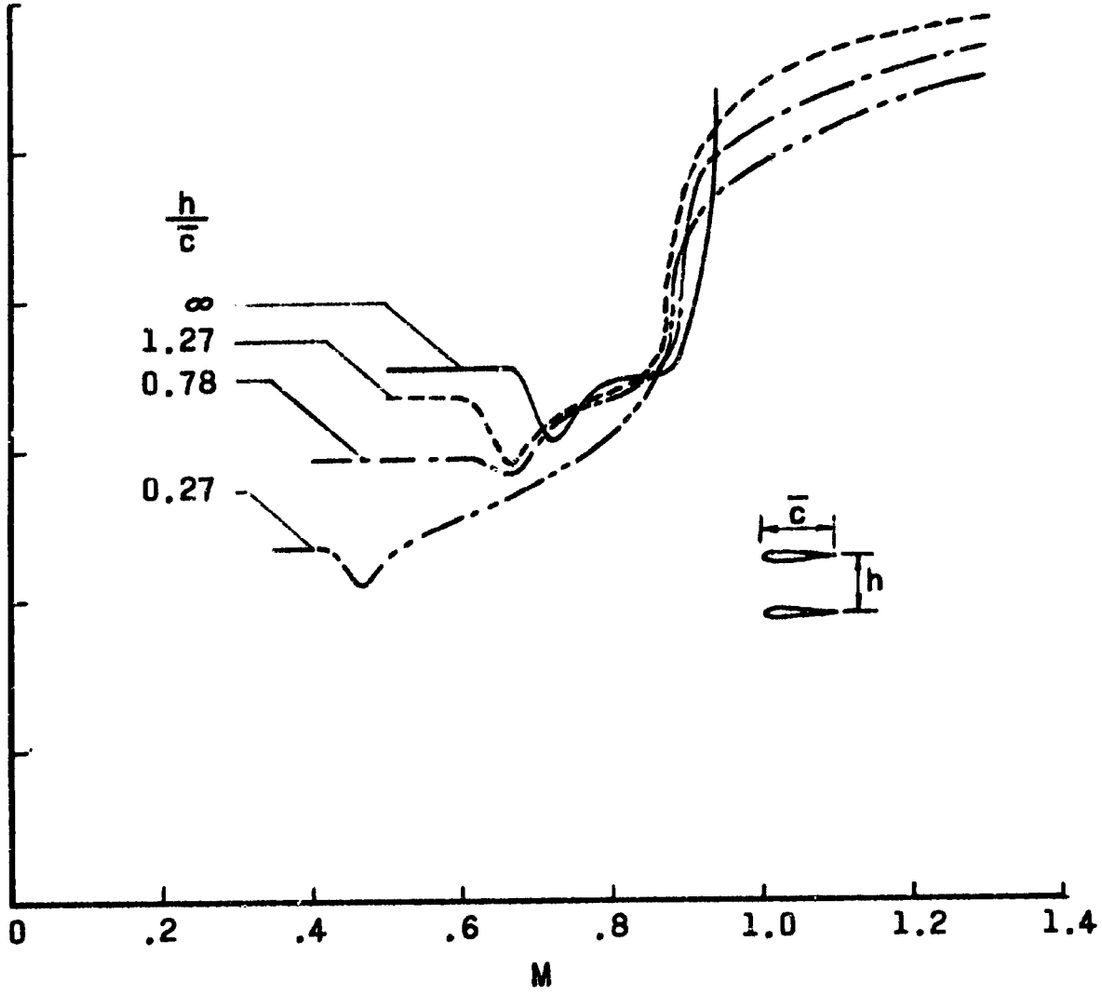

CONTROL SURFACE INSTABILITIES ON LIFTING-REENTRY VEHICLES

Another research program was conducted at Langley Research Center (ref. 16) with the final intent being to determine whether a control surface instability might exist for lifting-body reentry vehicle configurations at hypersonic speeds. One of the configurations studied was a 1/30-scale model of the HL-10 vehicle and is shown in figure 6. The photograph at the left shows the model at angle of attack, with trailing-edge control surfaces deflected for trim, mounted in the M = 15 Langley hypersonic aeroelasticity tunnel. The program was conducted to determine the aerodynamic in-phase or stiffness coefficient and the out-of-phase or damping coefficient for the flaps by the free oscillation technique. The variables of the program included vehicle angles of attack up to 25°, flap deflection angles up to 60°, and flap reduced frequencies from 0.01 to 0.04. The schlieren photograph on the right hand side of figure 6 illustrates the flow field associated with the model at 25° - angle of attack at a Mach number of 15.4 and Reynolds number per foot of 7.5×10^6. The flaps are deflected 35°. (Trim β with vehicle at $\alpha = 25°$ is about $\beta = 25°$.) Note the coalescence of the bow shock, the boundary-layer separation wedge induced shock, and the flap induced shock intersecting below but in the vicinity of the flap trailing edge. This intersection point was observed to move upstream with increasing flap angles, and to be unsteady for flap angles greater than about 30°, and become more violent for larger flap angles. This would not only affect the stability of the flaps themselves, but also their effectiveness as control devices.

CONTROL-SURFACE INSTABILITIES ON LIFTING-REENTRY VEHICLES

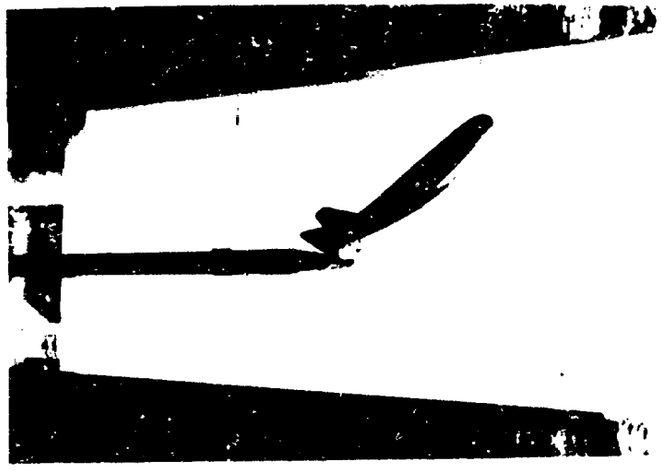

$1/30$-SCALE MODEL HL-10 VEHICLE

FLOW-FIELD DESCRIPTION AT M=15

AERODYNAMIC DAMPING RESULTS

Some control surface aerodynamic damping results from reference 16 are presented in figure 7. The results are presented as a function of an aerodynamic damping coefficient with flap deflection angle. The experimental data depicted by the solid circular symbols indicate a destabilizing trend of decreasing values of aerodynamic damping with increasing flap deflection angles. Negative aerodynamic damping values were measured for flap angles greater than about 37°. In contrast, modified Newtonian theory calculations shown as the solid line predicted a stabilizing trend and positive values of aerodynamic damping over the range of aeroelastic parameters tested. Other similar two-dimensional results obtained, but not presented here, showed good agreement between theory and experiment, suggesting that these destabilizing results are associated with interactions between the three-dimensional flow and thick trailing-edge flaps. However, the exact cause of the unstable phenomena was not determined.

AERODYNAMIC DAMPING RESULTS

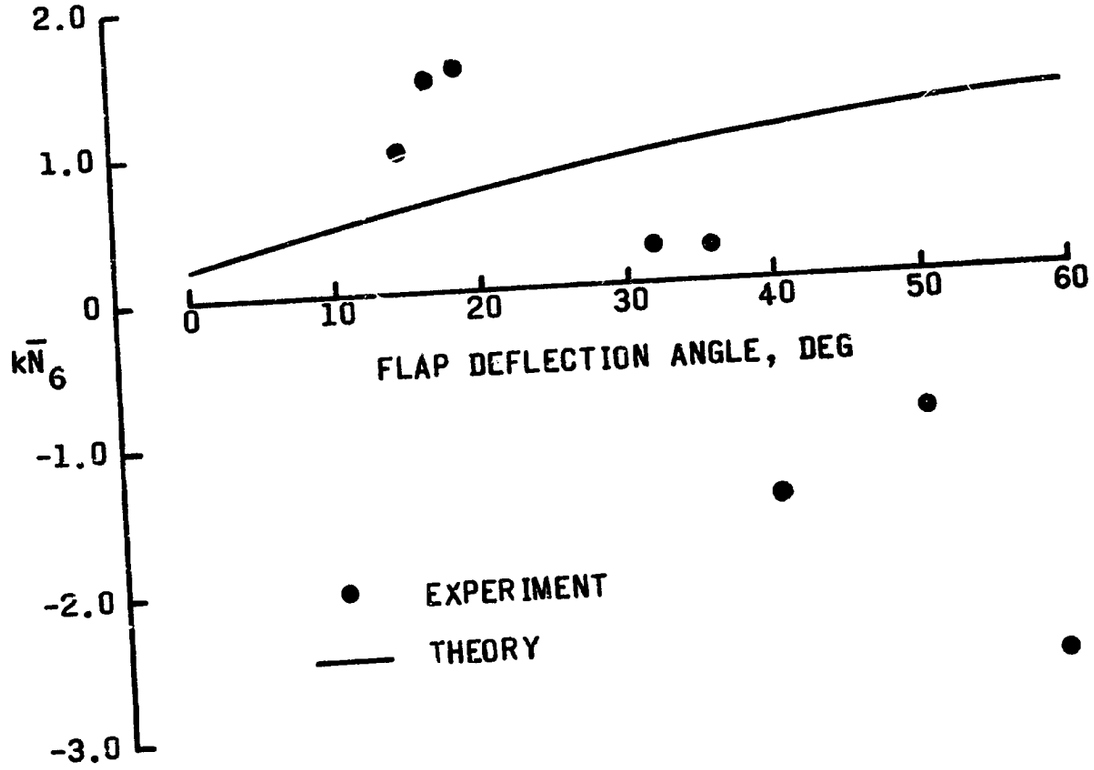

ANTICIPATED FLUTTER RESEARCH

In summary, figure 8 outlines some of the anticipated areas where continued effort is needed in order that sufficient flutter technology will be available in a timely manner to ensure a safe and reliable space shuttle vehicle.

In the area of planar lifting surface flutter (1), component model wind-tunnel studies should continue to be conducted on candidate space shuttle configuration designs. Flutter data should be obtained over the entire flight regime to provide reliable trends including the effects of blunt wings operating at high angles of attack. The transonic and maximum dynamic pressure regions of the flight should receive priority.

The stall flutter (2) problem may need both an analytical and experimental effort if the wing torsional stiffness is marginal. Wind-tunnel simulation of the transition maneuver from high to low angles of attack should be conducted on aeroelastically scaled wing models simulating Mach number and, in so far as possible, Reynolds number is essential. A parallel theoretical effort should be conducted to gain a better understanding of the effects of oscillation amplitude and the rate of change of angle of attack on stall flutter. The final objective being to develop a theory capable of analyzing stall flutter to the degree needed for prediction of wing amplitude response and the associated induced wing stresses during transition through the stall region.

For the interference flutter area, an evaluation is needed of some of the newer, more sophisticated analytical methods such as the method of Laschka (ref. 12) as to their applicability to the biplanar unsteady problem. For the higher speed regimes a quasi-steady theoretical approach seems both justifiable and feasible.

For control surfaces (4) a better understanding of the buzz phenomena is indicated including three-dimensional effects. Some related problem areas for control systems are found in the field of aeroservoelasticity.

The complete vehicle configuration flutter problem (5) warrants considerable attention. As with any new vehicle design, an aeroelastic proof-of-concept testing program is essential. For the 2-stage configuration due to the nature of its size and complexity, new, and perhaps, novel, wind-tunnel testing techniques will have to be developed. Test programs, as well as testing techniques, should be developed as soon as possible. Design and construction of complete aeroelastic models should be undertaken by the contractors as soon as design concepts become fixed. Testing programs, utilizing NASA and other facilities,

ANTICIPATED FLUTTER RESEARCH

1 PLANAR LIFTING SURFACES

- Component wind-tunnel studies

2 STALL FLUTTER

- Wind-tunnel simulation of transition maneuver
- Develop analysis for prediction of boundaries, amplitudes, and induced stresses

3 INTERFERENCE FLUTTER

- Comparison between existing analytical methods and new experimental results

4 CONTROL SURFACES

- Better understanding of buzz phenomena
- Aeroservoelasticity

5 LIFTING SURFACE - BODY

- Development of testing techniques
- Complete aeroelastic model wind-tunnel studies
- Refine and advance analytical methods

8

therefore, could be completed and the results in-hand prior to hardware production. This would allow the results, as they might impact the design, to be incorporated into the final configuration rather than after-the-fact as detrimental weight fixes or penalties.

A parallel analytical effort should share the high priority of this research effort as the current state of the art for lifting surface-body flutter is the least adequate.

REFERENCES

1. Garrick, I. E.: Emerging Trends in Aeroelasticity. Paper for the Küssner Anniversary Issue, Zeitschrift Für Flugwissenschaften, Sept. 1970.

2. Garrick, I. E. (Editor): Aerodynamic Flutter. AIAA Selected Reprint Series, Volume V, AIAA, New York, March 1969.

3. Victory, Mary: Flutter at High Incidence. R and M No. 2048, British ARC, 1943

4. Halfman, Robert L.; Johnson, H. C.; and Haley, S. M.: Evaluation of High Angle-of-Attack Aerodynamic Derivative Data a: Stall Flutter Prediction Techniques. NACA TN 2533, 1951.

5. Rainey, A. Gerald: Preliminary Study of Some Factors Which Affect the Stall Flutter Characteristics of Thin Wings. NACA TN 3822, March 1956.

6. Rainey, A. Gerald: Measurement of Aerodynamic Forces for Various Mean Angles of Attack on an Airfoil Oscillating in Pitch and on Two Finite Span Wings Oscillating in Bending with Emphasis on Damping in Stall. NACA Rept. 1305, 1957.

7. Regier, Arthur A.; and Rainey, A. Gerald: Effects of Mean Incidence on Flutter. Presented at the 7th Meeting Structural and Materials Panel, AGARD, NATO, Rome, Italy, March 26-April 2, 1958.

8. Goetz, Robert C.: Exploratory Study of Buffet and Stall Flutter of Space Shuttle Vehicle Wing Concepts. NASA LWP-872, May 22, 1970.

9. Ashley, H.: Some Recent Developments in Interference Theory for Aeronautical Applications. Archiwum Mechaniki Stosowanej 16, pp. 149-178, 1964.

10. Topp, L. J.; Rowe, W. S.; and Shattuck, A. W.: Aeroelastic Considerations in the Design of Variable Sweep Aeroplane. ICAS Paper No. 66-12, 5th ICAS Congress, London, 1966.

11. Laschka, B.; and Schmid, H.: Interference Between Wing and Horizontal/ Verticle Tail in Unsteady Subsonic Flow. Vereinigte Flugtechnische Werke, Munich, Com. Rep. M-51/68, 1968.

12. Sensburg, O.; and Laschka, B.: Flutter Induced by Aerodynamic Interference Between Wing and Tail. Paper presented at the joint conference of AIAA Structural Dynamics and Aeroelasticity Specialist/ASME-AIAA 10th Structures, Structural Dynamics, and Materials. New Orleans, Louisiana, April 14-16, 1969.

13. Lambourne, N. C.: Some Instabilities Arising from the Interactions Between Shock Waves and Boundary Layers. NPL/Aero/348, 1958.

14. Widmayer, E., Jr.: Aerodynamic Excitation of Flaps at M = 16. Martin Com. Int. Rept. No. S-38, Sept. 1961.

15. Morkovin, M. V.: Aerodynamic Background on High Speed Oscillations and Buzz. Martin Co., RM-162, Oct. 1963.

16. Goetz, Robert C., and Gibson, F. W.: Investigation of Control Surface Instabilities on Lifting Body Reentry Vehicles at M = 15.4. Prospective NASA TN- , 1970.

STATE OF THE ART FOR PANEL FLUTTER AS APPLIED TO SPACE SHUTTLE HEAT SHIELDS

Sidney C. Dixon and Charles P. Shore

NASA-Langley Research Center
Hampton, Virginia

SUMMARY

Heat shields considered for the space shuttle generally have flexible supports and may have orthotropic stiffness properties. The state-of-the-art for the supersonic flutter of this type of panel is briefly summarized. Results for the most general support conditions are not available, but considerable work has been done for panels with elastic edge restraint on two opposite edges. Results from these investigations which indicate the effects of elastic edge restraint, panel stiffness orientation, unequal support stiffness on opposite edges and elastic coupling to an elastic substructure are discussed. Four analytical methods presently considered for analysis of panels with arbitrary support on all four edges and experimental programs required for verification of these techniques are indicated.

INTRODUCTION

Heat-shield designs often involve a lightweight outer skin; the major design problem is one of supporting this outer skin so that it will survive in the airstream and, at the same time, will accommodate the thermal expansion due to the large temperature differences between shield and primary structure. The design techniques used to solve the problem generally lead to relatively stiff panels connected to a primary structure by flexible supports as indicated in the figure. The outer skins are often stiffened, for example corrugated sheets, and thus may have orthotropic stiffness properties. In some designs the supports are so closely spaced that they provide essentially continuous elastic support, whereas in other designs the spacing is so large that the attachments must be treated as discrete line or point supports; often the side edges are unsupported. Virtually no flutter results exist for panels with such edge support. However, some of the flutter characteristics of corrugation stiffened panels with continuous elastic support on two opposite edges and simple support on the other two edges have been determined, and both theory and experiment reveal a highly destabilizing effect of the elastic edge support (refs. 1 to 3). Thus even though heat shield panels may be relatively stiff, the influence of the elastic support may lead to panel flutter problems. Panel flutter instabilities are usually of limited amplitude, however very rapid fatigue-type failures have occurred in wind tunnel tests (refs. 1 and 4). Hence, it appears necessary to design heat shield panels that will not flutter.

In the present talk the influence of elastic edge support and elastic coupling to an elastic substructure on the supersonic flutter of panels will be discussed for panels with simple support on two opposite edges, as most information pertains to this type of panel. Proposed or needed investigations for panels with arbitrary edge support on all four edges will be indicated. All theoretical results to be presented were obtained from the two-dimensional steady aerodynamic approximation which yields accurate results for a wide range of Mach number and panel geometry for panels with nondeflecting edges. The ranges for which this approximation yields reliable results for panels with deflecting edges, however, has not as yet been ascertained.

TYPICAL HEAT SHIELD CONFIGURATIONS

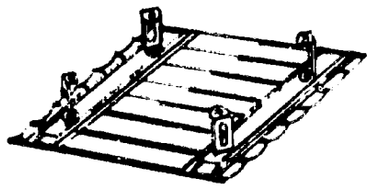

HAT STIFFENED CORRUGATED SKIN
WITH POINT SUPPORTS

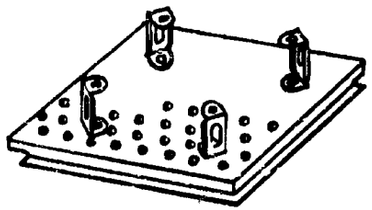

DIMPLED OR SANDWICH CONSTRUCTION
WITH POINT SUPPORTS

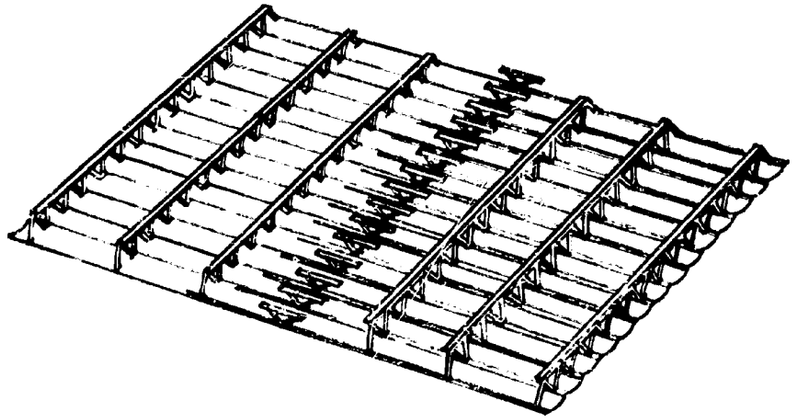

CORRUGATED SKIN WITH MULTIPLE SUPPORTS

SIGNIFICANT FLUTTER PARAMETERS

Some of the significant parameters that should be considered for flutter of heat-shield type panels are indicated in the figure. The numbers in parentheses indicate pertinent references which describe some of the investigations that have considered the effects of the various parameters; the list of references is in no wise complete. A recent comprehensive review of the state-of-the-art for panel flutter is given in reference 5.

The effects of most of the parameters listed have been studied in most detail using approximate aerodynamic theory. Although much progress has been made and the agreement with experiment is now generally good, many limitations in the analyses still exist. For example, studies of inplane load have usually been restricted to uniform loads and have neglected inplane shear, and studies of elastic deflectional edge restraint have been restricted to unstressed panels with equal springs on two opposite edges. Of all the parameters shown, the effect of elastic deflectional edge restraint appears to be the most significant, and also the most difficult to assess; one of the major difficulties is the determination of the edge support stiffness for actual hardware.

SIGNIFICANT FLUTTER PARAMETERS FOR HEAT-SHIELD TYPE PANELS

1. BOUNDARY LAYER (6, 7, 8, 9)[a]
2. FLOW ANGULARITY (10, 11)
3. BENDING STIFFNESSES (10)
4. ELASTIC COUPLING TO SUBSTRUCTURE (12, 13, 14)
5. ELASTIC EDGE RESTRAINT (2, 3, 15, 16)
6. TRANSVERSE SHEAR STIFFNESS (17)
7. INPLANE LOADS (18, 19, 20, 21)
8. DIFFERENTIAL PRESSURE (22, 23, 24)
9. THERMAL GRADIENTS (25)
10. CAVITY EFFECTS (22, 26)
11. DAMPING (14, 19)

[a] Numbers in parenthesis indicate pertinent references.

EFFECT OF ELASTIC DEFLECTIONAL EDGE RESTRAINT

The effects of continuous elastic deflectional edge restraint on two opposite edges on the flutter of corrugation stiffened panels are shown in the figure, which was taken from reference 16. The abscissa parameter K_D is a nondimensional deflectional spring parameter. In the ordinate flutter parameter b is the panel width, D_1 the panel stiffness in the direction of air flow, and D_{12} is the panel twisting stiffness. For the panel orientation shown, where the corrugations are normal to the air flow, the flutter results are a function of the parameter C, which is a ratio of the panel stiffnesses. The panel stiffness in the cross stream direction is D_2 and for the panel orientation shown $D_2 \gg D_1$.

The solid curve was calculated from the normal-mode Galerkin solution of reference 3 for the leading and trailing edge simply supported and $C = 7$; curves for smaller values of C would be above the curve shown.

The symbols represent experimental data for values of C ranging from 5.5 to 7. The panels had a wide variety of side edge-support conditions from very weak supports, with the ends of the corrugations unsupported, to very strong support where the ends of the corrugations were attached to a rigid substructure. The panels were not designed specifically for verification of theory and in fact most of the tests were made before the theory was available. The deflectional stiffnesses at the panel edges were not measured and were difficult to define analytically.

The data are seen to verify the trends of the theoretical curve and illustrate the fact that corrugation-stiffened panels tested to date have fluttered at dynamic pressures far less than the value provided by the conditions of all edges simply supported. Note that the largest experimental value of the flutter parameter is nearly an order of magnitude less than the theoretical value for simply supported edges.

EFFECTS OF ELASTIC DEFLECTIONAL EDGE RESTRAINT

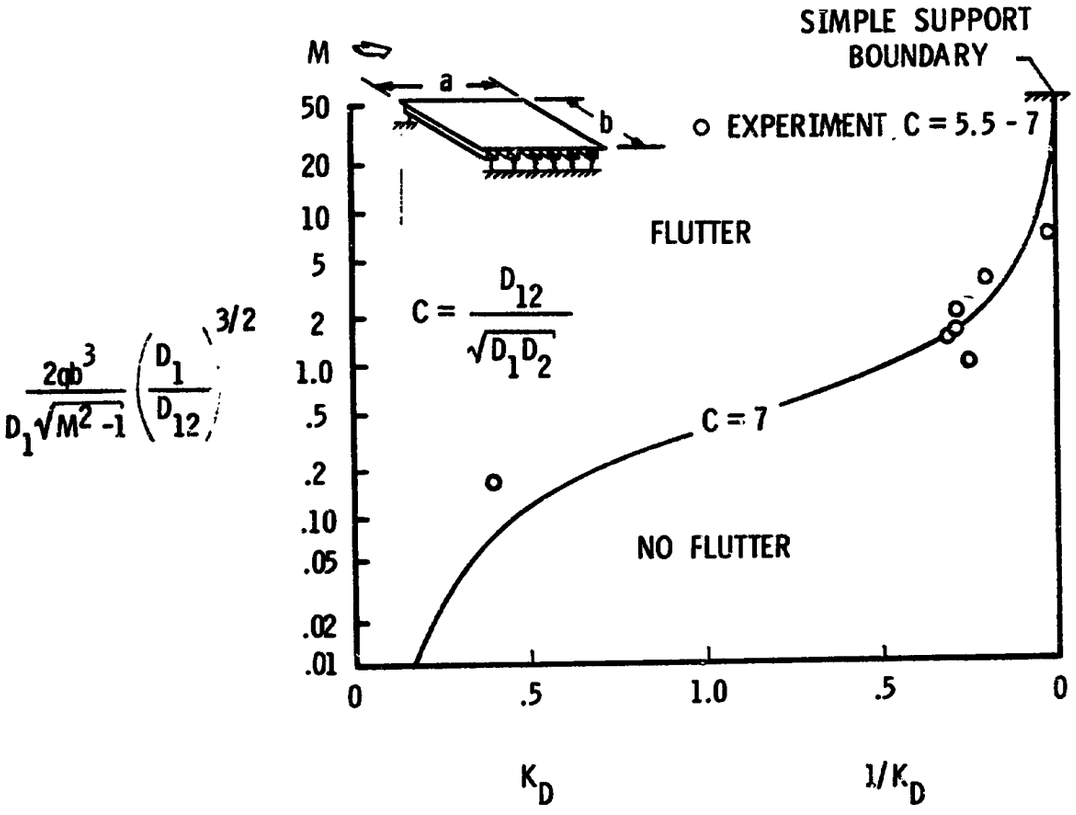

EFFECT OF STIFFNESS ORIENTATION ON FLUTTER BOUNDARY

The effect of stiffness orientation on the flutter boundary for a square corrugation-stiffened panel is shown in the figure, which was taken from reference 16. The abscissa parameter is the ratio of the panel twisting stiffness D_{12} to the larger of the panel bending stiffnesses D_2. The flutter parameter also contains D_2. Results are presented for $K_D = \infty$, which corresponds to simply supported edges, and $K_D = 10$. The solid curves are for the corrugations oriented normal to the air flow and were obtained from the normal-mode Galerkin Solution of reference 3 for $C = 7$. The dashed curves are for the corrugations oriented parallel to the airflow and were obtained from the exact solution of reference 3. An exact solution is possible for this orientation since the cross stream variation of the flutter mode shape is the sine function and the governing partial differential equation thus reduces to an ordinary differential equation with constant coefficients. The exact solution is independent of the stiffness parameter C.

The salient fact revealed by the results shown is that a panel with corrugations parallel to the air flow is much less susceptible to flutter than when the corrugations are normal to the air flow. In fact, flutter has not occurred in the few tests that have been made on orthotropic panels oriented with the direction of maximum flexural stiffness parallel to the direction of airflow. It should be noted that this orientation corresponds to the orientation of most proposed orthotropic heat shield designs.

Another significant fact revealed by the results is that the effect of elastic deflectional edge support is much less pronounced when the corrugations are parallel to the air flow, as compared to the effect when the corrugations are normal to the direction of air flow.

EFFECT OF STIFFNESS ORIENTATION ON FLUTTER BOUNDARY

$a/b = 1$

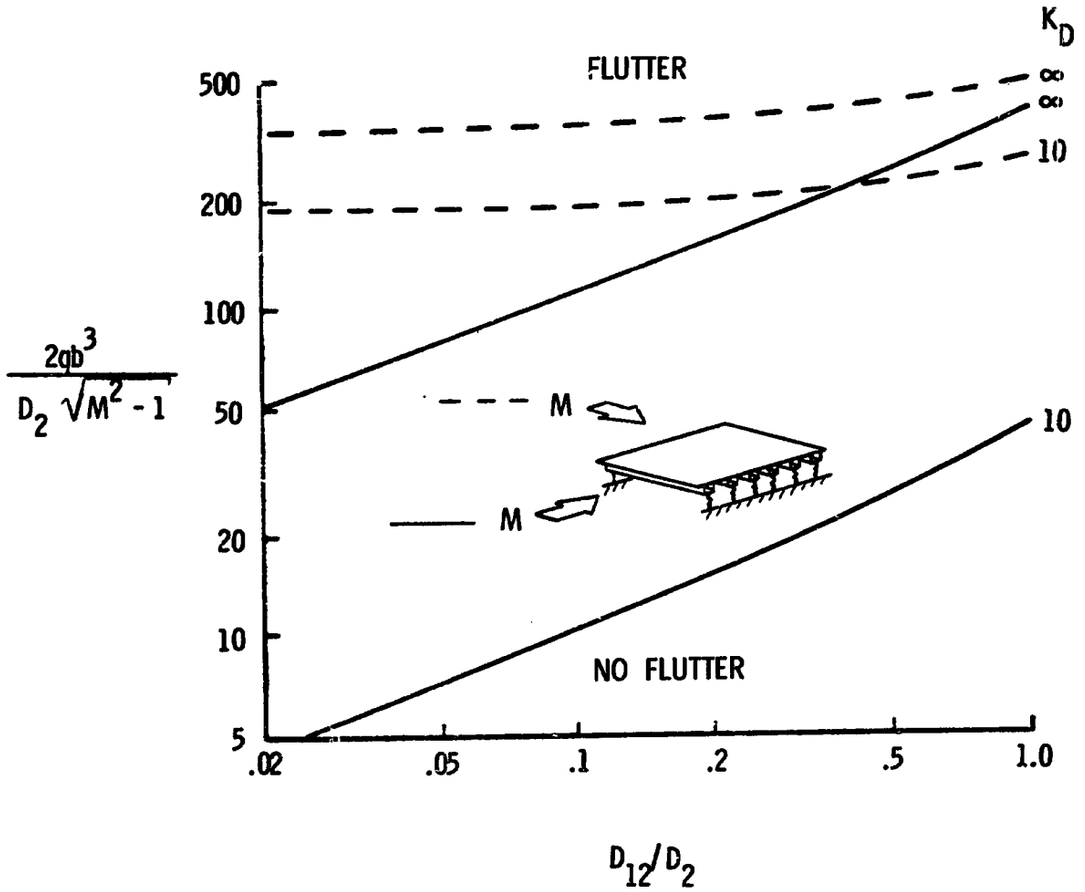

EFFECTS OF UNEQUAL ELASTIC

DEFLECTIONAL EDGE RESTRAINT

The results presented in the previous two figures were obtained from the analysis of reference 3 which has certain limitations. This analysis has recently been extended at the Langley Research Center to include the effects of normal inplane loads, damping, elastic torsional and rotational restraints, and unequal elastic restraint on opposite edges; the restriction that two opposite edges be simply supported still exists. Preliminary results indicating some effects of unequal deflectional springs are shown in the figure in terms of the flutter parameter and the ratio of the spring stiffness at the leading edge to the spring stiffness at the trailing edge; the side edges are simply supported. Results are presented for a square plate with stiffness ratios $D_{12}/D_2 = 0.05$ and $D_1/D_2 = 0$; the maximum flexural stiffness D_2 is in the direction of air flow. Results are presented for values of the spring stiffness parameter K_{D2} of 1, 5, and 10. For $K_{D2} = 1$ the effect of unequal springs is slight, and the results indicate a minimum flutter dynamic pressure for k_1/k_2 of about 0.8. For K_{D2} of 5 and 10 the flutter dynamic pressure increases monotonically with increasing values of K_{D1}. The value of the flutter parameter for $K_{D1} = 10$ and $K_{D2} = 5$ is 183, whereas for $K_{D1} = 5$ and $K_{D2} = 10$ the value is 130. Thus, these preliminary results suggest a panel is less susceptible to flutter if the larger spring is at the leading edge. The results also indicate that a significant difference in spring stiffnesses is required to affect a significant influence on the flutter results.

EFFECTS OF UNEQUAL ELASTIC DEFLECTIONAL EDGE RESTRAINT

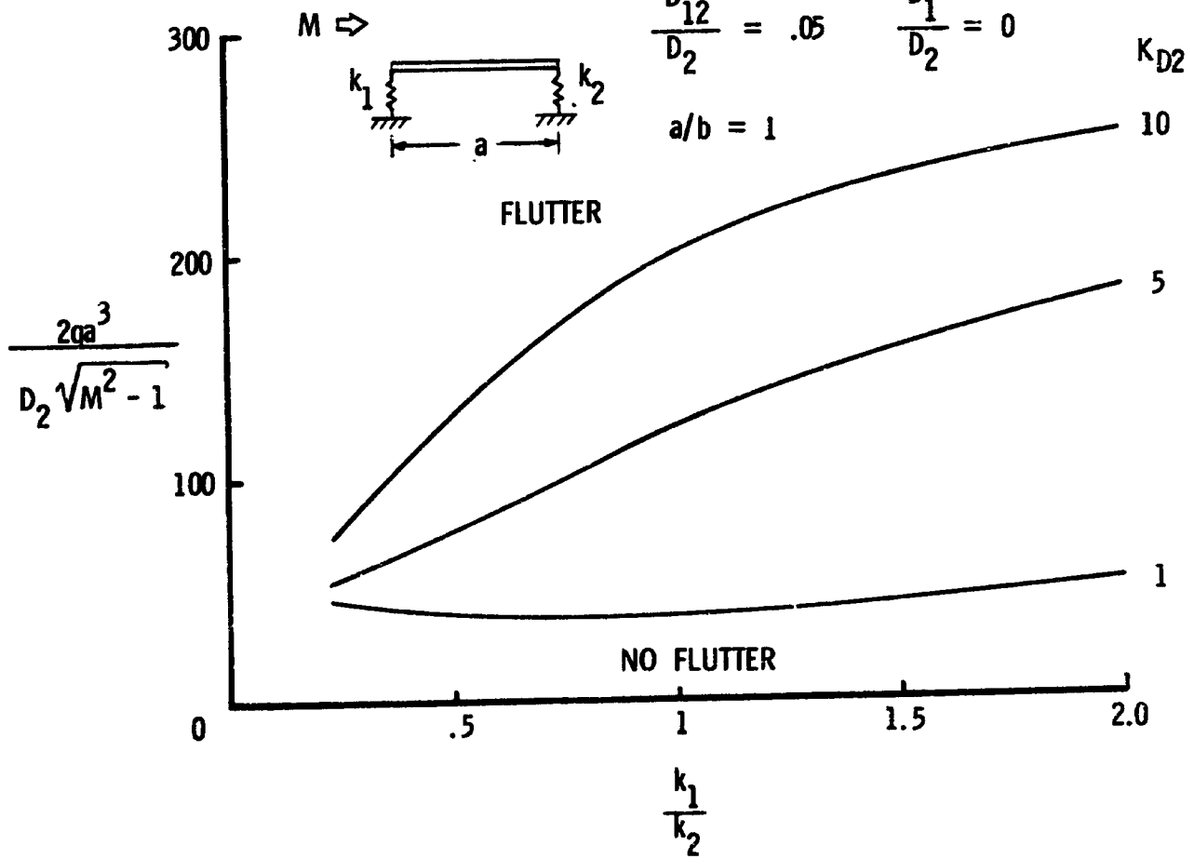

EFFECT OF ELASTIC COUPLING TO ELASTIC SUBSTRUCTURE

Some effects of the elastic coupling of two identical, isotropic parallel plates simply supported on all edges with supersonic flow over only one surface are shown in the figure. The results were taken from reference 13 and were calculated from a two-mode Galerkin solution. The results are presented in terms of a nondimensional spring stiffness parameter and the flutter parameter used previously. For $k = 0$ the results correspond to only a single plate. As can be seen, increasing the spring stiffness parameter to 10 is highly destabilizing but a further increase to a value of 20 is very stabilizing. Even more dramatic variations with k result when the effects of normal inplane loads are considered. It is apparent that the elastic coupling to an elastic substructure can significantly affect the flutter characteristics of panels and should be considered in analyses of heat shields. The analysis is presently being extended at the Langley Research Center to obtain an exact solution that includes the effects of orthotropic panel stiffnesses and elastic edge support at the leading and trailing edges for both panels. Both theory and experiment reveal that panels on continuous elastic foundations can experience subsonic flutter and divergence (refs. 13, 27, and 28); hence, extension of the analysis to account for these phenomena is needed.

EFFECT OF ELASTIC COUPLING TO ELASTIC SUBSTRUCTURE

$a/b = 1$

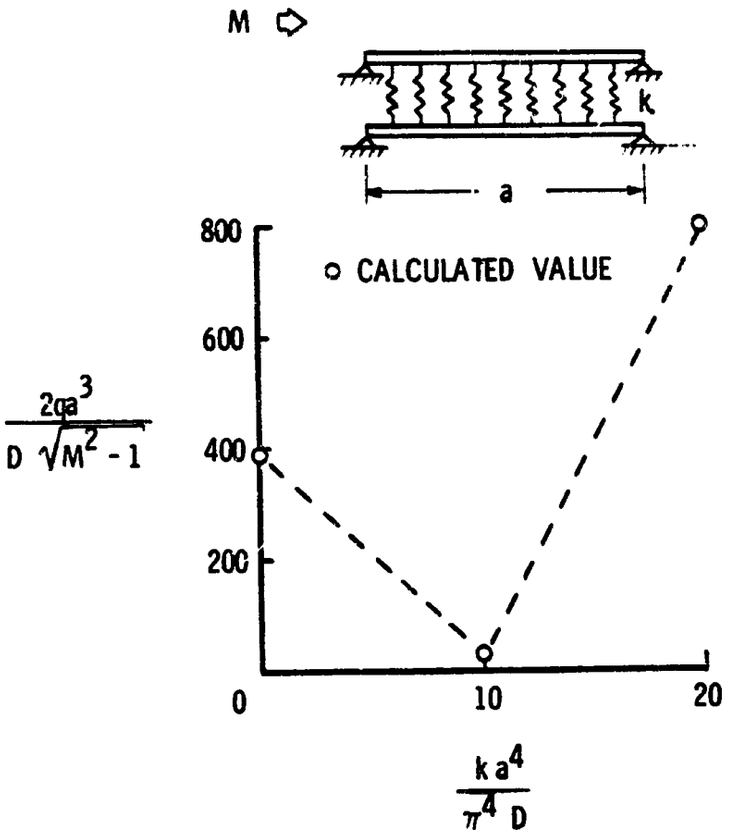

6

WIND TUNNEL TESTS OF HEAT-SHIELD TYPE PANELS

As a part of general studies of heat-shield type panels several models were tested in the Langley 9-by 6-foot thermal structures tunnel at a Mach number of 3.0, dynamic pressures from 1500 psf to 3000 psf, and stagnation temperatures from 450°F to 660°F (refs. 29 and 30). The panel shown in the figure is representative of one of the models tested. The outer skin was a thin (.01 in.) corrugated sheet which was attached to an elastic substructure by flexible supports. The other models also had corrugated skins, but the means of attachment to the substructure differed from the method shown. The models were tested with the corrugations both parallel and normal to the direction of air flow. No flutter was detected in any of the tests. It should be noted that the test conditions did not reproduce the environment for which the heat shields were designed; the temperatures were far too low, but the excessive dynamic pressure provided a rather severe test of the structural integrity of the models. For one model the corrugation depth was such that performance was marginal in resisting thermal buckling during radiant heating tests, yet the corrugation was stiff enough to perform satisfactorily in the wind-tunnel tests.

No vibration data were obtained for the models and no vibration or flutter calculations have been made. Vibration results for similar panels are presently being calculated at Langley Research Center by finite element methods (NASTRAN). Flutter analyses with existing theories would not be realistic as all edges of the panels were supported elastically which violates the restriction in existing analyses of two opposite edges simply supported.

REPRESENTATIVE HEAT SHIELD USED IN WIND TUNNEL TESTS

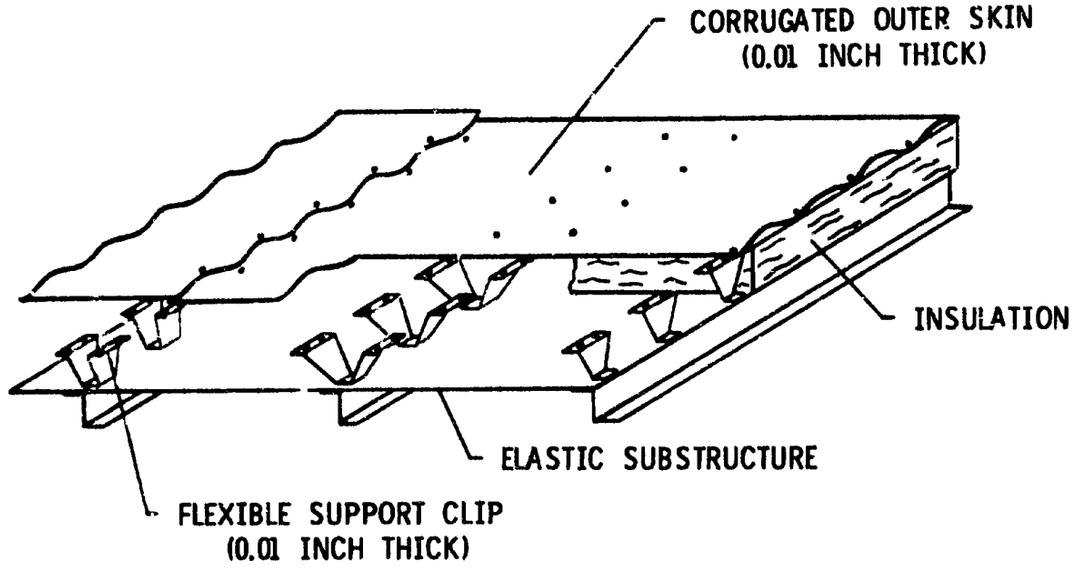

FLUTTER RESEARCH FOR PANELS WITH ARBITRARY SUPPORT CONDITIONS

Some of the anticipated flutter research effort for panels with arbitrary support conditions on all four edges are indicated in the figure. The numerical techniques and methematical modeling required to obtain accurate flutter predictions for complex heat shield panels will probably not be amenable to parametric studies of the many variables entering the problem. Hopefully, less rigorous analyses will be developed that are suitable for generating large amounts of information sufficiently accurate to establish reliable trends. Application of at least four analytical approaches is presently anticipated. Flutter results for relatively simple panels have been obtained from analyses based on finite element techniques (refs. 31 and 32) and finite difference techniques (ref. 13). It is presently anticipated that both of these techniques will be applied to the flutter of panels with arbitrary support conditions by personnel at the Langley Research Center. The NASTRAN system will be used for the finite element calculations; development of a finite difference analysis has just begun. The vibration characteristics of heat shield panels will be studied in considerable detail at Langley, and both theoretical and experimental modes and frequencies will be obtained. These results will be available for normal mode type analyses. Lagrangian multipliers were applied by Dowell (ref. 34) to the flutter of multibay panels, and he is presently developing this technique for panels with arbitrary support conditions.

The emphasis of the indicated analytical effort is on obtaining the ability to account for (1) the orthotropic stiffnesses of complex stiffened panels and (2) the effects of arbitrary support conditions on all four edges. However, it should be emphasized that the effects of the various parameters listed previously as well as the effects of deflecting panel edges on the accuracy of existing aerodynamic theories should also be assessed.

Two types of experimental programs are anticipated; tests on relatively simple models to check theoretical trends, and tests of models representative of actual heat shields. The latter tests would not only establish the accuracy of the theory but would also provide flutter data for proposed hardware. The test programs are still in the preliminary planning stages.

FLUTTER RESEARCH FOR PANELS WITH ARBITRARY SUPPORT CONDITIONS

ANALYTICAL EFFORT

1. FINITE ELEMENTS
2. FINITE DIFFERENCES
3. NORMAL MODE ANALYSIS
   (a) CALCULATED MODES
   (b) MEASURED MODES
4. LAGRANGIAN MULTIPLIERS

EXPERIMENTAL EFFORT

1. SIMPLE MODELS
2. MODELS REPRESENTATIVE OF ACTUAL HEAT SHIELDS

8

VIBRATION RESULTS FOR PANEL

SUPPORTED AT FOUR POINTS

Two of the numerical techniques proposed for analysis of flutter of panels with arbitrary supports have recently been applied to the vibration of an isotropic plate supported at four points (refs. 35 and 36). The figure shows theoretical and experimental results for the fundamental frequency of a square plate symmetrically supported at four points. The ordinate parameter is the nondimensional panel frequency where a is the panel length, m the panel mass per unit area, and D the panel bending stiffness. The abscissa parameter is the ratio of the support position to the panel half length.

The solid curve represents theoretical results from a two mode Lagrangian multiplier solution (ref. 35), the dashed curve represents results from a finite difference solution (ref. 36), and the symbols represent experimental data (refs. 36 and 37). The agreement between experimental data and theoretical results from both types of solutions is good; however, the results obtained by Lagrangian multipliers are in better agreement for support positions near the plate center.

The results indicate that the magnitude of the frequency is strongly affected by support position. The maximum frequency occurs when the supports are about halfway between the center of the plate and the plate edge, and is about a factor of two times the frequency for the supports at the plate center or at the corners. Since flutter results are strongly related to panel vibration characteristics, it appears reasonable to assume that support position will also have a significant influence on the flutter of point supported panels.

EFFECTS OF SUPPORT POSITION ON FUNDAMENTAL FREQUENCY OF A SQUARE PLATE

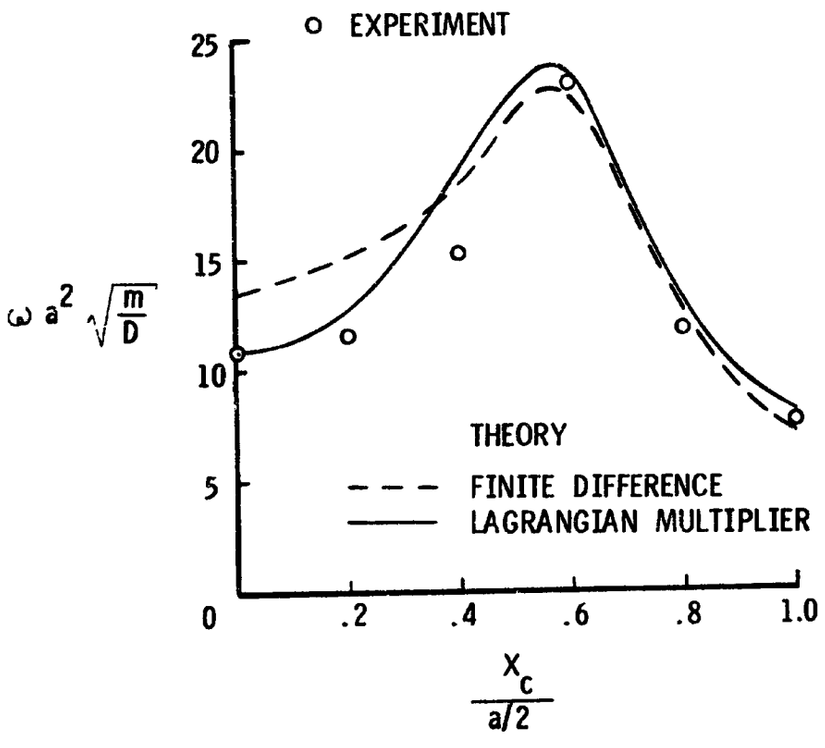

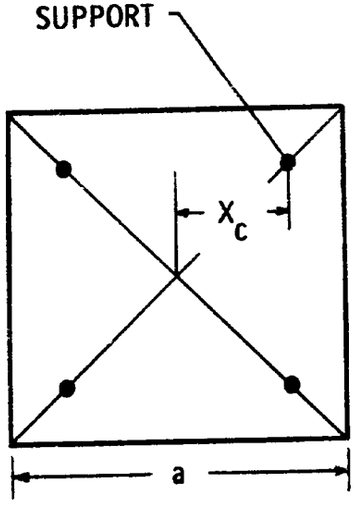

CONCLUDING REMARKS

Results for the supersonic flutter of orthotropic panels with elastic edge restraint have been presented. Both theory and experiment revealed that elastic deflectional edge restraint is highly destabilizing. Theoretical results indicated that orthotropic panels with the air flow in the direction of the maximum stiffness are much less prone to flutter than panels with the air flow normal to the direction of maximum stiffness. The effect of elastic coupling to an elastic substructure was shown to be either stabilizing or destabilizing depending on the stiffness of the elastic coupling.

Existing theories are restricted to panels with continuous elastic restraint on two opposite edges. In order to properly consider the flutter of heat-shield type panels, analytical capability is needed for panels with arbitrary support on all edges. Four possible analytical approaches were indicated: finite elements, finite differences, normal mode techniques, and Lagrangian multipliers. Two types of experimental programs were indicated: tests on relatively simple models to check theoretical trends, and tests of models representative of actual heat shields.

REFERENCES

1. Bohon, Herman L.: Experimental Flutter Results for Corrugation-Stiffened Panels at a Mach Number of 3. NASA TN D-2293, 1964.

2. Bohon, Herman L.: Flutter of Corrugation-Stiffened Panels at Mach 3 and Comparison with Theory. NASA TN D-4321, 1968.

3. Bohon, Herman L.; and Anderson, Melvin S.: Role of Boundary Conditions on Flutter of Orthotropic Panels. AIAA J. (4), 1241-1248, 1966.

4. Weidman, Deene J.: Experimental Flutter Results for Corrugation-Stiffened and Unstiffened Panels. NASA TN D-3301, 1966.

5. Dowell, E.H.: Panel Flutter: A Review of the Aeroelastic Stability of Plates and Shells. AIAA J. (8), pp. 385-399, 1970.

6. Dowell, E.H.: Theoretical-Experimental Correlation of Plate Flutter Boundaries at Low Supersonic Speeds. AIAA J. (7), pp. 1810-1811, 1969.

7. Dowell, E.H.: Generalized Aerodynamic Forces on a Flexible Plate Undergoing Transient Motion in a Shear Flow with an Application to Panel Flutter. AIAA Paper No. 70-76, presented at AIAA 8th Aerospace Sciences Meeting, New York, January 19-21, 1970.

8. Muhlstein, Lado, Jr.; Gaspers, Peter A., Jr.; and Riddle, Dennis W.: An Experimental Study of the Influence of the Turbulent Boundary Layer on Panel Flutter. NASA TN D-4486, 1968.

9. Gaspers, Peter A., Jr.; Mulstein, Lado, Jr.; and Petrott, Daniel N.: Further Experimental Results on the Influence of the Turbulent Boundary Layer on Panel Flutter. NASA TN D-5798, 1970.

10. Bohon, Herman L.: Flutter of Flat Rectangular Orthotropic Panels with Biaxial Loading and Arbitrary Flow Direction. NASA TN D-1949, 1963.

11. Kordes, Eldon E.; and Noll, Richard B.: Theoretical Flutter Analysis of flat Rectangular Panels in Uniform Coplanar Flow with Arbitrary Direction. NASA TN D-1156, 1962.

12. McElman, John A.: Flutter of Two Parallel Flat Plates Connected by an Elastic Medium. AIAA J. (2), pp. 377-379, 1964.

13. Johns, D.J.; and Taylor, P. W.: Vibration and Flutter of Parallel Flat Plates Connected by an Elastic Medium. Presented at AIAA/ASME 11th Structures, Structural Dynamics, and Materials Conference, Denver, Colo., April 22-24, 1970.

14. Dugundji, John: Theoretical Considerations of Panel Flutter at High Supersonic Mach Numbers. AIAA J. (4), pp. 1257–1266, 1966.

15. Bohon, Herman L.; and Dixon, Sidney C.: Some Recent Developments in Flutter of Flat Panels. J. Aircraft (1), pp. 280–288, 1964.

16. Bohon, Herman L.; Anderson, Melvin S.; and Heard, Walter L., Jr.: Flutter Design of Stiffened-Skin Panels for Hypersonic Aircraft. NASA TN D-5555, 1969.

17. Erickson, Larry L.; and Anderson, Melvin S.: Supersonic Flutter of Simply Supported Isotropic Sandwich Panels. NASA TN D-3171, 1966.

18. Hess, Robert W.: Experimental and Analytical Investigation of the Flutter of Flat Built-up Panels under Streamwise Inplane Load. NASA TR R-330, 1970.

19. Shore, Charles P.: Effects of Structural Damping on Flutter of Stressed Panels. NASA TN D-4990, 1969.

20. Shore, Charles P.: Flutter Design Charts for Stressed Isotropic Panels. Presented at AIAA Structural Dynamics and Aeroelasticity Specialist Conf., New Orleans, La., Apr. 16–17, 1969. To be published in J. Aircraft.

21. Eisley, J. G.; and Luessen, G.: Flutter of Thin Plates under Combined Shear and Normal Edge Forces. AIAA J. (1), pp. 620–626, 1963.

22. Dowell, E.H.; and Voss, H. M.: Experimental and Theoretical Panel Flutter Studies in the Mach Number Range 1.0 to 5.0. TDR-63-449, Dec. 1963, Aeronautical Systems Division, United States Air Force; also AIAA J. (3), pp. 2292–2304, 1965.

23. Ventres, C.S.; and Dowell, E.H.: Influence of Inplane Edge Support Flexibility on the Nonlinear Flutter of Loaded Plates. Presented at AIAA Structural Dynamics and Aeroelasticity Specialist Conf., New Orleans, La., Apr. 16–17, 1969.

24. Dowell, Earl H.: Nonlinear Oscillations of a Fluttering Panel. AIAA J. (4), pp. 1267–1275, 1966.

25. Schaeffer, Harry G.; and Heard, Walter L., Jr.: Supersonic Flutter of a Thermally Stressed Flat Panel with Uniform Edge Loads. NASA TN D-3077, 1965.

26. Zimmerman, N.H.; and Lemley, C.E.: Cavity Effect on Panel Flutter – Just How Significant? Presented at 40th Shock and Vibration Symposium, Hampton, Va., Oct. 21–23, 1969.

27. Dungundji, John; Dowell, Earl; and Perkin, Brian: Subsonic Flutter of Panels on Continuous Elastic Foundations. AIAA J. (1), pp 1146–1154, 1963.

28. Johns, D.J.: Static Instability of Rectangular Orthotropic Panels Subjected to Uniform In-Plane Loads and Deflection-Dependent Lateral Loads. ARC R&M No. 3569, 1967.

29. Anderson, Melvin S.; and Stroud, C.W.: Experimental Observations of Aerodynamic and Heating Tests on Insulating Heat Shields. NASA TN D-1237, 1962.

30. Wichorek, Gregory R.; and Stein, Bland A.: Experimental Investigation of Insulating Refractory-Metal Heat-Shield Panels. NASA TN D-1861, 1964.

31. Olson, Mervyn D.: Finite Elements Applied to Panel Flutter. AIAA J. (5), pp. 2267-2270, 1967.

32. Olson, Mervyn D.: Some Flutter Solutions Using Finite Elements. AIAA J. (8), pp. 747-752, 1970.

33. Kariappa; and Shomashekar, B.R.: Application of Matrix Displacement Methods in the Study of Panel Flutter. AIAA J. (7), pp 50-53, 1969.

34. Dowell, E.H.: The Flutter of Multibay Panels at High Supersonic Speeds. MIT Aeroelastic and Structures Research Laboratory Report ASRL 112-1, 1963.

35. Dowell, E.H.: Private Communication.

36. Johns, D.J.; and Nigaraj, V.T.: On the Fundamental Frequency of a Square Plate Symmetrically Supported at Four Points. J. Sound Vib. (3), pp. 404-410, 1969.

37. Tso, W.K.: On the Fundamental Frequency of a Four Point-Supported Square Elastic Plate. AIAA J. (4), pp 733-735, 1966.

THE RELEVANCE OF RECENT ADVANCES IN UNSTEADY AERODYNAMICS TO THE SPACE SHUTTLE PROGRAM

Walter J. Mykytow and J. J. Olsen

AFFDL
France

ABSTRACT

In the last ten years, progress in the linearized theory of unsteady aerodynamics has followed two courses, (a) the improvement of the numerical procedures for isolated lifting surfaces, and later (b) the extension of those methods to include the effects of mutual interference between two or more surfaces and bodies. This paper gives several examples of recent progress to illustrate that the prediction of steady or unsteady airloads on some complicated configurations, such as components of the Space Shuttle, can now be performed routinely and accurately. However, technological gaps exist and required research from the Space Shuttle viewpoint is delineated.

SECTION I

INTRODUCTION

Aeroelastic and structural dynamic considerations form a part of the most significant design conditions for large, very flexible and very light structures. Examples of problems or technical areas are flutter, divergence and control surface reversal and gust response. Others involving feedback or active control are load alleviation and mode stabilization. The accurate prediction and the reliable and safe control of the above phenomena require the capability to predict both the aerodynamic and structural dynamic characteristics with considerable confidence. This paper is a rapid review and evaluation of the state of the art in unsteady aerodynamics pertaining to various potential Space Shuttle designs and concludes with some comments and recommendations in this regard.

Proposed Space Shuttle configurations encompass many aspects which had to be ignored in earlier calculations of unsteady aerodynamic loads. Large fuselages, folded wing tips, interference between adjacent or tandem surfaces, and control surfaces were configurations which were not amenable to rigorous analysis ten years ago. Linearized methods which account for many of those factors are now available and in day-to-day usage. They bring the unsteady aerodynamic load predictions for a complex configuration such as some components of the Space Shuttle to a capability equivalent to the prediction for isolated planar wings of a decade ago. This paper will trace the development of linearized unsteady aerodynamic methods from the early considerations of airfoils and planar lifting surfaces to the present day capabilities for aeroelastic and dynamic analyses of configurations with control surfaces and multiple surface or body interactions. The following sections will discuss isolated lifting surfaces, control surfaces, intersecting surfaces, and interacting (but not intersecting) surfaces.

SECTION II

STATE OF THE ART

Isolated Lifting Surfaces

In the last ten years, tremendous progress has been made in the ability to use linearized theory to estimate unsteady aerodynamic airloads for aeroelastic and dynamic response problems. The progress in subsonic compressible flow methods rests on several important contributions. The first was made in 1940 by H.G. Kussner (Reference 1) who formulated the basic lifting surface theory which gives the now well known integral equation relating oscillating downwash to the surface integral of an influence function or kernel times unsteady pressure. Other important contributions were made in 1955 and 1959 by Watkins, Woolston, Cunningham, and Runyan (References 2 and 3), who developed forms of the kernel and mathematical procedures which then permitted the exploitation and practical application of the kernel function method. Since then, many other important contributions such as an early attempt to incorporate control surfaces have been made, and other improvements continue (References 4 - 8). The doublet-lattice method of Albano and Rodden (Reference 9) is another method which bypasses some of the difficulties of the kernel function method and has shown remarkable accuracy and ease of computation which makes it particularly attractive.

Progress in the prediction of unsteady supersonic airloads rests in the U.S. on contributions by Garrick and Rubinow (Reference 10) and, for three dimensional applications, the contributions of Pines, Dungundji and Neuringer (Reference 11) and Li (Reference 12) who suggested the Mach box approach about 1954. There then followed rapid developments of workable and practical Mach box methods for predicting the supersonic unsteady aerodynamics on isolated surfaces (References 13 - 16).

Control Surfaces

Methods to predict supersonic unsteady control surface airloads were investigated by Donato and Huhn (Reference 17) using Mach box techniques. Subsonic unsteady aerodynamic methods have been delayed because of complexities resulting from control surface hinge line and side edge singularities. However, Berman, Shyprykevich, and Smedfjeld (Reference 18) have explored the use of the kernel function method for the subsonic region using approximate expressions for the aileron pressure series. Ashley and Rowe (Reference 19) have presented a more rigorous formulation for the full span aileron on a subsonic lifting surface using the very notable contribution of Landahl (Reference 20). Further concentration and progress should lead to tractable methods for predicting the subsonic airload on partial span control surfaces oscillating in a subsonic flow. The Albano-Rodden doublet-lattice method can be applied to wings with control surfaces with a minimum of additional effort and is currently being used in that manner at several companies and at the AFFDL.

Intersecting Surfaces

Flutter prevention is a critical design condition for T-tail aircraft. This is emphasized by a few cases of actual in-flight catastrophic failures. Thus, the considerable effort devoted to prediction of T-tail unsteady aerodynamics for subsonic flow which started in the early 1960's is not surprising. Stark of Sweden (Reference 21) in 1964 produced a reversed flow method using doublets of integrated acceleration potentials to obtain the integral equations. Davies of the United Kingdom (Reference 22) extended his subsonic kernel function method to T-tails and reported extensive applications of his method also in 1964. Zwaan of the Netherlands (Reference 23) developed in 1967, a kernel method following suggestions given by Laschka (Reference 4) and Davies (Reference 22). Many versions of the subsonic T-tail kernel function method now exist in the U.S. although the procedure still requires considerable work. A general purpose subsonic kernel function method which is to be a development of the non-planar kernel function first given by Ashley (Reference 24) now is being developed by North American Rockwell Corporation for the AFFDL to handle T-tails, V-tails, cruciform tails, folded tips, etc., and is in the final stages of development. Many Space Shuttle configurations would be covered by this computer program.

The doublet-lattice method of Albano and Rodden (Reference 9) can also be applied to intersecting surfaces. Kalman, Rodden, and Giesing (Reference 25) have extended the method and have applied it to wing-pylon combinations, annular wings, wing and fuselage combinations, and wings in ground proximity as well as T-tails. An application to Stark's T-tail (Figure 1) and a comparison with other methods are given in Table 1. Agreement is excellent.

Andrew (Reference 26) is now developing a supersonic Mach box method for multiple intersecting surfaces. This is an extension of earlier work by Moore and Andrew (Reference 27) and Donato and Huhn (Reference 17) which could handle folded wing tips using the Mach box method.

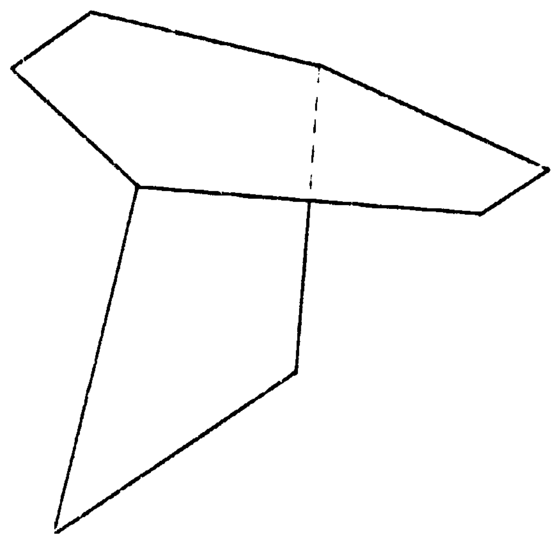

FIGURE 1. THE STARK T-TAIL

		[illegible]		[illegible]		[illegible]	
		[illegible]	[illegible]	[illegible]	[illegible]	[illegible]	[illegible]
DAVIES	YAW	[illegible]	[illegible]	[illegible]	[illegible]	[illegible]	[illegible]
STARK		[illegible]	[illegible]	[illegible]	[illegible]	[illegible]	[illegible]
FLR		-.0722	[illegible]	[illegible]	[illegible]	[illegible]	[illegible]
MDC		[illegible]	[illegible]	[illegible]	[illegible]	[illegible]	[illegible]
DAVIES	SIDESWAY	[illegible]	[illegible]	[illegible]	[illegible]	[illegible]	[illegible]
STARK		[illegible]	[illegible]	[illegible]	[illegible]	[illegible]	[illegible]
FLR		-.6236	[illegible]	0.0260	[illegible]	[illegible]	[illegible]
MDC		[illegible]	-.3565	[illegible]	[illegible]	[illegible]	[illegible]
DAVIES	ROLL	-.1248	-.1237	0.0150	-.0464	[illegible]	[illegible]
STARK		-.1247	[illegible]	0.0134	[illegible]	[illegible]	[illegible]
FLR		-.1235	-.1217	0.0148	-.0239	0.0179	-.0502
MDC		-.1270	-.1246	0.0154	-.0469	0.0186	[illegible]

TABLE 1 GENERALIZED FORCES FOR THE STARK T-TAIL

Interacting but not Intersecting Surfaces

Examples in this category include some Space Shuttle configurations with the booster and orbiter vehicles tied to each other, fuselage-to-fuselage, producing tandem airfoils having interactions between wings and tails. Recent flutter model investigations have indicated that the oscillating downwash shed by a wing has very significant influences on the horizontal tail unsteady airloads (References 28 - 31). These interactions produce detrimental effects and lower flutter speeds. Flutter speed trends cannot be predicted correctly unless this wing-on-tail interaction is included.

The AFFDL has applied the Rodden-Albano doublet-lattice method and the Albano kernel function method to a wing-fuselage-horizontal tail flutter model tested in the WPAFB five-foot subsonic wind tunnel (Reference 32).

The Albano kernel function method is an extension of Laschka's approach (References 33 - 35) and can be applied to non-planar wing-horizontal tail combinations providing the tail centerline is sufficiently displaced (10-15% semi-span) from the wing plane to avoid a singularity which is not accounted for in the current version. Relative dihedral angles between wing and tail planes are permissible.

Figure 2 shows the trend of flutter speed for the AFFDL subsonic flutter model for a wing sweep angle of sixty degrees. The wing sweep angle could be varied, but these sixty degree data are quite representative of results obtained. Results computed by AFFDL using the Rodden-Albano doublet-lattice method are shown in solid lines while experimental data are shown in dashed lines. The velocity data are plotted versus the frequency ratio of cantilever wing bending to uncoupled fuselage torsion. The velocity trend comparison between coplanar computed and experimental data is excellent. The relative agreement between corresponding experimental and computed data points at a given frequency ratio is good. Theory is about 15% conservative at frequency ratios where the flutter velocity is a minimum. This conservatism in computed results is thought to be due to viscous and wing blockage effects which produced less than ideal flow over the tail. The Albano kernel function method was also employed to compute flutter characteristics for the coplanar case and produced results essentially identical to the doublet-lattice method.

The dotted line on Figure 2 shows the experimental results obtained when the tail was rotated out of the wing plane to produce a relative dihedral angle of 45 degrees. Direct comparisons with kernel function computed data cannot be made since the tail centerline is in the plane of the wing introducing the previously mentioned singularity. However, indirect comparisons using a minimum displacement between wing and tail centerline shows that the incremental and beneficial change in flutter velocity should be about 15%. Thus, both theory and experiment validate the detrimental effects of wing unsteady aerodynamic interactions on the tail and the lower flutter velocities caused thereby for wing-fuselage-horizontal tail flutter.

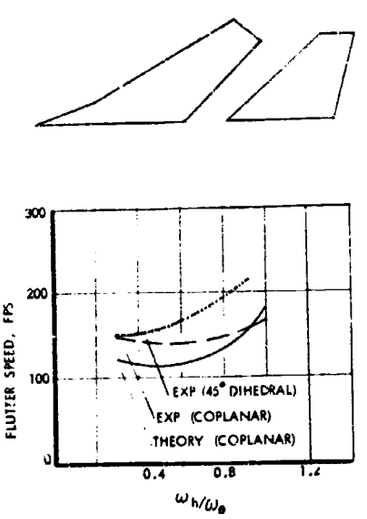

FIGURE 2. THE AFFDL SUBSONIC WING-TAIL FLUTTER MODEL

Albano has also applied his kernel function method to swept back, constant chord flutter models tested at high subsonic and transonic speeds by Cornell Aeronautical Laboratory (Reference 36). Typical experimental and computed results are given on Figure 3 for a given vertical and longitudinal tail position. Predicted results agree very well with the corresponding experimental data. This was found to be true for a wide range of vertical and longitudinal tail positions.

The AFFDL has applied the Rodden-Albano doublet-lattice and Albano kernel function method to several other configurations. Figure 4 shows lift coefficient results predicted by both methods for an oscillating wing-horizontal tail configuration which is now being used by AGARD as an evaluative standard. Agreement between both methods is excellent.

The Albano kernel function method has also been applied to the same AGARD configuration where the horizontal tail is displaced vertically a distance equal to 0.6 times the wing semi-span. Results are shown in Figure 5 together with coplanar data. The tail unsteady aerodynamic coefficients due to wing deflections are lowered significantly. Figure 5 also shows the effects when tail dihedral is also added to the vertically displaced tail. Tail coefficients due to wing deflections are further reduced with positive dihedral but are increased for negative dihedral as expected. Trends of these predicted coefficients appear to be correct.

Figure 6 shows the trend of the real parts of lift coefficients with Mach number as predicted by Laschka and Schmid (Reference 35) for pitching of a wing or horizontal tail. C_{A12} refers to lift on the wing due to tail pitching. C_{A21} refers to lift on the tail due to wing pitching. Corresponding data obtained by AFFDL using the Rodden-Albano doublet-lattice and Albano kernel function method are shown. Agreement among the three sets of data is excellent.

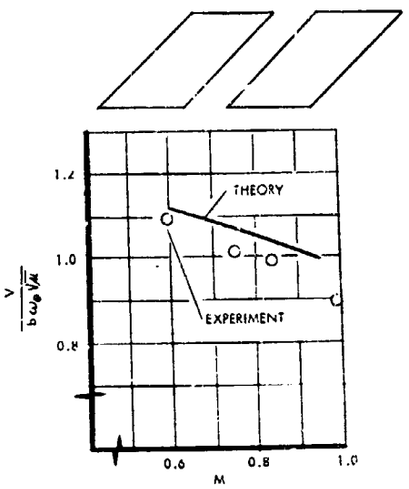

FIGURE 3. CAL TRANSONIC WING-TAIL FLUTTER MODEL
$\Delta Z/b = 0.4$, $\Delta X/b = 1.0$

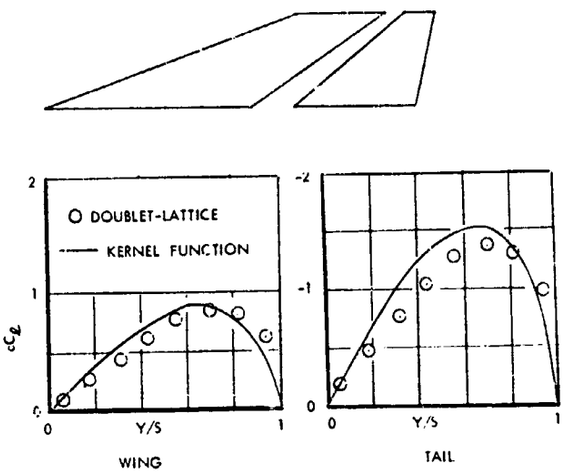

FIGURE 4. REAL SECTION LIFT COEFFICIENTS DUE TO WING TWIST, $M = 0.8$, $\frac{S\omega}{V} = 1.5$, COPLANAR CASE

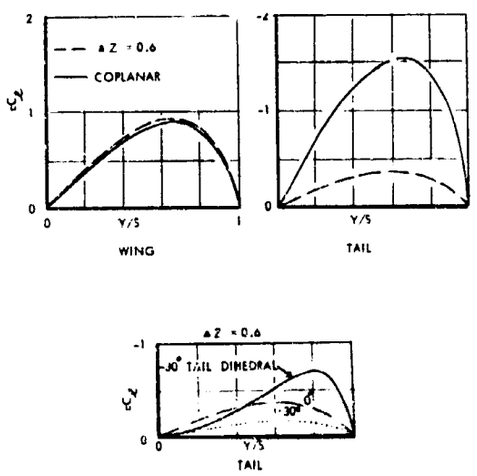

FIGURE 5. SECTION LIFT COEFFICIENTS DUE TO WING TWIST, $M = 0.8$, $\frac{S\omega}{V} = 1.5$, NON-PLANAR CASES.

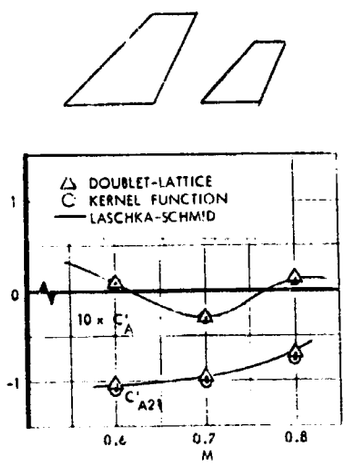

FIGURE 6. INTERFERENCE EFFECTS ON THE LASCHKA-SCHMID CONFIGURATION, $\frac{S\omega}{V} = 1.0$

Since one limit of tandem airfoils is a biplane configuration, the Albano kernel function method was applied to a biplane consisting of two identical AGARD wings with several vertical separations. Figures 7 and 8 give section lift coefficients due to plunging and pitch of one surface with the other fixed. These lift coefficients increase as the moving wing approaches the fixed wing.

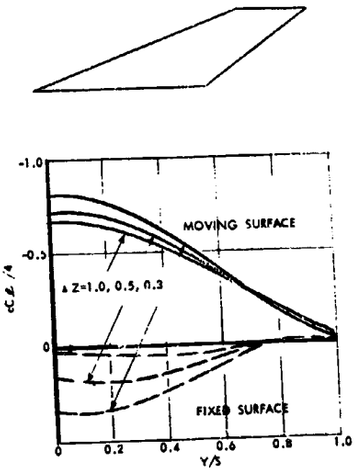

FIGURE 7. REAL LIFT COEFFICIENT DUE TO PLUNGE OF ONE SURFACE OF A BIPLANE, M = 0.8, $\frac{S\omega}{V} = 1.0$

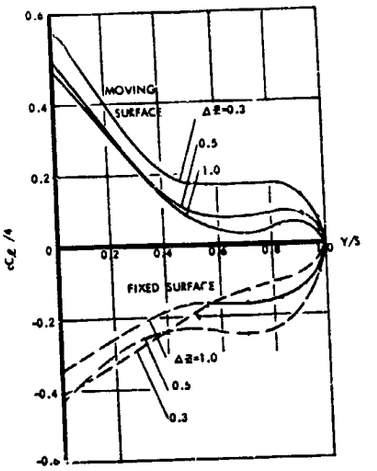

FIGURE 8. REAL LIFT COEFFICIENT DUE TO PITCH OF ONE SURFACE OF A BIPLANE, M = 0.8, $\frac{S\omega}{V} = 1.0$

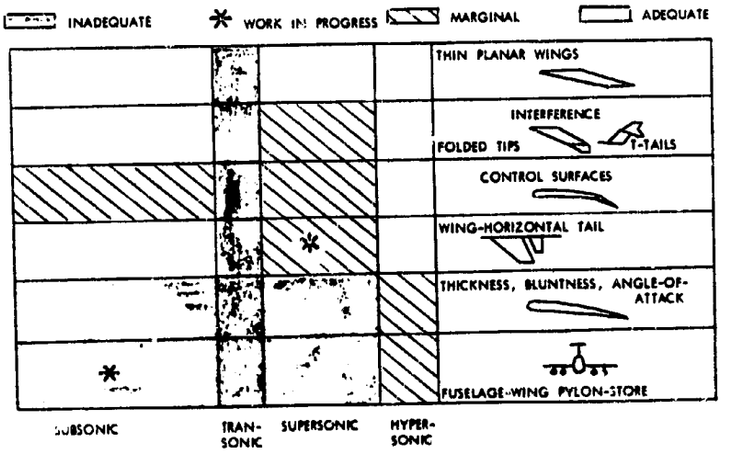

FIGURE 9. SUMMARY OF THE STATE OF THE ART

SECTION III

SUMMARY, CONCLUSIONS, AND RECOMMENDATIONS

The work of the last ten years in the linearized theory of unsteady aerodynamic flows has extended theory to multiple interfering surfaces. Production type computer programs are essentially available and have been checked against other methods and limited experimental data. The current work in the subsonic doublet-lattice method should bring capability in that method to nearly complete aircraft. On the other hand, the more classical subsonic kernel function theory still, while not far behind, is not in a production status for partial span control surfaces and, in some respects, for intersecting surfaces. Research emphasis could fill these gaps quickly. Current efforts should also place the supersonic Mach box method on a firm basis for wing-tail and intersecting surface interference problems. However, the computer programs are complex, and careful development and checking are paramount. Figure 9 is an overall summary of our estimate of the current state of the art.

The transonic area is generally the most critical area from aeroelastic and structural dynamic viewpoints but theoretical methods are most difficult and are not available today. Only token steps have been taken in the linearized theory for high frequency oscillations. It appears that nonlinear solutions will be unavoidable, but practical ideas for production analyses are few. Transonic unsteady aerodynamics remains the unsolved problem, and high priority efforts are required to produce methods useful in design and for the avoidance of serious problems. Transonic control surface unsteady aerodynamic methods are also needed to avoid buzz phenomena.

Subjects requiring attention and emphasis include control surfaces, interaction and interference effects from large or thick bodies or fuselages, non-sinusoidal or transient type unsteady aerodynamic coefficients for root locus forms of solution, and particularly, unsteady aerodynamic pressure measurements to validate theory or to form reliable estimates in design analyses. Thus, except as mentioned above, research in the last decade has contributed a remarkable, practical and relevant technology for prediction and avoidance of Space Shuttle dynamic and aeroelastic problems.

REFERENCES

1. Kussner, H., General Airfoil Theory, Luftfahrtforschung, Bd. 17, Lfg 11/12, NACA TM 979 (1941),(10 December 1940).

2. Watkins, C.E., Runyan, H.L., and Woolston, D.S., On the Kernel Function of the Integral Equation Relating the Lift and Downwash Distributions of Oscillating Finite Wings in Subsonic Flow, NACA Report 1234, (September 1955).

3. Watkins, C.E., Woolston, D.S., and Cunningham, H.J., A Systematic Kernel Function Procedure for Determining Aerodynamic Forces on Oscillating or Steady Finite Wings at Subsonic Speeds, NASA Technical Report R-48 (1959).

4. Laschka, B., The Potential and the Velocity Field for the Harmonically Oscillating Lifting Surface in Subsonic Streams, ZAMM Vol. 43, No. 7/8, (1963).

5. Rowe, W.S., Collocation Method for Calculating the Aerodynamic Pressure Distributions on a Lifting Surface Oscillating in Subsonic Compressible Flow, Proceedings of the AIAA Symposium on Structural Dynamics and Aeroelasticity, Boston, Mass., USA, (1965).

6. Ashley, H., Widnall, S., and Landahl, M.T., New Directions in Lifting Surface Theory, AIAA Journal, Volume 3, (January 1965).

7. Landahl, M.T., Stark, V.J.E., Numerical Lifting-Surface Theory - Problems and Progress, AIAA Paper 68-72, AIAA 6th Aerospace Sciences Meeting, (January 1968).

8. Cunninghan, A.M., A Rapid and Stable Subsonic Collocation Method for Solving Oscillatory Lifting Surface Problems by the Use of Quadrature Integration, AIAA/ASME 11th Structures, Structural Dynamics and Materials Conference, Denver, Colorado, (22-24 April 1970).

9. Albano, E., Rodden, W.P., A Doublet-Lattice Method for Calculating Lift Distribution on Oscillating Surfaces in Subsonic Flows, AIAA, Vol. 7, No. 2, (February 1969).

10. Garrick, I.E., and Rubinow, S.I., Flutter and Oscillating Air Force Calculations for an Airfoil in Two-Dimensional Supersonic Flow, NACA Report 846, (1946).

11. Pines, S., Dugundji, J., and Neuringer, J., Aerodynamic Flutter Derivatives for a Flexible Wing with Supersonic and Subsonic Edges, Journal of the Aeronautical Sciences, (October 1955).

12. Li, T.C., Aerodynamic Influence Coefficients for an Oscillating Finite Thin Wing, Chance Vought Aircraft, Inc., Report, (June 1954).

REFERENCES (Cont'd)

13. Zartarian, G., and Hsu, P.T., Theoretical Studies on the Prediction of Unsteady Supersonic Airloads on Elastic Wings. Part I. Investigations on the Use of Oscillatory Supersonic Aerodynamic Influence Coefficients, Wright Air Development Center Technical Report 56-97, Part I, (December 1955).

14. Zartarian, G., Theoretical Studies on the Prediction of Unsteady Supersonic Airloads on Elastic Wings. Part II. Rules for Application of Oscillatory Supersonic Aerodynamic Influence Coefficients, Wright Air Development Center Technical Report 56-97, Part II, (February 1956).

15. Voss, H.M., A Tabulation of Unsteady Supersonic Aerodynamic Influence Coefficients for the Square Box Grid, WADC TR 54-413, (May 1957).

16. Weatherill, W.H., and Zartarian, G., Application of Methods for Analyzing the Flutter of Finite Wings in Supersonic Flow, WADC-TR-58-459, (December 1958).

17. Donato, V.W., Huhn Jr. C.R., Supersonic Unsteady Aerodynamics for Wings with Trailing Edge Control Surfaces and Folded Tips, Air Force Flight Dynamics Laboratory Technical Report, AFFDL-TR-68-30, (August 1968).

18. Berman, J.H., Shyprykevich, P., and Smedfjeld, J.B., Unsteady Aerodynamic Forces for General Wing/Control-Surface Configurations, AFFDL-TR-67-117, (May 1968)

19. Ashley, H., and Rowe, W.S., On the Unsteady Aerodynamic Loading of Wings with Control Surfaces, Dedication to Professor H.G. Kussner's Seventieth birthday, (May 1970).

20. Lendahl, M., Pressure Loading Functions for Oscillating Wings with Control Surfaces, AIAA Journal, Vol. 6, No. 2, (February 1968).

21. Stark, V.J.E., Aerodynamic Forces on a Combination of a Wing and a Fin Oscillating in Subsonic Flow, Svenska Aeroplane Aktiebolaget Report Saab TN 54, (February 1964).

22. Davies, D.E., Generalized Aerodynamic Forces on a T-Tail Oscillating Harmonically in Subsonic Flow, Royal Aircraft Establishment Report Structures 295, (May 1964).

23. Zwaan, R.J., Calculated Results for Oscillating T-Tails in Subsonic Flow and Comparison with Experiments, National Aerospace Laboratory NLR, The Netherlands, Report MP 253, (August 1967).

24. Ashley, H., Linearized Time Dependent Loading of Intersecting Lifting Surfaces, North American Aviation, Inc., Report SID-63-1020, (1963).

25. Kalman, T., Rodden, W., and Giesing, J., Application of the Doublet-Lattice Method to Non-planar Configurations in Subsonic Flow, AIAA Atmospheric Flight Mechanics Conference, University of Tennessee Space Institute, (May 1970).

26. Andrew, L.V., Unsteady Aerodynamics for Advanced Configurations, Part VI, A Supersonic Mach Box Method Applied to T-Tails, V-Tails, and Top-Mounted Vertical Tails, Air Force Flight Dynamics Laboratory Technical Documentary Report, FDL-TDR-64-152, Part VI, (To Be Issued).

27. Moore, M.T., Andrew, L.V., Unsteady Aerodynamics for Advanced Configurations, Part IV, Application of the Supersonic Mach Box Method to Intersecting Planar Lifting Surfaces, Air Force Flight Dynamics Laboratory Technical Documentary Report, FDL-TDR-64-152, Part IV, (May 1965).

28. Topp, L.J., Rowe, W.S., Shattuck, A.W., Aeroelastic Considerations in the Design of Variable Sweep Airplanes, Fifth International Congress of the Aeronautical Sciences, London, England, (1966).

29. Shelton, J.D., Tucker, P.B., Davis, J.C., Wing-Tail Interaction Flutter of Moderately Spaced Tandem Airfoils, AIAA 6th Aerospace Sciences Meeting, (January 1968).

30. Sensberg, O., Laschka, B., Flutter Induced by Aerodynamic Interference Between Wing and Tail, (Entwicklungsring Süd Report No. 304-60), AIAA/ASME Structural Dynamics and Aeroelasticity Specialists Conference, New Orleans, Louisiana, (April 1969).

31. Triplett, W.E., Burkhart, T.H., and Birchfield, E.B., A Comparison of Methods for the Analysis of Wing-Tail Interaction Flutter, 8th Aerospace Sciences Meeting, American Institute of Aeronautics and Astronautics, New York, New York, (January 1970).

32. Mykytow, W.J., Noll, T.E., Huttsell, L.J., Shirk, M.H., Subsonic Flutter Characteristics of a Variable Sweep Wing and Horizontal Tail Combination, Air Force Flight Dynamics Laboratory Technical Report, AFFDL-TR-69-59, (To Be Issued).

33. Albano, E., Perkinson, F., and Rodden, W., Subsonic Lifting Surface Theory Aerodynamics for Flutter Analysis of Interfering Wing/Horizontal Tail Configurations, AFFDL-TR-70-59, (March 1970).

34. Laschka, B., Interfering Lifting Surfaces in Subsonic Flow, 29th AGARD Structures and Materials Panel Meeting, Istanbul, Turkey, (28 September - 8 October 1969).

35. Laschka, B., Schmid, H., Unsteady Aerodynamic Forces on Coplanar Lifting Surfaces in Subsonic Flow, Wing-Horizontal Tail Interference, Vereinigte Flugtechnische Werke GmbH Entarcklungs-Abteilung, Munchen, Germany, Report VFW M-72/66, (December 1966).

36. Balcerak, J.C., Flutter Tests of Variable Sweep Configurations, U.S. Flight Dynamics Laboratory Technical Report, AFFDL-TR-68-101, (September 1968).

TYPICAL SOURCES OF UNSTEADY FLOW

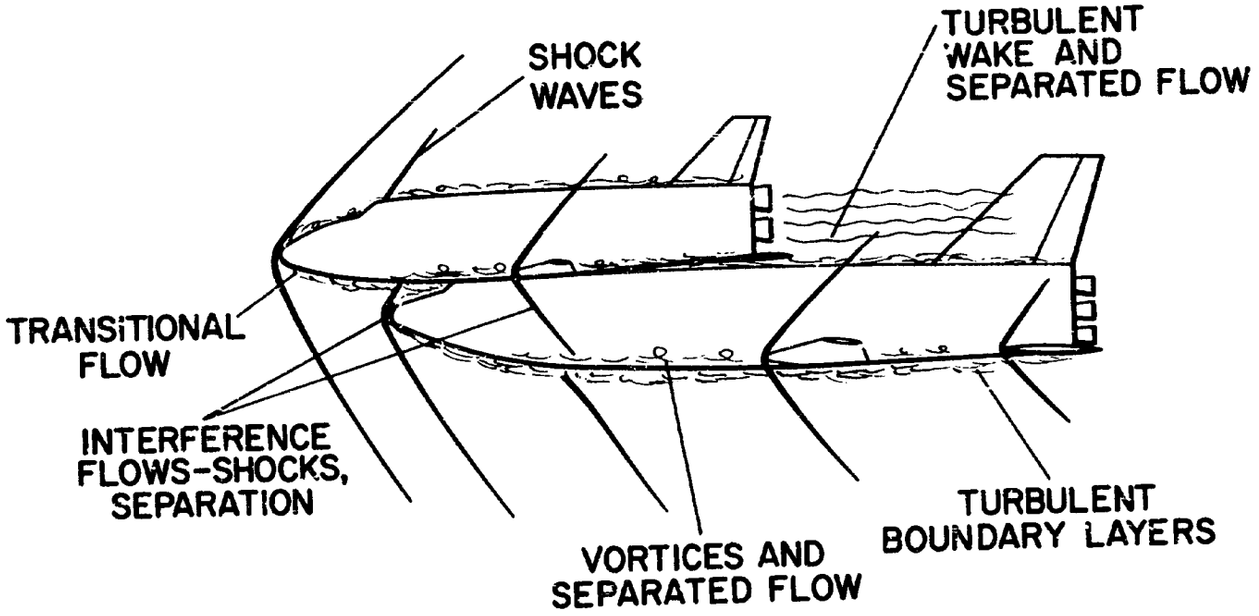

BUFFET AND AERODYNAMIC NOISE

By Charles F. Coe
Ames Research Center

INTRODUCTION

Buffeting has been defined by some dynamicists to be the response of a structure to unsteady aerodynamic flow. It has also been defined as the input loading to the structure by the unsteady aerodynamic flow. Without resolving which definition is more nearly correct, this paper will refer to buffeting as the random bending oscillations of overall vehicles and major structural components. Aerodynamic noise (which includes boundary-layer noise) is caused by the flow unsteadiness, and is related to the surface pressure fluctuations causing buffeting and local panel response.

The facing figure (#1) illustrates the main sources of flow unsteadiness causing aerodynamic noise and buffeting. The main sources are oscillating shock waves that occur at transonic and supersonic speeds, turbulent wakes, separated flow, attached turbulent boundary layers, vortices and possible flow separation from sharp cornered bodies, interference flows, and transitional flow. The sketch depicts the flow over the now familiar MSC space shuttle concept in the launch configuration. However, the same sources of unsteady flow would occur on any configuration for both the launch and reentry phases of flight.

BUFFET

At present, there is no analytical method available for prediction of buffet intensities. Consequently, such predictions must be based on experimental information generally obtained from wind-tunnel tests of scale models.

Previous experience from flight and wind-tunnel tests of aircraft and launch-vehicle configurations has shown that the severity of buffeting is largely dependent upon the extent of flow separation on the vehicle. Some of these previous data have shown the effects of airfoil profile on wing buffet, and that wings having thickness ratios greater than 10 percent can be expected to buffet at zero lift. All wings regardless of planform or profile will buffet when stalled. It can be expected therefore that currently envisioned space shuttle concepts will suffer from buffet, and that buffet loads will have to be carefully considered for each candidate configuration.

The first obvious question on shuttle vehicle buffeting concerns buffet of prospective wing configurations, particularly the MSC proposed straight wing. Results of some exploratory Langley tests reported in NASA LWP-872 are shown in the facing figure (#2) that confirm the expectation that a 12-percent-thick straight wing will buffet at zero angle of attack. These buffet boundaries for both a 3-percent-thick clipped delta wing and a 12-percent-thick straight wing indicate that the thin delta wing would be free of buffet at low angles of attack during launch but that the straight wing will buffet between M=0.8 and M=0.9. As expected, the boundaries indicate that both wings would buffet at high angles of attack.

WING BUFFET BOUNDARIES

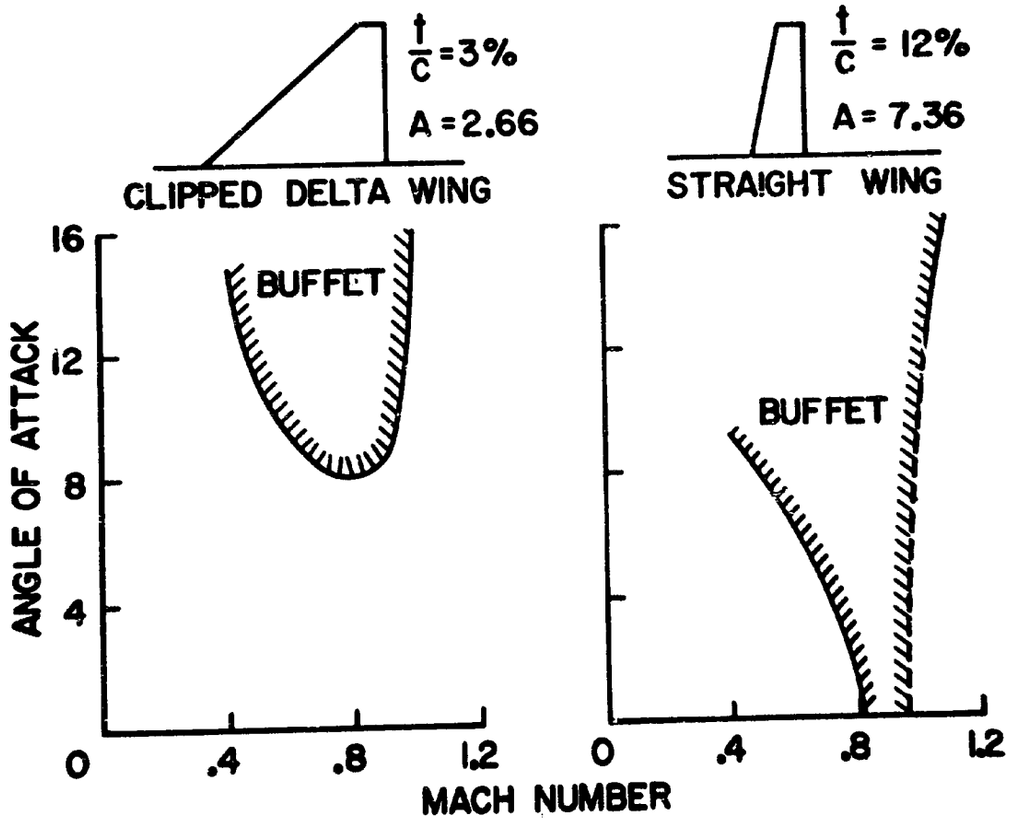

Examination of buffet boundaries is an appropriate first step, but boundaries yield no information on the potential severity of the problem. In order to gain some insight as to whether buffeting would be seriously detrimental to the straight wing, some very preliminary estimates of wing bending-moment fluctuations have been made, and are presented in the facing figure (#3). The results on the left show the ratio of maximum predicted full scale bending-moment fluctuations to the MSC design static-load limit for angles of attack up to 12°. These results, which were scaled from measurements on a 10-percent-thick wing, indicate that for normal launch conditions ($\alpha < 4°$) the bending-moment fluctuations would be less than 2 percent of the design static limit. An extreme launch condition angle of attack of 12° would result in a 10 percent of load-limit fluctuation. Recent Langley tests reported in NASA LWP-872 yielded a similar appraisal of the ratio of maximum peak amplitude of bending-moment fluctuations to static moment at $\alpha = 60°$. These results, shown on the right, indicate a maximum ratio of about 15 percent.

It should be kept in mind that the above-mentioned buffet intensity estimates are only first approximations. Additional tests of an elastically scaled model of the MSC straight wing are now in progress that will soon yield considerably more accurate results on low angle-of-attack wing buffeting intensities.

The estimation of the wing buffeting is critical to the wing design, but because of very large fuselages and empennages, wing buffet may not be the key factor responsible for the buffeting of the overall vehicle. Exploratory tests of a few launch-configuration concepts are therefore needed to appraise the effects of major geometric variables. Such tests are scheduled, and are noted in the summary of this paper.

PREDICTED WING BUFFET INTENSITIES

SCALED FROM
AMES AIRCRAFT BUFFET MODEL
t/c = 10%

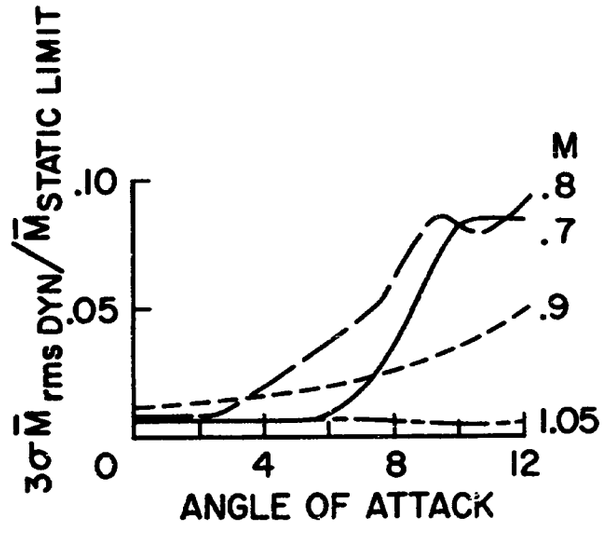

LWP 872
t/c = 12%

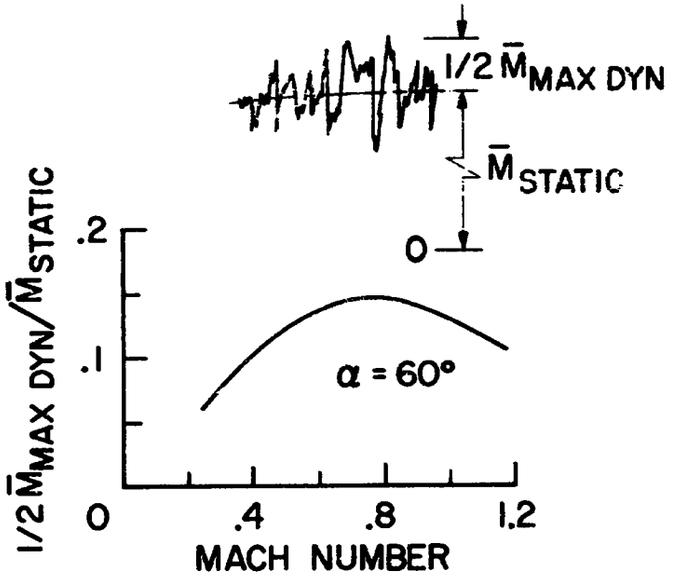

3

AERODYNAMIC NOISE

The information needed to fully describe the unsteady surface pressure field associated with aerodynamic noise is as follows: first, the intensity or magnitude of unsteady pressure; second, the location and area of coverage on a vehicle surface; third, the frequency spectra; and fourth, a pattern of spatial correlation. The intensity of fluctuating pressures is the easiest of the above listed information to acquire, and is consequently the most voluminous among the available experimental data that can be used for preliminary estimates of space shuttle unsteady pressures. The facing figure (#4) shows typical broadband intensities of local pressure fluctuations for different types of flow and the ranges of Mach numbers where data are available. The attached boundary layer which has the lowest intensity pressure fluctuations is in general the most thoroughly described statistically for $M < 3.5$. Attached boundary layer data for $M > 3.5$ are very sparse and lacking in description. Transitional flow which can result in high intensity pressure fluctuations has been investigated for intensity and spectra at only the two Mach numbers shown. Pressure fluctuations in regions of shock waves and separated flows have been studied quite extensively, and detailed spatial correlation and scaling information is nearing publication at Ames.

Aerodynamic noise is unfortunately very configuration sensitive, so that eventually a model of the final space shuttle configuration should be tested to establish a complete description of the unsteady pressure environment. In the meantime some exploratory space shuttle tests are needed to obtain preliminary data in regions of interference and possible vortex flows. Additional general research is also needed to acquire more complete statistical description of surface pressure fluctuations beneath hypersonic transitional and turbulent boundary layers.

INTENSITIES OF LOCAL PRESSURE FLUCTUATIONS

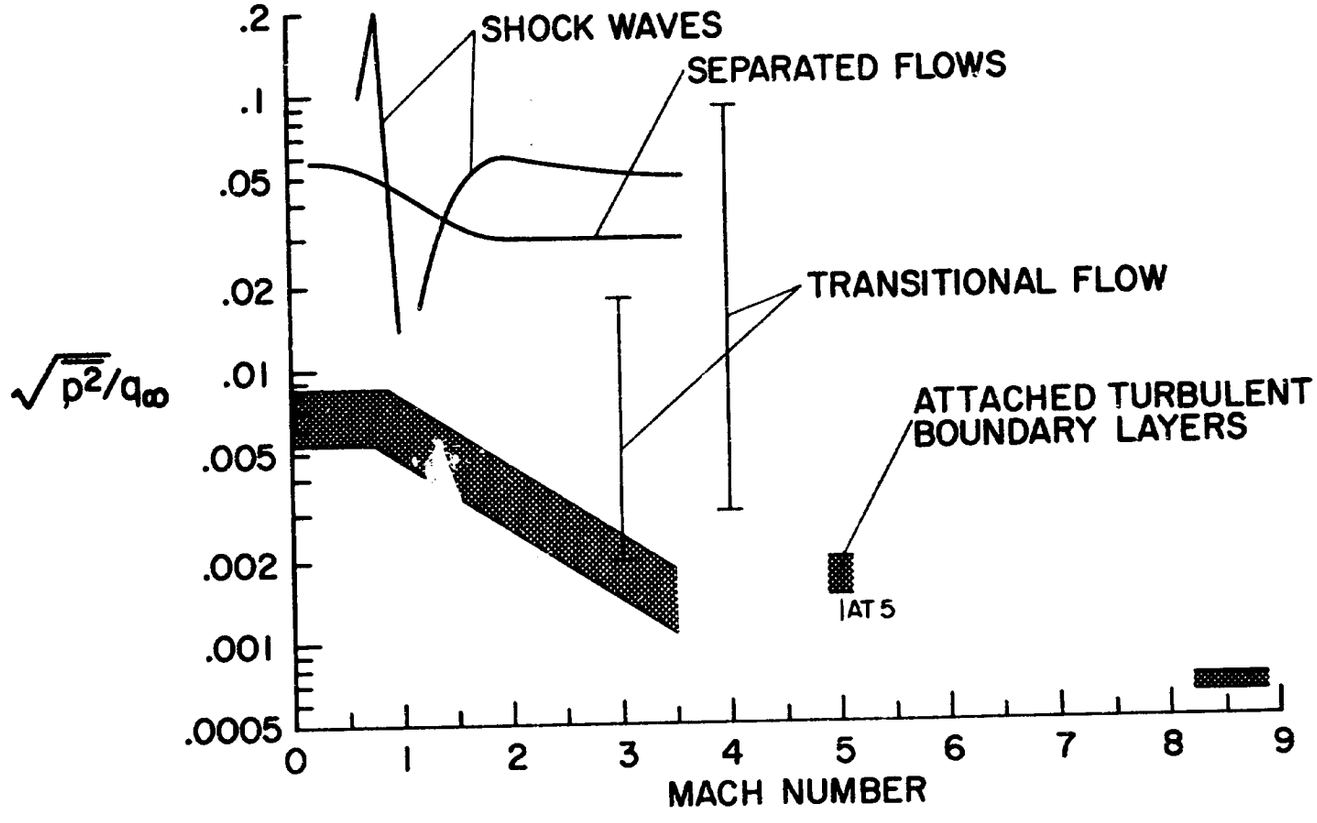

SUMMARY

In summary, buffet and aerodynamic noise are so configuration sensitive that the most critical research will be needed after final configuration selection. Some important interim research is in progress or planned, however, at NASA centers that will provide much needed preliminary design information. The key items of activity are tabulated in the facing figure (#5).

For BUFFET, exploratory tests are now in progress at Ames to determine the overall orbiter vehicle buffet loads of the MSC configuration during launch, and to estimate the unsteady loads at the booster attachment points. Elastic models are also under construction and will be tested to determine if the buffeting of a complete two-body launch vehicle will be significantly altered by changing wings from straight to delta planforms. Tests of an elastically scaled MSC straight wing are in progress that will yield more precise wing buffet information than is currently available. The planned MSFC investigation is to evaluate the possibility of critical aeroelastic effects using a quasi-steady aerodynamic technique. The last item under BUFFET is for ad hoc tests of the final configuration. Ames is indicated for support, and the question mark refers to uncertainties regarding contractor participation.

For AERODYNAMIC NOISE, aside from the need for an eventual final configuration study that will fully describe the surface pressure fluctuations, exploratory tests are planned at Ames that will identify and measure regions of high-intensity flow unsteadiness on candidate configurations. Some general research programs at MSFC and Ames that have application to shuttle vehicles are continuing with the objective of improving the statistical description of surface pressure fluctuations. Unsteady pressures due to high altitude plume induced flow separation is being studied by MSFC. Basic studies of hypersonic transitional and turbulent boundary layers are getting underway at Langley and Ames. Lastly an investigation is in progress at Ames to determine the effects of panel motion on aerodynamic noise. This is a potentially critical item for application to the calculation of response of thermal protection system panels to aerodynamic noise.

SUMMARY OF CURRENT AND PLANNED SUPPORTING RESEARCH

BUFFET – NEED TO EVALUATE BUFFET LOADS DURING LAUNCH AND REENTRY

• EXPLORATORY BUFFET TESTS OF LAUNCH CONFIGURATION CONCEPTS	ARC
• RIGID MODEL - MSC ORBITER LOADING ON BOOSTER	
• ELASTIC MODELS - BENDING RESPONSE OF COMPLETE LAUNCH VEHICLES WITH STRAIGHT AND DELTA WINGS	
• BENDING RESPONSE OF ELASTICALLY SCALED MSC STRAIGHT WING	
• EVALUATION OF AEROELASTIC EFFECTS INDUCED BY UNSTEADY SEPARATED FLOWS	MSFC
• AD HOC TESTS OF ELASTIC MODELS OF FINAL SELECTED CONFIGURATION FOR BOTH LAUNCH AND REENTRY CONDITIONS	ARC, ?

AERODYNAMIC NOISE – NEED SPECIFICATION OF INTENSITY, LOCATION, SPECTRA, AND SPATIAL CORRELATION OF UNSTEADY PRESSURES

• FLOW VISUALIZATION STUDIES TO IDENTIFY UNSTEADY FLOW REGIONS	ARC
• MEASUREMENT OF INTENSITIES, SPECTRA, AND SPATIAL CORRELATION	MSFC, ARC
• UNSTEADY PRESSURES DUE TO HIGH ALTITUDE PLUME INDUCED FLOW SEPARATION	MSFC
• BASIC STUDIES OF HYPERSONIC TRANSITIONAL AND TURBULENT BOUNDARY LAYERS	LRC, ARC
• EFFECTS OF PANEL MOTION ON AERODYNAMIC NOISE	ARC

PREVENTION OF COUPLED STRUCTURE-PROPULSION INSTABILITY (POGO) ON THE SPACE SHUTTLE

S. Rubin

The Aerospace Corporation
Los Angeles, California

INTRODUCTION

Many liquid-propellant rocket vehicles have experienced longitudinal vibration, nicknamed pogo after the jumping stick, due to an instability arising from interaction of the vehicle structure with the propulsion system. These vibrations can produce an intolerable environment for astronauts and equipment, can overload vehicle structure, and can lead to loss of propulsion performance. A NASA monograph concerned with the prevention of pogo is well on its way toward publication and should serve as a useful guide to design for the Space Shuttle.

The paper will briefly describe the nature of the pogo phenomenon, present a summary of past instabilities, relate the possible deleterious effects of pogo, and discuss the contents of the design criteria monograph. Finally, research tasks are recommended for support of pogo development activities on the Space Shuttle.

The pogo instability phenomenon results from a dynamic coupling of vibratory motion of the structure of a space vehicle with oscillations in the propulsion system. The simplified vehicle schematic at the left of chart 1 portrays a propellant tank, a feedline, and an engine. Imagine the engine to be comprised of a pump, a pump discharge line, and a thrust chamber. When the vehicle vibrates longitudinally, the pump and the propellant in the flexible tank undergo oscillatory motions. These two motions produce oscillatory flow in the feedline and in the pump discharge line. The flow oscillations lead to oscillations in engine thrust and in pressure at the pump inlet, which then act as regenerative forcing functions on the vehicle structure. Another type of propulsion-system behavior, involving an active tank-ullage pressurization system, may also lead to an instability termed ullage-coupled pogo as opposed to the above engine-coupled pogo.

A block diagram of this positive feedback process is also shown. The coupled structural-propulsion system is linearized to consider perturbations of the system variables to determine the degree of linear stability.

Of great significance is the relationship of natural frequencies of the structure with those of the propulsion system. The upper-right diagram shows the variation of natural frequencies of structural modes A and B and of a single propulsion system mode denoted by f^*. The frequency f^* changes primarily because the steady pressure at the inlets to pumps changes with time and the degree of pump cavitation thereby also changes. Coincidence of structural and propulsion natural frequencies strengthens the coupling which may lead to instability. Other important system characteristics are the gain and damping of the modes of the structural and propulsion systems. Pogo has been corrected in flight by introducing an accumulator into feedlines to maintain separation of significant modes of the structural and propulsion systems.

The results of stability analysis can be expressed in terms of the variation of damping of the coupled system with time, as depicted at the center right. System damping tends to decrease at frequency coincidences. As shown, the system mode involving the structural mode B has a damping ratio ζ_B which dips, but remains positive. However damping for the system mode involving structural mode A becomes negative and the system therefore becomes unstable in a linear sense.

A corresponding depiction of vehicle longitudinal acceleration appears at the lower right. When ζ_B dips, narrow-band random vibration in structural mode B tends to intensify. Later in time during the period of instability involving mode A, there appears a slowly varying limit cycle controlled by nonlinear behavior. Modeling the coupled system for accurate prediction of the limit-cycle behavior is beyond the state of the art.

CHART 1
NATURE OF POGO (ENGINE COUPLED)

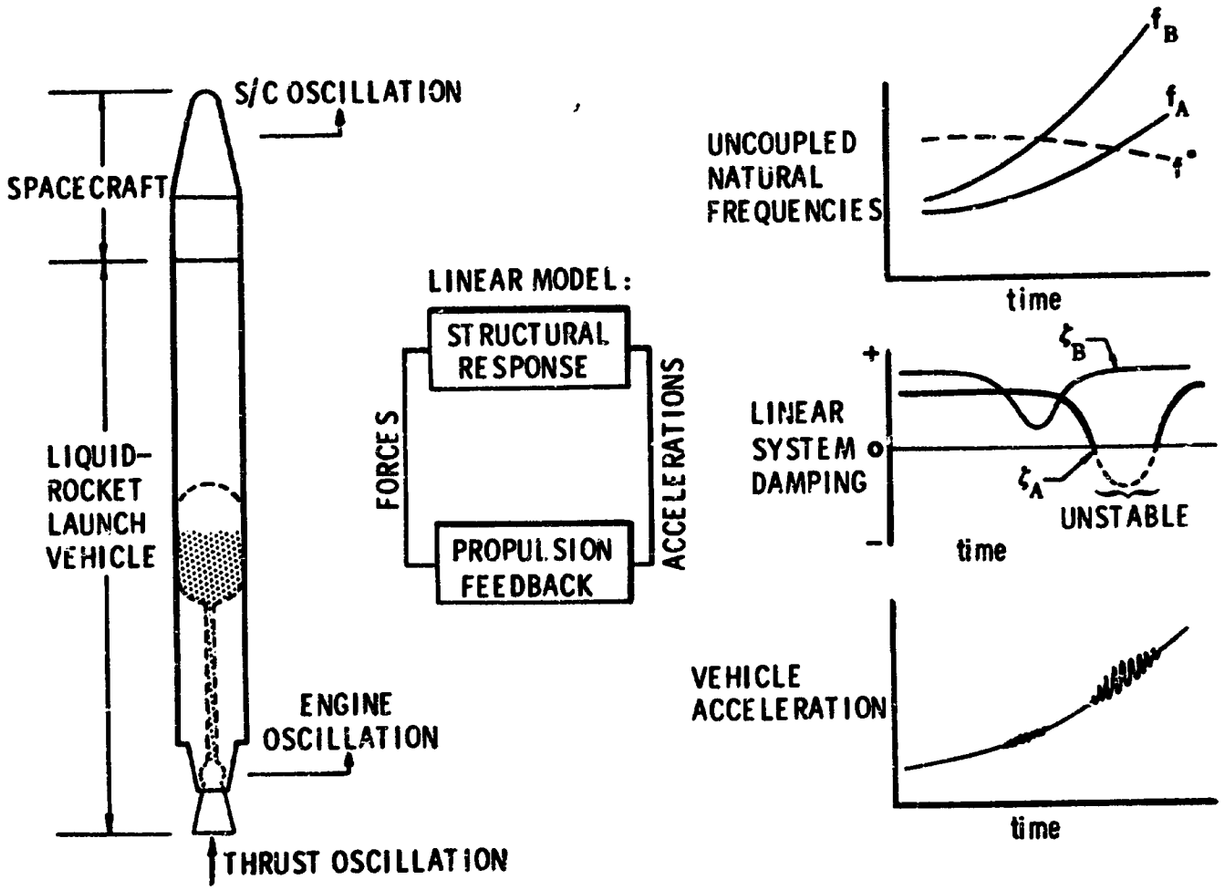

A compilation of information on engine-coupled pogo instabilities is shown on chart 2. Acceleration amplitudes at spacecrafts appear in the left plot and at engines in the right plot. The plots are intended to be an overall depiction of pogo history and should not be used for detailed comparisons among vehicles because of differences in measurement locations.

Bands 1-3 show ranges for certain consistently unstable Thor-family vehicles. Points and bands 4-8 are for Titan-family vehicle of the past. Among the Titan II vehicles, N-11 is unique in that is represents the first attempt to correct pogo with a feedline accumulator device. Unexpectedly vibration severity increased markedly, later it was recognized that the system had been incompletely understood. Failure of the N-11 mission occurred because large chamber pressure oscillations during pogo caused shutdown of the engines.

The Gemini-Titan vehicles were the first to have a pogo man-rating requirement and a limit of 1/4 g was imposed at the base of the Gemini capsule. Accumulators were incorporated into fuel and oxidizer feedlines of the Titan Stage I and the limit was not exceeded except on Gemini Titan-5 for which the two oxidizer accumulators were improperly charged prior to liftoff. All Titan III vehicles other than Titan IIIC-7 have been stable. Titan IIIB and advanced Titans have accumulators to prevent instability.

In connection with a man-rating requirement, an appropriate working-efficiency boundary taken from a proposed standard is shown in the left plot This boundary applies to short-term sinusoidal vibration of man in a back-to-chest direction. The degree of impairment of man's working efficiency of course depends on the nature of the task and other aspects of the environment. Note that the second Saturn V launch with Apollo 6 considerably exceeded this boundary; the first Saturn V vehicle did not pogo. Because of concern for the astronauts and for structural loading within the spacecraft, accumulators were introduced into the S-1C stage of later Saturn V vehicles and the instability has not reappeared during S-1C burn.

Suspicious indications of vibration during S-2 burn of early Saturn V vehicles and the Apollo 6 experience during S-1C burn led to the addition of accelerometers to detect S-2 pogo on the next Saturn V launch (Apollo 8). A 10 g amplitude at the center engine toward the end of S-2 burn was recorded in a local structural mode involving relatively large motion of the center engine. This instability was avoided on later vehicles by shutting down the center engine one minute early. However, the severity of lesser vibrations earlier in S-2 burn increased markedly in later flights. About 3.8 g was recorded at the center engine on Apollo 12 leading to consideration of system correction by means of a center-engine lox accumulator. Apollo 13 was not corrected, and even though it was virtually identical to Apollo 12, the vibration rose to 34 g! As with the Titan II N-11 vehicle, chamber pressure oscillations caused premature engine shutdown. The vibration mode is so local that less than 0.1 g was observed at the Apollo 13 spacecraft. Here is a striking example of the great sensitivity of pogo to small system changes — six launches of Saturn V/Apollo vehicles without large early S-2 vibration, then large vibration on Apollo 12, and enormous vibration on Apollo 13. Obviously the lack of a pogo problem on the first several launches is in itself an insufficient basis for a lack of concern.

The recent flight of the first Diamant B vehicle is exceptional in that the frequency was high (second longitudinal structural mode) and it is the only known occurrence of pogo during burn of a pressure-fed stage. The next paper deals with a new mechanism of feedback which may be important on the Diamant B.

CHART 2

POGO INSTABILITIES (ENGINE COUPLED)

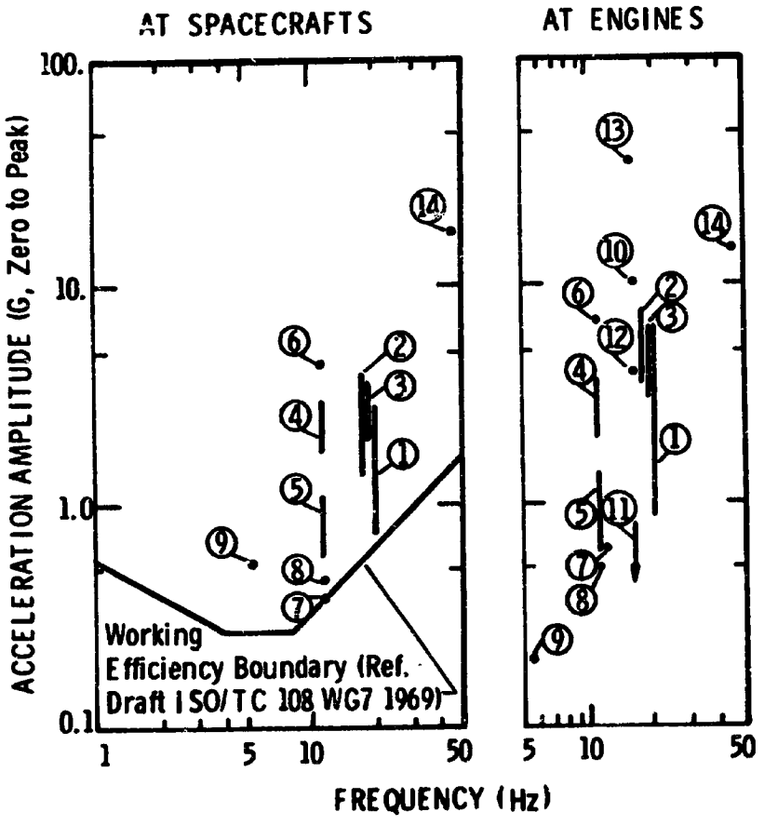

1 THOR/AGENA D
2 THORAD/AGENA D
3 THORAD/DELTA
4 TITAN II, EARLY
5 TITAN II
6 TITAN II, N-11
7 GEMINI TITAN-5
8 TITAN III C-7
9 SATURN V/APOLLO 6
• 10 SATURN V/APOLLO 8
• 11 SAT. V/PRE APOLLO 12
• 12 SATURN V/APOLLO 12
• 13 SATURN V/APOLLO 13
14 DIAMANT B
(• STAGE II)

Clearly the astronaut environment is a chief concern for the Space Shuttle. Man's sensitivity to vibration, and the levels of vibration which have resulted from pogo instability, strongly indicate the need to have stability in all modes involving significant motion in the spacecraft.

Although the number of cases of positively identified structural and equipment failures is small, such failures are also a major concern. Whereas man may often be the limiting factor in the system, for local instabilities near engines (socalled minipogos) the prime concern will be for structural failure and for the possibility of premature shutdown of engines.

CHART 3

POGO EFFECTS

- INTOLERABLE ENVIRONMENT FOR ASTRONAUTS AND EQUIPMENT
- OVERLOAD VEHICLE STRUCTURE
- ENGINE SHUTDOWN

A NASA Space Vehicle Design Criteria Monograph on pogo is currently being prepared by the writer under the auspices of the Langley Research Center. The monograph, currently in Reader's Copy form, is entitled "Prevention of Coupled Structure-Propulsion Instability (Pogo)"; the Task Manager at Langley is G. W. Jones, Jr.

An introductory section states the problem, discusses the need for attention to it, and presents the purpose, scope, and approach of the monograph. Basically the aim is to prevent pogo by modifying the system if necessary to achieve adequate linear stability.

The State-of-the-Art, Criteria, and Recommended Practices sections deal with the individual aspects shown on Chart 4. The Appendix deals with the assessment of the significance of the structural modes. Some 62 references to the literature are given.

CHART 4

DESIGN CRITERIA MONOGRAPH

PREVENTION OF COUPLED STRUCTURE-PROPULSION INSTABILITY (POGO)

- INTRODUCTION
- STATE-OF-ART
- CRITERIA
- RECOMMENDED PRACTICES
- APPENDIX
- REFERENCES

MATHEMATICAL MODELING
PREFLIGHT TESTING
STABILITY ANALYSIS
CORRECTIVE DEVICES
FLIGHT EVALUATION

The need for pogo stability has already been stressed. That stability must be demonstrated by a suitable combination of analysis and test. Since the achievement of a stable coupled system is the objective, analyses should be performed with a linearized mathematical model. Experimental data must be obtained to establish values for those model characteristics which significantly effect the resonant frequencies, gains, and dampings associated with modes of the structural and propulsion systems. Great care must be exercised so that tests are conducted in a manner to insure that small oscillation behavior is observed. This is particularly critical for determinations of structural-system damping and of turbopump dynamics.

Structural modeling for consideration of pogo on the Space Shuttle will be more complex than in the past owing to major three-dimensional coupling of motions resulting from asymmetric geometry of the vehicle. Based on past experience, particular attention must be paid to modeling of propellant tanks. Although a number of advanced tank-modeling approaches have been proposed in the last five years, these have not been sufficiently evaluated to determine the most suitable approach. The need is for a method to deal with both longitudinal and lateral oscillations and the effect of outflow oscillations into the feedlines to the engines. Also, detailed modeling will be required for engine-compartment structures to treat motions of such items as pumps, line bends, and engine support beams. Modal testing will be essential to the experimental verification of the structural-system model.

The overall structural system should be described for the model in terms of normal modes of vibration. The Appendix of the monograph provides a method for assessing the significance of the individual modes. Insignificant modes should be excluded to avoid unnecessary clutter in the analysis. The significant modes must be defined with considerable accuracy. The correctness of the model should be re-evaluated after modal analysis. The monograph recommends that modeling improvements be assessed and incorporated when they change a natural frequency by more than 5 percent or a structural gain by more than 10 percent.

Modeling of the propulsion system can begin on the basis of known properties of the propellants, flow-line geometries, and steady-state pressures and flows of the system. Only pump inlet cavitation can not be estimated from standard information.

Frequency-response testing of the turbopumps will be required. Uncertainties in results of past testing of turbopumps are believed to be largely the result of inadequate instrumentation and test procedures. Needed are pressure and flow instrumentation to detect low-amplitude oscillatory behavior. Flow instrumentation has not been available and pressure instrumentation ranges have been based on steady and large transient requirements. Also needed are test procedures which provide sufficient data to define completely the turbopump dynamics without requiring any assumptions of turbopump behavior. That is, the turbopump should be tested as if it were a "black box" to be described in terms of measured properties alone. Tests of the feedlines and of the overall propulsion system will also be required.

Pogo stability analyses which include the consideration of parameter uncertainties, should be performed early in the vehicle development process. The monograph refers to an approximate methods for an initial investigation of the possibility of incurring engine-coupled instability. With this method the significance of uncertainties in the system parameters can be initially

CHART 5

CRITERIA

- COUPLED SYSTEM SHALL BE STABLE
- ANALYZE WITH LINEARIZED MATH MODEL
- EXPERIMENTAL EVALUATION OF MAJOR CHARACTERISTICS
- PRIOR TO FLIGHT, VEHICLE CONSIDERED STABLE IF
  - ≥6 DB "DAMPING GAIN MARGIN" } NOMINAL CONDITIONS
  - ≥30° "STRUCTURAL PHASE MARGIN" } NOMINAL CONDITIONS
  - PROBABILITY OF INSTABILITY SMALL
- IF NECESSARY, ELIMINATE INSTABILITY BY SYSTEM MODIFICATION
- ACCURACY OF MATH MODEL SUBSTANTIATED BY VEHICLE FLIGHTS

assessed. As the vehicle progresses through its development phases and becomes better defined, increasingly detailed models should be constructed and stability analyses performed. Each cycle of stability analysis will provide information for a next round of refinements in the modal, including the possible consideration of corrective modifications for achieving stability. Moreover, the process will contribute to advanced planning for testing and to the early consideration of alternative corrective modifications for the standpoints of implementation, reliability, and influence on the function of other elements of the system. Analyses should continue with updated parameters and increasing refinement until flight data and postflight analyses have demonstrated acceptable stability of the space vehicle.

Special gain and phase margins are defined in the monograph and the 6 dB and 30 degree margins are minimum requirements for the nominal coupled system at each time of flight. These margins are defined so that any analytical technique that identifies an instability can be employed. This is achieved by prescribing that stability must be maintained for clearly specified modifications of the system. Complex mode shapes for the "nonclassical" normal modes of the coupled structure-propulsion system should be obtained to provide reference information for review of flight data.

It is recommended that the vehicle be considered stable when analyses performed show either (1) that the system is stable under extreme tolerance (worst-case) conditions or (2) that the probability of occurrence of an instability is less than an allowable value assigned on the basis of overall vehicle flight-worthiness considerations. A conservative approach is outlined for determining whether the probability of instability during flight is sufficiently small. A Monte Carlo analysis of feedline resonant frequencies may be involved.

Close-coupled accumulators for engine feedlines should be considered in any study of potential corrective modifications to achieve vehicle stability. Appropriate for cryogenic propellants are the metal-bellows type developed for Titan III vehicles and the gas-injection type developed for the Saturn V. Consideration should be given in the initial design phases to allow for possible future installation of such devices. A method is given for tentative sizing of an accumulator during early development of the vehicle. Requirements are identified for a development program to integrate accumulators into a propulsion system.

The initial several flights of the vehicle should be specially instrumented to obtain data which can be used to verify the mathematical model used for pogo stability analysis. A practical method to determine experimentally the degree of stability in flight has not been established. Due to the lack of such a method, the absence of an instability on an initial flight is far from a guarantee that the vehicle is adequately stable. Therefore only a well-verified mathematical model can provide confidence in the inherent stability of the vehicle. Special instrumentation is identified and data reduction techniques are suggested.

If an instability occurs in flight, the relative amplitude and phase of oscillations throughout the structural and propulsion systems indicate the "shape" of the unstable mode of the coupled system. This shape may be distorted by nonlinear effects at high amplitudes of oscillation. When the system is stable and sufficient coherency exists among the random oscillations of the system variables, spectral analyses should be performed to determine amplitude and phase relationships among variables. Coupled-system mode shapes determined from the flight data should be compared with analytical predictions for evaluation of the mathematical model. Natural

frequencies of structural modes can be readily detected through spectral density analysis of acceleration data. Resonant frequencies of feedlines have been more difficult to detect, but narrow-range pressure instrumentation should improve chances of success. A technique is available for evaluating individual portions of the structural dynamic model in cases of purely longitudinal vibration.

Pogo instability is potentially a major problem for every phase of rocket-powered flight of the Space Shuttle. A monograph is being prepared to make certain that the best advantage is taken of past experience.

There are two intrinsic limitations associated with current practices. First, the coupled structural-propulsion system can not be ground tested to directly evaluate pogo stability. Unfortunately, it appears that certain conflicting requirements rule out such testing. So analysis must be totally relied upon to obtain confidence in vehicle stability before flight.

Second, current practice does not permit the determination during flight of the coupled-system damping. It appears that the determination of system damping in flight requires the application of an artific[illegible] disturbance at various times of flight so that resulting oscillations in [illegible]stem modes can be discerned. Unless system damping can be deter[illegible]ed experimentally for initial flights, the mathematical model provides the only basis for assessing the degree of system stability.

Development of a reliable model demands considerable analysis and test activities throughout vehicle development. These activities must be carefully programmed into the planning to insure an orderly and timely development.

CHART 6

SUMMARY

- POGO IS MAJOR CONCERN FOR ALL ROCKET-POWERED PHASES
- MONOGRAPH PROVIDES CRITERIA AND RECOMMENDED PRACTICES
- RELIANCE ON MATH MODEL TO ASSURE ADEQUATE STABILITY EVEN AFTER SEVERAL FLIGHTS
  - STRONG INTERPLAY OF ANALYSIS AND TEST
  - POGO ACTIVITIES MUST BE CAREFULLY PROGRAMMED INTO DEVELOPMENT PLANS
- LIMITATIONS OF CURRENT PRACTICES
  - REQUIRE FLIGHT TO REALISTICALLY TEST COUPLED SYSTEM
  - INABILITY TO DETERMINE COUPLED-SYSTEM DAMPING IN FLIGHT

Four specific research objectives appear to be attainable and could contribute markedly to the technology for treating pogo instability. The first two listed on chart 7 would significantly improve our ability to define the propulsion system by test. The need for dynamic flow transducers is great. In addition practical means for testing a turbopump as a "black box" should be defined so that the pitfalls of deducing its behavior from overall propulsion-system behavior are avoided. For example, sinusoidal pulsing tests for two hydraulic boundary conditions at the turbopump discharge, with instrumentation for inlet and discharge dynamic pressure and flow, can yield the parameters of a "four-terminal network" which describes the turbopump.

A thorough evaluation of propellant-tank modeling methods is necessary. A number of modeling methods have been proposed, but their comparative capability for pogo needs have not been explored.

Because of a potentially large payoff, methods of inflight disturbance to determine system damping should be studied. It would appear that disturbances generated both within and external to the propulsion system should be considered.

CHART 7

TECHNOLOGY NEEDS

- DEVELOP TRANSDUCERS FOR PROPELLANT FLOW OSCILLATIONS
- DEVELOP TEST PLANS FOR COMPREHENSIVE MEASUREMENT OF TURBOPUMP DYNAMICS
- EVALUATE PROPELLANT-TANK MODELING METHODS
- INVESTIGATE METHODS FOR INFLIGHT EXCITATION TO MEASURE COUPLED-SYSTEM DAMPING

CONCLUSIONS

Knowledge of the pogo phenomenon is believed to be sufficient to permit pogo instability to be avoided on the Space Shuttle. The basis is provided by the criteria and recommended practices given in a forthcoming NASA monograph. The four identified research tasks should be carried out to support future analysis and test activities.

INFLUENCE ON THE POGO EFFECT OF THE AERODYNAMIC PHENOMENA IN A ROCKET AFTERBODY

Marcel BARRERE, Jacques POUTTES,
Office National d'Etudes et de Recherches Aérospatiales (ONERA)
92 - Châtillon, France

and Jean LEMOINE
Laboratoire de Recherches Balistiques et Aérodynamiques
27 - Vernon, France

1 - INTRODUCTION

The vibrations known as "POGO effect" result from a coupling between the structure, the tanks and lines, and the motor of a liquid propellant rocket stage. One of the elements of the coupling is due to the forces applied on the structure by periodical variations of the combustion chamber pressure. This paper aims at laying stress on the influence that aerodynamic phenomena in the afterbody may have on the value and the very nature of these forces. (Fig. 1)

After pointing out the main parameters of the problem, two particular cases will be briefly examined : a single nozzle rocket operating at low level (L. 17 booster of the DIAMANT B launcher), and a multi-nozzle rocket operating at high altitude.

2 - SETTING THE PROBLEM

In the methods generally used for forecasting the POGO effet, the efforts resulting from the periodic variations of the chamber pressure are computed by taking into account only the thrust coefficient of the propulsive nozzle in vacuum, but neglecting the effect of pressure variations on the other parts of the propulsive stage outside the nozzle proper. This assumption may be questionned, particularly when the base cross-section A_A is large, relative to the throat section A_t. If we call δp_A and δp_c the simultaneous pressure variations at the aft cross-section and in the chamber, δF_A and δT_v the thrust variations due to the forces on the aft section and on the intunnel walls of the nozzle (thrust in vaccum), it can be written: (Fig. 2)

$$\frac{\delta F_A}{\delta T_v} = \frac{A_A}{A_t C_T} \frac{\delta p_A}{\delta p_c}$$

C_T being the thrust coefficient in vaccum.

With this relation it is possible to appreciate the validity of the assumption generally retained, already mentioned, regarding the relative order of magnitude of $\delta F_A / \delta T_v$ for various frequencies.

The $A_A / A_t C_T$ depends only on the geometry of the after-body and the nozzle. In the case of L.17 (DIAMANT B), its value is 8 ; for the SATURN II stage, relative to 5 engines, it is 80.

The estimation of the ratio ($\delta p_A / \delta p_c$) is very difficult by theoretical means ; moreover its introduction in the forecasting of the stability of the POGO coupling entails that, for each frequency, its amplitude and phase are known.

A first semi-empirical approach is given hereafter for a single nozzle rocket operating in an air atmosphere, and a qualitative description of the phenomena that may take place in a multi-nozzle rocket operating at high altitude is indicated.

3 - SINGLE-NOZZLE ROCKET AT LOW ALTITUDE

The phenomena by which it is possible to express qualitatively the pressure variations δp_A in the aft section in correlation with the δp_c variations is as follows : any δp_c variation modifies, in a quasi-steady flow, the separation line between the jet and the surrounding atmosphere ; it may also change the nature and the intensity of the vortices issued from the jet. All these movements induce vibrations in the surrounding atmosphere , as a noise at the excitation frequency.

Bench experiments of the L.17 motor, aimed at measuring the noise around this rocket, show that there is an actual correlation between the pressure variations around the rocket and these of the chamber.

The noise generated by the nozzle is transmitted to the aft section ; its intensity decreasing with increasing distance, but if the aft part of the rocket is as a resonant cavity ; in that case, around the resonance frequency of the cavity, the pressure variations in the tank rear bulkhead may be very important.

Vibrations observed during the first flight of DIAMANT B seem to have to be attributed to such a phenomenon.

Acoustical tests of the rear fairing have been carried out showing that the frequency observed in flight is not far from that of the fairing. The results obtained are however difficult to analyze, as the excitation level that may be reached on the ground is low compared with that actually met in flight.

On the other hand, tests at reduced scall have been performed; they give a proof that the phenomenon actualy exists.Visualizations of the phenomena are prepared for the coming months.(Figs. 3 and 4)

The ratio ($\delta p_A / \delta p_c$) actually measured, at about the resonance frequency, reaches 3. This figure should be considered but as an order of magnitude for the full scale rocket, as it is not possible to respect all the similarity laws, especially for the damping, at the 1/40 scale model.

The analysis of the POGO effect on DIAMANT B has been performed by introducing measurements made on the ground, regarding in particular the damping of the structural mode. It appears that, taking into account the measurements during firing at rest, the acoustical measurements on the flight skirt or measurements on reduced scale models with air jets, the open-loop gain is such that vibrations of POGO type should diverge. (Fig. 5)

4 - MULTI-NOZZLE ROCKET IN VACUUM

It may be considered that an effect similar to that of a cavity at atmosphere pressure appears with multi-nozzle rocket operating in vacuum. In effect as a consequence of the jet convergence the pressure in the cavity limited by the jet exhausts

and the rear bulkhead may be rather large, as it has been proved by tests performed on reduced scale models.(Fig. 6)

This pressure is piloted by the pressure in the combustion chambers, and the problem lies in the determination of ($\delta p_A / \delta p_c$) as a function of frequency. This investigation has been recently initiated on a reduced scale model of a - 4 - nozzle rocket whose chamber pressure, supplied with compressed air, was modulated.

5 - CONCLUSION

The first ground tests carried out show that the aerodynamical phenomena on after-bodies may have a noticeable influence on vibrations of POGO type. The results already obtained on the ground on a single-nozzle configuration must be confirmed and made more accurate. It seems necessary to have experimental results available before ascertaining this effect on multi-nozzle configurations operating in vacuum.

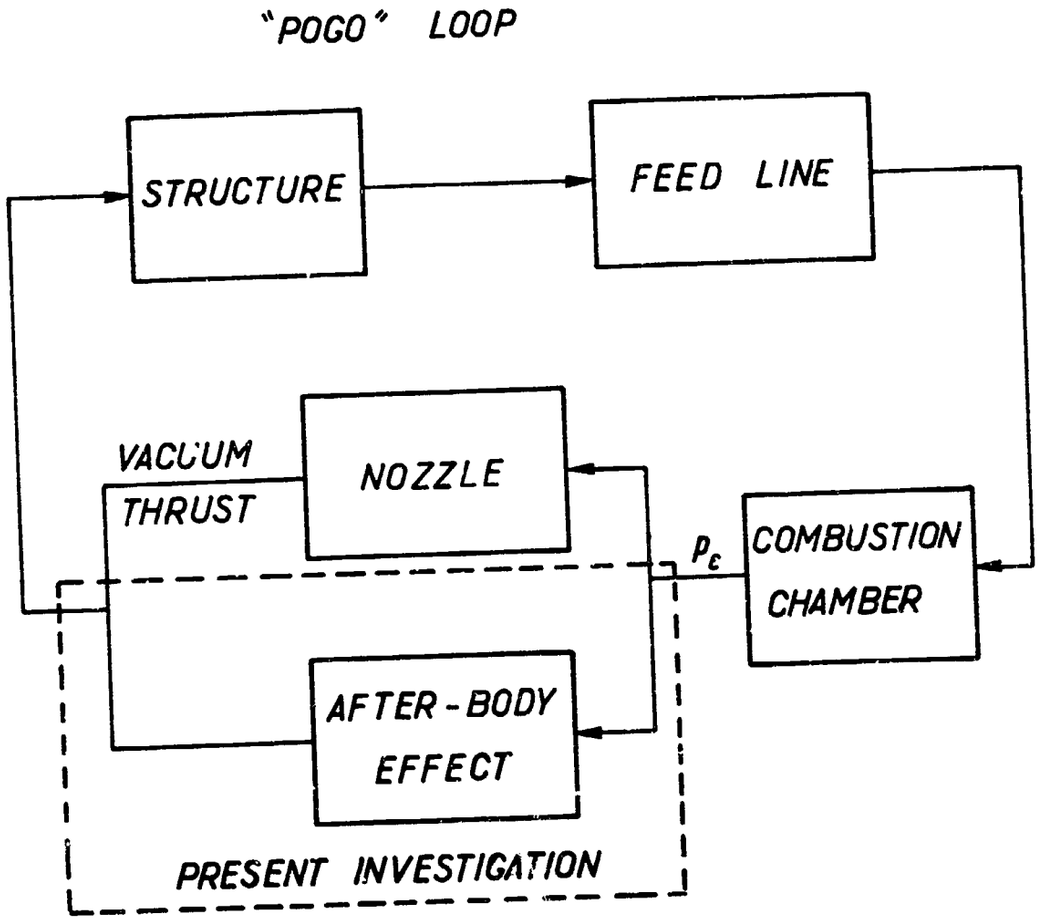
"POGO" LOOP
STRUCTURE
FEED LINE
VACUUM
THRUST
NOZZLE
p_c
COMBUSTION
CHAMBER
AFTER-BODY
EFFECT
PRESENT INVESTIGATION

Figure 1

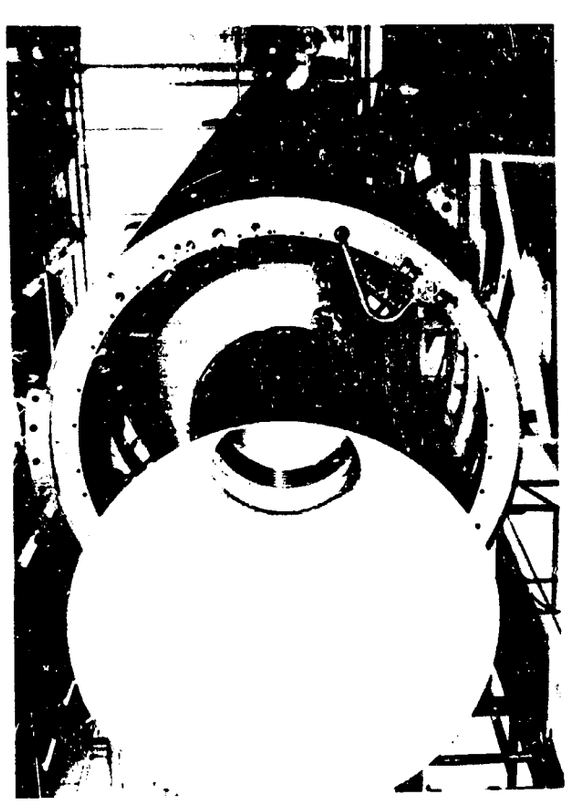

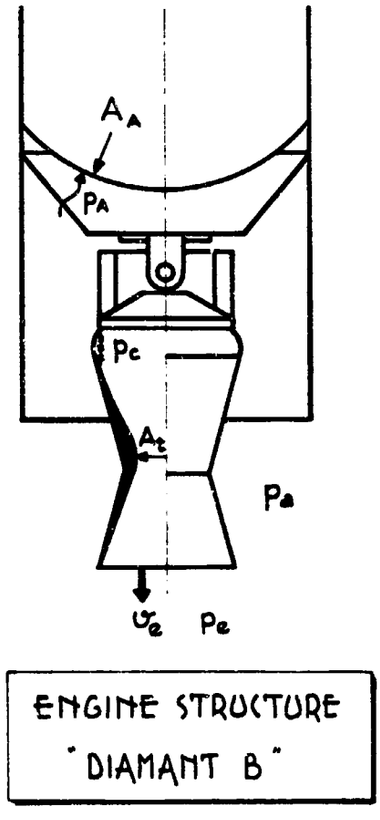

ENGINE STRUCTURE
"DIAMANT B"

Figure 2

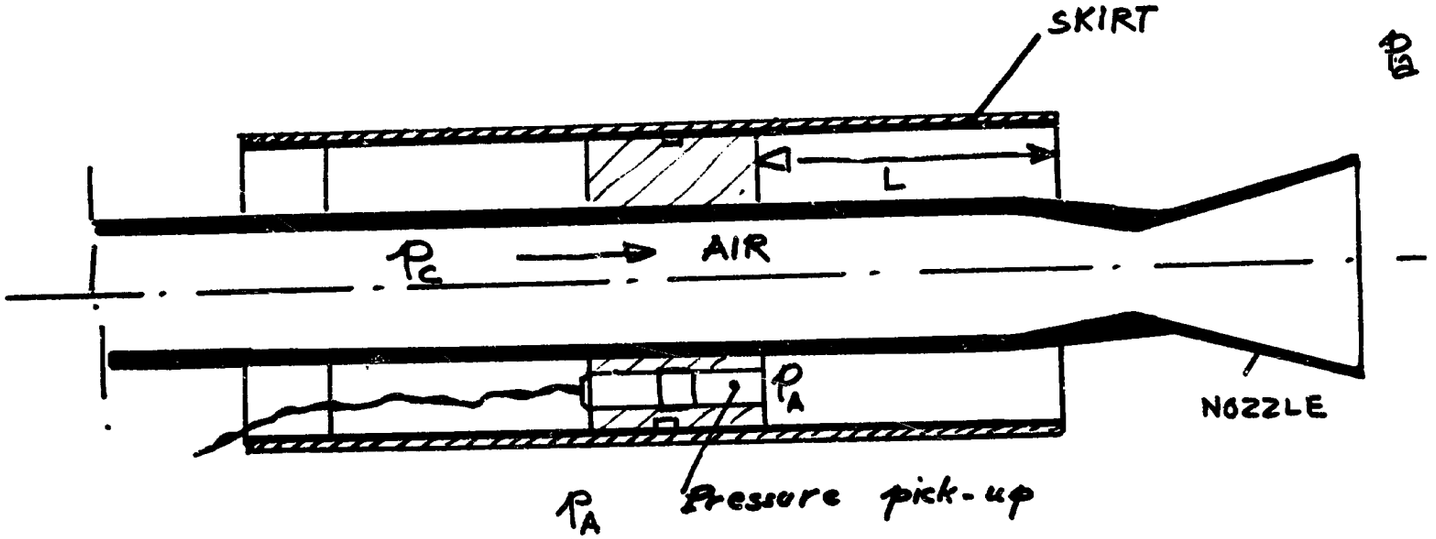

Parameters: P_A, P_c, P_a, L

ENGINE MODEL CONFIGURATION

Figure 3

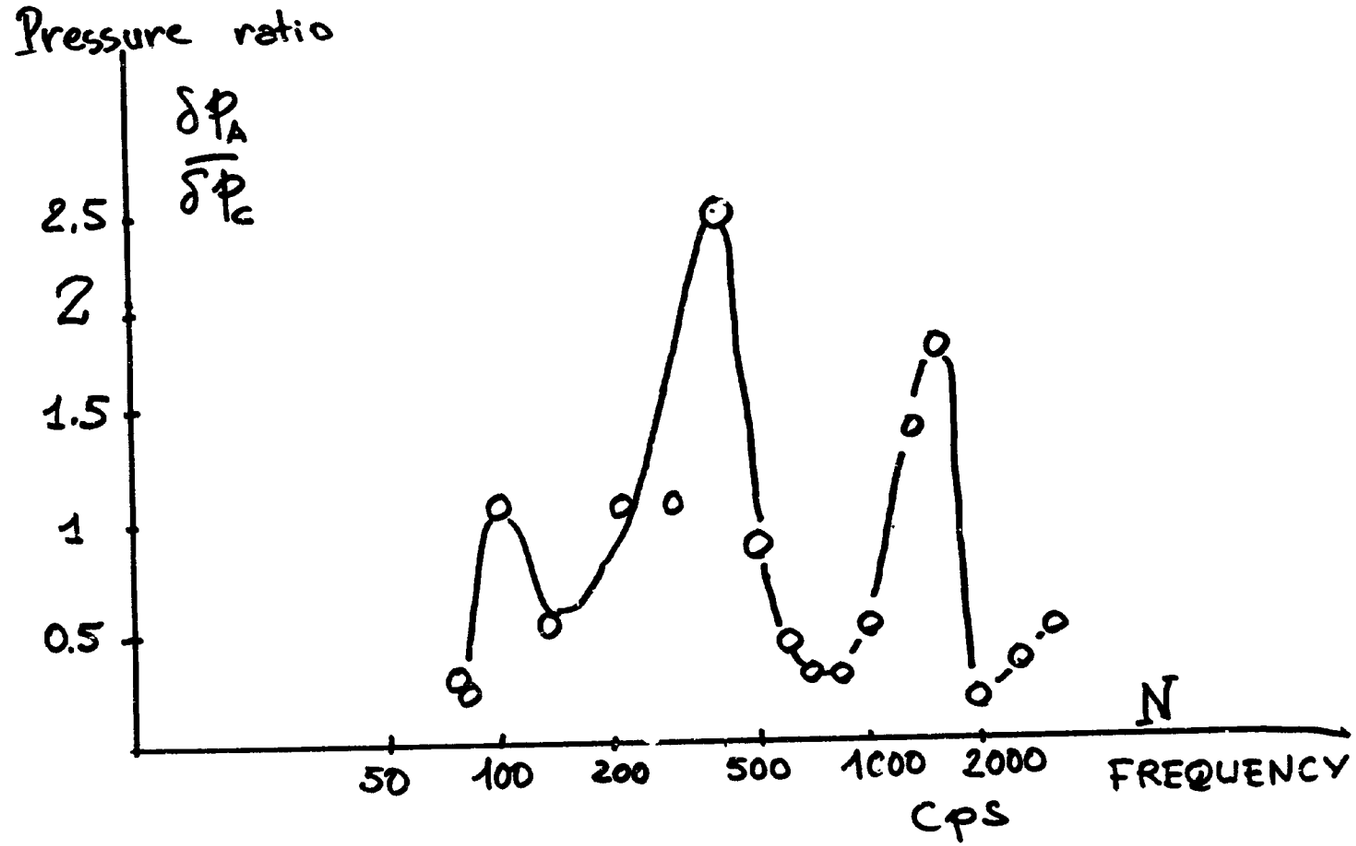

Evolution of the pressure ratio $\delta P_A / \delta P_c$ with N

Figure 4

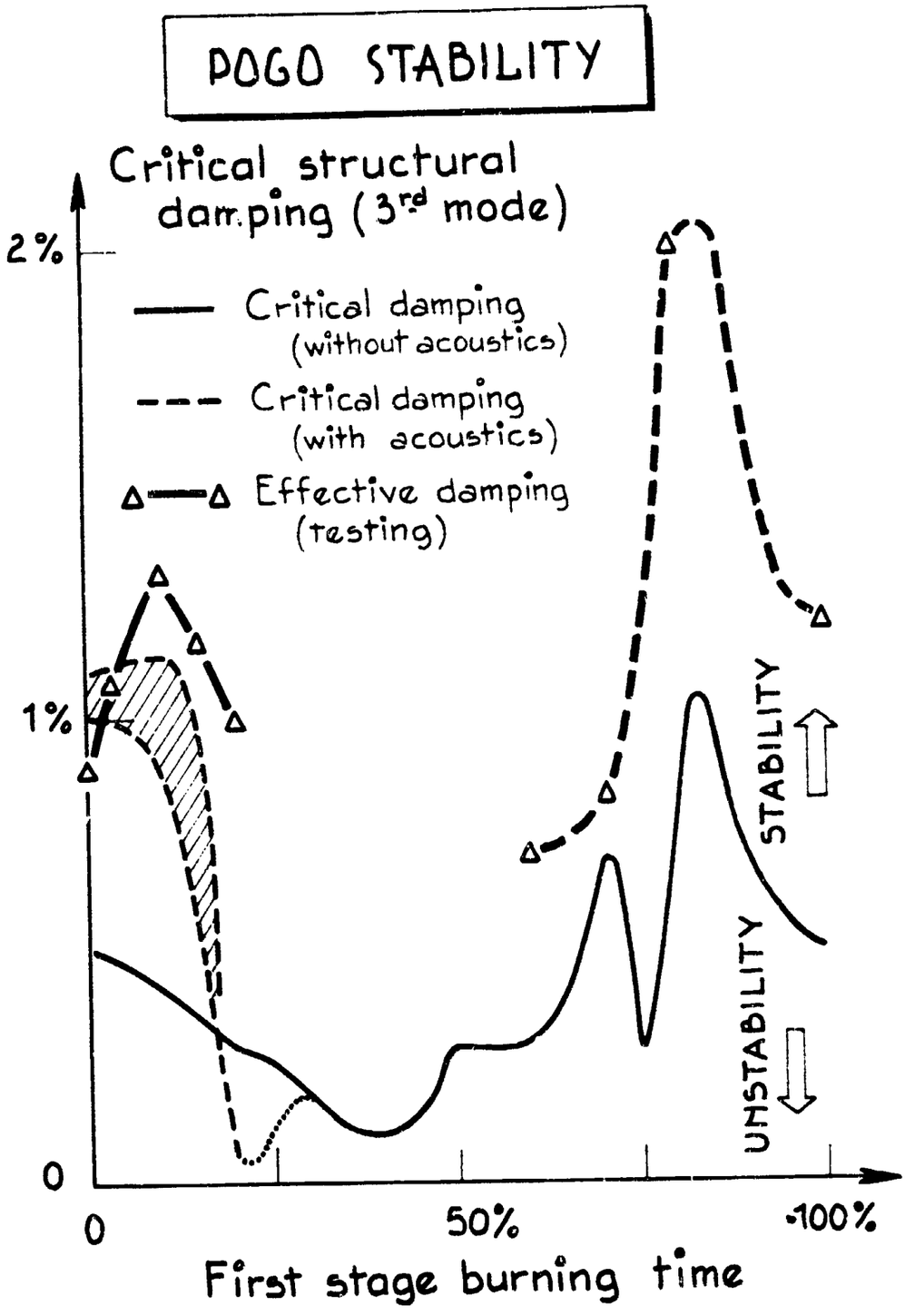
POGO STABILITY
Critical structural damping (3rd mode)
2%
1%
0
Critical damping (without acoustics)
Critical damping (with acoustics)
Effective damping (testing)
STABILITY
UNSTABILITY
0
50%
100%
First stage burning time

Figure 5

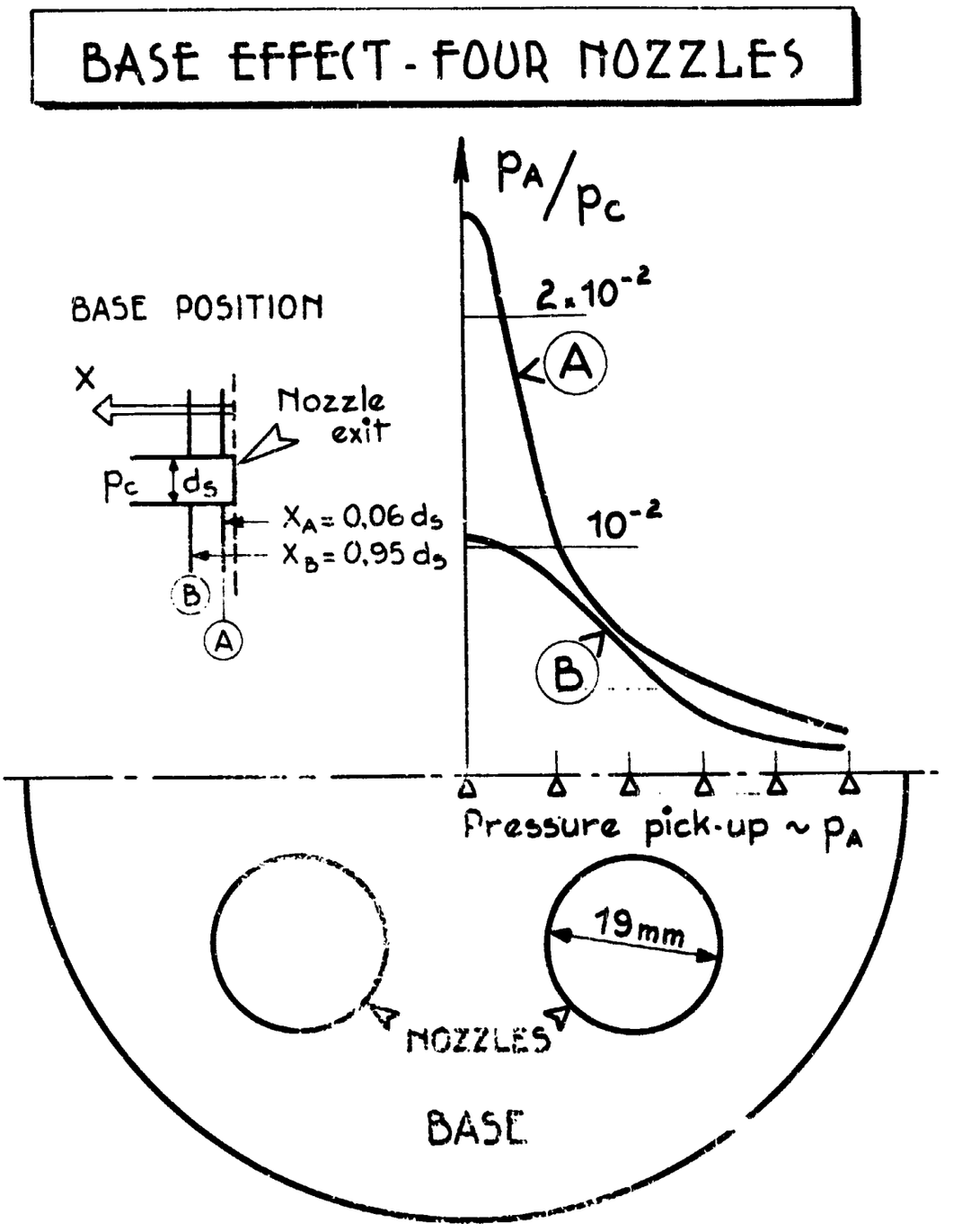
BASE EFFECT - FOUR NOZZLES
P_A/P_c
2.10^{-2}
A
10^{-2}
B
BASE POSITION
X
Nozzle exit
P_c
d_s
$X_A = 0,06\ d_s$
$X_B = 0,95\ d_s$
B
A
Pressure pick-up ~ P_A
19mm
NOZZLES
BASE

Figure 6

VIBRATION ENVIRONMENT

R. W. Schock
Marshall Space Flight Center
Huntsville, Alabama

INTRODUCTION

The space shuttle mission requirements such as high reliability, minimum refurbishment, minimum weight, and novel environmental combinations, impose singular considerations and requirements on the structural design. This is particularly true in the design of the thermal protection system (TPS). Unlike previous missile requirements the TPS must successfully withstand repeated applications of combined and separate thermal and vibration environments. Acoustic fatigue will therefore be a major consideration in the design of the TPS. The subsequent paper therefore presents some of the expected acoustic fatigue characteristics of TPS concepts, and defines areas where supporting research is needed to provide the required reliability and confidence in the TPS design.

Basic space shuttle TPS design concepts are shown on figure 1. They consist of the following:

A. Concept A consists of a radiative metallic structure with insulation attached either to primary structure or secondary structure, but in either case, the insulation does not contact the radiative structure. Aerodynamic loads are carried into primary load carrying structure by stand-off supports.

B. Concept B duplicates concept A except that the insulation is in contact with the radiative structure. The significance of this design will be shown later.

C. Concept C is the bonded ceramic foam type insulation which is structurally capable of direct aerodynamic load transfer.

D. Concept D is representative of an active cooling system in which the tubes shown here represent the heat exchanger used for transfer of re-entry heat from the TPS structure to a rejection exchanger or heat sink.

TPS DESIGN CONCEPTS

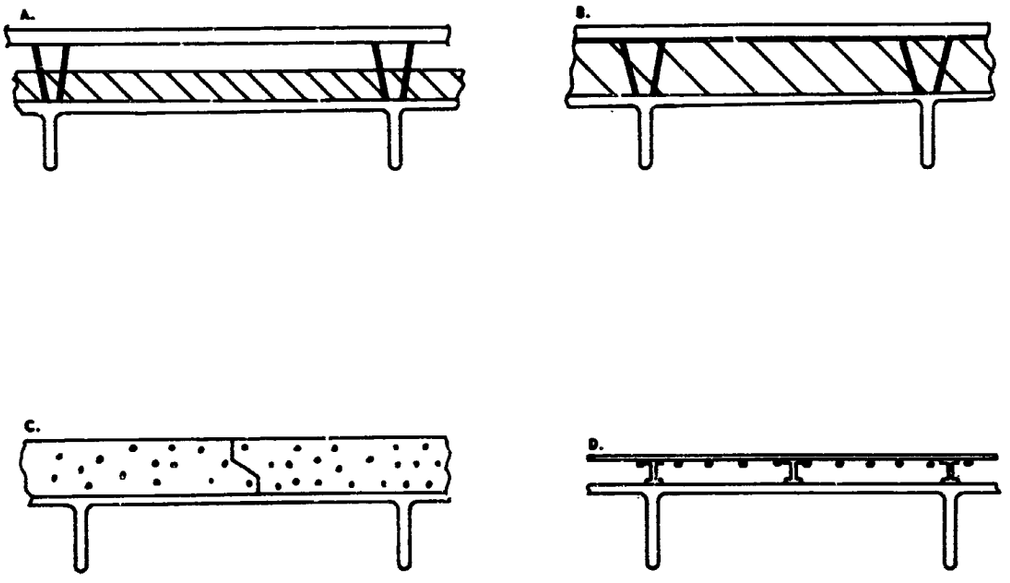

FIGURE 1

Since the purpose of this paper is to compare the vibration response and fatigue characteristics of each TPS concept, TPS design concept A was chosen as a baseline and preliminary vibration response characteristics were calculated. These are shown in figure 2.

The overall sound pressure level (db ref. 2×10^{-4} microbar), overall G_{rms} and duration of excitation for the indicated mission environment are shown for concept A. The levels were obtained from an acoustic spectral and structural areal density extrapolation of Saturn V, S-IVB data. Since this is a spectral extrapolation, an increase or decrease in overall sound pressure level does not necessarily cause a proportionate increase or decrease in overall G_{rms}. The objective of this figure is to indicate that for each mission cycle a severe vibration response will occur for a relatively short duration of time and a moderate response will occur for an extended length of time. This moderate response will occur simultaneously with a severe thermal environment. The levels shown for lift-off and MACH 1/MAX Q are approximately equal to the levels obtained on lightly loaded Saturn V upper stage structure for the same mission-phase. It should be noted however, that Saturn V structure was required to survive only one mission cycle environment whereas the TPS system must survive repeated application.

VIBRATION RESPONSE OF METALLIC RADIATIVE
HEAT SHIELD CONCEPTS

MISSION ENV	OVERALL SPL DB	OVERALL GRMS	DURATION OF EXCITATIONS
LIFTOFF	157.5	30	10 SEC
MACH 1 MAX Q	159.5	40	40 SEC
RE-ENTRY	152.5	5	800–1200

FIGURE 2

Figure 3 provides a simplified comparative evaluation of the vibration response characteristics and fatigue life potential of the various TPS design concepts. The graph illustrates the relative response RMS stress levels for the same acoustic excitation source versus time. The graph purposely has no values assigned to either axis since the purpose of the figure is to provide representative trends rather than absolute information which is unavailable. For purposes of illustration the acoustic excitation is assumed constant.

Concept A, with its high area to weight ratio and low damping value would be expected to have the highest vibration response (G_{rms}), and resulting RMS stress level for well coupled acoustic excitation. This concept would therefore have the least acoustic fatigue mission life potential.

Concept D with its lower area to weight ratio should have a lower response with resulting lower RMS stress. Therefore concept D should have a higher acoustic fatigue life potential.

Concept C is shown as a dashed line since no information could currently be obtained for the response of panels protected by this method. Since it is a rigidized fibrous material it would be expected to provide significant joint damping to any supporting metallic structure and therefore reduce structural response significantly. Its ability to survive even a moderate vibration environment and, particularly, low frequency vehicle dynamics is currently undefined. From the supporting structure standpoint, it does subjectively appear to incorporate a high acoustic fatigue life potential.

TPS SYSTEM RESPONSE TRENDS

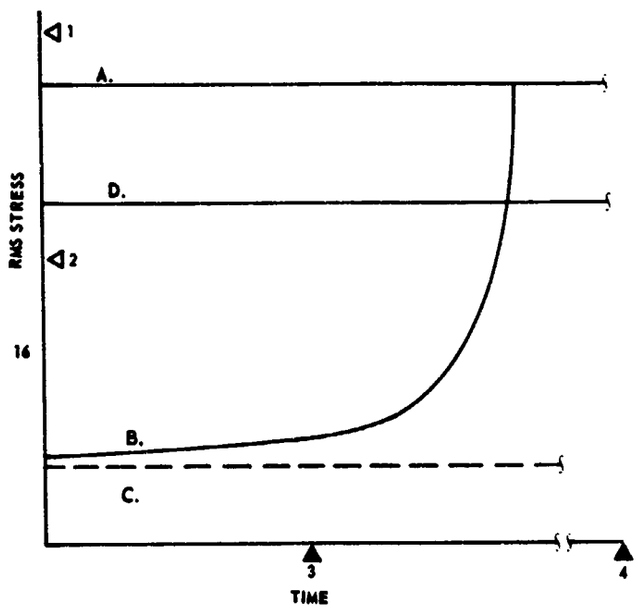

ACOUSTIC FATIGUE
MISSION LIFE POTENTIAL

CONCEPT	POTENTIAL
A	4
B	2
C	1
D	3

FIGURE 3

Concept B has an interesting and advantageous vibration response characteristic. Since the radiative panel is supported by a limp fibrous, highly damped insulation, its initial response to acoustic excitation should be significantly lower than an identical unsupported panel. Unless an adequate insulation can be developed that will withstand the dynamic bearing condition imposed by the moderate panel response, the insulation will structurally degrade in the bearing areas. As the insulation degrades, the panel becomes less damped, the panel response increases, and the insulation degradation rate increases. The panel configuration will finally approach concept A and will have a vibration response and resulting stress equal to concept A. Stated another way, the acoustic fatigue life potential is a function of the rate of insulation degradation. This characteristic could be advantageously employed to provide extended mission life fatigue potential.

All concepts could probably be designed to have an RMS stress level below the material endurance limit point 1. The resulting TPS system weight would, in all probability, be prohibitive. With TPS system weight a primary driving function, the response of large area to weight ratio structures will be above the endurance limit (point 2). Therefore, a finite fatigue life will result. If this fatigue life is greater than an acceptable refurbishment schedule (point 3), then any concept will be adequate. However, if a minimum refurbishment rate is a major objective (point 4), then TPS design concepts providing for induced panel damping at a minimum weight penalty must be developed.

To provide for the reliability, inherent in space shuttle objectives, the required research and development in the area of acoustic fatigue is presented in figure 4.

Due to the novel design concepts required to accomplish TPS system objectives, existing data is non-existant. Before fatigue life assessments can be performed, representative forced response characteristics of TPS type structure must be established.

Basic S/N curves for TPS material must be defined before reliable estimations of fatigue life can be obtained.

The effects of combined thermal and aerodynamic environments on the mission life of proposed TPS designs and materials must be determined.

To provide for experimental verification of TPS system designs and shuttle component life tests, the relative forcing efficiency of re-entry aerodynamic excitation and standard plan wave, reverberation chamber test modes must be determined, and test exaggeration factors established, to provide reasonable qualification test times.

REQUIRED RESEARCH & DEVELOPMENT

PROBLEM AREA	STATE OF THE ART	NEEDED RESEARCH
1. VIB RESPONSE PREDICTION TECH.	1. SEMI-EMPIRICAL TECHNIQUES DEPEND ON REP DATA	1. RESPONSE CHARACTERISTICS OF TPS TYPE STRUCTURE
2. HIGH TEMP MATERIAL FATIGUE PROPERTIES	2. PAUCITYOF DATA PARTICULARLY RANDOM	2. DEVELOPMENT OF HIGH TEMP MATERIAL S/N DATA
3. FATIGUE LIFE PREDICTION	3. CUMULATIVE FATIGUE TECH PROVIDES INFINITE LIFE IN MODERATE ENVIRONMENTS	3. EFFECTS OF COMBINED THERMAL & AERODYNAMIC ENVIRONMENTS ON FATIGUE LIFE
4. FATIGUE LIFE TEST VERIFICATION	4. ACOUSTIC REVEBRATION AND PLANE WAVE CHAMBERS	4. TEST EXCITATION VRS FLIGHT FORCING FUNCTION EFFICIENCY. TEST EXAGGERATION FACTORS.

Figure 4

CONCLUSIONS

Acoustic fatigue will be a significant design consideration for the space shuttle thermal protective system. Although not an insurmountable problem, significant research and development effort is required to obtain confidence in the reliability and mission life potential of any selected concept.

N70-36612

ACOUSTIC ENVIRONMENT CHARACTERISTICS OF THE SPACE SHUTTLE

Jesse H. Jones

NASA-Marshall Space Flight Center
Huntsville, Alabama

INTRODUCTION

The science of acoustics is the study of the generation, repagation and reception of mechanical waves in an elastic media. Acoustics as defined in this manner covers a wide variety of problem areas. The areas that are of primary concern with regard to the Space Shuttle are: (1) rocket jet noise environment and its effects upon the structural integrity of the Space Shuttle vehicle as well as its effect upon the operational aspects of the GSE in the near and mid-field areas during launch, (2) siting and personnel hazard considerations with respect to the surrounding civilian community due to the sound being propagated into these areas, (3) inflight fluctuating pressure environments during the sub, trans, super and hypersonic flight regime and it's effect upon the structural integrity of the Space Shuttle vehicle, (4) blast environment due to a catastrophic failure of the Space Shuttle, (5) the sonic boom associated with orbiter reentry and booster return flight, (6) the structural dynamic response characteristics of the Space Shuttle vehicle and (7) acoustic fatigue and it's effect on the repeated use of the Space Shuttle vehicle.

Each of these problem areas must be examined in detail in order to realistically assess their influence on the total mission reliability and success of the Space Shuttle system.

Due to the limited time available, it is not possible to discuss all of these problem areas, therefore, I would like to briefly discuss two of these areas and present the results of the preliminary analysis of the acoustic environmental characteristics of the Space Shuttle system. The two areas which will be discussed are the rocket engine environment developed during holddown and in a general sense the inflight fluctuating pressure environment developed during the trans and supersonic Space Shuttle exit flight regime. Further, I would like to present a specific aerodynamic phenomena that is of a growing concern to those of us at MSFC and to discuss the possible influence of this phenomena on the Space Shuttle system. This phenomena is commonly referred to at MSFC as the "High Altitude Plume Induced Flow Separation Phenomena".

Rocket Engine Acoustic Environment

Since the initial formulation of the jet noise theory by Lighthill [1] many sophisticated theories have emerged. The most notable ones are those developed by [2] Ribner, [3] Phillips and [4] Williams. Each of these theories emphasized a different point of view. Lighthill by his acoustic analogy approach developed a volume of acoustic sources in terms of a stress tensor whereas Ribner utilized the "simple-source" technique, i.e., monopole, dipole and quadrapole. Phillips presented his theory in terms of a convected wave equation the solution of which is restricted to high speed flows, i.e., Mach wave radiation. Williams in extending the theory of Lighthill emphasized the effects of high speed convection and Mach wave radiation. Recently, Peters [5] and Pao [6] have introduced new aspects into the jet noise theory. Peter's theory emphasizes a non-isentropic convected wave equation. Pao's theory is actually an extension of the Phillips approach, the solution of which is valid for all transonic and supersonic Mach numbers.

All of these theoretical approaches requireddetailed knowledge of the mean and turbulent characteristics of the exhaust flow field and their practicability is restricted by the fact that they only apply to free undeflected exhaust flows. These theories have provided valuable insight into the basic noise generation mechanisms of jet or rocket exhaust flows and much has been accomplished through their study. In the final analysis however, whenever it is desired to provide acoustic environmental estimates of actual situations, such as the Space Shuttle during holddown,some form of empirical techniques and/or model tests have to be employed.

The comments which follow will be directed towards the techniques used for estimating the acoustic environmental characteristics of the Space Shuttle developed during holddown, (or static firing). These comments are not necessarily restricted to only this area but apply equally as well in the other areas of acoustic prediction; i.e., ground plane environment in the mid- and far-field areas, launch environment, etc.

Definition of the decailed acoustic environmental characteristics of space vehicle systems is usually accomplished in three distinct phases. The first phase is the preliminary environmental definition by using an empirical technique to obtain an estimate of the environment. Once this has been completed, the second phase can be initiated. This phase consists of planning, designing and conducting of model test programs utilizing scale models of the propulsion system to be used on the full scale vehicle. The third phase then consists of scaling the resulting model data to the full scale configuration. The second and third phases are normally performed as soon as firm design information on the propulsion system is known. Full scale testing is additionally employed to verify the estimated environments.

Many empirical techniques have been devised throughout the years. All of these techniques rely in one manner or another upon the principle of an "apparent source model" [7,8] and are based upon the principles of dynamic similarity. For the case of the Space Shuttle environment, this apparent source model consists of

a non-dimensional function which describes the location of the "apparent-sources" and another non-dimensional function for determining the strength of the acoustic source. This technique was employed in predicting the Space Shuttle environment and the results are presented in Figure 1. A nominal thrust of 400,000 pounds per engine and 13 engines was used in computing these environments. Figure 1 depicts the overall sound pressure level in dB (RE: 0.00002 N/m^2), as a function of Space Shuttle station. In the aft region of the Shuttle, the environment is on the order of 165 to 170 dB's and in the crew compartment area the environment is on the order of 152 to 154 dB's. The spectral distribution of the acoustic energy, in one-third octave band sound pressure level form, at two selected Space Shuttle stations, is presented in Figure 2. In the aft region of the Shuttle, i.e., Station 160, the energy is primarily high frequency in nature and is distributed over a wide range of frequencies with the maximum energy being located in the 500 Hertz one-third octave band. In the crew compartment area, the overall sound pressure level has decreased to approximately 154 dB with most of the energy decrease occurring at the high frequencies and the frequency distribution of the energy is centered about the 100 Hertz one-third octave band. These preliminary estimates were obtained utilizing existing data from conventional rocket engines; i.e., those with chamber pressure on the order of 800 to 1200 psi. The Space Shuttle propulsion system will however, have chamber pressures operating at more than twice the pressures of these conventional engines; i.e., 3000 psi, and the effect of this increase chamber pressure on the inherent acoustical characteristics is not known at this time. This is one of the factors which needs emphasizing during the second phase of the environmental definition, the model test phase. Plans for this phase are in progress and the primary objectives will be to: (1) assess the influence of the increased chamber pressure on the acoustical characteristics, (2) delineate the influence of the non-conventional cluster arrangement of the rocket engines on the resulting acoustic pressure field, (3) study the effects of deflectors; i.e., could be beneficial to TPS, (4) define the spectral characteristics of the radiated pressure field, (5) define the spatial correlation characteristics of the acoustic pressure field. Definition of the spatial correlation characteristics is required in order to provide a realistic assessment of the dynamic structural response, electronic design and qualification characteristics of the Space Shuttle. With the reuseability concept being applied to the Shuttle, the necessity of defining the correlation characteristics is even more acute from a fatigue standpoint. Therefore, adequate assessment of dynamic response is mandatory (hence proper environmental acoustic tests need to be conducted) in order to insure the structural integrity of the Shuttle and avoid costly redesign of Shuttle component due to fatigue.

ANTICIPATED ACOUSTIC ENVIRONMENT
FOR
SPACE SHUTTLE DURING HOLDDOWN

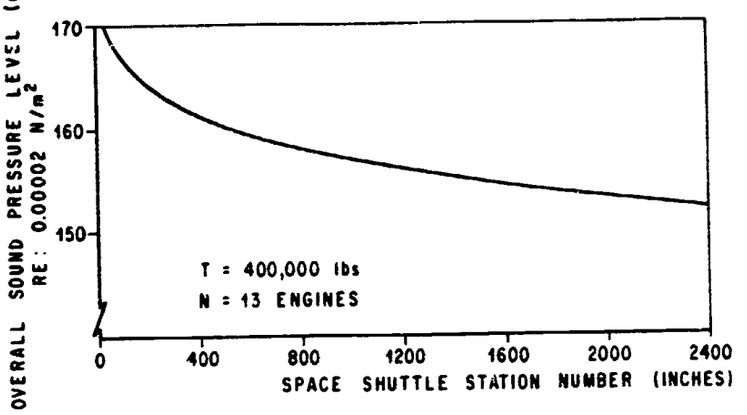

FIG. 1

ANTICIPATED ACOUSTIC ENVIRONMENT
AT SELECTED STATIONS
DURING HOLD DOWN OF SPACE SHUTTLE

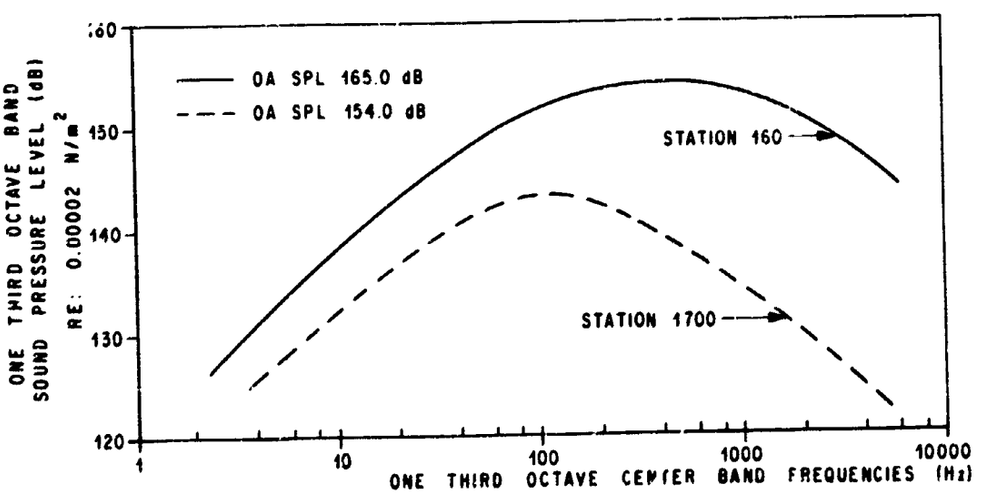

FIG 2

Inflight Fluctuating Pressures

Definition of the inflight fluctuating pressure environment is almost entirely determined by empirical means and/or model testing. Delineation of the fluctuating pressure environment is also accomplished in several distinct phases similar to those employed in defining the rocket noise environment. The first phase is to determine, through empirical means, the total energy and the spectral content of the energy associated with several different types of aerodynamic flow regions encountered during Space Shuttle flight. The fluctuating pressure environment is determined primarily by the external geometrical characteristics of the Space Shuttle and therefore once the design has been established the second phase can be initiated. This phase consists of establishing the location of the many different types of aerodynamic flow regions as a function of the flight conditions to be experienced during Space Shuttle flight, i.e., Mach number, angle of attach, dynamic pressure, etc. This phase is normally accomplished by flow visualization processes such as shadowgraphs, Schlerien or some other means. The third phase consists of conducting a scale model wind tunnel test of the Space Shuttle and the fourth phase is the scaling of the model test results to the full scale configuration. Full scale flight measurements are then required to verify and modify the design and qualification environments. The second, third, and fourth phases of the environmental definition are normally initiated after the design has been frozen.

Many experimental programs have been conducted in order to define the fluctuating pressure characteristics in distinct flow regimes associated aircraft or space vehicle flight. Most notably are those experimental studies of; Bull [9] , Bull and Willis [10] , and Serafini [11] in regions of attached turbulent boundary layers; Kistler [12] , in regions of separated flow; Chyu and Hanley [13] , and Coe [14] on an ogive cylinder in attached and separated flow regions and; Robertson [15,16] , in regions of protuberance induced environments. These experimental results plus numerous inhouse experimental results at MSFC obtained from a 4% scale model wind tunnel test program of the Saturn V vehicle were used to obtain typical fluctuating pressure environment in four distinct flow regions associated with the Space Shuttle flight. These preliminary environments were defined for regions of; (1) attached turbulent boundary layers, (2) separated flow, (3) oscillating shock and (4) separated flow/oscillating shock interaction, and the results are presented in Figures 3 and 4 in one-third octave band sound pressure level form. These environmental estimates are considered valid for maximum dynamic pressures of approximately 500 to 700 psi.

In regions of attached turbulent boundary layer, Figure 3, the overall fluctuating pressure level (OAFPL) is approximately 142.0 dB and for the separated flow region the OAFPL is approximately 152.0 dB. The separated flow region contains considerably more low frequency energy than the turbulent boundary layer region. In Figure 4, the OAFPL is approximately 152.0 dB for the separated flow/oscillating shock interaction region; the total energy is the same as that for a typical separated flow region but the frequency distributions of the energy is shifted an order of magnitude lower in frequency. For the region of oscillating shock, the frequency distribution of the energy is narrow band in nature and centered in the low frequency range of the spectrum with an OAFPL of 169.0 dB.

ANTICIPATED FLUCTUATING PRESSURE ENVIRONMENT DEVELOPED DURING SPACE SHUTTLE FLIGHT FOR SELECTED FLOW REGIONS

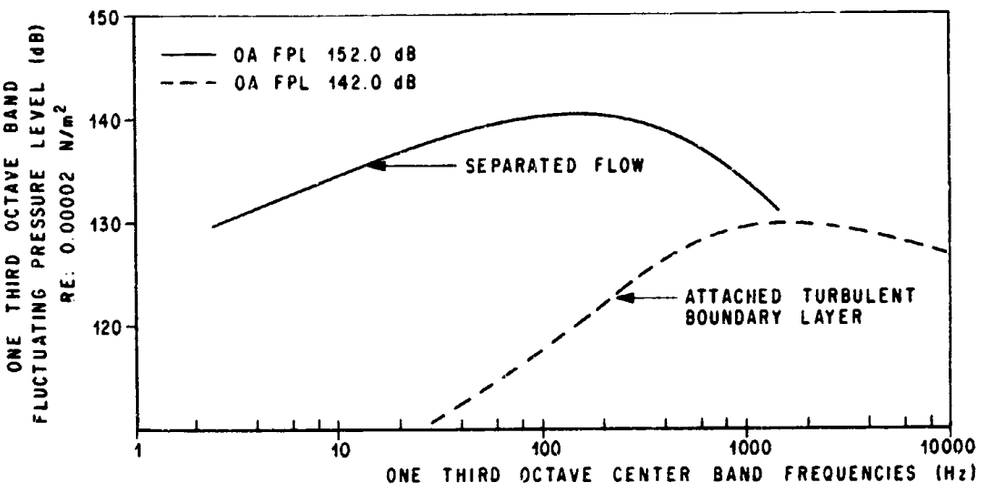

FIG 3

ANTICIPATED FLUCTUATING PRESSURE ENVIRONMENT DEVELOPED DURING SPACE SHUTTLE FLIGHT FOR SELECTED FLOW REGIONS

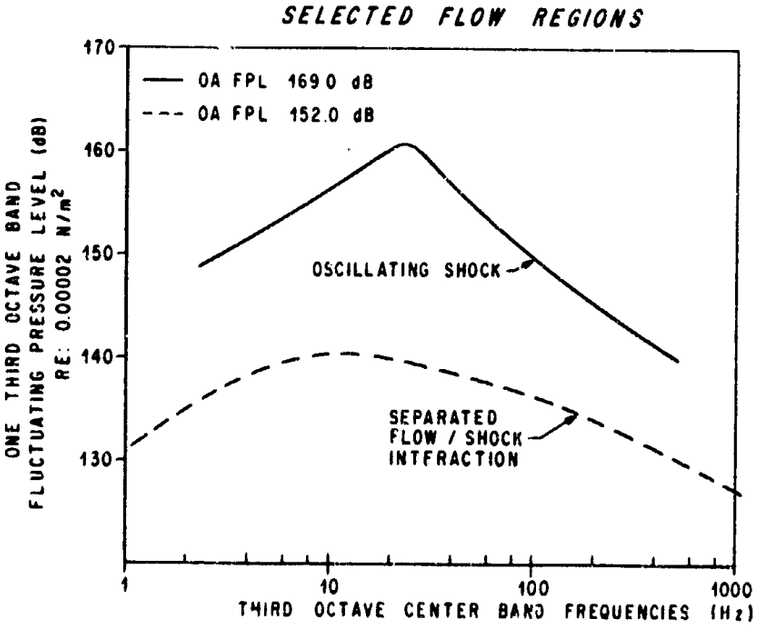

FIG 4

The detailed environmental definition will be established after the Space Shuttle configuration has been defined. Due to the asymmetric nature of the Space Shuttle, the flow visualization and model test phases will have to be much more extensive and well defined than usual. During the model test phase, it is planned to obtain the spectral and spatial correlation characteristics of the fluctuating pressure field. Again, complete definition of the spatial correlation properties, the cross power spectral density in particular, is required in order to realistically assess the structural integrity of the Space Shuttle system.

Plume Induced Flow Separation

During all of the past flights of the Saturn V vehicle, an aerodynamic phenomena has occurred about which very little information is known. This phenomena is known as the high altitude plume induced flow separation phenomena and it is illustrated in Figure 5. This figure was obtained from a single frame of a movie film which was taken by a camera that was mounted in an Air Force "chase plane" that recorded the sequence of events during the second flight of the Saturn V vehicle, AS-502. The time at which this frame was taken was approximately 133 seconds into the flight. It can be seen from this figure that at the leeward side (the left side), the visible portion of the flame front is at the interstage region of the vehicle; between the S-IC boost stage and the S-II second stage. The flight and atmospheric conditions at this time is shown in Figure 6. The flight Mach number was 5.44 with an angle of attack of 2 degrees and a dynamic pressure of 62.6 PSF. Vehicle altitude at this time was 150,000 feet with the corresponding ambient pressure and density of 2.7 PSF and 0.00011 pounds per cubic foot respectively.

The start of the movement of the flame front forward on the vehicle occurs early during the flight of the Saturn V, typically around 90 seconds into the flight. It appears, that as the vehicle travels along its prescribed trajectory, the rocket exhaust plume interacts with the surrounding air stream and thereby creates a large region of separated flow adjacent to the vehicle. This causes the exhaust products of the rocket engines to be recirculated into the separated flow region. As the vehicle gains altitude, the expanding exhaust plume causes an additional enlargement of the region of separated flow and consequently, there is a very rapid and sometimes violent forward movement of the flow separation front on the vehicle. Figure 7 depicts the movement of this flow separation front as obtained from analysis of the chase plane movies taken of the flight of AS-502. Near the end of the boost phase of the Saturn V flight, typically 150 seconds, the separated flow region completely engulfs the S-IC stage and has traveled a total distance of approximately 125 feet. If a similar movement occurs on the Space Shuttle, approximately 60% of the Shuttle would be immersed in the separated flow region.

In an effort to acquire more information about this phenomena, an inflight measurement program was implemented on AS-505. This measurement program consisted of ten dynamic pressure transducers which were flush mounted in the intertank region of the S-IC stage. Six transducers were located in a ring around the vehicle and two each were aligned in a longitudinal direction along Position I and III of the vehicle. The instantaneous fluctuating pressure time history for two of the measurements are shown in Figure 8. The frequency response of the telemetry system used for the measurements at Station 757 and 837 were from 0-8.4 hertz and 0-14.0 hertz respectively. The fluctuating pressure levels that were obtained were unexpectedly high. As the separated flow front moved past each transducer the pressure time histories were initially clipped and then gradually decayed as the front continued to move forward. The fluctuating pressure levels at which clipping occurred were typically on the order of 155 to 158 dB with the predominate frequency on the order of 2 to 3 Hertz. There were many problems encountered in attempting to obtain measurements in this type of flow region, the major ones being those of the radiant energy from the

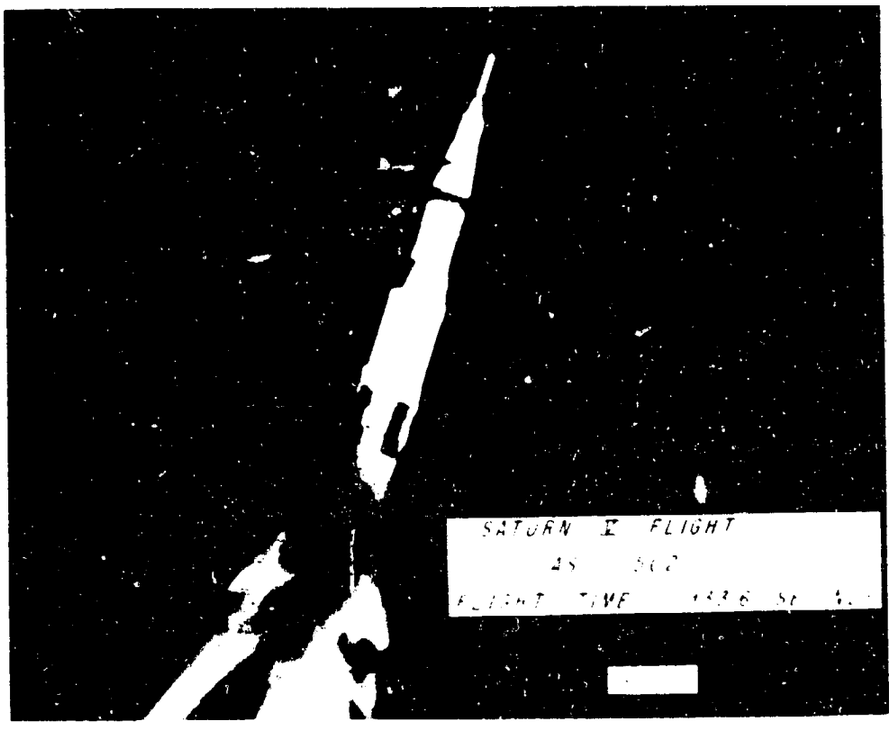

AS – 502 PLUME INDUCED
FLOW SEPARATION
CONDITIONS AT 133 sec FLIGHT TIME

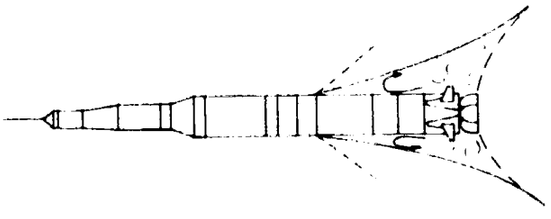

MACH NO 5 44

DYN PRESS 62 6 PSF (2993 N/m^2)

ANGLE OF ATTACK 2 0 DEG

ALTITUDE 150,000 FT (45,700 m)

AMBIENT DENSITY 00011 lbs/FT^3
(00178 kg/m^3)

AMBIENT PRESSURE
2 7 PSF (131 7 N/m^2)

FIG 6

AS – 502 FLOW SEPARATION FRONT
VS
FLIGHT TIME

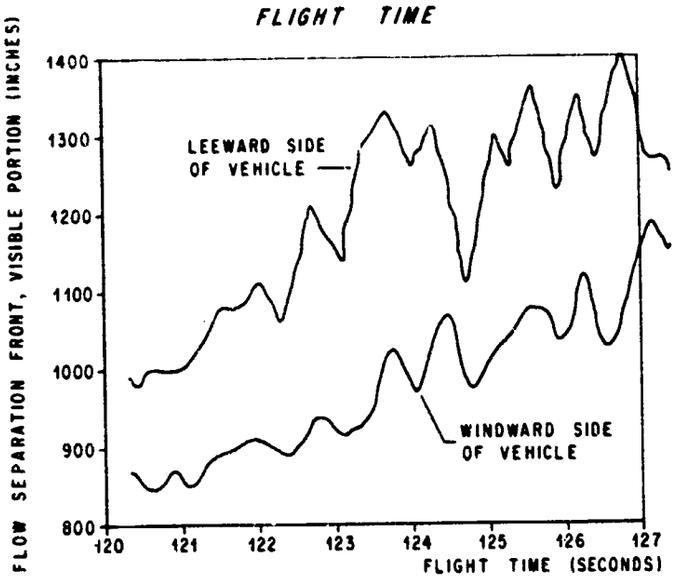

FIG 7

FLUCTUATING PRESSURE ENVIRONMENT
IN REGION OF PLUME INDUCED FLOW SEPARATION
AS – 505

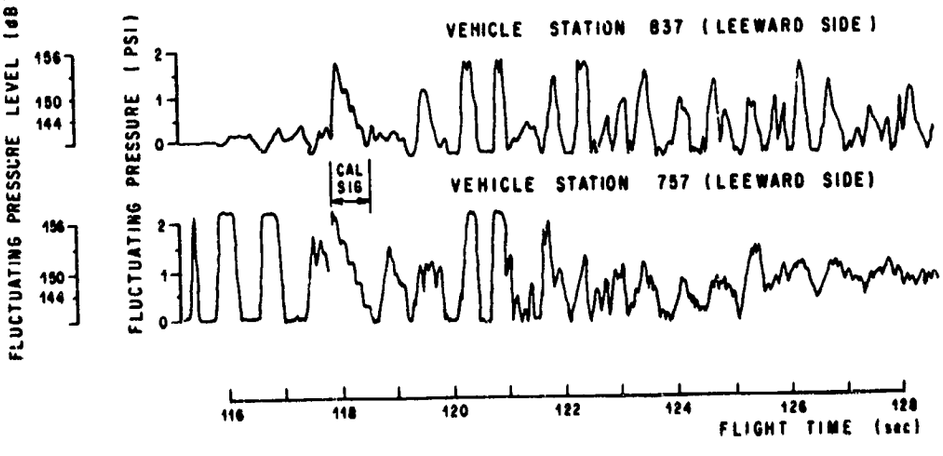

FIG 8

flow, temperature and vibration. Transient light energy from the flow causes extraneous signal output of the transducers that were used, therefore, a thin piece of aluminum foil had to be placed between the diaphragm and the protecting cover cap. The temperature caused a bias to be produced in the data. Efforts to compensate for this temperature bias were made prior to launch, but the effects of this bias can still be seen in the data. The transducer used had a vibration compensation network that served to minimize the effects of the vibration. All efforts have been made to insure the accuracy of the data. Admittedly the data does seem unrealistically high, however, no justifiable reasons have been found to invalidate the results shown in Figure 8.

The following points should be carefully considered if these levels are indeed accurate; (1) what effect does this type of environment have on the aerodynamic surface and especially the thermal protection system (TPS) of the Shuttle?; (2) to what extent will this asymmetric flow field load the Shuttle?; (3) how does this loading affect the control system?; (4) will the exhaust flow products contaminate the orbiter rocket engines and the orbiter surface itself?

A study program is underway at MSFC in an attempt to gain a better understanding of the exact nature of this phenomena. From this study an experimental program will be designed and implemented in order to obtain fluctuating pressure data and basic flow characteristics under this type of simulated flow conditions.

Concluding Remarks

Efforts are underway at MSFC to determine the preliminary environmental estimates in the other acoustic problem areas associated with the Space Shuttle, i.e., ground plane environment in near, mid and far-field during holddown and launch, blast, etc., that was discussed earlier. The results of these studies will be reported when they become available.

With regard to the two areas that were briefly discussed, the following remarks are given:

a. Rocket Noise Environment

(1) Preliminary estimates of the acoustic environment developed by the propulsion system of the Space Shuttle have been determined. These estimates are state-of-the-art estimates and are adequate for preliminary design requirements.

(2) A model test program is presently being designed to obtain the spectral and spatial correlation characteristics of the radiated pressure field associated with the Space Shuttle. A preliminary experimental program is planned to determine the effect of the increased chamber pressure as well as the non-conventional cluster arrangement of the engines and deflector effects.

b. Inflight Fluctuating Pressure Environment

(1) Preliminary estimates of the typical fluctuating pressure environments in selected aerodynamic flow regions expected during Space Shuttle flight have been determined. Again, these preliminary estimates are adequate for the preliminary design requirements of the Shuttle.

(2) Flow visualization tests are presently being planned. The results of these tests will be used to design a scale model wind tunnel test program ot obtain detailed fluctuating pressure information for all Space Shuttle flight regimes.

(3) An analytical study is presently in progress with regard to the plume induced flow separation phenomena. The results of this study will be used to design an experimental test program to more clearly and accurately define the magnitude of the unsteady pressure and basic flow characteristics associated with this phenomena.

References

1. Lighthill, M.J., "On Sound Generated Aerodynamically I., General Theory", Proc. Roy. Soc. Vol. A211, 564-578 (1952).

2. Ribner, H.S., "Aerodynamic Sound from Fluid Dilatations. A Theory of the Sound from Jets and Other Flows", Univ. of Toronto Inst. Aerospace Studies, UTIA Rep. 86 (1962).

3. Phillips, I.M., "On the Generation of Sound by Supersonic Turbulent Shear Layers", J. Fluid Mechanics, Vol. 9, pp. 1-28 (1960).

4. Flowes Williams, J.E., "The Noise from Turbulence Convected at High Speed", Phil. Trans. Roy. Soc., London. Vol. A255, 469-503 (1963).

5. Peters, A.C., and Cottrell, J.W., "An Investigation to Define the Propagation Characteristics of a Finite Amplitude Pressure Wave", NASA-CR-735 (1967).

6. Pao, S.P., "A Generalized Theory on Noise Radiated by Supersonic Turbulent Shear Layers", Wyle Laboratories Report, WR 70-1 (1970).

7. Dyer, I., "Estimate of Sound-Induced Missile Vibration", Chapter 9 of Random Vibration edited by Crandell, Mass. Institute of Technology, (1958).

8. Wilhold, G.A., et. al., "Acoustic Energy Hazards", Vol. 1, Chapter 7, General Safety Engineering Design Criteria, JANNAF Hazards Working Group, CIPA Publications No. 194 (1970).

9. Bull, M.K., "Wall Pressure Fluctuations Associated with Subsonic Turbulent Boundary Layer Flow", J. Fluid Mech., Vol. 28, pt 4, p. 179, (1967).

10. Bull, M.K., and Willis, J.L., "Some Results of Experimental Investigations of the Surface Pressure Field Due to a Turbulent Boundary Layer", AASU Rept. 199. (Nov. 1961).

11. Serafini, J.S., "Wall Pressure Fluctuations and Pressure Velocity Correlations in a Turbulent Boundary Layer", NASA TR R-165 (1958).

12. Kistler, A.L., "Fluctuating Wall Pressure Under a Separated Supersonic Flow", J. Acoustic. Soc. Am., Vol. 36, no. 3, p. 543 (1964).

13. Chyu, W.J., and Hanly, R.D., "Power and Cross-Spectra and Space-Time Correlations of Surface Fluctuating Pressures at Mach Numbers Between 1.6 and 2.5 AIAA paper no. 68-77, (Jan. 1968).

14. Coe, C.F., "Surface-Pressure Fluctuations Associated with Aerodynamic Noise", Basic Aerodynamic Noise Research Conference, NASA SP-207 (1969).

15. Robertson, J.E., "Characteristics of the Static and Fluctuating Pressure Environments Induced by Three-Dimensional Protuberances at Transonic Mach Numbers", Wyle Laboratories Research Staff Report WR 69-3, (June 1969).

16. Robertson, J.E., "Fluctuating Pressures Induced by Three-Dimensional Protuberances", Wyle Laboratories Report WR-70-10 (1970).

DYNAMIC RESPONSE OF ANTENNA STRUCTURES IN A LAUNCH ENVIRONMENT

A. C. S. Payden

Canadair Limited
Montreal, Canada

SUMMARY

The dynamic responses of various proposed designs of an antenna-feedhorn combination for a communications satellite to random excitation in the launch environment were determined using beam and plate finite elements idealizations, in both normal mode and impedance solutions, and applying power spectral density techniques.

Statistical results in the form of mean square values, exceedances of load levels and cumulative damage formed the design criteria.

The same digital programs can be used to determine space shuttle responses for various dynamic loading considerations, particularly during launch and staging. Sets of compatible elements which could be used in the finite element idealization of the complex space shuttle structure are presented.

1.0 INTRODUCTION

This paper deals with methods of analysis and criteria for the design of a flexible structure in a random loading environment. The particular problem of concern is the design of an antenna for a communications satellite, considering the random character of the launch vibration environment.

A sketch of the antenna mounted on the spacecraft and enclosed by the payload envelope is shown in Figure 1. Significant points in the spacecraft as well as the antenna are shown. The random excitation during the launch phase is assumed to be applied in the form of accelerations in all directions at the base of the spacecraft. That is to say, it is applied at the point of attachment to the launch vehicle.

ANTENNA AND SPACECRAFT AS MOUNTED ON LAUNCH VEHICLE

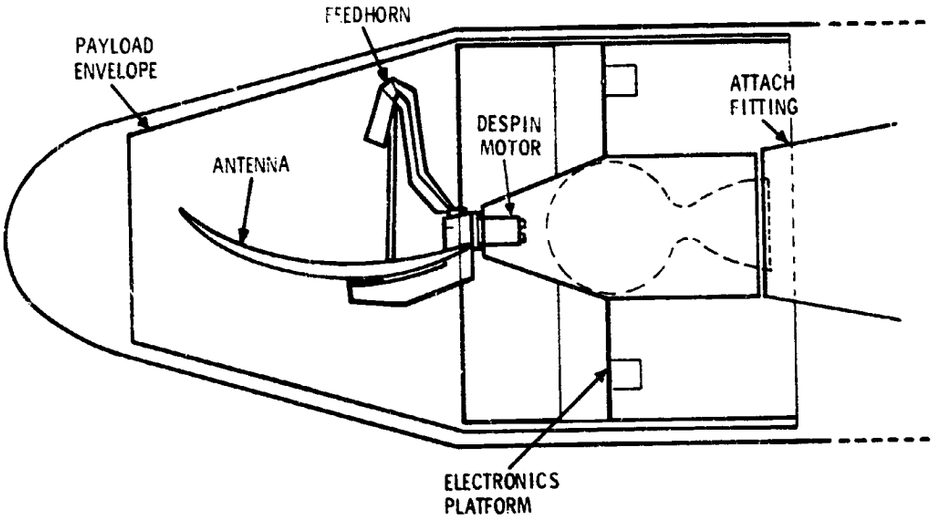

FIGURE 1

2.0 ANTENNA DESIGNS

Various antenna designs were proposed, using different materials and different basic configurations. A typical design is shown in Figure 2. Here the antenna dish is curved, and the feedhorn is connected directly to it, as well as being cantilevered from its base. Another design was such that the feedhorn needed only to be connected to the base, at the despin motor assembly.

Three different configurations were considered for the antenna dish itself.

a) The first was a formed thin plate attached to a gridwork of beams. Materials considered were aluminum, beryllium, titanium, and carbon.

b) The second design used a honeycomb sandwich material. The formed sandwich dish was mounted on a central post. Proposed materials for the honeycomb and face sheets were aluminum, and titanium. The central post had to be quite stiff and a carbon composite material was chosen. The feedhorn was also of the same material.

c) The third design was a stretchable alloy wire mesh supported by a tubular space frame. This frame could be made from aluminum, beryllium, titanium or carbon.

TYPICAL ANTENNA CONFIGURATION

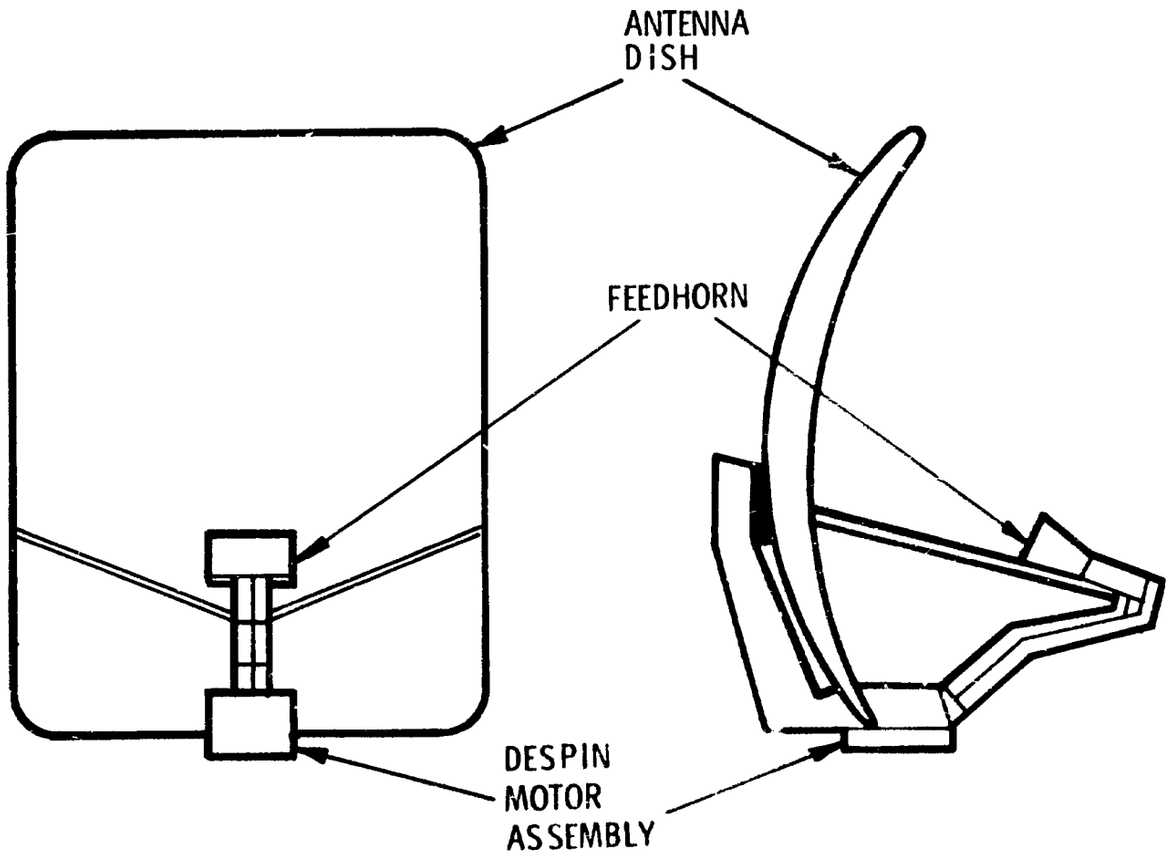

FIGURE 2

3.0 ANALYTICAL METHOD

3.1 Structural Representation

In order to perform a dynamic analysis of a complex structure such as that of the antenna-feedhorn combination, the first requirement is a set of stiffness or influence coefficients, and a corresponding set of masses. The method chosen yields the stiffness coefficients by simulating the structure by an assembly of finite elements, using the direct stiffness method. For preliminary design, where a great many models were run, lumped masses were used, because of the substantially fewer number of operations required. However, for final design, consistent masses were used, with added lumped masses at certain discrete node points. The consistent masses allow for a much more accurate representation of the dynamic properties of a structure.

Descriptions of work previously carried out by Canadair in finite element analysis are contained in References 5 and .

3.2 Finite Element Idealizations

Beam and plate elements used in the finite element representations of the various antenna designs are shown in Figure 3. These elements have six degrees of freedom per node.

For the first antenna structure, the formed flat plate on a gridwork, the beam elements were used to idealize

TRIANGULAR PLATE ELEMENT

BEAM ELEMENT

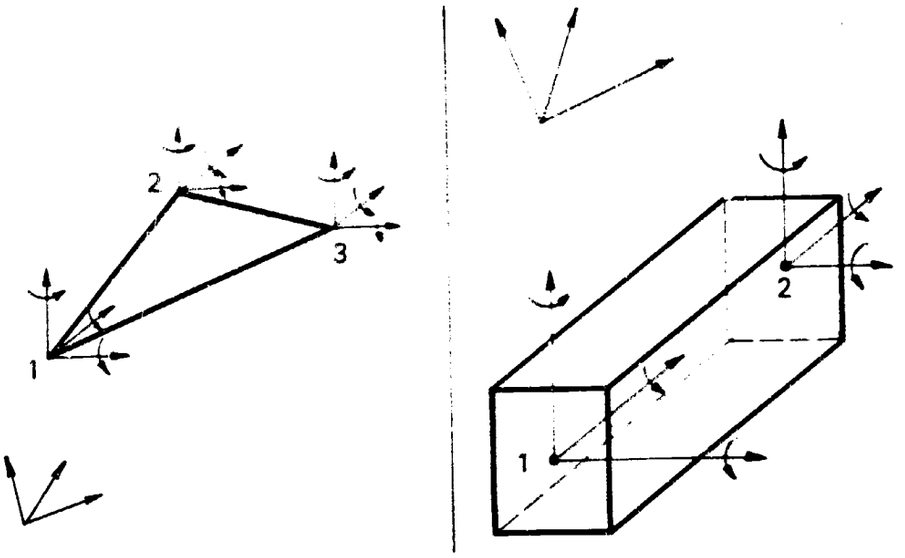

FIGURE 3

the gridwork, and the triangular plate elements were used to represent the curved dish. For the second configuration, flat triangular shell elements were used to represent the formed sandwich dish, and the beam elements the central post.

For the mesh designs, the beam elements were used to represent the back-up truss structure, as shown in Figure 4.

The feedhorn was represented by a series of beams, as shown in Figure 5, for all the designs.

Since the vibration of the spacecraft itself substantially affects the vibration of the antenna structure, the spacecraft was represented by a series of tapered beams, as shown in Figure 6, the representation being obviously coarser than that of the main structure of interest.

3.3 Solution Procedure

3.3.1 Reduction

The only effective limitation on the size of the original stiffness matrix and hence the number of nodes in the representation is the bandwidth. However, the eigenvalue routines available to determine the natural frequencies and mode shapes of the structure are not efficient, for large order matrices, and impose a limit

FINITE ELEMENT REPRESENTATION OF TRUSS NETWORK BACK UP STRUCTURE FOR MESH ANTENNA DESIGN

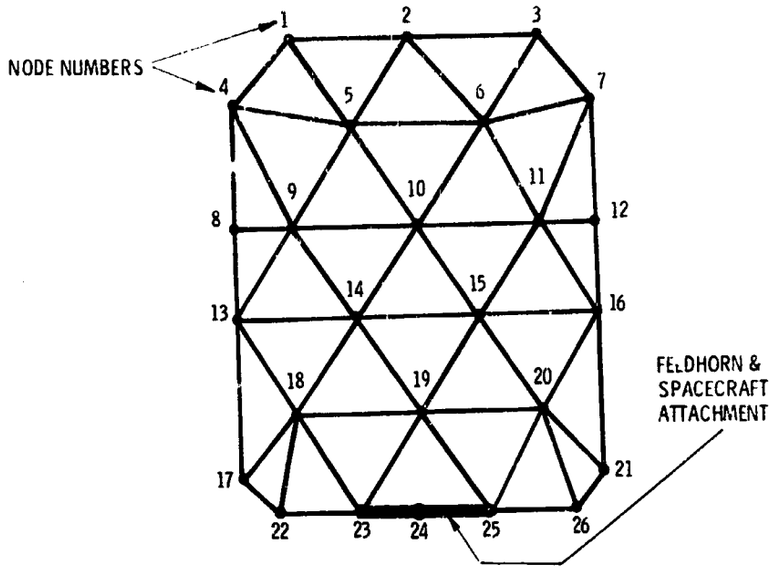

FIGURE 4

FINITE ELEMENT REPRESENTATION OF FEED HORN USING BEAMS

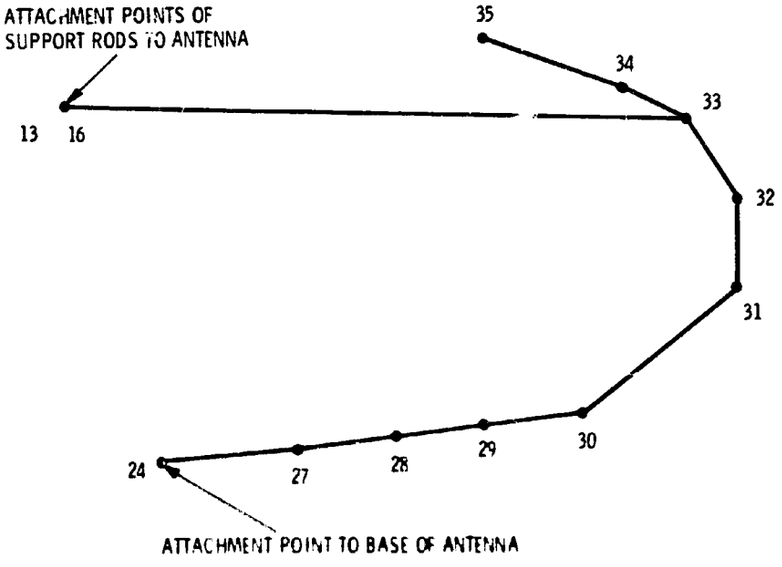

FIGURE 5

FINITE ELEMENT REPRESENTATION OF SPACECRAFT USING TAPERED BEAMS

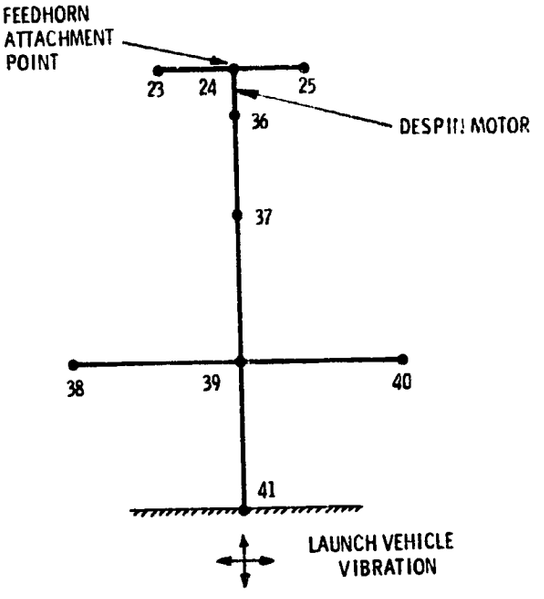

FIGURE 6

ON-LINE MATRIX REDUCTION

STIFFNESS:

$$K_{ij}^{\nabla} = K_{ij} - \frac{K_{ik}K_{kj}}{K_{kk}} \qquad (1)$$

CONSISTENT MASS:

$$M_{ij}^{\nabla} = M_{ij} - \frac{K_{ik}M_{kj}}{K_{kk}} - \frac{M_{ik}K_{kj}}{K_{kk}} + \frac{K_{ik}M_{kk}K_{kj}}{K_{kk}K_{kk}} \qquad (2)$$

TABLE 1

of somewhere near the order 100. Also, if the impedance method of solution is to be used, only small order matrices may be solved efficiently, timewise.

Hence, the original matrix size must be reduced by retaining only a certain number of degrees of freedom and eliminating the rest, by application of the principle of virtual work.

The equations used for the reduction are shown in Table 1. The reduction of the stiffness matrix is carried out on-line, as given by equation (1). No matrix inversion is required.

If lumped masses are used, the mass of the structure is lumped at the retained degrees of freedom.

If consistent masses are used, a simultaneous on-line reduction of the mass matrix is performed according to equation (2).

3.3.2 Eigenvalue Solution

The natural frequencies and mode shapes of the structure for the reduced number of degrees of freedom are then found using the eigenvalue routine.

3.3.3 Transfer Function Solution

The vibration level of the structure over the entire frequency range is found by first determining the response of the retained degrees of freedom to unit sinusoidal accelerations at the base of the spacecraft for

the natural frequencies, as well as for intermediate frequencies, using either the impedance or the normal mode method of solution.

Details of the two methods are as follows, while more complete discussion may be found in reference 1.

3.3.3.1 Impedance Method

The equations are as shown in Table 2. Equation (3) is the matrix formulation for the equations of motion of the system, with base acceleration excitation, where:

$[M]$ = mass matrix, either lumped or consistent

$[K]$ = stiffness matrix

$\{\ddot{x}\}$ = accelerations

$\{x\}$ = displacements

ig = structural damping

$\{\ddot{y}\}$ = base acceleration, zero in directions where there is no excitation.

The complex impedance matrix $[Z]$ is formed as in equation (4), for a sinusoidal excitation of frequency W.

The equations of motion thus become equation (5) for a unit base acceleration excitation.

The solution for the displacements and/or accelerations is straightforward inversion of the complex $[Z]$ matrix and multiplication by the right hand side as shown by equations (6) and (7).

IMPEDANCE METHOD

$$[M]\{\ddot{x}\} + (1+ig)[K]\{x\} = -[M]\{\ddot{z}\} \qquad (3)$$

$$[Z] = \left[-w^2[M] + (1+ig)[K]\right] \qquad (4)$$

$$[Z]\{x\} = -w^2[M]\{1\} \qquad (5)$$

$$\{\ddot{x}\} = -w^4[Z]^{-1}[M]\{1\} \qquad (6)$$

$$\text{or } \{x\} = -w^2[Z]^{-1}[M]\{1\} \qquad (7)$$

TABLE 2

3.3.3.2 Normal Mode Method

The equations are as shown in Table 3.

The basic equations of motion for the system are the same as before, represented by equation (3).

A transformation to generalized coordinates $\{q\}$, given by equation (8), is applied using the matrix of mode shapes $[\phi]$ obtained from the eigenvalue solution.

The equations of motion are then premultiplied by $[\phi]^T$. The diagonal generalized mass matrix $[M_R]$ and the generalized stiffness $[K_R]$ are defined by equations (9) and (10) where the ω_n are the natural frequencies.

The left hand side being now diagonal, the equations of motion are decoupled, and the generalized coordinates q_i can be solved independently using equation (12).

Equation (8) is then used to obtain the actual displacements.

This is a much more satisfactory method for the solution of large order dynamic problems. It allows decoupling of the equations of motion, so that no inversion of large complex matrices is required, and also allows reduction of the number of degrees of freedom.

NORMAL MODE METHOD

$$[M]\{\ddot{x}\} + (1 + ig)[K]\{x\} = -[M]\{\ddot{z}\} \tag{3}$$

$$\{x\} = [\phi]\{q\} \tag{8}$$

$$[Mr] = [\phi]^T [M] [\phi] \tag{9}$$

$$[Kr] = [W^2 n][Mr] \tag{10}$$

$$\left[-W^2[Mr] + (1+ig)[W^2 n][Mr]\right]\{q\} = -W^2[\phi]^T[M]\{1\} \tag{11}$$

$$\{q\} = \frac{-W^2[\phi]^T[M]\{1\}}{-W^2[Mr] + (1+ig)[W^2 n][Mr]} \tag{12}$$

TABLE 3

3.3.4 Discussion of Methods

The preliminary designs were examined on a remote access terminal connected to a high speed IBM 360-75 computer. The main problem was one of storage, as only 100K were available to the user, although temporary storage disks could also be used. The impedance method was deemed to be more practical for the solution of these problems, and reductions were made to the original stiffnesses to allow final solutions of approximately 16-20 degrees of freedom. For final design, the solutions were run on Canadair's own IBM 360-65 computer with 365K working memory and vast tape and disk capability. For larger order problems (i.e. for a larger number of retained degrees of freedom), the normal mode method was and should be used, so that there is no need to invert large order complex matrices. The impedance method may be used as a check on the normal mode solutions.

Sinusoidal launch vibration specifications are then satisfied by merely scaling up or down the transfer functions found for one g excitation.

3.4 Response to Random Excitation Using Power Spectral Density Methods

Once the response (i.e. transfer function) to a unit sinusoidal excitation has been computed, the response to the random excitation of the launch environment is computed using power spectral density (PSD) methods.

The basic equations are shown in Table 4.

Equation (14) relates the random character of the response, as a function of frequency, to that of the excitation through the modulus of the transfer function where

Φ_{OUT} - power spectral density of response

$|TF|^2$ - transfer function modulus

Φ_{IN} - power spectral density of excitation, assuming that the excitation behaves as a stationary Gaussian random process.

The root mean square value $\bar{A}$ of any response, as well as the number of zero crossings N_o can then be found by numerical integration of equations (15) and (16), respectively.

The exceedances N of any acceleration or load level y is then obtained from equation (17), commonly known as Rice's equation.

Descriptions of related work on power spectral density methods carried out by Canadair are contained in References 3 and 4.

POWER SPECTRAL DENSITY EQUATIONS

$$|TF| = \left| \ddot{x} \right| * \text{conjugate} \left| \ddot{x} \right| \qquad (13)$$

$$\mathcal{I}_{out} = |TF|^2 \mathcal{I}_{in} \qquad (14)$$

$$\bar{A} = \left[\int_0^{\Omega c} \mathcal{I}_{out} \, dw \right]^{1/2} \qquad (15)$$

$$No = \frac{\left[\int_0^{\Omega c} w^2 \mathcal{I}_{out} \, dw \right]^{1/2}}{\bar{A}} \qquad (16)$$

$$N = No \, e^{-\left(y^2 / 2\bar{A}^2\right)} \qquad (17)$$

TABLE 4

4.0 [illegible] RESPONSE

Curves showing the power spectral density of the launch environments provided by two possible launch vehicles, the Thor Delta and the Atlas Burner II, are shown plotted in Figure 7 as a function of frequency.

The response PSD of the lateral acceleration of the tip, for one antenna model, is as shown in Figure 8, for a Thor Delta launch vehicle. Natural frequencies can be seen at 18, 39, 107 cps, etc.

From this PSD, the root mean square level of the acceleration was found to be 7.58 g, and the number of zero crossings 325.4 per second.

The plot of the number of exceedances of each g level is shown in Figure 9.

RANDOM VIBRATION LEVEL OF SPACECRAFT AT SEPARATION PLANE

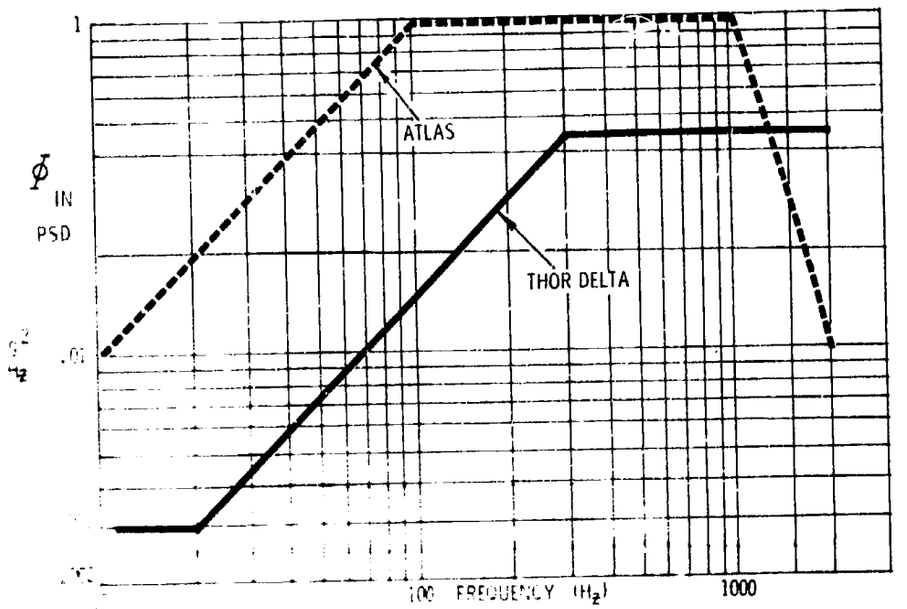

PLOT OF POWER SPECTRAL DENSITY OF ANTENNA TIP LATERAL ACCELERATION IN RESPONSE TO RANDOM EXCITATION AT BASE OF SPACECRAFT

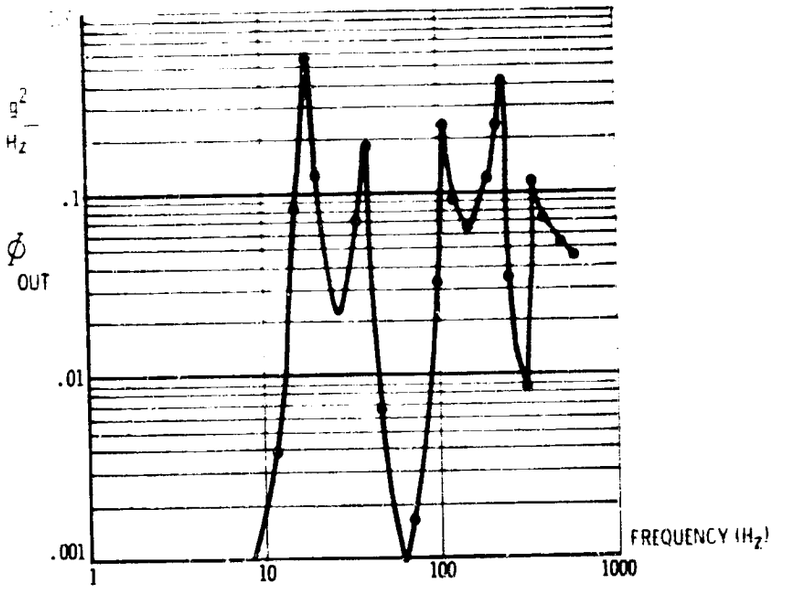

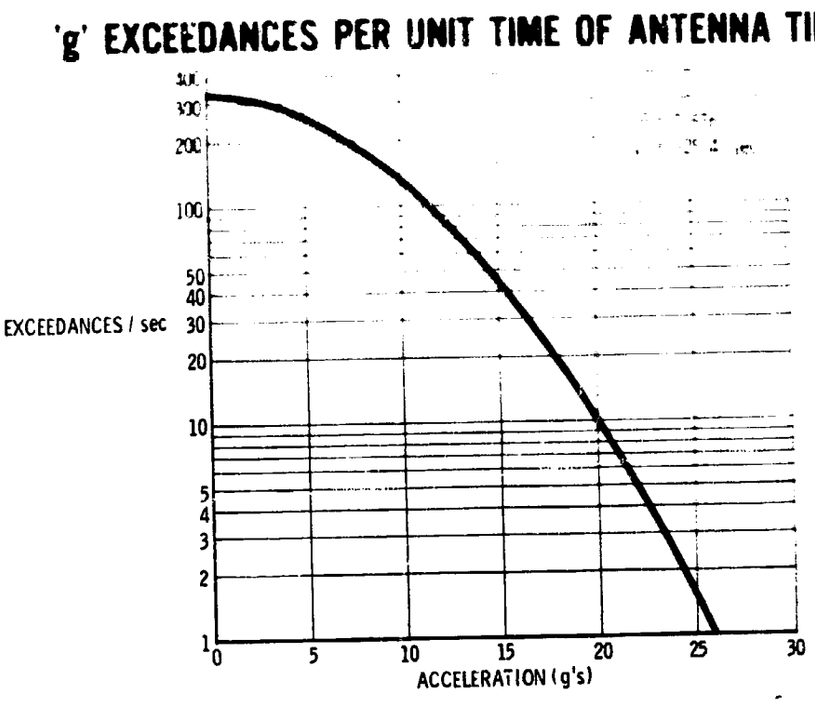
'g' EXCEEDANCES PER UNIT TIME OF ANTENNA TIP
EXCEEDANCES / sec
300
200
100
50
40
30
20
10
5
4
3
2
1
0
5
10
15
20
25
30
ACCELERATION (g's)

FIGURE 9

5.0 FATIGUE ANALYSIS

Two different methods were followed in applying these results to fatigue, one for preliminary design, and one for final design. The two methods both used the theory of Cumulative Damage as a final point in assessing the fatigue life, but arrived at the result in slightly different ways.

For the preliminary design, stresses were computed for a 10 g loading at the tip of the antenna. The exceedance curve for g's was entered at successive g loadings to give the number of times these g's were exceeded per second. These numbers were then multiplied by the time in the environment, to give the total number of exceedances of that level. This was repeated for increasing g levels until the total number of exceedances for a level was less than one. The static solution for the 10g load was then factored to these discrete g loadings and the spectrum of fatigue stresses obtained, with rectangular and triangular load patterns assumed. The number of stresses at the various stress levels was given by the number of exceedances for the g acceleration levels. The cumulative fatigue damage was then estimated from equation (18), using a scatter factor of 4.5.

$$\text{Fatigue} = \sum_i \frac{n_i}{N_i} \qquad (18)$$

where n_i = number of cycles experienced at level i

N_i = number of cycles to failure at level i

Conventional wisdom says the total summation should be less than one in order that failure does not occur

For final design, a more sophisticated procedure was required. Once the displacements δ_R are computed at the retained degrees of freedom by either the normal mode or impedance method, the displacements δ_E at the eliminated degrees of freedom can be found from the original stiffness matrix, which has been stored on tape, by using Equation (19), where K_{21} and K_{22} are elements of the original partitioned stiffness matrix.

$$\delta_E = \frac{\delta_R \ K_{21}}{K_{22}} \tag{19}$$

Once the displacements for all the degrees of freedom are found, the stresses can be determined on each element by re-entering the element subroutines. These stresses now become the transfer functions per unit base acceleration. When multiplied by the input PSD and the numerical integrations performed as before, the rms stresses, zero crossings and the exceedances of various stress levels per unit time are obtained. The stress exceedance curve is entered for a series of successively increasing stress levels until the exceedance for the time in the launch environment is less than one. The cumulative damage equation is then formed as before, using these stress levels. Thus, an estimate of the fatigue life of each element in the structure is obtained.

For elements where there is effectively no interaction between stresses, the basic exceedance equation is applicable. For elements where combined stresses are significant, the exceedances of a series of factored structural interaction boundaries are found, using the method of Houbolt, as given in Reference 2. The number of cycles to failure should then be that value as specified for the combined stress level.

CONSTANT STRAIN ELEMENTS

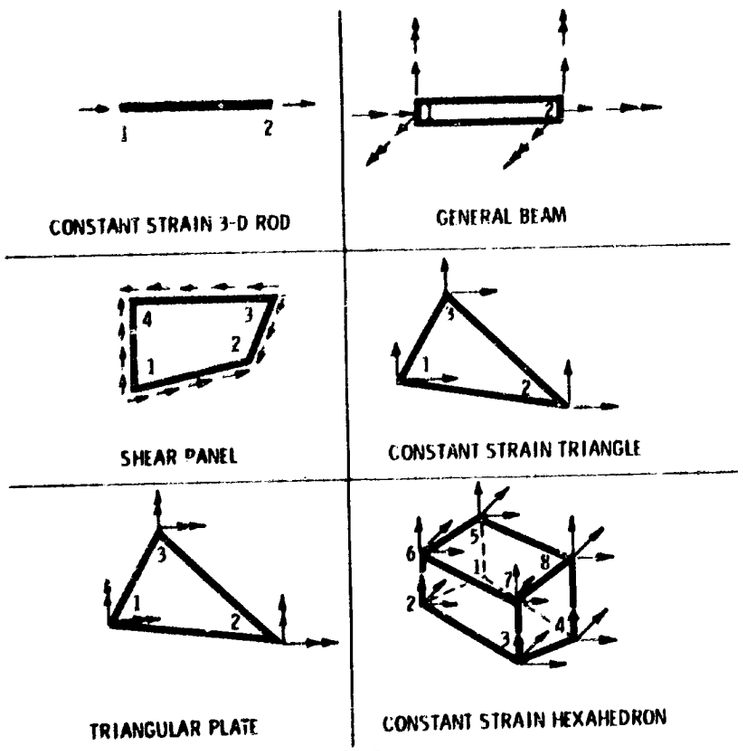

FIGURE 7

LINEAR-STRAIN ELEMENTS

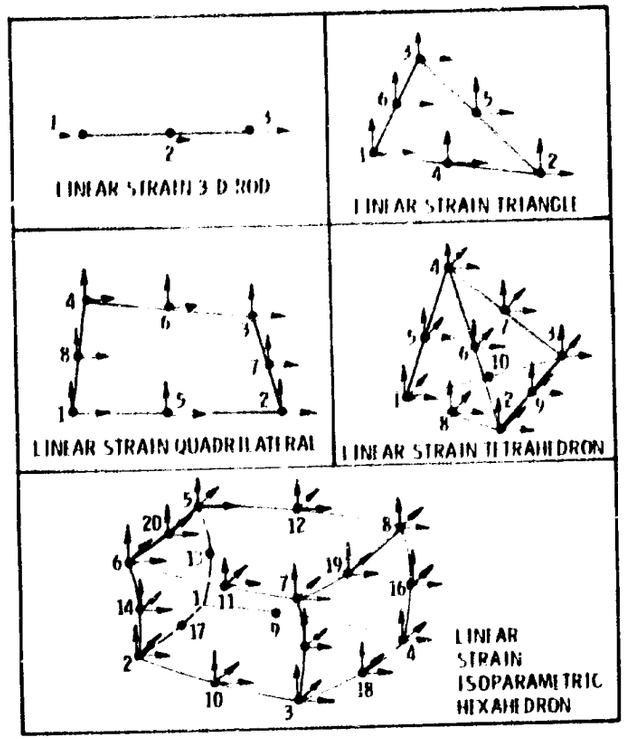

FIGURE 8

6.0 CONCLUSIONS AND RECOMMENDATIONS

These methods have proven most satisfactory in the design of the antenna-feedhorn combination. The same programs used to analyse the antenna response during launch can equally well be used to analyse dynamic structural vibrations in the space shuttle, particularly during launch and staging. However, a much larger choice of elements is necessary than were required for the antenna, in order that the complex shuttle structure be represented accurately.

A large number of elements have been thoroughly developed and tested under research grants from the Canadian Defence Research Board.

Two different sets of compatible elements that could be used in idealizing the shuttle structure have been assembled and are presented here.

The first group, shown in Figure 10, have corner nodes only. They allow linearly varying displacements within the element, and hence have constant strain.

The second group of elements, as shown in Figure 11, have intermediate nodes along their edges. This allows the displacements to vary quadratically: hence, the elements have a linear strain capability. The hexahedron is also isoparametric, allowing the faces of the element to represent curved surfaces.

These elements could easily represent the two craft shuttle configuration; using the normal techniques described, and employing either discretion in choosing the retained degrees of freedom, or the method of substructures, the dynamic response of the structure may be determined, and fatigue life of the elements estimated.

7.0 REFERENCES

1. Hurty, W.C. and Rubinstein, M.F., "Dynamics of Structures", Prentice Hall 1964.

2. Houbolt, J.C., "Exceedances of Structural Interation Boundaries for Random Excitation". AIAA Journal vol. 6, no. 11, Nov. 1968, pg. 2175.

3. Edwards, R.G. and Hayden, A.C., "Gust Analysis Procedure" Canadair Report ERR-CL-RAS-00-100, March 1968.

4. Hayden, A.C. and Edwards, R.G., "PSD Techniques - Experiments with Random Excitation". Canadair Report ERR-CL-RAS-00-177, 1969.

5. Tinawi, R. and Norwood, M., "Finite Element Analysis of Composite Wing Structures" Canadair Report ERR-CL-RAS-00-175, 1969.

6. Tinawi, R., "A Study of Various Idealizations for Wing Structures and Numerical Procedures Involved using Matrix Methods". AIAA/ASME Structures, Structural Dynamics and Materials Conference, April 1969.

SPACE VEHICLE RESPONSE TO ATMOSPHERIC DISTURBANCES

Robert S. Ryan

NASA-Marshall Space Flight Center
Huntsville, Alabama

The objective of dynamics analysis is to predict the vehicle response (load) statistically (probability of expectancies of load) using a vehicle model which is known only in some bounded fashion (nominal plus spreads), and an input force (winds) either as an ensemble of individual winds or as a statistical quantity. The prediction and interpretation of the response of a space vehicle to atmospheric disturbances are very complicated because the vehicle response depends on, and interacts with, the various characteristics of the wind (magnitude, shear, gust), the vehicle dynamics (rigid body, elastic body, propellant oscillations, aerodynamic loading), the control system (attitude control, modal suppression, path control), and the statistical characteristics of each of these subsystems or variables. Technology associated with space vehicle response is, therefore, concerned with many facets or disciplines. These can be categorized as: (1) dynamic models for structure, liquid propellant, aerodynamic forces, control system, environment (atmospheric disturbances), and overall combined system; (2) analysis techniques for frequency response, time response, and stability analysis, including appropriate techniques for statistical description or interpretation of results; (3) criteria for evaluation of results such as flutter boundaries, handling qualities, response goals, stability goals, design goals (probability of launch in worst wind month, etc.); and (4) methods for alleviation or suppression or excessive loads.

Obviously, one cannot treat all of these areas in one paper. Therefore, only major items will be mentioned with emphasis placed on the analysis area. The approach taken will be to present state of the art approaches and to identify the basic technology development needed for the Space Shuttle concept. In addition, special inflight dynamic problems which are expected for the Space Shuttle vehicle due to its varied mission and innovated design will be identified.

SPACE VEHICLE RESPONSE TO ATMOSPHERIC DISTURBANCES

The objective of dynamic analysis is to predict the vehicle response (load) statistically (probability of expectancies of load) using a vehicle model which is known only in some bounded fashion (predicted nominal plus tolerances), and an input force (usually winds) either as an ensemble of individual winds or as a statistical quantity.

The degree of accuracy with which we can make these predictions determines the structural integrity of the vehicle which can be traded directly into greater payload capability. This same accuracy is parlayed into the control system requirements and design. The more accurate the vehicle's dynamic characteristic predictions are, the less the requirement for control system redundancy; thus, such accuracy saves cost and produces greater reliability and can result in payload savings, added structural lifetime, and crew comfort.

The Space Shuttle vehicle, as now envisioned, is payload sensitive, fatigue sensitive (reusable), and requires a highly integrated avionics system to meet the total mission requirements. The stringent mission requirements and design ground rules require that a very accurate and efficient dynamic analysis be developed if the Space Shuttle is to become a reality.

SPACE VEHICLE RESPONSE TO ATMOSPHERIC DISTURBANCES

PROBLEM: SIMULATION OF DYNAMIC LOADS AND RESPONSE OF SPACE SHUTTLE VEHICLES

OBJECTIVES: PREDICT VEHICLE DYNAMIC RESPONSES AND LOADS WITH AN ACCURATE, DEFINABLE, PROBABILITY LEVEL.

IMPACT: VEHICLE STRUCTURAL INTEGRITY, PAYLOAD, AND CONTROL SYSTEM REQUIREMENTS

REQUIREMENTS FOR DETERMINING DYNAMIC LOADS AND RESPONSE

Accurate and efficient dynamic analysis is dependent upon five basic factors: (1) Analytical or test derived models of subsystems which are combined into the overall system model. This overall system model must include accurate descriptions of the subsystems, liquid propellant, structural dynamics, control system, aerodynamic forces, and flight mechanics trajectories; (2) An accurate description of the environment compatable with the analysis technique. This is as important as the model because it is the major excitation force of both static and dynamic lateral loads; (3) Analysis procedures which are efficient, lead to understanding, and provide accuracy of the results; (4) Performance criteria. These are necessary for performance goal settings, both in the design and verification phase; otherwise, ultra-conservative designs result; (5) Active load reduction techniques (mainly control system) is necessary as a final means of meeting design goals and mission constraints.

REQUIREMENTS FOR DETERMINING DYNAMIC LOADS AND RESPONSES

I. **MODELS**

A. SUBSYSTEMS

B. SYSTEM

II. **DESCRIPTION OF ENVIRONMENT**

III. **ANALYSIS PROCEDURES**

IV. **PERFORMANCE CRITERIA**

V. **LOAD REDUCING TECHNIQUES**

FLIGHT PHASES REQUIRING LOADS CALCULATIONS

All major areas of the flight profile from the launch pad to the return landing require accurate predictions. Each phase can, and usually does, design a particular area or structural subsystem of the vehicle. The chart lists all the major areas of concern; however, only the ascent phase will be covered in this presentation (asterisk) because of time limitation. Many of the points covered will be applicable to the other mission phases.

FLIGHT PHASES REQUIRING LOADS CALCULATION

- ON PAD
- LIFT-OFF
- * ASCENT
- SEPARATION
- DOCKING
- RE-ENTRY
- CRUISE
- LANDING

MODEL REQUIREMENTS

The system model should include, but not necessarily be limited to, the listing shown on Chart 4. Accurate models of these various subsystems allow a choice to be made as to the degree of sophistication needed for a particular analysis. In the final design phase and assessment phase, all the model details must be included.

MODEL REQUIREMENTS

- 6-D RIGID BODY TRAJECTORY
- STATIC AEROELASTIC EFFECTS
- NON-IDEAL CONTROL SYSTEM *(FILTERS, LAGS)*
- ENVIRONMENT *(WIND DESCRIPTION)*
- BENDING MOMENT OR LOADS
- 3-D STRUCTURAL MODES
- PROPELLANT SLOSHING MODES
- NON-LINEAR, LOCAL AERODYNAMIC FORCES
- PROPULSION SYSTEM

SYSTEM MODELING

The state-of-the-art of dynamics system modeling has reached a high level of sophistication in the last few years. System equations for a six-degree-of-freedom trajectory, using three-degree-of-freedom elastic body descriptions, have been formulated. Nonlinear quasi-steady aerodynamic distributions were incorporated, as well as nonideal control systems (filters and lags). Programmed control system gains, time-varying co-efficients, and some means of account for data tolerances, are available.

Even with these advancements, adequate models are still the major problem. A recent publication from NASA Electronics Research Center entitled "Trends in Control Research and Technology," surveys the most pressing problems facing control engineers. Modeling was listed by a number of the experts as being one of the major areas of research needing attention today. John B. Lewis, Pennsylvania State University, says, "There is absolutely no substitute for a thorough knowledge of the system. It is a tedious and time-consuming process requiring much ingenuity to obtain useful system models on which the control design can be based. Good general test procedures are needed so that even complex systems can be satisfactorily described." N. Lefkowitz, Case Western Reserve, says, "We need much more effective means of modeling systems and abstracting from the model the attributes that are relevant to the decision-making and control problem.

Much of the modeling technology which is needed for vehicle response to disturbances is covered in other papers dealing with the basic substances. Their importance dictates a restatement of the basic areas. They include more accurate elastic body characteristics that include local effects at sensor locations and mass cross-coupling. Particular emphasis is needed on joints and localized damping. Nonstationary aerodynamics in a practical form for response is a dire need, as well as work in defining accurately the data spreads associated with the characteristics of these subsystems so that they can be statistically accounted for in the response analysis. Finally, an efficient statistical procedure is needed for analyzing these data tolerances in conjunction with the response analysis.

SYSTEM MODEL

STATE OF ART:

- 6-D TRAJECTORY
- 3-D ELASTIC BODY
- QUASI-STEADY AERODYNAMICS
- PROGRAMMED CONTROL SYSTEM GAINS
- RSS PARAMETER VARIATIONS

TECHNOLOGY NEEDED:

- NON-STATIONARY AERODYNAMICS
- IMPROVED SUBSYSTEM MODELS
- METHODS FOR ESTIMATION OF SUBSYSTEM DATA ACCURACIES
- EFFICIENT STATISTICAL PROCEDURES FOR ANALYZING DATA TOLERANCE EFFECTS ON RESPONSES

VEHICLE LOADS CHARACTERISTICS

Dynamic analysis of present launch vehicles has produced some basic results applicable to future space vehicle design and the development of technology. The basic wind loads acting on a vehicle can be expressed as a lateral bending moment with the longitudinal loads added to these effects. This bending moment can, in general, be simplified to be a function of the angle of attack, control force deflection, and elastic body accelerations. Other effects are generally small for vehicles of the Saturn type. Three basic dynamic effects influence design of the vehicle structure: ground winds, inflight winds of high dynamic pressure regions, and first stage shutdown transient. Typical structural design areas for the Saturn V/Apollo are shown on figure 1. Figure 2 shows two very important effects: (1) That from a rigid vehicle standpoint, the design of the nose of the vehicle is predominantly influenced by the aerodynamics. This is illustrated by the solid curve R(x) which is the ratio of the bending moment partial due to angle of attack to the bending moment partial due to control force $R(x) = \frac{M'_\alpha}{M'_\alpha}$. (2) The percentage of total bending moment resulting from bending dynamics. Here again, the vehicle nose is the culprit with the major portion of the bending moment in this region resulting from bending dynamics. Additional effects on the Saturn / Apollo vehicle loads were gust penetration which had no appreciable effects and static aeroelasticity, which increased the engine deflection by approximately 2 to. With the large aerodynamic surfaces present on the Shuttle vehicle and its complex structural design, these effects can be compounded from those experienced on the Saturn vehicles. Technology then must be extended in the aeroelasticity area of local nonstationary aerodynamics, gust penetration, static aeroelasticity, and structural dynamic modeling.

VEHICLE LOAD CHARACTERISTICS

BENDING MOMENT $M_B(x) = M_{\dot{\beta}} \left[R(x)\alpha(t) + \beta(t) \right] + \Sigma M_{\dot{\eta}_\mu} \ddot{\eta}_\mu(t) + \Sigma M_{\dot{\xi}_s} \ddot{\xi}_s(t) + M_T$

1. SATURN V DESIGN LOADS

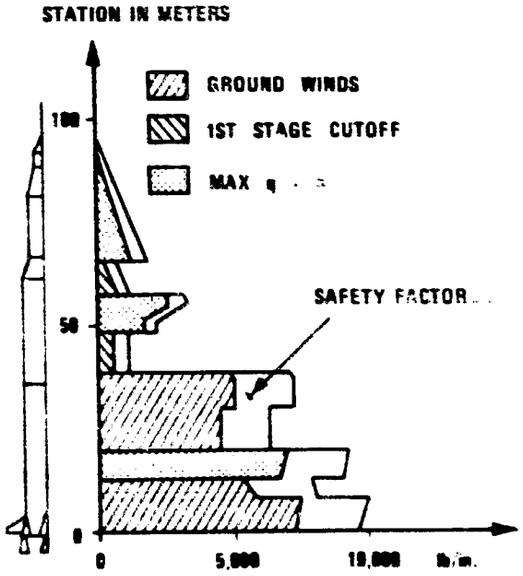

TOTAL STRUCTURAL LOADS

2. AERODYNAMICS, THRUST FORCE, AND BENDING DYNAMICS

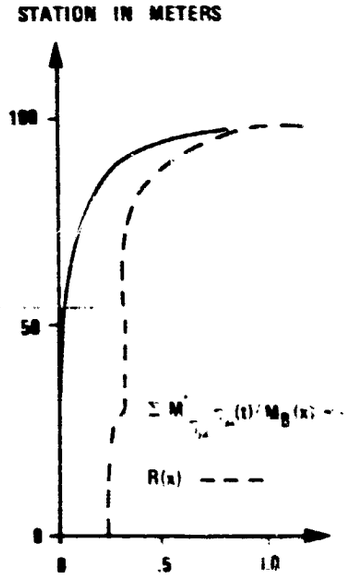

RATIO

3. STATIC AEROELASTIC EFFECTS FOR SATURN V, β INCREASED 20%

4. GUST PENETRATION EFFECTS FOR SATURN V, NEGLIGIBLE

ENVIRONMENT

Four distinct types of wind inputs are available for the appropriate response analysis: (1) discrete, (2) power spectra, (3) nonstationary (stochastic), and (4) individual wind soundings. The accuracy of the vehicle response is obviously directly proportioned to the accuracy and understanding of these inputs.

Discrete winds are used mainly as synthetic profiles and 1-cosine gusts. The state-of-the-art profiles are based on many individual soundings and are available for ETR, SAMTEC, White Sands, and Wallops. Wind shear is a conditional shear based on a reference level wind speed. Technology needed for these discrete profiles is a development of joint statistics of the shears and wind speeds.

Power spectra exceedance models for longitudinal, lateral, and vertical gust components are available on a worldwide basis. The power spectra vertical wave lengths of 100m to 2,000m are available for the ETR test range. Additional development is needed to determine the cross spectrum from these same data in order to determine more accurate response data.

A nonstationary wind representation is available based on the Rawinsonde profiles (1000m increments) for ETR, and contains interlevel correlations. The major development in this area is the shaping filters and inter-level correlations for the high frequency wind characteristics ($100 \leq \lambda < 2{,}000$m).

Detail wind profiles (Jimsphere) based on 25m increments are available for ETR, SAMTEC, White Sands, and Wallops. The present samples are not adequate to duplicate the wind speed and wind shear statistics of the Rawinsonde ensemble. The turbulence portion is adequate. Either a larger wind sample is needed or a statistical procedure developed to correct the present sample.

ENVIRONMENT

WIND INPUT	STATE OF ART	TECHNOLOGY REQUIRED
I DISCRETE		
a. SYNTHETIC	a. WIND SPEED ENVELOPES, ETR, SAMTEC WHITE SANDS, AND WALLOPS. WIND SHEAR CONDITIONAL ON REFERENCE LEVEL WIND SPEED, ETR, AND SAMTEC	JOINT STATISTICS OF SHEARS AND WIND SPEED
b. 1-COSINE	b. ETR AND SAMTEC	
II POWER SPECTRA (PSD)	a. NASA 100 M - 2000M 5-15 KM ALTITUDE. ZONAL, MERIDIONAL, SCALAR, ETR	a. CROSS SPECTRUM
	b. USAF EXCEEDANCE MODEL FOR LONGITUDINAL, LATERAL AND VERTICAL GUST COMPONENTS WORLDWIDE BASIS	b. ADEQUATE
III NON STATIONARY (STOCHASTIC)	BASED ON RAWINSONDE INTERLEVEL CORRELATIONS. ETR	INTERLEVEL CORRELATIONS AND SHAPING FILTERS FOR HIGH FREQUENCY (100M - 2000M)
IV JIMSPHERE WIND ENSEMBLE	a. 2000 PROFILES ETR 500 PROFILES SAMTEC, WHITE SANDS AND WALLOPS	• SAMPLE NOT ADEQUATE FOR WIND SPEED AND SHEARS. TURBULENCE PART ADEQUATE

ANALYSIS PROCEDURES

Analysis procedures fall into the same categories as the environment: (1) discrete inputs, (2) harmonic analysis, (3) nonstationary (stochastic), and (4) Monte Carlo. The analysis using discrete inputs is well known and covers various degrees of sophistication from simple planar point time analysis to full 6-D trajectories with 3-D elastic modes and nonlinear aerodynamics. This analysis procedure is adequate.

Generalized harmonic analysis is well developed for both loads and lifetime analysis of linear point time systems. This approach has not been generally extended to include cross spectrum wind models or analysis techniques.

Nonstationary (stochastic) procedures are state-of-the-art for linear time-varying systems which include a wind filter for 1,000m wave lengths. Methods for determining response to mean wind and adding the results from the stochastic process are available. Extending this approach to nonlinear systems, with the development of the high frequency wind model, would produce a very valuable tool in loads analysis. This approach also needs a method for lifetime prediction.

The final approach, the most desirable because no basic restricting assumptions are necessary, is the modified Monte Carlo which flies the vehicle through an ensemble of individual wind profiles, computes the vehicle outputs, and analyzes them in a statistical manner (response level versus probability). (See slide # 9 .) This approach is state-of-the-art for a 6-D rigid body trajectory, nonlinear time-varying coefficients, nonideal control, propellant oscillations, and planar elastic modes. Present state-of-the-art computation time for one trajectory using a hybrid computer is seven seconds. Technology development involves more efficient models and computational procedures that produce desired accuracy while reducing machine run time. Additional developments include procedures for incorporating data spreads (tolerances), nonlinear local angle-of-attack aerodynamics, and a procedure (mentioned under "winds") for correcting the wind sample.

ANALYSIS PROCEDURES

APPROACH	STATE-OF-ART	TECHNOLOGY NEEDED
I DISCRETE INPUTS	• SYNTHETIC WIND PROFILE • RAMP, STEP, IMPULSE, COSINE ALL FOR EITHER LINEAR OR NON-LINEAR TIME VARYING COEFFICIENTS	ADEQUATE
II HARMONIC ANALYSIS	• LINEAR POINT TIME SYSTEM • LOADS AND LIFETIME	CROSS SPECTRUM WIND MODEL AND ANALYSIS TECHNIQUES
III NONSTATIONARY (STOCHASTIC)	• LINEAR TIME VARYING SYSTEM • MEAN WIND PLUS WIND FILTER (STOCHASTIC) 1000M ACCURACY	• NONLINEAR TIME-VARYING SYSTEM • ACCURATE WIND MODEL (HIGH FREQUENCY) • LIFETIME PREDICTION
IV MONTE-CARLO	• HYBRID 6-D SIMULATION 6 SECONDS PER WIND • NONLINEAR TIME-VARYING • SIMPLIFIED PLANAR ELASTIC BODY • NONIDEAL CONTROL • PROPELLANT OSCILLATIONS • SIMPLIFIED LOCAL ANGLE-OF-ATTACK AERODYNAMICS • 2000 JIMSPHERE WIND PROFILES • OUTPUT AS PROBABILITY, VARIANCE AND MEAN	• 3-D ELASTIC BODY WITH NONLINEAR LOCAL ANGLE-OF-ATTACK AERODYNAMICS • COMPUTER PROCEDURES AND MODELING TECHNOLOGY TO GAIN ADDITIONAL COMPUTER SPEED AND ACCURACY • WIND SAMPLE CORRECTION TO ACCOUNT FOR WIND SPEED AND SHEAR DISCREPANCIES • DATA TOLERANCE PROCEDURES FOR EFFECTS ON RESPONSES

PERFORMANCE CRITERIA

Vehicle dynamic response analysis and response reduction techniques require accurate performance criteria as a base for interpertation and design goals. A state-of-the-art optimal approach (Honeywell's) is based on a mean wind and a stochastic wind (1,000m wave length accuracy); ideal state and wind sensing, with constraints on gimbal angle, gimbal rate, and vehicle drift. Bending moment response is usually chosen for optimization.

Technology is required for nonideal state estimation which includes sensor choice and location criteria, an improved optimal procedure for computation efficiency and greater model detail, and a verification of present optimal criteria. Extension of the criteria to include other responses in conjunction with the bending moment is needed (example, acceleration at cockpit), and the development of a time-varying analog of the frozen point time criteria is highly desirable as a simplified means of evaluating system response.

PERFORMANCE CRITERIA

STATE OF ART:

- WIND – MEAN WIND PLUS STOCHASTIC (1000M ACCURACY)
- IDEAL STATE AND WIND SENSING
- CONSTRAINTS ON GIMBAL ANGLE, GIMBAL RATE, AND VEHICLE DRIFT
- OPTIMIZED TO BENDING MOMENT
- FROZEN TIME POINT CRITERIA

TECHNOLOGY NEEDED:

- NON-IDEAL STATE ESTIMATION
- 25M STOCHASTIC WIND MODEL
- IMPROVED OPTIMAL PROCEDURE FOR COMPUTER EFFICIENCY AND GREATER MODEL DETAIL
- ESTABLISH VALIDITY OF PRESENT CRITERIA AND MODIFY TO CORRECT DISCREPANCIES
- DEVELOP CRITERIA FOR BENDING MOMENT PLUS OTHER RESPONSES SUCH AS CREW COMFORT (ACCELERATION OF CREW STATION)
- TIME VARYING ANALOGY OF FROZEN POINT CRITERIA

BENDING MOMENT VERSUS PROBABILITY

Typical results for the bending moment for an ensemble of 1,000 winds is shown for the Saturn V/Apollo type launch vehicle. The results are given for the total wind ensemble and for the wind ensemble with the turbulence filtered out. Accelerometer feedback gain, g_2, is used as the parameter. The only restriction in this probability statement is not in the method of analysis but in the accuracy of the wind ensemble since the method is not restricted by linearity or stationarity assumptions.

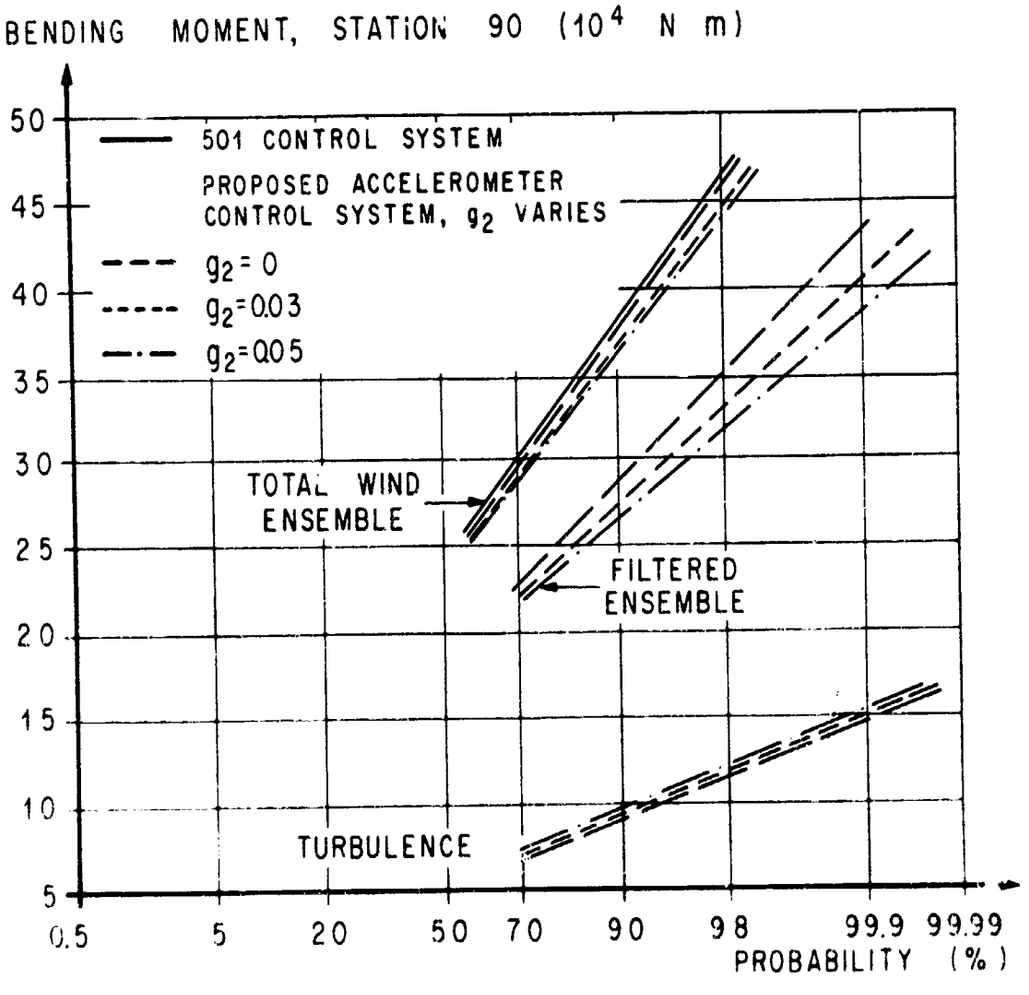

LOAD RELIEF AND MODAL SUPPRESSION

This topic is covered in detail by other authors. The inclusion of the chart is merely for additional emphasis to the importance of reduction techniques and the emphasis it places on other technology requirements such as model accuracy.

The basic technology areas are passive reduction techniques (mean wind biasing), active reduction techniques, performance criteria, state estimation and separation, and efficient analysis techniques. All of these should be pursued simultaneously.

LOAD RELIEF AND MODAL SUPRESSION

STATE OF ART:

- PROGRAMMED GAINS
- SENSOR CHOICE: ACCELEROMETERS, RATE GYROS, POSITION GYROS
- MONTHLY MEAN WIND TRAJECTORY BIASING (ALL PLANES)
- MIXED STATE ESTIMATION

TECHNOLOGY NEEDED:

- ADAPTIVE GAIN SCHEMES
- PREFLIGHT WIND BIASING SCHEMES
- INFLIGHT WIND SENSING AND WIND BIASING
- TECHNIQUES FOR DESIGNING PRACTICAL OPTIMAL SUBSYSTEM CONTROLLER USING OPTIMAL PERFORMANCE CRITERIA AS GOAL
- SEPARATE (MODES) STATE ESTIMATION
- TECHNIQUE FOR MINIMUM INTERFERENCE (COUPLING) THROUGH CONTROL SYSTEM
- SENSOR CHOICE AND LOCATION CRITERIA
- MORE EFFICIENT ITERATION PROCEDURES

SPECIAL SHUTTLE LOADS PROBLEMS

The final chart lists special Shuttle load problems that are potential technology areas. Whether state-of-the-art techniques can be used to analyze and solve these problems will be determined only through analysis. High priority must be given to these areas early to determine their design problem potential and, hence, determine if additional technology is needed.

SPECIAL SHUTTLE LOADS PROBLEMS
(POTENTIAL TECHNOLOGY AREAS)

1. AERODYNAMICALLY STABLE LAUNCH VEHICLE FORCES TRADES BETWEEN PERFORMANCE, DRIFT, AND LOADS.
2. MASS AND AERODYNAMIC BIAS FORCES CREATE A STATIC OR TRIM LOAD DURING ASCENT.
3. MASS OFFSETS AND DYNAMIC MASS COUPLING CREATE DYNAMIC LOADS THROUGH LATERAL LONGITUDINAL COUPLING.
4. AEROELASTIC PROBLEMS DURING ASCENT MAGNIFIED OVER PREVIOUS SPACE VEHICLES DUE TO LARGE LIFTING SURFACES.
5. LIFT-OFF TWANG LOADS ARE MAGNIFIED DUE TO MASS OFFSETS AND LARGE AERODYNAMIC SURFACES.
6. ASCENT LOADS ARE A TRADE OFF BETWEEN BODY LOADING AND WING LOADING.

CONCLUSIONS

The critical technology areas for Space Shuttle vehicle response to atmospheric disturbances are presented on the chart. Other less critical but highly desirable areas were identified in each basic area. Many of the areas shown fall into the various disciplines of Space vehicle design and should receive more in-depth discussions by specialists in these areas; however, they are of utmost importance to response analysis.

CONCLUSIONS

CRITICAL TECHNOLOGY

- PERFORMANCE CRITERIA
- NONSTATIONARY AERODYNAMICS
- ADAPTIVE LOAD RELIEF SCHEMES
- CRITERIA FOR CONTROL SENSOR CHOICE AND LOCATION
- MORE ACCURATE SYSTEM MODELS AND FASTER COMPUTATIONAL TECHNIQUES
- MODAL OR SUBSYSTEM DECOUPLING TECHNIQUES (HARDWARE AND CONTROL)
- TECHNIQUES FOR ACCURATELY INCORPORATING DATA TOLERANCES IN RESPONSES.

ASSESSMENT OF THE POTENTIAL FOR LOAD ALLEVIATION CONCEPTS FOR SPACE SHUTTLE VEHICLES

R. H. Lassen and J. H. Wykes

North American Rockwell

INTRODUCTION

The space shuttle vehicle (SSV) concept utilizes reusable booster and orbiter vehicles to place a variety of payloads into earth orbits for an order-of-magnitude lower cost than that of previous launch-vehicle/spacecraft combinations. The structural weight of reusable booster and orbiter vehicles is a key item in determining the eventual payload and consequent economic feasibility of the SSV. Thus concepts that might result in saving vehicle structural weight must be given serious consideration as early as possible in the design process.

The mated booster-orbiter configuration functions as a combined launch vehicle and aircraft and experiences the structural dynamic response problems of each. The many aerodynamic surfaces of proposed SSV configurations will result in response to atmospheric turbulence over a broad frequency band. Additional excitation of the mated vehicles, as well as each craft separately, will be induced by separated flow or buffeting, interference effects, and interaction of shock waves with the boundary layer. The possibility of high stress, low cycle fatigue must be considered due to the multiple reuse requirement of this program. High loading conditions will occur during boost flight, in maneuvers, and at entry-cruise transition, and the aerodynamic surfaces may be flutter-prone either during the transonic-high dynamic pressure flight regime or in transversing the stall region following high angle of attack entry. One way of coping with many of these problems is to strengthen and/or stiffen the basic load carrying structure. The effect of the resulting weight increase, however, could so seriously jeopardize the payload capability that the SSV mission could not be accomplished

During the past decade or so, automatic control systems have been designed to alleviate induced loads and/or control structural mode dynamics of flexible vehicles. Many studies have been made and several flight programs have demonstrated a variety of benefits and advantages for both aircraft and launch vehicles. The application of such systems and concepts to the aforementioned shuttle vehicle problem areas is suggested as one potential means of meeting the very stringent structural mass fraction requirements of the SSV. This paper briefly reviews the state-of-the-art in load alleviation and mode control, discusses some of the recent techniques, and assesses the potential of such systems for the SSV. Finally, some of the problems requiring solution, and the supporting programs to supply these solutions, are outlined.

LOAD ALLEVIATION AND STRUCTURAL MODE CONTROL SOME RECENT STUDIES AND EXPERIMENTAL PROGRAMS

Because of mission requirements and basic physical differences, the approaches to the study of load relief and structural mode control systems have been different for launch vehicles and aircraft. We have arbitrarily selected several aircraft-oriented programs which have provided both analytical and flight test validation of important load relief and structural mode control concepts. These types of systems have direct application to the SSV configurations because of the use of aerodynamic surfaces.

One analytical study initiated in 1964 for the Air Force Flight Dynamics Laboratory used the XB-70 to study flexible vehicle effects. It was demonstrated that accelerations and structural loads due to structural motion can be alleviated by a control system that increases the damping ratio of the structural modes. The effects on sensing, control force application, coupling and adaptability to changing conditions were studied. It was shown that a relatively simple, practical, conventional control system can be designed to provide phase and gain stabilization of the structural modes under varying flight conditions. This system was called ILAF for Identical Location of Accelerometer and Force. (Fig. 1)

Another Air Force-sponsored program (1965), best known by the name Gust Alleviation and Structural Dynamic Stability Augmentation System (GASDSAS), used analytical and fixed-base simulation techniques to explore gust alleviation and structural mode control systems, ride quality effectiveness and interface problems with handling qualities, displays and terrain following. Building on the results of the XB-70 study, practical solutions were achieved for problems of force generation, system stability, and interference with the regular stability augmentation. Theoretical applications were made to the Advanced Manned Strategic Aircraft (AMSA), the C-5A, and F-111 vehicles. Practical applications of modern optimal control theories were also developed during this study.

Under a jointly sponsored NASA/Air Force program, a combined analytical-flight test project to verify the ILAF concept on the XB-70 was undertaken in 1969. An ILAF system was designed as an add-on to the airplane's stability augmentation system to control only the symmetric structural modes using the existing elevons as force generators. Analytical evaluations showed that the system would be stable and effective in controlling the first three structural modes without degrading handling qualities. Pilot comments and flight test records verified the fact that the system improved crew ride quality in atmospheric turbulence.

Another important analytical-flight test program was conducted for the Air Force Flight Dynamics Laboratory using the B-52 aircraft. This program is best known by the name Load Alleviation and Mode Stabilization (LAMS) and was conducted to demonstrate the capabilities of an advanced flight control system to alleviate gust loads and control structural modes on a large flexible aircraft using existing aerodynamic control surfaces as force producers. A direct lift system was also studied. Flight demonstration of the LAMS flight control system was conducted to provide a comparison of analytical and experimental data. The results obtained showed that significant reduction in fatigue damage rates were obtained. (Fig. 1)

LOAD ALLEVIATION AND STRUCTURAL MODE CONTROL
SOME RECENT ANALYTICAL AND EXPERIMENTAL PROGRAMS

PROGRAM	PURPOSE/RESULTS
CONTROL OF ELASTIC MODES OF FLEXIBLE AIRCRAFT (1964)	INVESTIGATE TECHNIQUES FOR ACTIVE CONTROL OF STRUCTURAL MODES OF A FLEXIBLE VEHICLE USING XB-70 AS ANALYTICAL MODEL. A SIMPLE SUCCESSFUL TECHNIQUE CALLED IDENTICAL LOCATION OF ACCELEROMETER AND FORCE (ILAF) CONCEIVED.
GUST ALLEVIATION AND STRUCTURAL DYNAMIC STABILITY AUGMENTATION SYSTEM (GASDSAS) 1965	ANALYTICAL AND FIXED BASE SIMULATION EMPLOYED TO STUDY EFFECTS OF GASDSAS ON RIDE QUALITY AND INTERFACE PROBLEMS WITH HANDLING QUALITIES, DISPLAYS AND TERRAIN FOLLOWING. AMSA PRINCIPAL STUDY VEHICLE; C-5, F-111 APPLICATIONS DEMONSTRATED. SYSTEMS PERFORMED WELL AND INTERFACE PROBLEMS SOLVED.
XB-70 FLIGHT TEST PROGRAM, INVESTIGATION OF CONTROL OF ELASTIC MODES, 1968	FLIGHT TEST PROGRAM TO VERIFY ILAF CONCEPTS. A SYSTEM DESIGNED AND IMPLEMENTED TO CONTROL SYMMETRIC MODES USING ELEVONS. PILOT COMMENTS AND FLIGHT RECORDS DEMONSTRATED IMPROVEMENT IN RIDE QUALITY.
LOAD ALLEVIATION AND MODE STABILIZATION (LAMS) 1966	ANALYTICAL AND FLIGHT TEST PROGRAMS USING THE B-52 TO DEMONSTRATE ADVANCED CONTROL SYSTEM CONCEPTS TO ALLEVIATE GUST RESPONSE AND CONTROL STRUCTURAL MODES. FLIGHT TEST RESULTS OBTAINED SHOWED SIGNIFICANT REDUCTIONS IN FATIGUE DAMAGE RATES.

TYPICAL SENSOR & FORCE GENERATOR LOCATIONS

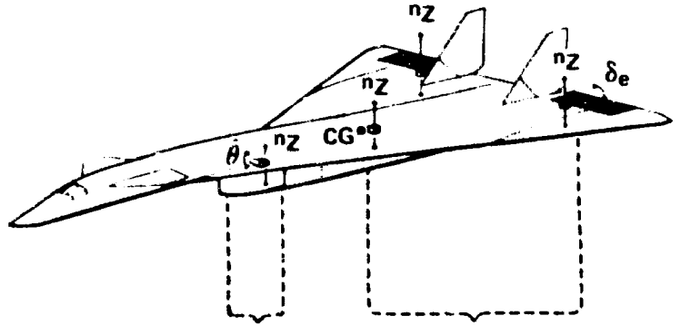

XB-70 SAS & ILAF LONGITUDINAL SYMMETRIC
FLIGHT CONTROL SYSTEM

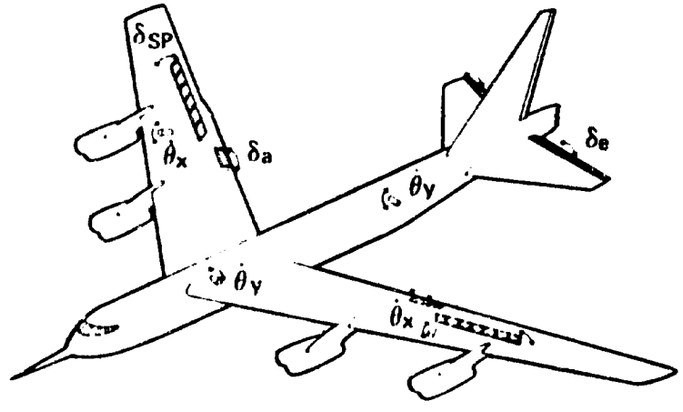

B-52 LAMS SYSTEM SENSOR & CONTROL SYSTEM
SURFACE LOCATIONS FOR
LONGITUDINAL - SYMMETRIC MODES

SYSTEM ADVANTAGES

The chart shows the major benefits to be obtained from using various load alleviation and/or mode control schemes. Obviously, not all systems can provide all these advantages, nor are they designed to do so. However, it is important to note that when fly-by-wire concepts are employed, as on the SSV, implementation of multiple functions is much easier. Early participation of the control system designer and the structural analyst is especially important in the requirement for force generators where use of already existing control surfaces generally compromises the system effectiveness.

Implementation of an automatic control system to reduce gust and buffet response can reduce peak accelerations, loads, and bending moments with potential saving in weight due to reduced fatigue damage rate. Improvement in ride quality is also possible. Systems to control gust responses on flexible vehicles using basic stability augmentation, direct lift and structural mode control techniques have the largest technology background of analysis and test. Little has actually been done in studying the control of buffet response; in principle structural mode control techniques should be applicable. The potential savings in weight to a given vehicle design due to gust alleviation and buffet control can only be assessed after all factors impacting on strength and stiffness have been determined. A number of gust load and fatigue analyses of large flexible aircraft have shown that, in general, these vehicles have not been fatigue limited to a great extent. This means that structural material provided for discrete loads (gust and maneuver) and for stiffness (stability, control, and flutter) have provided more than enough material to cover most fatigue requirements.

Obtaining required flutter margins through use of automatic control of aerodynamic surfaces is becoming increasingly attractive. This is particularly so since fly-by-wire technology is developing the redundancy techniques and actuation hardware required to obtain reliability equivalent to basic structure. Thus, weight saving may be possible through reduction of a lifting surface's basic stiffness. Next to gust response control, this concept has developed a considerable analytical and technology background. The type of flutter to be controlled, lightly damped or explosive, will affect the details of the approach to be utilized.

With the advent of fly-by-wire technology, the possibility of saving weight and reducing drag by reducing the horizontal and vertical tail sizes, and thus reducing static stability has received considerable attention. The basic stability required would be achieved using automatic controls. A balance between the reduced tail size and control surface size and deflection limits set by take-off rotation, maneuver, and stability augmentation requirements must be achieved.

By proper attention to the location of control forces required to maneuver a vehicle the aerodynamic loadings can be shaped to reduce design bending moments and thus save weight. Combined direct lift concepts together with structural mode stabilization concepts show attractive potential for implementing this idea.

SYSTEM ADVANTAGES

CONCEPT	OBJECTIVE/APPROACH	BENEFITS
CONTROL GUST AND BUFFET RESPONSE	REDUCE PEAK ACCELERATIONS, LOADS AND BENDING MOMENTS	SAVE WEIGHT THROUGH LOWER FATIGUE DAMAGE RATE, IMPROVE RIDE QUALITY
FLUTTER MARGIN CONTROL	REDUCE AERODYNAMIC SURFACE STIFFNESS REQUIREMENTS	SAVE WEIGHT
RELAXATION OF INHERENT STATIC STABILITY	REDUCE SIZE OF HORIZONTAL AND VERTICAL STABILIZERS	SAVE WEIGHT REDUCE DRAG
MANEUVER LOAD CONTROL	SHAPE AERO LOADING TO REDUCE BENDING MOMENTS	SAVE WEIGHT

KEY DESIGN CONSIDERATIONS

The key design elements of any active load alleviation and structural mode control system are the sensors and control forces and their final effectiveness is dependent upon the control laws utilized.

Most load alleviation and structural mode control systems developed for winged vehicles over the past decade have employed vehicle motion response sensors such as rotary and linear accelerometers and gyros. Structural motion sensing strain gages have been studied but have not received wide acceptance. In addition to these, launch vehicle and missile studies have found gust sensing vanes and pressure sensors effective.

On vehicles with lifting surfaces, the source of the controlling forces have made use of the normal type trailing edge controls; that is the flaps, ailerons, and elevators. Leading edge surfaces are receiving increased attention. Tip controls and spoilers have also been utilized. Often times these controls have been designed to do double duty as part of the basic maneuver and stability augmentation control systems as well as part of the load alleviation and structural mode control system. While having control surfaces do double duty can be advantageous when the dual requirements are not too constraining, it has been found that small auxiliary surfaces strictly for structural mode control can be efficient and effective.

On launch vehicles and missiles, engine gimballing has been studied extensively to obtain thrust vectoring for control of low frequency load relief and structural mode control. On future vehicles of the SSV type it appears that reaction jets also could be effective control force sources for load alleviation and structural mode control. However, on a relatively continuous demand basis, these reaction jet forces may require more on-board power or fuel than the actuating system needed for aerodynamic surfaces.

Over the past decade considerable research and development effort has been expended on defining the required control laws between sensors and control forces required to accomplish the load alleviation and structural mode control functions without impeding basic maneuver and stability augmentation control. In seeking a simpler fundamental approach within these constraints North American Rockwell, through Air Force sponsored research, identified the ILAF approach. By placing the sensing element (accelerometer) at the force input point and taking advantage of normal actuation and aerodynamic lags, with some assist from electronic compensation, a structural damping force is obtained which is effective over a wide range of vehicle and flight conditions. The Air Force-sponsored LAMS program conducted by Boeing and Honeywell is representative of a more complex but effective sensor blending approach using both accelerometers and gyros which results in an integrated stability augmentation and load alleviation and mode stabilization system. Optimal control theories were effective in synthesizing these types of systems.

Launch vehicle and missile control laws for load relief have been constrained by the use of engine gimballing for control forces to control of vehicle rigid body motions although studies have shown that control of fundamental flexure modes might prove anvantageous. Gyros rather than accelerometers have been utilized because of the thrust vector control approach and the fact that large thrust accelerations make acceleration alignment a problem.

KEY DESIGN CONSIDERATIONS

SENSORS

- ACCELEROMETERS (ROTARY AND LINEAR) — MOTION SENSING
- GYROS — MOTION SENSING
- STRAIN GAGES — MOTION SENSING
- VANES — EXCITATION SOURCE (GUST) SENSING
- PRESSURES — EXCITATION SOURCE (GUST) SENSING

FORCE GENERATORS

- TRAILING EDGE CONTROLS (FLAPS, AILERONS, ELEVATORS)
- LEADING EDGE CONTROLS
- TIP CONTROLS
- SPOILERS
- ALL MOVEABLE SURFACES (HORIZONTAL TAILS, VERTICAL TAILS, CANARDS)
- THRUST VECTOR CONTROL
- REACTION JETS

CONTROL LAWS

- IDENTICAL LOCATION OF ACCELERATION AND FORCE (ILAF)
- SENSOR BLENDING (THROUGH OPTIMAL TECHNIQUES)
- SIMPLE FEEDBACK

ASSESSMENT OF LOAD ALLEVIATION AND STRUCTURAL MODE CONTROL POTENTIAL FOR SSV

Having reviewed the current state-of-the-art, examined some studies and flight program results, and discussed some important system hardware features, this section examines the application of all this technology to the SSV.

By relying on automatic controls to provide a satisfactory equivalent static stability, it may be possible to reduce the horizontal and vertical tail sizes with a savings in weight. The potential for doing this is rated fair to good. The lack of current in-depth study of the amount of tail size reductions possible contributes to the cautious comment. In addition, the current lack of ability to produce large capacity multiple redundant actuation units adds further caution. The actuation unit is one of the main differences to keep in mind when making comparisons between Apollo and SSV fly-by-wire systems. It is, of course, the technology developed in the redundancy and reliability of the electronic components of fly-by-wire systems like Apollo that suggests some optimism in evaluating this approach.

The use of an active flutter control system on the SSV to reduce rigidity requirements has a good chance for success. All of the lifting surfaces are expected to have their minimum flutter margins during boost while in the transonic flight region. During reentry, stall flutter of these lifting surfaces may also be of concern even though the dynamic pressure will be much reduced. Leading edge, trailing edge, and tip controls as well as reaction jets are possible force generation sources. The control would provide for margin only. While the vehicles would be vulnerable for flutter on every flight, during boost the exposure time is relatively short. The potential for controlling stall flutter also exists and the overall assessment is "good".

Maneuver load control for the booster during entry and turn and for the orbiter during transition is rated of fair to good potential. The qualification shading of fair is related to the fact that sufficient analyses have not been accomplished to determine if a weight penalty exists due to these maneuvers. If a design penalty exists, surface locations and the low frequency surface actuation demands make the chance good for potential weight savings.

The potential for obtaining benefits from controlling response to gusts and buffet to reduce bending moments and improve ride quality and structural fatigue are rated fair to good. The strength designs of the lifting surfaces could be set by the q magnitudes during boost where the peak values of this parameter could be caused by gust. The maximum exposure to gusts and maximum dynamic pressure occur almost simultaneously. The chances of implementing an automatic control system to reduce these design loads are rated good since much of the state-of-the-art technology exists for this kind of application. The SSV's are flexible and the crew will be subjected to some acceleration environment. However, the fact that the crew will have mainly a monitoring function except during docking, and the fact that the exposure time will be relatively short, indicates gust and buffeting will have little effect on crew efficiency or safety and ride quality improvement is not critical. Studies have shown that structural response due to buffeting is mainly first wing bending; thus control surfaces near the tip should be able to damp this relatively low frequency motion if this is determined to be desirable.

ASSESSMENT OF LOAD ALLEVIATION AND STRUCTURAL MODE CONTROL POTENTIAL FOR SSV

CONCEPTS	SSV CONSIDERATION	POTENTIAL
REDUCE STATIC STABILITY	MAY BE DESIGN CONDITION FOR SOME TAIL SURFACES	FAIR TO GOOD
FLUTTER MARGIN CONTROL	HIGH Q, TRANSONIC AND LOW SUPERSONIC IMPORTANT	GOOD
	STALL FLUTTER MAY BE IMPORTANT	
MANEUVER LOAD CONTROL	BOOSTER ENTRY/TURN AND ORBITER TRANSITION MAY BE KEYS	FAIR TO GOOD
	STRENGTH DESIGN OF LIFTING SURFACES IMPORTANT	
CONTROL RESPONSE TO GUST/BUFFET	RIDE CONTROL NOT THOUGHT CRITICAL AND STRUCTURAL FATIGUE NOT LIKELY	FAIR TO GOOD

PRECEDING PAGE BLANK NOT FILMED.

POSSIBLE AERODYNAMIC CONTROLS & REACTION JET FORCE LOCATIONS FOR LOAD-ALLEVIATION & STRUCTURAL-MODE CONTROL SYSTEMS

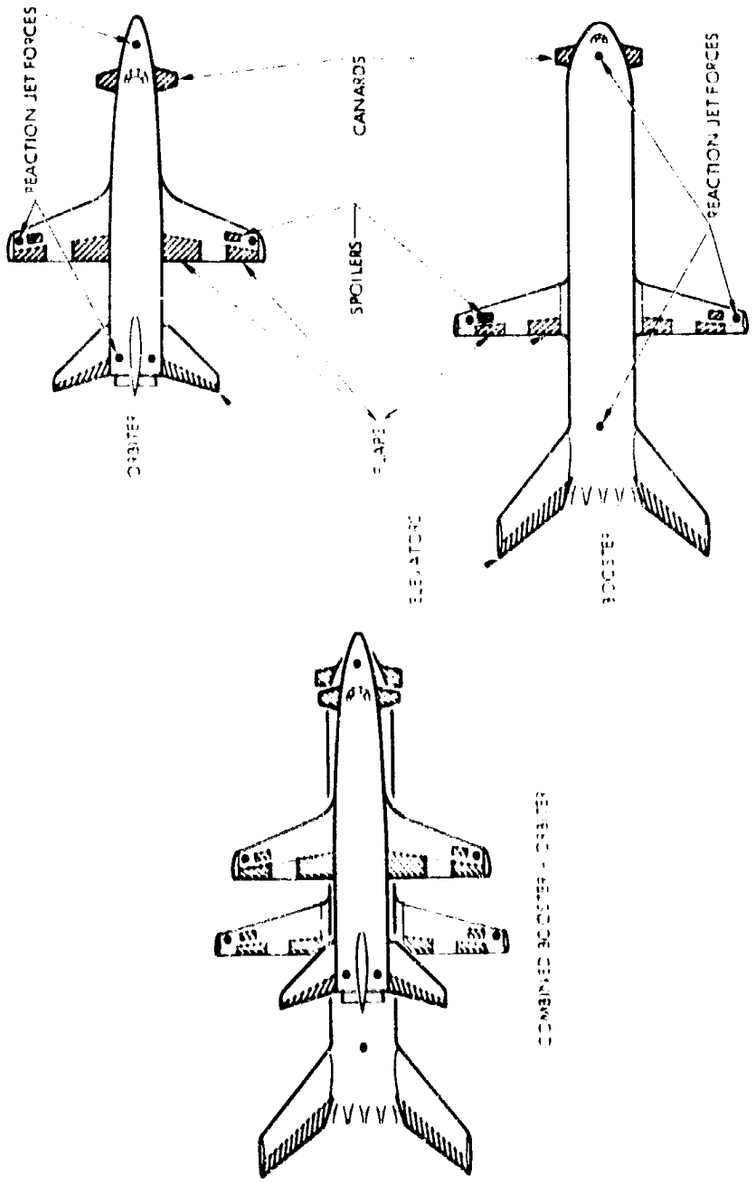

CONCLUSIONS AND RECOMMENDATIONS

The use of load alleviation and structural mode control concepts for SSV should be explored in more detail. Sufficient analytical and flight test experience exists for both aircraft and launch vehicles to give an overall good possibility of success of this approach. In addition, the existing fly-by-wire avionics technology gives confidence of being able to provide the required safety and reliability in this portion of the hardware system. However, the unique nature of the space shuttle vehicle results in complex problems in system design. Adequate verification that these problems have been solved will require the best analytical efforts supported by structural and aerodynamic tests of specific models of the SSV. To assure that an adequate system will evolve, a number of research and development activities must be pursued.

To isolate the potential problems of applying load relief and structural mode control systems to the SSV, the primary structural design conditions must be identified. This requires in-depth analyses of all conditions affecting strength and stiffness as a development level of effort. These analyses must identify the structural response to maneuver loads, gust and buffet, and to flutter. Currently, satisfactorily accurate analytical calculations can be made for maneuver loads, gust loads, and flutter characteristics. The analytical capability for estimating excitations from buffet and dynamic interference loads is not adequate and improved methods are needed as well as experimental data from wind tunnel model test programs to confirm all calculations.

Any system design synthesis will require detailed knowledge of the vehicles structural dynamics (mode shapes, frequencies, generalized masses, and structural damping) for the range of weight conditions to be experienced. This information is required to locate sensors and control forces for solutions to the problems identified in the earlier analyses. The desirability or the need to use reaction jets must be determined, taking into account the fact that within the atmosphere the jet flow induces a secondary pressure field on the aerodynamic surface from which it emits. This causes the jet force magnitude to become a function of flow regions through which the vehicle flies, - subsonic, transonic, supersonic, and hypersonic.

As the problem definitions are sharpened and an active control system design evolves, interface conflicts with the vehicle configuration and design ground rules will arise. One example might be the desire to have minimum penetration of the orbiter lower surfaces for heat protection reasons versus the need for positive and negative forces from a given control surface. Trade-off studies may be required to determine whether adding a separate aerodynamic surface as a force generator is better than using existing surfaces.

Finally, detailed tests will be needed to verify that the aerodynamic characteristics of the selected force generators will provide the desired inputs. Also a development program should be initiated to insure that actuators of sufficient capacity and redundancy will be available.

CONCLUSIONS AND RECOMMENDATIONS

- LOAD ALLEVIATION AND STRUCTURAL MODE CONTROL SYSTEM FOR SSV SHOULD BE INVESTIGATED IN MORE DETAIL
- SUGGESTED RESEARCH AND DEVELOPMENT SEQUENCE:
  - IN-DEPTH ANALYSES TO DETERMINE DESIGN LOADS & STIFFNESSES
  - SUPPORTING WIND TUNNEL TESTS TO CONFIRM STUDIES
  - SELECTION OF SPECIFIC LOAD CONDITIONS AND STIFFNESS REQUIREMENTS THAT ACTIVE CONTROL SYSTEM CAN INFLUENCE
  - SYNTHESIZE A SPECIFIC LOAD ALLEVIATION/MODE CONTROL SYSTEM
  - CONDUCT TESTS TO INVESTIGATE AERODYNAMICS OF FORCE GENERATORS
  - INITIATE DEVELOPMENT OF MULTIPLE-REDUNDANCY ACTUATORS